SURVIVAL IN EXTREME ENVIRONMENTS – ADAPTATION OR DECOMPENSATION?, VOLUME I

EDITED BY: Torkjel Tveita, Ingrid Eftedal and Sanjoy Deb
PUBLISHED IN: Frontiers in Physiology

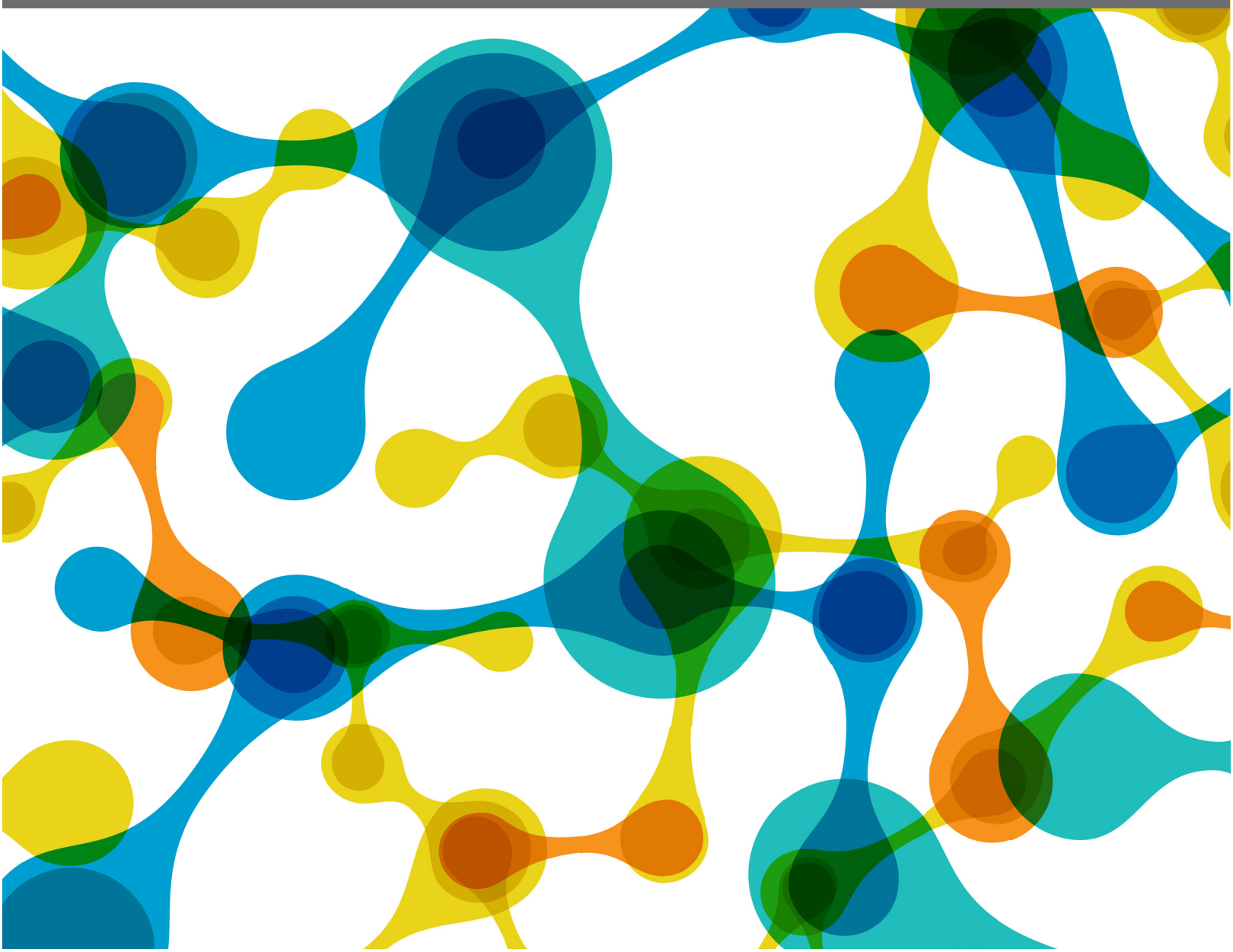

frontiers Research Topics

frontiers

ISSN 1664-8714
ISBN 978-2-88974-590-6
DOI 10.3389/978-2-88974-590-6

About Frontiers

Frontiers is more than just an open-access publisher of scholarly articles: it is a pioneering approach to the world of academia, radically improving the way scholarly research is managed. The grand vision of Frontiers is a world where all people have an equal opportunity to seek, share and generate knowledge. Frontiers provides immediate and permanent online open access to all its publications, but this alone is not enough to realize our grand goals.

Frontiers Journal Series

The Frontiers Journal Series is a multi-tier and interdisciplinary set of open-access, online journals, promising a paradigm shift from the current review, selection and dissemination processes in academic publishing. All Frontiers journals are driven by researchers for researchers; therefore, they constitute a service to the scholarly community. At the same time, the Frontiers Journal Series operates on a revolutionary invention, the tiered publishing system, initially addressing specific communities of scholars, and gradually climbing up to broader public understanding, thus serving the interests of the lay society, too.

Dedication to Quality

Each Frontiers article is a landmark of the highest quality, thanks to genuinely collaborative interactions between authors and review editors, who include some of the world's best academicians. Research must be certified by peers before entering a stream of knowledge that may eventually reach the public - and shape society; therefore, Frontiers only applies the most rigorous and unbiased reviews.
Frontiers revolutionizes research publishing by freely delivering the most outstanding research, evaluated with no bias from both the academic and social point of view. By applying the most advanced information technologies, Frontiers is catapulting scholarly publishing into a new generation.

What are Frontiers Research Topics?

Frontiers Research Topics are very popular trademarks of the Frontiers Journals Series: they are collections of at least ten articles, all centered on a particular subject. With their unique mix of varied contributions from Original Research to Review Articles, Frontiers Research Topics unify the most influential researchers, the latest key findings and historical advances in a hot research area! Find out more on how to host your own Frontiers Research Topic or contribute to one as an author by contacting the Frontiers Editorial Office: frontiersin.org/about/contact

SURVIVAL IN EXTREME ENVIRONMENTS – ADAPTATION OR DECOMPENSATION?, VOLUME I

Topic Editors:
Torkjel Tveita, UiT The Arctic University of Norway, Norway
Ingrid Eftedal, Norwegian University of Science and Technology, Norway
Sanjoy Deb, University of Westminster, United Kingdom

Citation: Tveita, T., Eftedal, I., Deb, S., eds. (2022). Survival in Extreme Environments – Adaptation or Decompensation?, Volume I. Lausanne: Frontiers Media SA. doi: 10.3389/978-2-88974-590-6

Table of Contents

frontiers in Physiology

EDITORIAL
published: 04 February 2022
doi: 10.3389/fphys.2022.836210

Editorial: Survival in Extreme Environments – Adaptation or Decompensation?, Volume I

Torkjel Tveita[1,2]*, *Ingrid Eftedal*[3,4] *and Sanjoy Deb*[3,5]

[1] *Anesthesia and Critical Care Research Group, Department of Clinical Medicine, UiT, The Arctic University of Norway, Tromsø, Norway,* [2] *Division of Surgical Medicine and Intensive Care, University Hospital of North Norway, Tromsø, Norway,* [3] *Department of Circulation and Medical Imaging, Faculty of Medicine and Health Sciences, NTNU Norwegian University of Science and Technology, Trondheim, Norway,* [4] *Faculty of Nursing and Health Sciences, Nord University, Bodø, Norway,* [5] *Centre for Nutraceuticals, School of Life Sciences, University of Westminster, London, United Kingdom*

Keywords: diving, hunting, fishing, extraction work, farming

Editorial on the Research Topic

Survival in Extreme Environments – Adaptation or Decompensation?, Volume I

The history of human migration is also the history of successful biological interactions with new environments, where maintenance of body homeostasis is the fundamental property. Equilibrium of body homeostasis is the product of many regulatory physiologic mechanisms and seems to result from a natural resistance to change from a pre-existing optimal biological condition. Chronic or functional adaptation is the product of processes which may run for the whole life of an individual. Human adaptive processes may take thousands of years, like the process of standing and walking erect or adaptation to living at a high altitude which is possible due to some adaptation, but these ongoing processes need much more time to be optimal. However, the focus of the Research Topic is related to acute adaptation to a new equilibrium which may take place within seconds. Challenges to maintain biological equilibrium in a new environment, or more simply, to stay alive, include climate, ambient temperature and pressure, high altitude, water immersion, and the immediate access to naturegiven resources like food, water, and shelter. When humans are exposed to extreme environments, accidents may occur; the victims are no longer adapted and may decompensate due to hyper/hypothermia, oxygen deprivation, high-/low ambient pressures, or drowning. Professional workers like divers, extraction industry workers, anglers and hunters, seamen, or people seeking these elements during leisure or recreational activity, all depend on their ability to adapt, but share the same potential threat that their biological homeostasis will disrupt in case of an accident. The rescuers, on the other hand, may often meet other challenges, like lack of practice to institute proper care of patients with these relatively rare conditions, or worse, attempting to treat such decompensated patients where the guidelines for treatment are not yet written. To write these guidelines, we are in urgent need of new knowledge. Due to obvious reasons, some of this new knowledge of complex pathophysiologic mechanisms evoked by accidents can only be collected from animal models experiments. However, novel techniques allow us to conduct clinical studies on subjects during their daily activities under harsh working conditions. Due to the very intrinsic integrative nature of the physiological mechanisms involved in adaptation—or not—to extreme environmental challenges, it is sometimes difficult to understand them in their entirety. Fortunately, new opportunities have arisen with the advent of biomolecular techniques, providing tools to better understand the interactions between the different levels of integration within the body, allowing us to see the bigger picture.

Edited and reviewed by:
Johannes Van Lieshout, University of Amsterdam, Netherlands

***Correspondence:**
Torkjel Tveita
torkjel.tveita@uit.no

Specialty section:
This article was submitted to Clinical and Translational Physiology, a section of the journal Frontiers in Physiology

Received: *15 December 2021*
Accepted: *06 January 2022*
Published: *04 February 2022*

Citation:
Tveita T, Eftedal I and Deb S (2022) Editorial: Survival in Extreme Environments – Adaptation or Decompensation?, Volume I. Front. Physiol. 13:836210. doi: 10.3389/fphys.2022.836210

In this Research Topic we present a valuable collection of new preclinical and clinical research data with the potential as background information to broaden our insight into how to improve our physiologic adaptation, or at least to be better prepared when meeting a challenging environment. We have collected data with translational potential to better manage critical care conditions after exposure to such environments.

Anecdotal information exists on how to face and survive harsh environments. Those living by the north Atlantic coastline learned early from offshore fishermen that to stay alive out there you must keep warm and get enough rest. The message was that becoming chilly or sleepless may be as dangerous as consuming alcohol due to the potential threat of losing mental control. Aspects of this information are elegantly taken into the research lab and presented by Færevik et al. in the Research Topic. They showed that test persons, adequately dressed for an ambient temperature of −2°C, limited to 6 h exposure time during the night after a good night sleep before that, remained mentally alert and warm. Likewise, over the past 60 years, an understanding exists that victims of accidental hypothermia may survive even if rewarming is started after prolonged periods of cardiac arrest, and the saying "Nobody is dead until warm and dead" has become a slogan. The main reason is that over the same years the medical health care system, from prehospital care to in hospital advanced medical care, together have managed to reduce morality of accidental hypothermia from 52 to 80% at the beginning to the present 28–35%. However, this success rate is closely linked to accidental hypothermia patients without cardiac arrest, whereas survival rate of patients in cardiac arrest is much lower. The recommended treatment of hypothermic cardiac arrest is rapid patient transfer under continuous cardiopulmonary resuscitation (CPR) to a hospital equipped for in-hospital rewarming using extracorporeal membrane oxygenation (ECMO). But sometimes, mostly due to weather conditions, patient transport to a hospital with ECMO might be impossible and the search for alternative methods to ECMO rewarming must be investigated. In the preclinical experimental work by Nivfors et al. an alternative method, warming by continuous perfusion of the pleural cavity with warm water (Closed thoracic lavage) was tested out following 3 h of continuous CPR. This work demonstrated the positive effect of CPR at reduced core temperature (27°C) to maintain organ perfusion, but also demonstrated the need for ECMO rewarming as thoracic lavage failed to establish a perfusing rhythm during rewarming. The work by Mohyuddin et al. demonstrated two facts; the hemodynamic stability of an intact experimental model with spontaneous circulation to undergo cooling and rewarming, as well as the positive effects of the adrenergic agent epinephrine, to support cardiovascular function during hypothermia. This work may also underline the clinically recognized differences in survival between patients with cardiac arrest vs. maintained spontaneous circulation. When rewarming patients with maintained spontaneous circulation they regularly have an increase in total vascular resistance. In addition, they may suffer from may suffer from a varying degree of cardiac failure. This calls for immediate pharmacologic interventions for circulatory support, but a lack of consensus of pharmacologic strategy in hypothermic patients exists. In principle, pharmacologic interventions during acute cardiac failure contain two elements: vasodilation or myocardial support, or their combination. We saw that the cardiac supportive effects of epinephrine were also maintained at low temperatures, but the pharmacologic effects of vasodilating substances during hypothermia are so far not well-described. The work by Lund Selli et al. shows that the vasodilator effects of the phosphodiesterase 5 (PDE5) inhibitor, sildenafil, to inhibit the elimination of cGMP, to maintains vascular smooth muscle activity (vasodilation), is maintained during *in vitro* cooling to 20°C.

Cold-water divers also experience hypothermia, and those who are cold during the ascent from diving may be at increased risk of decompression sickness (DCS). DCS is a multifaceted disease with a wide range of symptoms and contributors. Gaustad et al. used a temperaturecontrolled rodent model to target effects of a 2°C drop in core temperature during decompression on post-dive vascular bubble formation and hemodynamic function. They found no changes in bubble formation to substantiate increased DCS risk. However, cardiac output and stroke volume fell after the dive, possibly because of reduced left ventricular preload secondary to increased pulmonary resistance. Other have found reduced cardiac output to be associated with increased muscular sympathetic nerve activity, but as there was no post-dive increase in total peripheral vascular resistance in Gaustad's study this explanation appears less likely. Whether the observed outcome was triggered by undetected bubbles remains to be explored. Rodents are also useful preclinical models for pharmacological interventions aimed at alleviating injury to divers. Zhou et al. reported a favorable outcome of normobaric oxygen (NBO) in combination with inhibition of mitogenactivated protein kinase MEK1/2 on DCS in rats with spinal cord injury. They found that the combination resulted in lower incidence of DCS compared to that of animals treated with NBO or MAK1/2 inhibitor alone, and propose that the effect is attributable to increased expression of heat shock protein HSP32.

As useful as animal models are for understanding of physiology and pathology, clinical medicine still depends on studies of human subjects. But controlled prospective studies of human maladaptation are difficult. Provoking potentially life-threatening disease in healthy subjects is for obvious reasons not possible, and the variety in symptoms and severity associated with DCS complicates the Research Topic. Magri et al. overcame this in a study of immune and inflammatory changes in divers with DCS. The detailed insight of the molecular ethiology of DCS provides possible starting points for the search for biomarkers and drugable targets for prevention and improved treatment.

Saturation diving is an extreme occupation where individuals are exposed to a high-pressure hyperoxic environment for prolonged periods. Individuals must adapt to physiological stress to maintain health and physiological function. Monnoyer et al. demonstrated that a 4-weeks in this environment during a commercial saturation dive at 200 m resulted in transient alterations to the oral microbiome. This oral microbiome offers some fascinating insight into both oral and systemic health and disease states, with imbalances in the oral microbial

ecosystem may manifest in disturbances to health. This investigation found transient changes in oral bacterial diversity and abundance following decompression. These changes were maintained throughout the bottom phase of the dive and appeared to return to pre-dive levels on return to the surface. This attenuation of anaerobic activity during the bottom phase may contribute to a saturation diver's health outcome. Several factors determine the health and wellbeing during a saturation. An area of notable interest is the role of the diet. Deb et al. present the first analysis of energy expenditure during a commercial saturation dive. Several interesting observations were presented, which may have significant practical implications. It was evident that divers were in a substantial negative energy balance during the 10-day measurement period, with overall energy expenditure being positively correlated with the time spent working underwater. It is apparent that there is an intrinsic link between diet, occupational work and the environmental exposure of saturation diving. These investigations provide insight into the adaptive physiological responses to commercial saturation diving and present interesting avenues to improve the health and wellbeing of occupational divers.

Taken together, studies in this Research Topic present consequences of exposure to extreme environments, and potentional effects of adaptational interventions. This new information on the consequences may support the development of updated guidelines intended to improve safety and survival.

AUTHOR CONTRIBUTIONS

All authors listed have made a substantial, direct, and intellectual contribution to the work and approved it for publication.

Conflict of Interest: The authors declare that the research was conducted in the absence of any commercial or financial relationships that could be construed as a potential conflict of interest.

Publisher's Note: All claims expressed in this article are solely those of the authors and do not necessarily represent those of their affiliated organizations, or those of the publisher, the editors and the reviewers. Any product that may be evaluated in this article, or claim that may be made by its manufacturer, is not guaranteed or endorsed by the publisher.

frontiers in Physiology

ORIGINAL RESEARCH
published: 27 April 2021
doi: 10.3389/fphys.2021.669355

Shifts in the Oral Microbiota During a Four-Week Commercial Saturation Dive to 200 Meters

Roxane Monnoyer[1], Kjersti Haugum[2,3], Jacky Lautridou[1], Arnar Flatberg[2], Astrid Hjelde[1] and Ingrid Eftedal[1,4]*

[1]Department of Circulation and Medical Imaging, Faculty of Medicine and Health Sciences, NTNU Norwegian University of Science and Technology, Trondheim, Norway, [2]Department of Clinical and Molecular Medicine, Faculty of Medicine and Health Sciences, NTNU Norwegian University of Science and Technology, Trondheim, Norway, [3]Department of Medical Microbiology, Clinic of Laboratory Medicine, St. Olavs Hospital, Trondheim University Hospital, Trondheim, Norway, [4]Faculty of Nursing and Health Sciences, Nord University, Bodø, Norway

During commercial saturation diving, divers live and work under hyperbaric and hyperoxic conditions. The myriads of bacteria that live in and on the human body must adjust to the resultant hyperbaric stress. In this study, we examined the shifts in bacterial content in the oral cavity of saturation divers, using a metagenomic approach to determine the diversity in the composition of bacterial phyla and genera in saliva from 23 male divers before, during, and immediately after 4 weeks of commercial heliox saturation diving to a working depth of circa 200 m. We found that the bacterial diversity fell during saturation, and there was a change in bacterial composition; with a decrease at the phylum level of obligate anaerobe *Fusobacteria*, and an increase of the relative abundance of *Actinobacteria* and *Proteobacteria*. At the genus level, *Fusobacterium*, *Leptotrichia*, *Oribacterium*, and *Veillonella* decreased, whereas *Neisseria* and *Rothia* increased. However, at the end of the decompression, both the diversity and composition of the microbiota returned to pre-dive values. The results indicate that the hyperoxic conditions during saturation may suppress the activity of anaerobes, leaving a niche for other bacteria to fill. The transient nature of the change could imply that hyperbaric heliox saturation has no lasting effect on the oral microbiota, but it is unknown whether or how a shift in oral bacterial diversity and abundance during saturation might impact the divers' health or well-being.

Keywords: acclimatization, decompression, heliox saturation, microbiome, metagenomic, bacterial phyla, bacterial genera

OPEN ACCESS

Edited by:
Jorge G. Farias,
University of La Frontera, Chile

Reviewed by:
Jean-Pol Frippiat,
Université de Lorraine, France
Alessandro Marroni,
DAN Europe Foundation, Malta

****Correspondence:***
Roxane Monnoyer
roxane.monnoyer@ntnu.no

Specialty section:
This article was submitted to Environmental, Aviation and Space Physiology, a section of the journal Frontiers in Physiology

Received: *18 February 2021*
Accepted: *06 April 2021*
Published: *27 April 2021*

Citation:
Monnoyer R, Haugum K, Lautridou J, Flatberg A, Hjelde A and Eftedal I (2021) Shifts in the Oral Microbiota During a Four-Week Commercial Saturation Dive to 200 Meters. Front. Physiol. 12:669355. doi: 10.3389/fphys.2021.669355

INTRODUCTION

Commercial saturation diving is used to perform long-term subsea work at greater depths. During saturation diving operations, the divers live within a pressurized, hyperbaric chamber system in a heliox atmosphere (a mix of oxygen and helium) for longer periods, normally limited to 28 days (DMAC, 2006). The divers commute to work from the hyperbaric chamber system to the sea bottom in a diving bell. Although saturation diving is generally considered safe, the environmental conditions encountered by the divers are still a matter of health concern (Brubakk et al., 2014). Preserving health in harsh environments requires successful

acclimation of the body's physiological mechanisms. In this respect, the multiple microorganisms living in or on the body are also involved; i.e., the various microbiota that constitutes the human microbiome. Since the first appearance of the term microbiota in 2001 (Lederberg and McCray, 2001) and the recent development of metagenomics study tools, a large number of studies have emerged emphasizing the dual role of microorganisms inhabiting the human body in health protection as well as the development of diseases (Scannapieco, 2013; Wade, 2013; Yamashita and Takeshita, 2017; Sharma et al., 2018; Zheng et al., 2020). They interact with the host's immune system and affect central metabolic processes (Chu and Mazmanian, 2013; Belkaid and Hand, 2014).

Divers are exposed to several stress factors during hyperbaric saturation (Bosco et al., 2018), which may also affect the composition and activity of the microbial communities. Bacteria residing in the divers' oral cavity, the oral microbiota, come directly into contact with the hyperbaric breathing gases. It has been proposed that oral bacteria contribute to their host's health and fitness beyond the oral cavity. For instance, they may be involved in the control of cardiovascular function by nitric oxide (NO) *via* their essential function in the regulation of nitrate (NO_3^-) production (Hyde et al., 2014; Cutler et al., 2019), and are thought to play a role in autoimmune disease susceptibility (Nikitakis et al., 2017). The effects of hyperbaric heliox saturation on the human oral microbiome have yet to be determined.

This study was designed to examine the effects of commercial saturation diving on the bacterial content of the oral microbiota. A metagenomic approach was used to determine the composition of bacterial phyla and genera in divers' saliva before, during, and immediately after 4 weeks of commercial heliox saturation diving.

MATERIALS AND METHODS

Ethics

The study was conducted during a commercial saturation diving operation in the Mediterranean Sea, March–April 2018. The protocol was approved in advance by the Norwegian Regional Committee for Medical and Health Research Ethics (REK), approval number 2018/1184. Divers who passed the pre-saturation medical examination and were committed to saturation onboard the Dive Support Vessel (DSV) Deep Arctic were eligible for participation. They were informed of the aim and scope of the study and provided written consent before inclusion. The experimental procedures were conducted according to the Declaration of Helsinki principles for ethical human experimentation.

Study Subjects

Initially, 30 certified saturation divers, all male non-smokers, were enrolled in the study for the duration of a 28-day work assignment in hyperbaric heliox saturation. All held valid health certificates for work in saturation and fulfilled the operator's requirement for aerobic fitness with maximum oxygen uptake capacity $VO_{2max} \geq 40$ L/min. **Table 1** describes the study subject characteristics prior to saturation. The study did not interfere with the divers' lifestyle, whether diet, activity outside of operational requirements, nor the use of dentifrice. In the final analysis, we included only divers from whom four sets of saliva samples were successfully obtained, resulting in data from 23 of the 30 divers.

TABLE 1 | Study subject characteristics prior to saturation (n = 23).

	Mean	Range
Age (years)	44	31–60
BMI (kg/m^2)	26.8	20.2–31.2
VO_2 max (L/min)	48	44–60

BMI, body mass index; VO_2 max, maximum oxygen uptake capacity.

Saturation Diving

Saturation diving was performed according to the contractor's procedures as previously described (Łuczyński et al., 2019). In summary, the divers were compressed in a heliox atmosphere over a period of about 6 h to a storage depth of 178–192 meters of seawater (msw). They remained at storage depth throughout the bottom phase for 21 days, during which time they performed daily shifts of underwater work in teams of three at depths of 191–207 msw. Each shift lasts 12 h, 7 days per week. A dive bell was used to transport the divers between the pressure chamber and the underwater work site. When the bottom phase was completed, the divers were decompressed back to atmospheric pressure over a period of 8 days.

During the bottom phase, the partial pressure of oxygen (ppO_2) was kept at 40 kPa in the pressure chamber and 60–80 kPa during the bell-runs. During decompression, the ppO_2 was increased to 50 kPa until a depth of 13 msw was reached, and from there on ppO_2 was gradually reduced to 21%. After reaching the surface, the divers stayed on the vessel for another 24 h for observation for decompression sickness, before they left the vessel. The saturation profile is shown in **Figure 1**.

Saliva Collection

Saliva samples were collected at four time-points for each diver, as shown in **Figure 1**. D0 is at surface before saturation, D2 and D5 are on days 2 and 5 during bottom phase, and D28 is the day decompression was completed and the divers were back to surface. The divers themselves collected the saliva and were instructed not to brush their teeth before sampling. All sampling was undertaken ≥2 h after the last meal and collected in an all-in-one kit for stabilization of microbial nucleic acids (OMNIgene ORAL OM-505, DNA Genotek, Ottawa, Canada). Samples obtained on days 2 and 5, while the divers were pressurized, were decompressed back to surface pressure through an airlock shortly after collection. During the collection period, samples were stored in a fridge in the vessel hospital. At the end of the operation, all samples were transported collectively to the Norwegian University of Science and Technology (NTNU) for analysis. The bottom phase time-points for sample collection were chosen based on earlier reports on hematology in saturation

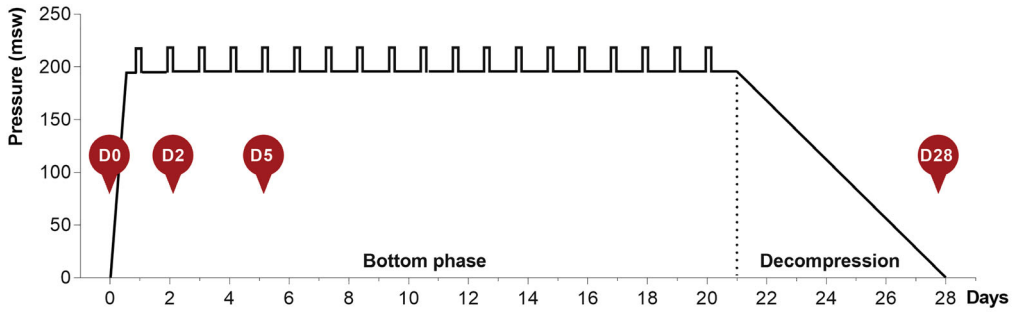

FIGURE 1 | The 28-day heliox saturation profile. Hyperbaric saturation was done in a heliox atmosphere with 6 h compression, 21-day bottom phase, and 7-day decompression. Daily underwater work excursions (bell-runs) in the bottom phase are indicated by vertical bars. Saliva collection time-points are shown as red circles: D0, before saturation; D2 and D5, days 2 and 5 of the bottom phase; D28, after decompression.

diving, and are in agreement with recent data on mice lung and gut microbiota in response to hyperoxia (Hofso et al., 2005; Ashley et al., 2020). At the time of sample collection, the divers had already performed at least on round of heliox saturation during the same diving campaign. The baseline (day 0) samples, therefore, also represent the status of the diver's microbiota 4–6 weeks after a similar exposure.

16S Library Preparation for Metagenome Sequencing

16S metagenomic sequencing libraries were prepared according to the QIAseq 16S Region Panel protocol (Qiagen, Hilden, Germany). In brief, 4 nanograms (ng) of genomic DNA extracted from the saliva samples (n = 92) were used as a template for PCR of the 16S V2–V3 and V4–V5 regions, in separate reactions using Illumina primers/reagents. The resulting 16S amplicons were purified using AMPure XP beads (Beckman Coulter, Inc., Indianapolis, IN, United States). Purified PCR products from each sample were pooled and thereafter subjected to a second PCR amplification step, where dual samples indices and Illumina sequencing adaptors were added, according to the manufacturer's instructions. A second PCR clean-up step was performed using AMPure XP beads (Beckman Coulter, Inc., Indianapolis, IN, United States), before the validation of the sequencing library using an Agilent High Sensitivity DNA Kit on a BioAnalyzer (Agilent Technologies, Santa Clara, CA, United States). Individual sample libraries were pooled and normalized to 10 pM, prior to sequencing of 2 × 300 cycles with a MiSeq V3 flowcell on a MiSeq instrument, according to the manufacturer's instructions (Illumina, Inc. San Diego, CA, United States). Sequence reads were demultiplexed and converted from BCL to fastq file format using bcl2fastq2 conversion software V2.20.0422 (Illumina, Inc. San Diego, CA, United States).

Bioinformatics

The sequencing data were merged and analyzed using the Quantitative Insights Into Microbial Ecology (QIIME2, version 2019.10) pipeline (Caporaso et al., 2010). All following procedures in this section were conducted in the QIIME2 environment using QIIME2 plugins. Demultiplexed paired-end reads from MiSeq (2 × 300 bp) were trimmed to remove primers and poor quality bases with fastp (version 0.20.0; Chen et al., 2018). The trimmed sequences were denoised and clustered with DADA2 (Callahan et al., 2016). The generated amplicon sequence variants (ASVs) were assigned to taxonomy using a targeted classifier. Briefly, we extracted sequences from the SILVA database (version 132) at a similarity threshold of 99% with locus-specific sequences from V2–V3 and V4–V5 QIAseq 16S primers and a targeted Naive Bayes trained on the extracted sequences. The QIIME2 phylogeny plugin was applied to construct the rooted phylogenetic tree by employing the FastTree program (Price et al., 2009). Based on the taxonomy generated, we filtered our feature-table to include only assigned reads of the taxonomic kingdom Bacteria and exclude reads assigned to mitochondria or chloroplasts. The generated BIOM file and phylogenetic trees were further imported into Phyloseq for comparison and visualization (McMurdie and Holmes, 2013).

Statistical Analysis

To estimate the diversity of the oral microbiota within individuals, i.e., the richness and evenness of the bacterial community (Kim et al., 2017), different indexes of the alpha diversity within samples such as the Shannon index were calculated by the function estimate_richness and the beta diversity between samples was calculated on a Bray-Curtis distance measure by the function ordinate using the Phyloseq package on R studio. Significance between groups in the PCoA subspace of the first two components was estimated by permuted Anova (permANOVA) from the vegan package. Statistical analysis on the Shannon index and the relative abundance at the phylum and genus level was done in IBM SPSS Statistics software Version 26.0. Normal distribution of the data was confirmed by visual inspection of Q-Q plots and Shapiro-Wilk's test for normality ($p > 0.05$), either directly or after the data were transformed. If the data were still non-normal after transformation, a non-parametric analysis was applied. A one-way repeated measures ANOVA, with Bonferroni *post hoc* adjustment for multiple comparisons, was used to assess within diver differences in Shannon index and relative abundance of phyla and genera between the four time-points. Differences were considered significant at $p < 0.05$. If the

assumption of sphericity was violated, as assessed by Mauchly's test which assumes homogeneity for $p > 0.05$, a Greenhouse-Geisser correction was applied. In the case of non-normal data, Friedman's test was applied and pairwise comparisons were performed with a Bonferroni correction for multiple comparisons.

Data Repository

The data for this study have been deposited in the European Nucleotide Archive (ENA) at EMBL-EBI under accession number PRJEB40804.[1]

RESULTS

Ten different bacterial phyla were detected by taxonomic analysis of the 16S rRNA sequencing data from saliva collected from 23 divers before, during, and at the end of 4 weeks of commercial heliox saturation diving. The analysis of alpha diversity within samples, i.e. species richness and evenness using the Shannon index, showed a significant drop during the bottom phase (4.028 ± 0.47 for day 2, and 4.089 ± 0.48 for day 5, $p < 0.001$), compared to the baseline (day 0; 4.398 ± 0.33). However, the alpha diversity returned to baseline after the decompression (**Figure 2A**). The beta diversity is shown in **Figure 2B**.

Taken altogether, the total abundance of the 10 detected phyla did not significantly change during heliox saturation (**Figure 3**).

In general, five phyla were dominant in all the samples: *Firmicutes* (34%), *Proteobacteria* (27%), *Bacteroidetes* (17%), *Actinobacteria* (11%), and *Fusobacteria* (9%). Five other phyla were detected at lower levels (<1%), including *Patescibacteria*, *Epsilonbacteræota*, *Tenericutes*, *Spirochaetes*, and *Synergistetes*. Moving down the taxonomic tree, the most abundant significantly altered genera belonged to the phyla *Firmicutes* (genus *Veillonella* and *Oribacterium*), *Proteobacteria* (genus *Neisseria*), *Actinobacteria* (genus *Rothia* and *Actinomyces*), and *Fusobacteria* (genus *Fusobacterium* and *Leptotrichia*) (**Figure 4**).

The relative abundance of *Firmicutes*, *Fusobacteria*, and *Bacteroidetes* decreased during the first 5 days of the bottom phase, but only significantly so for *Fusobacteria*. Within the phylum *Firmicutes*, one of the dominant genera, *Veillonella*, decreased at day 2 ($p = 0.047$) and day 5 ($p = 0.004$), as well as the genus *Oribacterium*, that also decreased but only at day 2 of the bottom phase ($p = 0.040$; **Figure 4A**). In the phylum *Fusobacteria*, decreases in abundance were observed for the genus *Fusobacterium* at day 2 ($p < 0.0005$) and day 5 ($p = 0.027$), and in genus *Leptotrichia* at day 2 ($p = 0.0022$). We also observed a decrease in the genus *Prevotella* from *Bacteroidetes* but non-significant (**Figures 4B,C**). Conversely, during the bottom phase, at day 2, the abundance of *Actinobacteria* and *Proteobacteria* increased. In these phyla, genus *Rothia* (*Actinobacteria*) increased at day 2 ($p = 0.009$; **Figure 4D**), while genus *Neisseria* (*Proteobacteria*) increased at day 2 ($p = 0.010$) and day 5 ($p = 0.022$; **Figure 4E**). However, all changes observed during the bottom phase were abolished at the end of the dive.

DISCUSSION

In this study, we surveyed the oral bacterial microbiota of divers during 4 weeks of commercial heliox saturation diving. Using a taxonomic analysis through 16S rRNA sequencing, we identified 10 abundant bacterial phyla in saliva collected before, during, and immediately after saturation, and this composition is coherent with other studies that describe the human oral microbiota (Palmer Jr., 2014). We found that the microbial diversity was reduced during saturation and that the relative abundance of *Proteobacteria*, *Actinobacteria*, and *Fusobacteria* changed significantly. In each phylum, these changes were mostly due to their most abundant genera, including a shift from obligate anaerobes (*Fusobacterium*, *Leptotrichia*, *Veillonella*, and *Oribacterium*) to aerobic/facultative anaerobic bacteria (*Neisseria* and *Rothia*). To our knowledge, this is the first study to address the relationship between hyperbaric environments and oral microbiota.

In our study, we observed that the alpha diversity of the oral microbiota was reduced during hyperbaric heliox saturation, indicating that either the richness and/or evenness of the microbial communities changed. The relative abundance of *Fusobacteria* decreased during saturation, whereas *Proteobacteria* and *Actinobacteria* increased. The most probable explanation is that the evenness of the oral microbiota was impacted by the drop of *Fusobacteria* during the bottom phase together with the raise of *Proteobacteria* abundance, in particular the *Neisseria* genus – of which this phylum alone made up more than 30% of the total abundance during the bottom phase. Furthermore, the absence of change in the total abundance during saturation (**Figure 2B**) indicates that the environmental conditions inherent to the dive merely created a shift in the microbial balance between the different genera and therefore phyla. In apparent contrast with our results, a recent study on commercial saturation divers' gut microbiota reported no change in alpha diversity, but a decreased abundance of the genus *Bifidobacterium*, which are in fact *Actinobacteria* (Yuan et al., 2019).

This discrepancy may be explained by the fact that the oral microbiome is directly in contact with the breathing mixture during the dive and thus is more reactive to the steep changes in pressure and oxygen availability. Oral bacteria can be classified according to their oxygen needs and their ability to metabolize it in different environments regarding each site of the mouth from tooth surfaces to supragingival and subgingival regions. Obligate aerobes are found to grow optimally at atmospheric concentrations of oxygen (~20%), whereas microaerophiles prosper best well-below normal atmospheric concentrations. Unlike obligate anaerobes that cannot tolerate oxygen and thrive only under anoxic conditions; facultative anaerobes can grow by fermentation, use other terminal electron acceptors for anaerobic respiration, or their ability to breathe aerobically. Aerotolerant anaerobes as the name suggests can tolerate the

[1]https://www.ebi.ac.uk/ena/browser/view/PRJEB40804

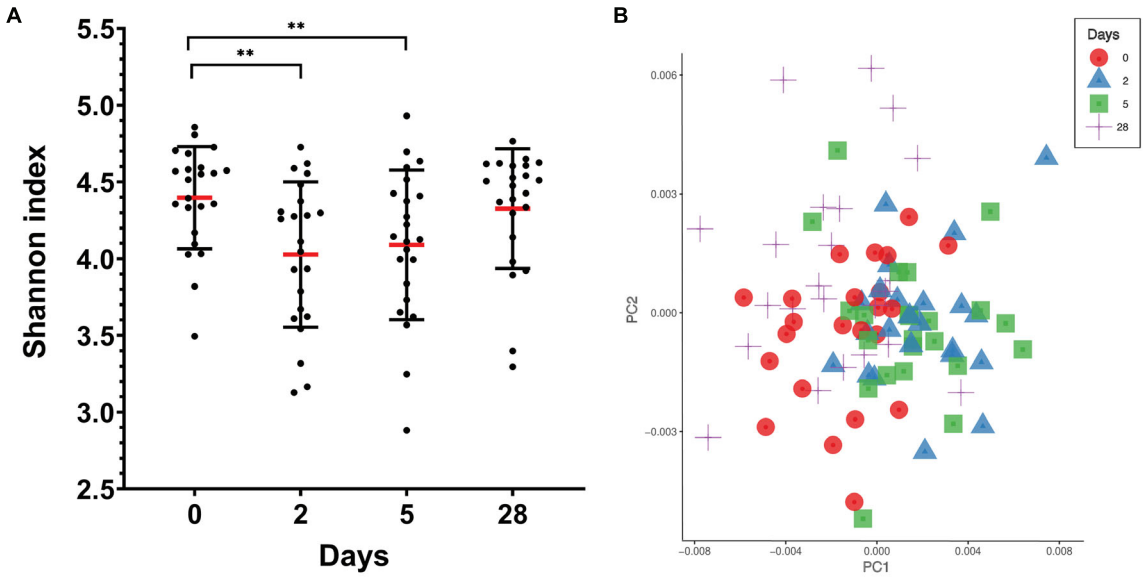

FIGURE 2 | Oral microbiota diversity in saliva from commercial saturation divers (n = 23) before, during, and after 28 days of heliox saturation. **(A)** The alpha diversity within samples, i.e., species richness and evenness, is given by the Shannon index (**p < 0.001). Means (red line) and individual values are shown. Error bars are ±1 SD. **(B)** Principal coordinate analysis (PCoA) plot of beta-diversity for individual samples showing the first two principal components (PC1 and PC2) using Bray-Curtis distances (p = 0.001 using permANOVA). Colored symbols indicate times of sample collection. In both panels, day 0, before saturation; days 2 and 5, during the bottom phase; day 28, after decompression.

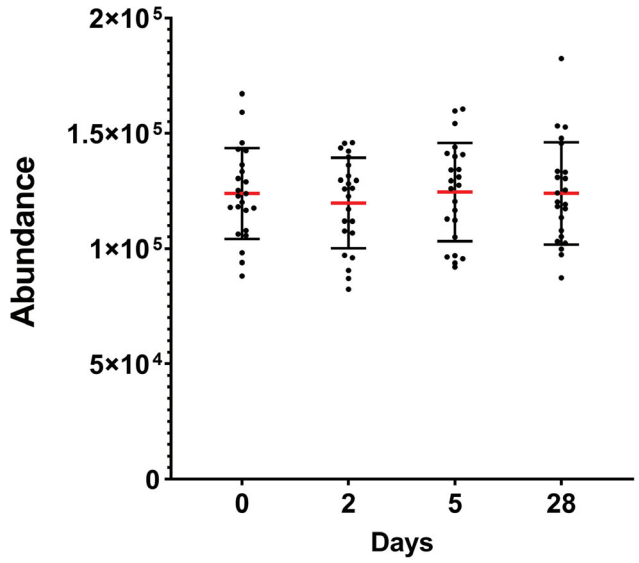

FIGURE 3 | Total abundance of the oral bacterial communities in saliva from commercial saturation divers (n = 23) before, during, and after 28 days of heliox saturation, displayed as the number of reads for all detected OTU after 16S sequencing. For each time-point, means (red line) and individual values are shown. Error bars are ±1 SD. Day 0, before saturation; days 2 and 5, during the bottom phase; day 28, after decompression.

presence of oxygen, but do not benefit from aerobic respiration and thrive optimally without oxygen (Morris and Schmidt, 2013). Many facultative anaerobes rapidly become anaerobic as the oral biofilm develops, which explains the predominance of obligate anaerobic bacteria in the mouth (Wade, 2013).

Hyperbaric hyperoxia in the divers' breathing gas is a likely contributing factor to the bacterial shift we observed. It has been noted that hyperoxia gave a selective relative growth advantage to oxygen-tolerant respiratory microbial species (e.g., *Staphylococcus aureus*) in patients with respiratory failure who received high concentrations of therapeutic oxygen. In parallel, using neonatal and adult mouse models, the same authors demonstrated that lung and gut bacterial communities were altered within 24 and 72 h, respectively, in mice exposed to hyperoxia (Ashley et al., 2020). To overcome the toxic effects of oxygen, both aerobic and facultative anaerobic organisms contain a highly regulated complex of antioxidant defense enzymes such as catalase or superoxide dismutase as well as other enzymatic and non-enzymatic defense mechanisms against the toxic effects of reactive oxygen species (ROS; Brioukhanov and Netrusov, 2007; Henry et al., 2014). These have been particularly well-described in the two pathogens in the species *Neisseria* (*Neisseria gonorrhoeae* and *Neisseria meningitidis*), when even within the same genus, Neisserial species appeared to have different contents of antioxidant enzymes (Archibald and Duong, 1986; Seib et al., 2004, 2006). Our divers were exposed to hyperoxia during the bottom phase, with ppO_2 of 40 kPa in the pressurized living chambers and up to 60–80 kPa during the bell-run excursions, which is double to triple the amount of oxygen in normobaric air.

An increase in oxygen availability has been reported to induce gut dysbiosis, thus driving an uncontrolled luminal expansion of the family *Enterobacteriaceae*, which are facultative anaerobic (Rivera-Chavez et al., 2017). Nevertheless, it is difficult to draw comparisons between the oral and the gut microbiome in relation to the normoxic and hyperoxic conditions because

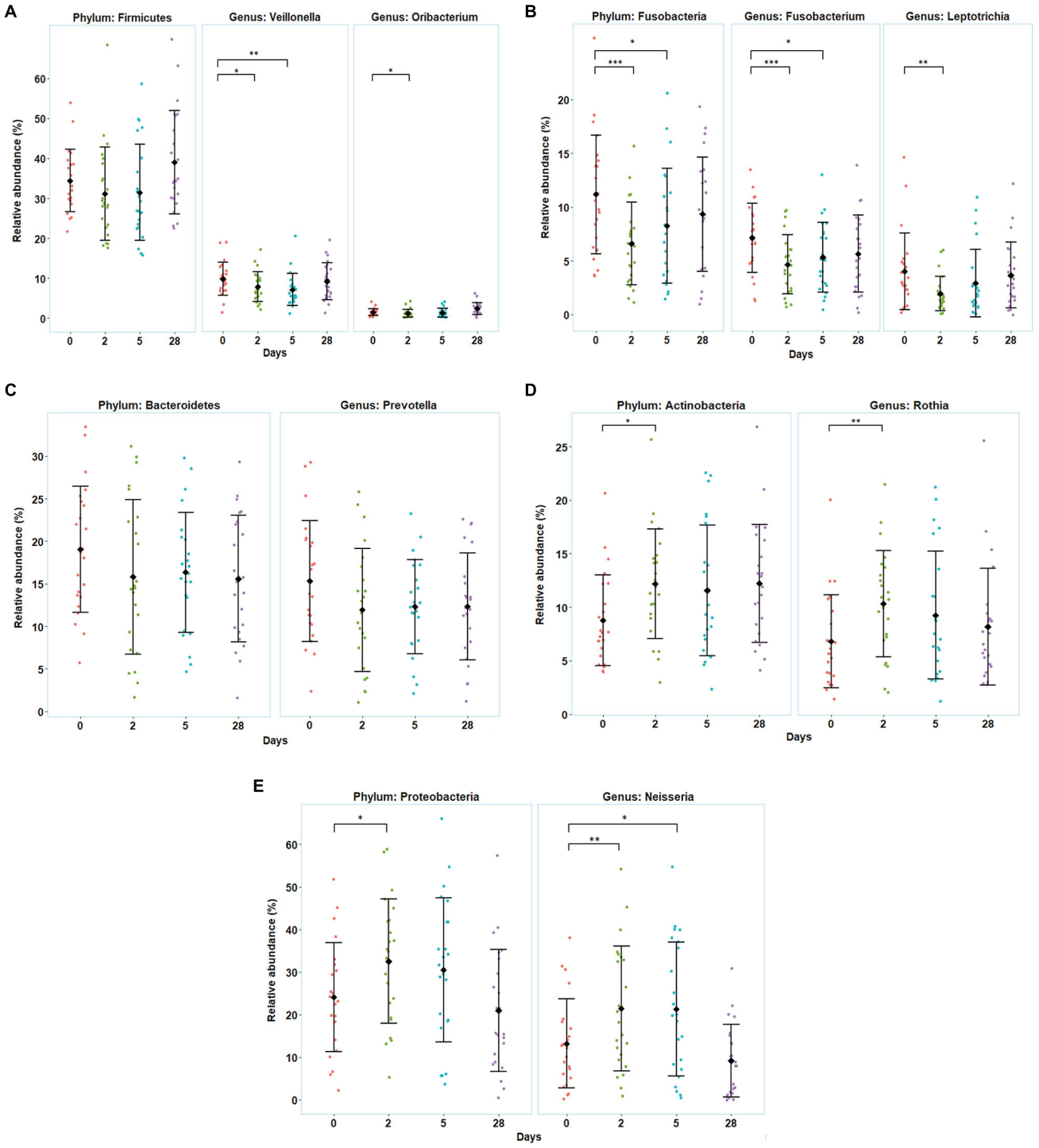

FIGURE 4 | Variation in the divers' oral microbiota before (day 0), during the bottom phase (days 2 and 5), and after decompression (day 28) from heliox saturation diving. **(A–E)** Observed shifts in the relative abundance of the five most abundant bacterial phyla, along with their significantly altered genera. For each time-point: mean (♦) and individual values are shown. Error bars are ±1 SD (*$p \leq 0.05$; **$p \leq 0.01$; and ***$p \leq 0.001$). The relative abundance is given in percentage of total bacterial sequences.

the gut microbiome is usually more stable than the oral microbiome in terms of environmental conditions. However, we can compare the gut microbiome and the neonatal gut microbiome. The latter being more abundant in oxygen, it is frequently dominated by facultative anaerobes such as *Proteobacteria* species (Guaraldi and Salvatori, 2012). By consuming the oxygen in the 1st week of life, these facultative anaerobes create a more suitable environment for obligate

anaerobes such as *Fusobacteria* (Kelly et al., 2018). The hyperoxic conditions experienced by the divers during the bottom phase may thus be inadequate for *Fusobacteria*, which might in turn leave space for *Proteobacteria*.

The gut microbiota also seems to be related to the host response to hypobaric hypoxia exposure associated with increased inflammation and risk of infection (Hartmann et al., 2000; Khanna et al., 2018). High altitude tends to be positively correlated with obligate anaerobes (Maity et al., 2013; Suzuki et al., 2019) and is associated to relative abundance of *Prevotella* (Karl et al., 2018). It has recently been described that intermittent hypoxia can induce alterations in the gut microbiota (Moreno-Indias et al., 2015; Ramos-Romero et al., 2020). Together, these results suggest that obligate anaerobes may have a competitive advantage under hypoxic conditions over aerobes that require oxygen.

What might the consequences be of a shift in diversity and abundance of bacteria during saturation diving? Most studies on the oral microbiome established associations between oral health conditions and the bacterial composition in saliva. Indeed, healthy periodontal conditions were mainly related to the genus *Neisseria*, while the predominance of the genera *Prevotella* and *Veillonella* was associated with periodontal diseases (Yamashita and Takeshita, 2017). In addition, many studies also associate the gut microbiome to human health. A raise of *Proteobacteria* abundance in the gut microbiome has been linked to pathologies such as obesity (Zhu et al., 2013) and Type 2 diabetes (Larsen et al., 2010; Zhang et al., 2013). *Proteobacteria* also appear to be associated with extraintestinal diseases such as asthma and chronic obstructive pulmonary disease (COPD), making it a common microbial signature of states linked to various degrees with inflammation (Rizzatti et al., 2017). However, it is still unclear whether a transient bacterial shift from *Fusobacteria* to *Proteobacteria* in the oral microbiota may have an impact on the divers' health. Additional studies should be conducted to investigate the bacterial metabolic pathways altered during saturation diving.

LIMITATIONS

This study imposed no restrictions on the divers' routines or diet. Since they worked overlapping shifts over the 24-h day, the time for saliva collections varied accordingly. We can, therefore, not rule out possible effects of circadian variation which may have a functional impact on bacterial activity (Takayasu et al., 2017). The divers were also free to choose individually from daily selections of meals from the vessel galley. A modest association between diet and oral microbiota has been reported (Kato et al., 2017). However, these limitations are not expected to cause false-positive results.

CONCLUSION

We identified changes in the abundance of three bacterial phyla in the oral microbiota during commercial heliox saturation diving: *Fusobacteria* decreased, whereas *Proteobacteria* and *Actinobacteria* increased during the bottom phase. At the genus level, there was a decrease in the relative abundance of *Fusobacterium*, *Leptotrichia*, *Oribacterium*, and *Veillonella*, and an increase of *Neisseria* and *Rothia*. However, no changes persisted at the end of the decompression. The transient nature of the change could imply that hyperbaric heliox saturation has no lasting effect on the oral microbiota, but it is unknown whether and how the bacterial shift during saturation may impact the divers' health or well-being.

DATA AVAILABILITY STATEMENT

The datasets presented in this study can be found in online repositories. The names of the repository/repositories and accession number(s) can be found at: https://www.ebi.ac.uk/ena/browser/view/PRJEB40804.

ETHICS STATEMENT

The studies involving human participants were reviewed and approved by Norwegian Regional Committee for Medical and Health Research Ethics (REK). The patients/participants provided their written informed consent to participate in this study.

AUTHOR CONTRIBUTIONS

RM, KH, and IE designed the study. IE collected the material. RM, JL, AH, and AF conducted the analyses. RM initiated the manuscript. All authors contributed in the writing and approval of the final version.

FUNDING

This study is part of a Knowledge-Building Projects for Industry, placed at NTNU, Norway and funded from the Norwegian Research Council's Large-scale Programme for Petroleum Research (PETROMAKS2), project no. 280425, *via* an integral part dedicated to research on Health, Safety, and Environment (HSE) in the petroleum sector.

ACKNOWLEDGMENTS

We gratefully acknowledge the contributions of the divers, captain, and crew on DSV Deep Arctic. Access to the 2018 Bahr Essalam diving campaign was granted by TechnipFMC and Mellitah Oil and Gas B.V. The 16S library prep, sequencing, and bioinformatics analysis were performed in close collaboration with the Genomics Core Facility (GCF), Norwegian University of Science and Technology (NTNU). GCF is funded by the Faculty of Medicine and Health Sciences at NTNU and Central Norway Regional Health Authority. Christina G Ås, St. Olav's University Hospital, aided in data repository submission.

REFERENCES

Archibald, F. S., and Duong, M. N. (1986). Superoxide dismutase and oxygen toxicity defenses in the genus *Neisseria*. *Infect. Immun.* 51, 631–641. doi: 10.1128/IAI.51.2.631-641.1986

Ashley, S. L., Sjoding, M. W., Popova, A. P., Cui, T. X., Hoostal, M. J., Schmidt, T. M., et al. (2020). Lung and gut microbiota are altered by hyperoxia and contribute to oxygen-induced lung injury in mice. *Sci. Transl. Med.* 12:eaau9959. doi: 10.1126/scitranslmed.aau9959

Belkaid, Y., and Hand, T. W. (2014). Role of the microbiota in immunity and inflammation. *Cell* 157, 121–141. doi: 10.1016/j.cell.2014.03.011

Bosco, G., Rizzato, A., Moon, R. E., and Camporesi, E. M. (2018). Environmental physiology and diving medicine. *Front. Psychol.* 9:72. doi: 10.3389/fpsyg.2018.00072

Brioukhanov, A. L., and Netrusov, A. I. (2007). Aerotolerance of strictly anaerobic microorganisms and factors of defense against oxidative stress: a review. *Appl. Biochem. Microbiol.* 43, 567–582. doi: 10.1134/S0003683807060014

Brubakk, A. O., Ross, J. A., and Thom, S. R. (2014). Saturation diving; physiology and pathophysiology. *Compr. Physiol.* 4, 1229–1272. doi: 10.1002/cphy.c130048

Callahan, B. J., McMurdie, P. J., Rosen, M. J., Han, A. W., Johnson, A. J., and Holmes, S. P. (2016). DADA2: high-resolution sample inference from Illumina amplicon data. *Nat. Methods* 13, 581–583. doi: 10.1038/nmeth.3869

Caporaso, J. G., Kuczynski, J., Stombaugh, J., Bittinger, K., Bushman, F. D., Costello, E. K., et al. (2010). QIIME allows analysis of high-throughput community sequencing data. *Nat. Methods* 7, 335–336. doi: 10.1038/nmeth.f.303

Chen, S., Zhou, Y., Chen, Y., and Gu, J. (2018). Fastp: an ultra-fast all-in-one FASTQ preprocessor. *Bioinformatics* 34, i884–i890. doi: 10.1093/bioinformatics/bty560

Chu, H., and Mazmanian, S. K. (2013). Innate immune recognition of the microbiota promotes host-microbial symbiosis. *Nat. Immunol.* 14, 668–675. doi: 10.1038/ni.2635

Cutler, C., Kiernan, M., Willis, J. R., Gallardo-Alfaro, L., Casas-Agustench, P., White, D., et al. (2019). Post-exercise hypotension and skeletal muscle oxygenation is regulated by nitrate-reducing activity of oral bacteria. *Free Radic. Biol. Med.* 143, 252–259. doi: 10.1016/j.freeradbiomed.2019.07.035

DMAC (2006). The duration of saturation exposures and surface intervals following saturations. In DMAC 21. London, UK: DMAC.

Guaraldi, F., and Salvatori, G. (2012). Effect of breast and formula feeding on gut microbiota shaping in newborns. *Front. Cell. Infect. Microbiol.* 2:94. doi: 10.3389/fcimb.2012.00094

Hartmann, G., Tschöp, M., Fischer, R., Bidlingmaier, C., Riepl, R., Tschöp, K., et al. (2000). High altitude increases circulating interleukin-6, interleukin-1 receptor antagonist and C-reactive protein. *Cytokine* 12, 246–252. doi: 10.1006/cyto.1999.0533

Henry, L. G., Boutrin, M. C., Aruni, W., Robles, A., Ximinies, A., and Fletcher, H. M. (2014). Life in a diverse oral community—strategies for oxidative stress survival. *J. Oral Biosci.* 56, 63–71. doi: 10.1016/j.job.2014.03.001

Hofso, D., Ulvik, R. J., Segadal, K., Hope, A., and Thorsen, E. (2005). Changes in erythropoietin and haemoglobin concentrations in response to saturation diving. *Eur. J. Appl. Physiol.* 95, 191–196. doi: 10.1007/s00421-005-1381-9

Hyde, E. R., Andrade, F., Vaksman, Z., Parthasarathy, K., Jiang, H., Parthasarathy, D. K., et al. (2014). Metagenomic analysis of nitrate-reducing bacteria in the oral cavity: implications for nitric oxide homeostasis. *PLoS One* 9:e88645. doi: 10.1371/journal.pone.0088645

Karl, J. P., Berryman, C. E., Young, A. J., Radcliffe, P. N., Branck, T. A., Pantoja-Feliciano, I. G., et al. (2018). Associations between the gut microbiota and host responses to high altitude. *Am. J. Physiol. Gastrointest. Liver Physiol.* 315, G1003–G1015. doi: 10.1152/ajpgi.00253.2018

Kato, I., Vasquez, A., Moyerbrailean, G., Land, S., Djuric, Z., Sun, J., et al. (2017). Nutritional correlates of human oral microbiome. *J. Am. Coll. Nutr.* 36, 88–98. doi: 10.1080/07315724.2016.1185386

Kelly, D., Yang, L., and Pei, Z. (2018). Gut microbiota, fusobacteria, and colorectal cancer. *Diseases* 6:109. doi: 10.3390/diseases6040109

Khanna, K., Mishra, K. P., Ganju, L., Kumar, B., and Singh, S. B. (2018). High-altitude-induced alterations in gut-immune axis: a review. *Int. Rev. Immunol.* 37, 119–126. doi: 10.1080/08830185.2017.1407763

Kim, B. R., Shin, J., Guevarra, R., Lee, J. H., Kim, D. W., Seol, K. H., et al. (2017). Deciphering diversity indices for a better understanding of microbial communities. *J. Microbiol. Biotechnol.* 27, 2089–2093. doi: 10.4014/jmb.1709.09027

Larsen, N., Vogensen, F. K., van den Berg, F. W. J., Nielsen, D. S., Andreasen, A. S., Pedersen, B. K., et al. (2010). Gut microbiota in human adults with type 2 diabetes differs from non-diabetic adults. *PLoS One* 5:e9085. doi: 10.1371/journal.pone.0009085

Lederberg, J., and McCray, A. T. (2001). 'Ome sweet'omics—a genealogical treasury of words. *Scientist* 15:8.

Łuczyński, D., Lautridou, J., Hjelde, A., Monnoyer, R., and Eftedal, I. (2019). Hemoglobin during and following a 4-week commercial saturation dive to 200 m. *Front. Physiol.* 10:1494. doi: 10.3389/fphys.2019.01494

Maity, C., Lahiri, P., Adak, A., Ghosh, K., Pati, B. R., and Mondal, K. C. (2013). Hypobaric-hypoxia induces alteration in microbes and microbes-associated enzyme profile in rat colonic samples. *Biomed. Environ. Sci.* 26, 869–873. doi: 10.3967/bes2013.013

McMurdie, P. J., and Holmes, S. (2013). Phyloseq: an R package for reproducible interactive analysis and graphics of microbiome census data. *PLoS One* 8:e61217. doi: 10.1371/journal.pone.0061217

Moreno-Indias, I., Torres, M., Montserrat, J. M., Sanchez-Alcoholado, L., Cardona, F., Tinahones, F. J., et al. (2015). Intermittent hypoxia alters gut microbiota diversity in a mouse model of sleep apnoea. *Eur. Respir. J.* 45, 1055–1065. doi: 10.1183/09031936.00184314

Morris, R. L., and Schmidt, T. M. (2013). Shallow breathing: bacterial life at low O_2. *Nat. Rev. Microbiol.* 11, 205–212. doi: 10.1038/nrmicro2970

Nikitakis, N. G., Papaioannou, W., Sakkas, L. I., and Kousvelari, E. (2017). The autoimmunity-oral microbiome connection. *Oral Dis.* 23, 828–839. doi: 10.1111/odi.12589

Palmer, R. J. Jr. (2014). Composition and development of oral bacterial communities. *Periodontol.* 64, 20–39. doi: 10.1111/j.1600-0757.2012.00453.x

Price, M. N., Dehal, P. S., and Arkin, A. P. (2009). FastTree: computing large minimum evolution trees with profiles instead of a distance matrix. *Mol. Biol. Evol.* 26, 1641–1650. doi: 10.1093/molbev/msp077

Ramos-Romero, S., Santocildes, G., Pinol-Pinol, D., Roses, C., Pages, T., Hereu, M., et al. (2020). Implication of gut microbiota in the physiology of rats intermittently exposed to cold and hypobaric hypoxia. *PLoS One* 15:e0240686. doi: 10.1371/journal.pone.0240686

Rivera-Chavez, F., Lopez, C. A., and Baumler, A. J. (2017). Oxygen as a driver of gut dysbiosis. *Free Radic. Biol. Med.* 105, 93–101. doi: 10.1016/j.freeradbiomed.2016.09.022

Rizzatti, G., Lopetuso, L. R., Gibiino, G., Binda, C., and Gasbarrini, A. (2017). Proteobacteria: a common factor in human diseases. *Biomed. Res. Int.* 2017:9351507. doi: 10.1155/2017/9351507

Scannapieco, F. A. (2013). The oral microbiome: its role in health and in oral and systemic infections. *Clin. Microbiol. Newsl.* 35, 163–169. doi: 10.1016/j.clinmicnews.2013.09.003

Seib, K. L., Tseng, H. J., McEwan, A. G., Apicella, M. A., and Jennings, M. P. (2004). Defenses against oxidative stress in *Neisseria gonorrhoeae* and *Neisseria meningitidis*: distinctive systems for different lifestyles. *J. Infect. Dis.* 190, 136–147. doi: 10.1086/421299

Seib, K. L., Wu, H. J., Kidd, S. P., Apicella, M. A., Jennings, M. P., and McEwan, A. G. (2006). Defenses against oxidative stress in *Neisseria gonorrhoeae*: a system tailored for a challenging environment. *Microbiol. Mol. Biol. Rev.* 70, 344–361. doi: 10.1128/MMBR.00044-05

Sharma, N., Bhatia, S., Sodhi, A. S., and Batra, N. (2018). Oral microbiome and health. *AIMS Microbiol.* 4, 42–66. doi: 10.3934/microbiol.2018.1.42

Suzuki, T. A., Martins, F. M., and Nachman, M. W. (2019). Altitudinal variation of the gut microbiota in wild house mice. *Mol. Ecol.* 28, 2378–2390. doi: 10.1111/mec.14905

Takayasu, L., Suda, W., Takanashi, K., Iioka, E., Kurokawa, R., Shindo, C., et al. (2017). Circadian oscillations of microbial and functional composition in the human salivary microbiome. *DNA Res.* 24, 261–270. doi: 10.1093/dnares/dsx001

Wade, W. G. (2013). The oral microbiome in health and disease. *Pharmacol. Res.* 69, 137–143. doi: 10.1016/j.phrs.2012.11.006

Yamashita, Y., and Takeshita, T. (2017). The oral microbiome and human health. *J. Oral Sci.* 59, 201–206. doi: 10.2334/josnusd.16-0856

Yuan, Y., Zhao, G., Ji, H., Peng, B., Huang, Z., Jin, W., et al. (2019). Changes in the gut microbiota during and after commercial helium-oxygen saturation diving in China. *Occup. Environ. Med.* 76, 801–807. doi: 10.1136/oemed-2019-106031

Zhang, X., Shen, D., Fang, Z., Jie, Z., Qiu, X., Zhang, C., et al. (2013). Human gut microbiota changes reveal the progression of glucose intolerance. *PLoS One* 8:e71108. doi: 10.1371/journal.pone.0071108

Zheng, D., Liwinski, T., and Elinav, E. (2020). Interaction between microbiota and immunity in health and disease. *Cell Res.* 30, 492–506. doi: 10.1038/s41422-020-0332-7

Zhu, L., Baker, S. S., Gill, C., Liu, W., Alkhouri, R., Baker, R. D., et al. (2013). Characterization of gut microbiomes in nonalcoholic steatohepatitis (NASH) patients: a connection between endogenous alcohol and NASH. *Hepatology* 57, 601–609. doi: 10.1002/hep.26093

Conflict of Interest: TechnipFMC sponsored helicopter transfers and boarding on the DSV Deep Arctic for IE.

The remaining authors declare that the research was conducted in the absence of any commercial or financial relationships that could be construed as a potential conflict of interest.

frontiers in Physiology

BRIEF RESEARCH REPORT
published: 26 May 2021
doi: 10.3389/fphys.2021.687605

The Assessment of Daily Energy Expenditure of Commercial Saturation Divers Using Doubly Labelled Water

Sanjoy K. Deb[1,2], Eimear Dolan[3], Catherine Hambly[4], John R. Speakman[4,5], Olav Eftedal[6], Mohammed Gulrez Zariwala[1] and Ingrid Eftedal[2,7]*

[1] Centre for Nutraceuticals, School of Life Sciences, University of Westminster, London, United Kingdom, [2] Department of Circulation and Medical Imaging, Faculty of Medicine and Health Sciences, Norwegian University of Science and Technology, Trondheim, Norway, [3] Applied Physiology and Nutrition Research Group, University of São Paulo, São Paulo, Brazil, [4] Institute of Biological and Environmental Sciences, University of Aberdeen, Aberdeen, United Kingdom, [5] Centre of Excellence in Animal Evolution and Genetics, Chinese Academy of Sciences, Kunming, China, [6] Equinor ASA, Stavanger, Norway, [7] Faculty of Nursing and Health Sciences, Nord University, Bodø, Norway

OPEN ACCESS

Edited by:
Costantino Balestra, Haute École Bruxelles-Brabant (HE2B), Belgium

Reviewed by:
Jacek Kot, Medical University of Gdańsk, Poland
Pasquale Longobardi, Hyperbaric Center of Ravenna, Italy

***Correspondence:**
Sanjoy K. Deb
S.Deb@westminster.ac.uk

Specialty section:
This article was submitted to Environmental, Aviation and Space Physiology, a section of the journal Frontiers in Physiology

Received: *29 March 2021*
Accepted: *03 May 2021*
Published: *26 May 2021*

Citation:
Deb SK, Dolan E, Hambly C, Speakman JR, Eftedal O, Zariwala MG and Eftedal I (2021) The Assessment of Daily Energy Expenditure of Commercial Saturation Divers Using Doubly Labelled Water. Front. Physiol. 12:687605. doi: 10.3389/fphys.2021.687605

Commercial saturation divers are exposed to unique environmental conditions and are required to conduct work activity underwater. Consequently, divers' physiological status is shown to be perturbed and therefore, appropriate strategies and guidance are required to manage the stress and adaptive response. This study aimed to evaluate the daily energy expenditure (DEE) of commercial saturation divers during a 21-day diving operation in the North Sea. Ten saturation divers were recruited during a diving operation with a living depth of 72 metres seawater (msw) and a maximum working dive depth of 81 msw. Doubly labelled water (DLW) was used to calculate DEE during a 10-day measurement period. Energy intake was also recorded during this period by maintaining a dietary log. The mean DEE calculated was 3030.9 ± 513.0 kcal/day, which was significantly greater than the mean energy intake (1875.3 ± 487.4 kcal; $p = 0.005$). There was also a strong positive correction correlation between DEE and total time spent performing underwater work ($r = 0.7$, $p = 0.026$). The results suggested saturation divers were in a negative energy balance during the measurement period with an intraindividual variability in the energy cost present that may be influenced by time spent underwater.

Keywords: saturation diving, extreme environment, hyperbaric, energy expenditure, doubly labelled water

INTRODUCTION

Saturation diving is an extreme environmental occupation, with extended exposure to a confined, hyperbaric, hyperoxic environment to allow subsea activity for prolonged periods. The hyperbaric environment places unique demands on the human body that challenges the physiological, cognitive, and physical functions of professional saturation divers. These challenges may cause immunosuppression, reduce body mass, and alter the gut microbiome environment (Brubakk et al., 2014; Yuan et al., 2019). Although longitudinal studies to assess the chronic health-related

implications of saturation diving is sparse, purported long-term consequences include reduced musculoskeletal health and impaired cognition (Ross et al., 2007; Brubakk et al., 2014).

Given the potential health-related consequences of prolonged exposure to this environmental stressor, there is a clear need to develop strategies to support acclimatisation, adaptation, and management of physiological perturbations that these unique environmental conditions bring. Appropriate and targeted nutritional interventions represent some such potential mitigation approach and are believed to play a vital role in managing a saturation divers physiology, health and wellness (Deb et al., 2016). For example, oral antioxidant supplementation has been reported to reduce hepatic oxidative damage during saturation diving (Ikeda et al., 2004). Furthermore, commercial saturation diving results in changes to the gut microbiome by reducing Bifidobacterium and short-chain fatty acid (Yuan et al., 2019), both of which can also be modulated by nutritional intervention (Ojeda et al., 2016). Despite emerging research highlighting the importance of nutrition for saturation divers' health, there remains a gap in knowledge on this occupation's unique dietary needs (Deb et al., 2016).

Energy requirements are a fundamental component of dietary guidelines, as it provides a quantitative assessment of physiological and behavioural energy cost of an individual within their environment (Speakman, 1999). Commercial saturation divers self-reported their daily activity within the chamber's confinement to be low (Dolan et al., 2016), with the main activity (and therefore activity-related energy expenditure) occurring during underwater excursions. This underwater activity's energy requirements are unknown; although, reports suggest that this can vary between diving operations depending on the tasks performed (Gernhardt and Lambertsen, 2002; Dolan et al., 2016). Taken together, the changes in daily physical activity in the chamber, the atmospheric conditions and the energy cost of underwater activity may all theoretically influence daily energy expenditure (DEE) during commercial saturation diving. However, to date, an accurate assessment of DEE during the real-life offshore work environment has not been undertaken. Establishing the energy requirements of saturation diving is essential to formulate appropriate nutritional guidelines to support occupational divers' health and well-being (Deb et al., 2016). Therefore, the purpose of this study was to determine the average DEE of occupational saturation divers who are undertaking a 21-day commercial dive in the North Sea using the gold standard energy assessment technique of doubly labelled water (DLW).

METHODS

Participants and Saturation Dive

Ten operational and medically certified divers were recruited with the following characteristics (mean ± SD), age: 47 ± 8.4 years; height: 180.4 ± 7.4 cm; bodyweight: 89.0 ± 10.2 kg; and BMI: 27.3 ± 1.9. Prior to entering the saturation chamber, all participants underwent a medical examination by a trained health professional and body weight was also recorded to the nearest 0.1 kg (SECA, Birmingham, United Kingdom). The Norwegian Regional Committee approved the study protocol for Medical and Health Research Ethics (REK; approval number: 2018/1184). The participants provided their written informed consent before volunteering for the study.

Saturation Dive Operation

Diving operations took place in October–November 2019, off the west coast of Norway and were conducted per the NORSOK U-100 requirements (Standards Norway, 2014). All participants were part of the same diving operation; therefore, they were exposed to similar dive conditions with a living depth of 72 metres seawater (msw) resulting in a maximum working depth of 81 msw. In the chamber the oxygen pressure was maintained at 380 mbar and this increased to 756 mbar during the bell run. The temperature was adjusted to maintain the thermal comfort of divers and typically maintained between 28 and 30°C. The dive operation was up to 18 days, with divers spending 14 days in a saturation at the living depth of 72 msw followed by a 3–4 days decompression period. The divers organised into 4 teams of 3 and working in overlapping 12 h shift patterns with a new 3-man shift starting every 6 h throughout a 24-h cycle. The divers had 12 h off between each shift. The dive teams worked in rotation; for every third shift, the divers provided support from the diving bell and did not perform any activities underwater. For the purposes of this study, an underwater excursion was defined the duration of a wet bell run during shifts where the divers undertook activity in the water, as one diver would remain dry in the bell throughout any given shift. Each diver completed 7.4 ± 1.7 underwater excursions on average during this operation, with an average underwater working period of 193.1 ± 25.9 min per excursion. The total time that a diver spent in water during this saturation operation was 1066.8 ± 417.9 min across the 21-day saturation dive. It was not possible to measure the underwater excursion's intensity, but the divers subjectively reported that the underwater excursions were approximately half the length of the typical 5.30 h underwater working period, and the workload was perceived as "light." Examples of work performed during underwater excursions during this operation include: Installation of blind flange plugs, pipe support installation, seal replacements, bell mouth installation, and inspection works.

Measurement of Daily Energy Expenditure

The DLW stable isotope technique was used to measure energy expenditure. This is the gold-standard method that provides a safe and non-invasive procedure to determine energy expenditure (Westerterp, 2017). Participants completed a 10-day sampling period commencing 3 days after they were compressed to hyperbaric pressure equivalent to 72 msw. A second-morning void urine sample (∼ 1 ml) was collected to determine isotope analysis prior to the oral administration of a liquid bolus dose of hydrogen (deuterium ^{2}H) and oxygen (^{18}O) stable isotopes in the form of water ($^{2}H_{2}{}^{18}O$). Additional water was added to the glass vials, and the participants were asked to drink this to ensure

the full dose was ingested. A pre-prepared standardised dose, based on the weight of the subjects, was made in the Energetics Research Laboratory, Aberdeen and sent to the vessel to reduce any inconsistencies in dose preparation in the field. The dose was weighed to four decimal places. The prescribed dose was 10% ^{18}O and 5% deuterium ^{2}H based on a 90 kg participant using the following equation:

$$^{18}\text{O dose} = \left[0.65\ \left(\text{body mass, g}\right) \times \text{DIE}\right]/\text{IE} \quad (1)$$

where DIE is the desired initial enrichment (DIE = 618.923 × body mass (kg)−0.305) and IE is the initial enrichment (10%) 100,000 ppm.

Following the DLW administration, a morning urine sample (second void) was taken every 24 h for the subsequent 9 days (see **Figure 1** for an overview of the study protocol) and kept in sealed containers. All urine samples were passed out of the saturation chamber *via* a hatch where they underwent decompression to the surface pressure. The urine containers were decompressed with unfastened lids, standing upright in a rack to avoid spillage. The lids were closed when the containers were collected from the hatch at surface pressure after decompression. The samples were subsequently frozen at −24 °C and stored on the vessel, before being transported to the laboratory in Aberdeen, United Kingdom, using a temperature-controlled cube (VeriCor Medical Systems, Holmen, WI, United States), where they remained frozen until analysis.

Analysis of the isotopic enrichment of urine was performed blind, using a Liquid Isotope Water Analyser (Los Gatos Research, United States) (Berman et al., 2012). Initially the urine was vacuum distilled, and the resulting distillate was used for analysis. Samples were run alongside five lab standards for each isotope and international standards to correct delta values to ppm. Daily isotope enrichments were $\log_e$ converted and the elimination constants (k_o and k_d) were calculated by fitting a least squares regression model to the $\log_e$ converted data. The back extrapolated intercept was used to calculate the isotope dilution spaces (N_o and N_d). A two-pool model, was used to calculate rates of CO_2 production as recommended for use in humans (Speakman et al., 2021; Eq. 2).

$$rCO_2 = 0.4554{*}N{*}[(1.007{*}\,K_O) - 1.043{*}\,K_d)]{*}22.26 \quad (2)$$

where k_o and k_d are in units of d^{-1} and rCO_2 is in L d^{-1}. Subsequently, rCO_2 was used to determine DEE using the following equation:

$$TEE = rCO_2{*}\left(1.106 + \left(\frac{3.94}{0.85}\right)\right){*}\left(\frac{4.194}{10^3}\right) \quad (3)$$

TEE is calculated in megajoules per day and subsequently converted into kcal per day for statistical analysis. For the purposes of this study an estimated respiratory quotient (RQ) of 0.85 was used, as this is often used during field-based studies where it is not possible to determine RQ (Butler et al., 2004). Furthermore, research suggests that despite a change in atmospheric conditions, expired O_2 consumption and CO_2 production (parameters used to calculate RQ) remain similar during a 17-day simulated saturation dive with a hyperoxic-helium gas mixture compared to surface ambient environment (Dressendorfer et al., 1977). An RQ of 0.85 was therefore deemed to be appropriate for analysis.

Energy Intake

The kitchen on board the vessel controlled access to food. Participants were able to choose their diets from a daily menu throughout the day. The diver's food choices and estimated portion sizes were recorded during the 10-day measurement period in a dietary log by the dive support team and researcher onboard. The dietary logs were assessed for completeness by a qualified nutritionist before analysis, with seven participants providing complete dietary logs that were subsequently analysed. A nutritional analysis software (Nutritics, United Kingdom) was used to determine the average daily energy intake during the 10-day measurement period.

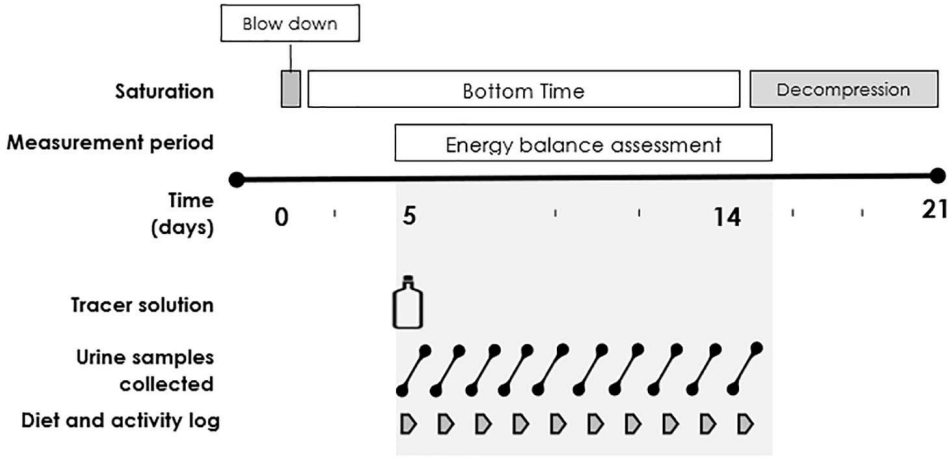

FIGURE 1 | Outline of the study protocol.

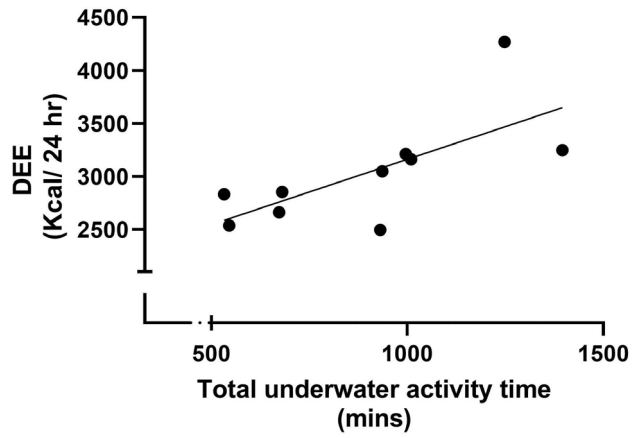

FIGURE 2 | Shows the significant strong positive correction reported between DEE and total time spent performing underwater work ($r = 0.7$, $p = 0.026$).

Statistical Analysis

Statistical analyses were performed using statistical software package SPSS (SPSS, version 22, IBM, United States). The Q–Q plots and Shapiro–Wilk test demonstrated that all variables were normally distributed. A paired *t*-test was used to test the difference between DEE and energy intake. Pearson's correlation was conducted to assess the relationship between total time spent performing underwater activity during the measurement period and the DEE. Statistical significance was accepted at $p < 0.05$.

RESULTS

During the 10-day measurement period participants complete on average 3.8 ± 1.2 underwater excursions, with a range from 2 to 6 excursions. Overall, participants spent 895.0 ± 273.8 min conducting wet bell runs, and each excursion was 237.8 ± 33.7 min on average. The mean actual DEE determined *via* DLW across the 10-day measurement period was 3030.9 ± 513.0 kcal/day, ranging from 2495 to 4268 kcal/day. When normalised for body mass, DEE was 32.5 ± 5.1 kcal/kg body mass/day and ranged between 28.6 and 40.1 kcal/kg body mass/day. Pearson's correlation analysis revealed a significant strong positive correction reported between DEE and total time spent performing underwater work ($r = 0.7$, $p = 0.026$; **Figure 2**).

The average dietary intake was 1875.3 ± 487.4 kcal throughout the measurement period, which compared to actual energy expenditure, resulted in a significant 1021.1 ± 724.7 kcal negative energy balance ($p = 0.005$; **Figure 3A**). While this difference is substantial, one diver did consume enough calories during the measurement period, demonstrating that divers can meet the energy requirements of saturation diving (**Figure 3B**). Despite several divers not meeting the energy requirements during the 10-day measurement period, this was not reflected in body mass changes pre to post-dive. The diver's average body mass remained unchanged.

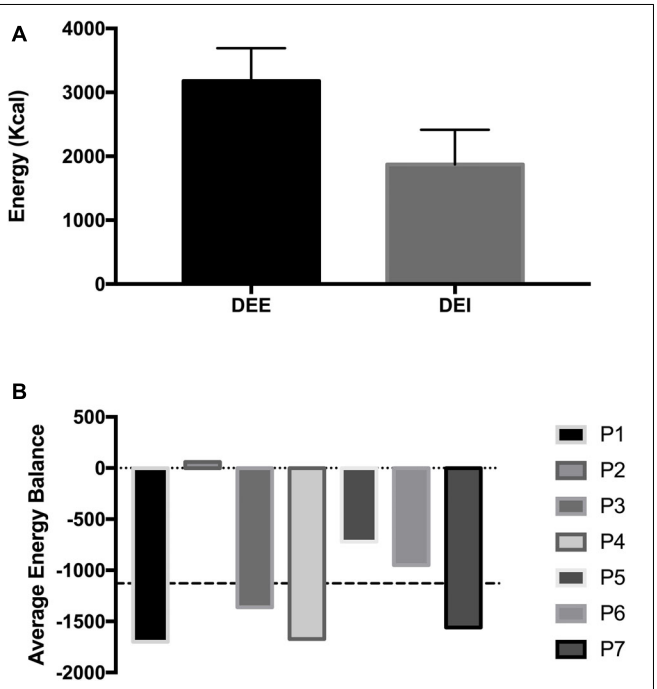

FIGURE 3 | Panel **(A)** shows the mean daily energy expenditure (DEE) measured *via* DLW and mean daily energy intake (DEI) of saturation divers during a commercial operation in the North Sea. Panel **(B)** shows the individual energy balance (DEE–DEI) with commercial saturation divers. The dashed line represents the mean energy balance.

DISCUSSION

This research study was the first to determine the average DEE of saturation divers during a live commercial diving operation in the North Sea. The data suggests a considerable individual variation in DEE between divers, with a range spanning 1745 kcal. This variability remained when DEE was normalised for body mass. There was a significant correlation between DEE and the total duration of underwater activity during the 10-day measurement period, with divers who spent more time in the water expending more energy. Energy intake was also reported to be significantly lower than average DEE, suggesting most of the divers did not attain an energy balance during the 10-day sampling period in saturation. The saturation divers and diving industry stakeholders should be aware that a divers' dietary energy requirements must be personalised due to the intraindividual variability in DEE and energy intake in divers participating in the same diving operation.

While the current investigation reported a high DEE, it was not possible to establish if these requirements are more substantial than the demand within normobaric normoxic conditions (i.e., surface conditions) when physical activity and movement is matched. Early research by Seale et al. (1994) suggested that the hyperbaric heliox environment resulted in a significant DEE increase compared to the surface. Similarly, the authors utilised the DLW technique to determine DEE at the surface and hyperbaric conditions equivalent to 50 and 317 msw,

using a saturation dive simulation without underwater excursions for 9 and 14 days, respectively. Participants had a significant 13 ± 4% increase in DEE at 50 msw compared to the surface, but no further significant DEE increases occurred with greater atmospheric pressure. The authors postulated that this increase might be explained by the hyperbaric atmosphere creating a greater gas density, thereby increasing airway resistance that results in more work required for respiration (Moon et al., 2009). Furthermore, helium (an inert gas required to create the hyperbaric environment) possesses a conductivity six times greater than air and subsequently increases heat exchange from the body (Hong et al., 2011). Together, these environmental factors may contribute to an increased DEE in commercial saturation divers.

This study observed that increases DEE were strongly correlated with total time spent conducting underwater activities, suggesting dive activities may be a primary determinant of DEE during commercial diving. The knowledge of physiological responses and intensities of underwater work for commercial saturation divers is limited. The physical and physiological demand of matched activity is however, greater in water compared to the surface due to the water density providing external resistance (Pendergast and Lundgren, 2009) and with greater depth the higher pressure increases the work of breathing (Moon et al., 2009). Within a commercial diving setting, saturation divers conduct several different tasks associated with the design and (de)construction of underwater structures, e.g., oil rigs. The intensity of the underwater work performed in this current study was reported to be low; however, previous reports of subjective workloads of different diving activities indicate certain activities require higher levels of endurance and strength (Gernhardt and Lambertsen, 2002). Therefore, the overall DEE in saturation divers is likely to be influenced by the intensity of underwater work, and a diver's energy intake should be altered based on the task. There needs to be more research to understand the energy demand of various tasks that saturation divers perform underwater so that an accurate DEE can be calculated.

A theoretical analysis of calorie expenditure of open water diving in non-saturation divers suggested that dives that involve minimal movement may require 5.4 kcal/min with a range of between 3.8 and 8.1 kcal/min (Michniewski, 2020). With increased physical demand, this is suggested to go to 9.8 kcal/min and a range of 7.1–11.8 kcal/min. Consequently, providing an interesting insight into the energy demands of underwater activity; although, the differing equipment requirements and unique characteristics of saturation diving, these values cannot be directly applied. While underwater activity is likely to be a contributor to DEE, this study cannot discern the energy cost that is attributed to the resting metabolic rate (RMR) and activity-related expenditure. The RMR accounts for approximately 60% of DEE at sea level, contributing to a normal physiological process in a rested, post-absorptive and thermoneutral state (Pizzagalli et al., 2017). Given the change in atmospheric conditions, it is feasible that RMR during a saturation dive may also change compared to the surface. Further work should aim to measure the RMR of divers during hyperbaric hyperoxic exposure using indirect calorimetry. This will allow the prediction of energy expenditure during underwater activity to be calculated.

Knowledge of RMR may also help to explain some of the variability in DEE between divers. An individual's weight and body composition influence their RMR, as a greater mass of metabolically active tissue (i.e. fat free-mass), results in a greater RMR (Amaro-Gahete et al., 2018). The participants' body composition in the current study could not be measured, and further work should consider the influence of a diver's body composition on the energy cost during a diving operation. In addition, those partaking in rotating shift patterns may also experience changes to their RMR and DEE as energy metabolism is subject to diurnal variation (Shaw et al., 2019). This study's sample size was insufficient to discern any differences between divers on different shift patterns, but future research and nutritional guidelines for saturation divers should consider this.

During the saturation dive, dietary intake assessment revealed that divers consume significantly fewer calories than their DEE. While the current study is the first to demonstrate this during a commercial operation, existing research suggests that individuals may be prone to a negative energy balance during saturation diving simulations and have reported a reduced daily calorie intake (Webb et al., 1977; Collis, 1983; Smith et al., 2004). In the present study, this negative energy balance was not however, accompanied by a change in body weight, which is commonly cited to occur following commercial diving operations (Busch-Stockfish and Von Bohken, 1992). Theoretically, if a −1128 ± 725 kcal deficit was maintained throughout the 21-day saturation dive, a 3 kg weight loss may be expected. As weight did not change, it suggests that the calculated daily energy intake may be underestimated, which is a common error in dietary assessment research. In this study, however, dietary intake was restricted to the vessel's food availability on a given day and food had to be passed into the chamber. As dietary logs were written as the divers were making their menu choices, this study did not rely on dietary recall or memory, which is cited as a source of error in dietary assessment (Naska et al., 2017). Equally, the energy expenditure and intake outside of the 10-day measurement period were not recorded; therefore, the energy balance across the full 21-day saturation dive is unknown, and the subsequent implications on body mass cannot be confirmed.

Maintaining an energy balance has important implications; however, saturation divers experience several unique food intake barriers. These include, but not limited to, the reduction in taste and palatability of certain foods, food availability based on differing shift patterns and a lack of appetite following underwater work (Deb et al., 2016). One participant in this study achieved an average energy balance, demonstrating that divers can attain their required energy intake. Nevertheless, further understanding is needed to identify the factors that influence a diver's nutritional behaviours, so appropriate guidance and recommendations can be presented to the diving industry to account for the personalised needs of saturation divers.

The concept of personalised nutrition education uses information on individual characteristics to develop targeted nutrition advice, support or services that assist people in

achieving a sustained behaviour change and improving health (Ordovas et al., 2018). In the context of saturation diving, these individual characteristics refer to unique challenges of their occupation and their onshore behaviours, preferences, and barriers to healthy eating. Furthermore, the on and off work schedule adds a further challenge to adopting a healthy lifestyle and nutrition habits. Research suggests that a sense of fatigue post saturation can last 1–10 days, with divers reporting varied timescales of returning to daily habits (Imbert et al., 2019). A personalised nutritional education approach should consider and encourage strategies that will help divers' practice sustainable nutritional behaviours to help achieve energy balance during an operation and maintain their diet quality to promote cardiovascular health, body composition, and healthy ageing.

The current study presents a high degree of ecological validity, although the investigations' field-based nature brings some limitations and opens additional research questions to address. Data in this study were collected in the same diving operation; therefore, all the divers were exposed to similar depths, conditions and work activities. Previous research in simulated conditions suggests that dive depth may not affect average DEE (Seale et al., 1994); this has not been tested in an operational setting within commercial saturation divers who perform underwater work. Equally, this study saw divers undertake an average of 7.4 underwater excursions across the whole dive, which is less than a typical operation. Given the activity underwater is a large part of a divers daily physical movement, other operations may result in a higher DEE.

Caution should be taken before applying the outcome of this study to the diving population, given the possibility of overestimating DEE due to confounding variables and the unique environmental conditions of saturation diving. For instance, the hyperbaric hyperoxic-helium environment may increase RQ above the estimated 0.85 used to determine DEE. Little is known about the metabolic changes during saturation diving; however, evidence suggests that changes in lipid metabolism are non-significant during experimental saturation dives at 70 m. Although during deeper dives to <200 m, changes in lipid metabolism are expressed through changes in blood metabolites (Buravkova and Popova, 2007). Divers in the current study had a living depth of 72 msw and a maximum working depth of 81 msw, suggesting changes in lipid metabolism, and therefore an increased RQ, is less likely. Future studies should consider indirect calorimetry during saturation exposure to allow direct assessment of RQ and therefore, increase the accuracy of DEE calculations *via* DLW. Equally, future studies may consider monitoring body composition pre and post dive using accurate techniques, such as dual X-ray absorptiometry (DEXA), which can help identify if the negative energy balance resulted in changes in body fat percentage and muscle mass of the divers. No changes in body weight were observed in the current study and while this may be explained by increased fluid intake to account for any loss in body weight, this study did not monitor fluid intake. As such, this study cannot conclude with certainty that saturation divers experience a negative energy balance during a commercial operation due to the potential overestimation in DEE or underestimation of DEI. Nevertheless the findings in this study corroborate previous research during simulated saturation dives that indicate divers may experience an elevated DEE (Seale et al., 1994) and may also reduce DEI (Webb et al., 1977; Collis, 1983; Smith et al., 2004).

CONCLUSION

In conclusion, this study is the first to assess the energy expenditure of saturation divers during a commercial saturation dive using DLW. Considerable variability in DEE was reported, along with a mismatch between DEE and energy intake during the 10-day measurement period. This suggests that the dietary intake requirements and practices can vary between divers, and a personalised approach to nutritional intake may be needed. The study outcomes are drawn from a single diving operation, where all participants performed similar dive activities and exposed to similar environmental conditions. Further offshore field research should aim to understand the causes of DEE variability and the factors that may influence a diver's nutritional intake. Saturation divers have a unique nutritional requirement due to occupational demands. As such, the dietary recommendations for saturation divers must be cognisant of these factors to promote their health and well-being. Addressing these factors requires continued personalised nutrition support from the diving industry and contractors to ensure meaningful and sustainable changes.

DATA AVAILABILITY STATEMENT

The raw data supporting the conclusions of this article will be made available by the authors, without undue reservation.

ETHICS STATEMENT

The studies involving human participants were reviewed and approved by the Norwegian Regional Committee approved the study protocol for Medical and Health Research Ethics (REK; approval number: 2018/1184). The patients/participants provided their written informed consent to participate in this study.

AUTHOR CONTRIBUTIONS

SD and IE contributed to the conception and design of the study. IE performed the data collection. CH and JS conducted the DLW analysis. SD wrote the first draft of the manuscript. All authors contributed to manuscript revision, read, and approved the submitted version.

ACKNOWLEDGMENTS

The authors gratefully acknowledge the contributions of the divers, captain and crew on the DSV Deep Arctic. Access to the 2018 Bahr Essalam diving campaign was granted by TechnipFMC and Mellitah Oil & Gas B.V.

REFERENCES

Amaro-Gahete, F., Jurado-Fasoli, L., De-la-O, A., Gutierrez, Á, Castillo, M., and Ruiz, J. (2018). Accuracy and validity of resting energy expenditure predictive equations in middle-aged adults. *Nutrients* 10:1635. doi: 10.3390/nu10111635

Berman, E. S. F., Fortson, S. L., Snaith, S. P., Gupta, M., Baer, D. S., Chery, I., et al. (2012). Direct analysis of δ2H and δ18O in natural and enriched human urine using laser-based, off-axis integrated cavity output spectroscopy. *Anal. Chem.* 84, 9768–9773. doi: 10.1021/ac3016642

Brubakk, A. O., Ross, J. A. S., and Thom, S. R. (2014). Saturation diving; physiology and pathophysiology. *Compr. Physiol.* 4, 1229–1272. doi: 10.1002/cphy.c130048

Buravkova, L. B., and Popova, Y. A. (2007). Effects of various hyperbaric gas mixtures on metabolic parameters of human blood. *Hum. Physiol.* 33, 603–613. doi: 10.1134/S0362119707050118

Busch-Stockfish, M., and Von Bohken, B. (1992). Evaluation of energy requirements from body mass, lean body mass, fat content, and energy intake in GUSI dives - PubMed. *Undersea Biomed. Res.* 19, 263–270.

Butler, P. J., Green, J. A., Boyd, I. L., and Speakman, J. R. (2004). Measuring metabolic rate in the field: the pros and cons of the doubly labelled water and heart rate methods. *Funct. Ecol* 18, 168–183. doi: 10.1111/j.0269-8463.2004.00821.x

Collis, S. A. (1983). The conduct of metabolic balances during simulated deep dives. *Hum. Nutr. Appl. Nutr* 37, 46–53.

Deb, S. K., Swinton, P. A., and Dolan, E. (2016). Nutritional considerations during prolonged exposure to a confined, hyperbaric, hyperoxic environment: recommendations for saturation divers. *Extrem. Physiol. Med.* 5:1. doi: 10.1186/s13728-015-0042-9

Dolan, E., Deb, S., Stephen, G., and Swinton, P. (2016). Brief communication: self-reported health and activity habits and attitudes in saturation divers - PubMed. *Undersea Hyperb. Med.* 43, 92–101.

Dressendorfer, R., Hong, S., Morlock, J., Pegg, J., Respicio, B., Mith, R., et al. (1977). Hana kai ii: a 17-day dry saturation dive at 18.6 ATA. V. Maximal oxygen uptake - PubMed. *Undersea Biomed. Re* . 4, 283–296.

Gernhardt, M. L., and Lambertsen, C. (2002). in *Bennett and Elliotts' Physiology and Medicine of Diving*, 5th Edn, eds A. Brubakk and T. Neuman (Amsterdam: Elisevier).

Hong, S. K., Bennett, P. B., Shiraki, K., Lin, Y.-C., and Claybaugh, J. R. (2011). "Mixed-gas saturation diving ," in *Comprehensive Physiology*, ed. R. Terjung (Hoboken, NJ: John Wiley & Sons, Inc), 1023–1045. doi: 10.1002/cphy.cp040244.

Ikeda, M., Nakabayashi, K., Shinkai, M., Hara, Y., Kizaki, T., Oh-Ishi, S., et al. (2004). Supplementation of antioxidants prevents oxidative stress during a deep saturation dive. *Tohoku J. Exp. Med.* 203, 353–357. doi: 10.1620/tjem.203.353

Imbert, J. P., Balestra, C., Kiboub, F. Z., Loennechen, Ø, and Eftedal, I. (2019). Commercial divers' subjective evaluation of saturation. *Front. Psychol* 9:2774. doi: 10.3389/fpsyg.2018.02774

Michniewski, P. (2020). Energy Expenditure of swimmers and scuba divers. *Polish Hyperb. Res.* 69, 91–96. doi: 10.2478/phr-2019-0023

Moon, R. E., Cherry, A. D., Stolp, B. W., and Camporesi, E. M. (2009). Pulmonary gas exchange in diving. *J. Appl. Physiol.* 106, 668–677. doi: 10.1152/japplphysiol.91104.2008

Naska, A., Lagiou, A., and Lagiou, P. (2017). Dietary assessment methods in epidemiological research: current state of the art and future prospects. *F1000Research* 6:926. doi: 10.12688/f1000research.10703.1

Ojeda, P., Bobe, A., Dolan, K., Leone, V., and Martinez, K. (2016). Nutritional modulation of gut microbiota - the impact on metabolic disease pathophysiology. *J. Nutr. Biochem.* 28, 191–200. doi: 10.1016/j.jnutbio.2015.08.013

Ordovas, J. M., Ferguson, L. R., Tai, E. S., and Mathers, J. C. (2018). Personalised nutrition and health. *BMJ* 361:bmj.k2173. doi: 10.1136/bmj.k2173

Pendergast, D. R., and Lundgren, C. E. G. (2009). The underwater environment: cardiopulmonary, thermal, and energetic demands. *J. Appl. Physiol.* 106, 276–283. doi: 10.1152/japplphysiol.90984.2008

Pizzagalli, D. A., Webb, C. A., Dillon, D. G., Tenke, C. E., Kayser, J., Goer, F., et al. (2017). The effect of megestrol acetate on oral food and fluid intake in nursing home residents: a pilot study. *Am. J. Clin. Nutr.* 13, 97–103. doi: 10.1093/ajcn/41.1.21

Ross, J. A. S., Macdiarmid, J. I., Osman, L. M., Watt, S. J., Godden, D. J., and Lawson, A. (2007). Health status of professional divers and offshore oil industry workers. *Occup. Med. (Chic. Ill).* 57, 254–261. doi: 10.1093/occmed/kqm005

Seale, J., Thorp, J., Conway, J., Rumpler, W., and Haberman, K. (1994). Energy expenditure and fluid production in hyperbaric He-O2 environments using doubly labeled water - PubMed. *Undersea Hyperb. Med.* 21, 199–208.

Shaw, E., Leung, G. K. W., Jong, J., Coates, A. M., Davis, R., Blair, M., et al. (2019). The impact of time of day on energy expenditure: Implications for long-term energy balance. *Nutrients* 11:2383. doi: 10.3390/nu11102383

Smith, S. M., Davis-Street, J. E., Vernell Fesperman, J., Smith, M. D., Rice, B. L., and Zwart, S. R. (2004). Nutritional status changes in humans during a 14-day saturation dive: the NASA extreme environment mission operations V project. *J. Nutr.* 134, 1765–1771. doi: 10.1093/jn/134.7.1765

Speakman, J. R. (1999). The cost of living: field metabolic rates of small mammals. *Adv. Ecol. Res.* 30, 177–297. doi: 10.1016/S0065-2504(08)60019-7

Speakman, J. R., Yamada, Y., Sagayama, H., Berman, E. S. F., Ainslie, P. N., Andersen, L. F., et al. (2021). A standard calculation methodology for human doubly labeled water studies. *Cell Rep. Med.* 2:100203. doi: 10.1016/j.xcrm.2021.100203

Webb, P., Troutman, S. J., Frattali, V., Dressendorfer, R. H., Dwyer, J., Moore, T. O., et al. (1977). Hana Kai II: a 17 day dry saturation dive at 18.6 ATA. II. energy balance. *Undersea Biomed. Res.* 4, 221–246.

Westerterp, K. R. (2017). Doubly labelled water assessment of energy expenditure: principle, practice, and promise. *Eur. J. Appl. Physiol.* 117, 1277–1285. doi: 10.1007/s00421-017-3641-x

Yuan, Y., Zhao, G., Ji, H., Peng, B., Huang, Z., Jin, W., et al. (2019). Changes in the gut microbiota during and after commercial helium-oxygen saturation diving in China. *Occup. Environ. Med.* 76, 801–807. doi: 10.1136/oemed-2019-106031

Conflict of Interest: SD was awarded funding by Equinor which funds part of this research study. IE was funded Norwegian Research Council and Equinor on behalf of PRSI Pool (Petromaks2 project no. 280425). OE is currently employed by Equinor. The conception, design and analysis of the study were conducted independently of the funder with no commercial involvement.

The remaining authors declare that the research was conducted in the absence of any commercial or financial relationships that could be construed as a potential conflict of interest.

frontiers in Physiology

ORIGINAL RESEARCH
published: 01 June 2021
doi: 10.3389/fphys.2021.674430

MEK1/2 Inhibition Synergistically Enhances the Preventive Effects of Normobaric Oxygen on Spinal Cord Injury in Decompression Sickness Rats

*Quan Zhou[1†], Xiangyang Meng[1†], Guoyang Huang[1†], Hongjie Yi[2], Juan Zheng[1], Kun Zhang[1] and Weigang Xu[1]**

[1] Department of Diving and Hyperbaric Medicine, Naval Special Medical Center, Naval Medical University, Shanghai, China,
[2] Department of Hyperbaric Oxygen, The First Affiliated Hospital, Naval Medical University, Shanghai, China

OPEN ACCESS

Edited by:
Ingrid Eftedal,
Norwegian University of Science and Technology, Norway

Reviewed by:
Simin Berenji Ardestani,
Aarhus University, Denmark
Xuehua Liu,
Capital Medical University, China

***Correspondence:**
Weigang Xu
wg_hsu@163.com

[†]*These authors have contributed equally to this work*

Specialty section:
This article was submitted to Environmental, Aviation and Space Physiology, a section of the journal Frontiers in Physiology

Received: *01 March 2021*
Accepted: *19 April 2021*
Published: *01 June 2021*

Citation:
Zhou Q, Meng X, Huang G, Yi H, Zheng J, Zhang K and Xu W (2021) MEK1/2 Inhibition Synergistically Enhances the Preventive Effects of Normobaric Oxygen on Spinal Cord Injury in Decompression Sickness Rats. Front. Physiol. 12:674430. doi: 10.3389/fphys.2021.674430

A previous study from our team found that hyperbaric oxygen (HBO) pretreatment attenuated decompression sickness (DCS) spinal cord injury by upregulating heat shock protein 32 (HSP32) via the ROS/p38 MAPK pathway. Meanwhile, a MEK1/2-negative regulatory pathway was also activated to inhibit HSP32 overexpression. The purpose of this study was to determine if normobaric oxygen (NBO) might effectively induce HSP32 while concurrently inhibiting MEK1/2 and to observe any protective effects on spinal cord injury in DCS rats. The expression of HSP32 in spinal cord tissue was measured at 6, 12, 18, and 24 h following NBO and MEK1/2 inhibitor U0126 pretreatment. The peak time of HSP32 was observed at 12 h after simulated air diving. Subsequently, signs of DCS, hindlimb motor function, and spinal cord and serum injury biomarkers were recorded. NBO-U0126 pretreatment significantly decreased the incidence of DCS, improved motor function, and attenuated oxidative stress, inflammatory response, and apoptosis in both the spinal cord and serum. These results suggest that pretreatment with NBO and U0126 combined can effectively alleviate DCS spinal cord injury in rats by upregulating HSP32. This may lead to a more convenient approach for DCS injury control, using non-pressurized NBO instead of HBO.

Keywords: decompression sickness, spinal cord injury, normobaric oxygen, MEK1/2, U0126, heat shock protein 32

INTRODUCTION

Decompression sickness (DCS) is caused by inert gas bubbles forming in tissues and vessels following inadequate decompression in diving, aviation, and space activities (Vann et al., 2011). The overall rates of DCS per dive are 0.01–0.019% among recreational divers, 0.01–0.019% in scientific divers, 0.030% in U.S. Navy divers, and 0.095% in commercial divers (Vann et al., 2011; Mahon and Regis, 2014). Various tissues and organs are involved in DCS from the skin to the central nervous system, and the involvement of the spinal cord may cause serious sequelae, such as back pain, paresthesia, or acroparalysis (Blatteau et al., 2011; Saadi et al., 2019). Neurologic DCS accounts for 20–40% of all DCS, and spinal cord injury accounts for about 77% of neurologic DCS, even

after active treatment, and more than 20% sequelae remain afterward (Blatteau et al., 2011; Mahon and Regis, 2014; Saadi et al., 2019). While complete resolution following treatment remains elusive, DCS, especially with spinal cord injury, is addressed mainly through prevention but, other than adhering to established decompression schedules, there are few other preventive strategies.

Hyperbaric oxygen (HBO), the practice of administering pure oxygen to patients while being exposed to ambient pressure greater than one absolute atmosphere, is widely used in DCS treatment (Moon, 2014). By increasing blood oxygen partial pressure and extending oxygen diffusion, HBO accelerates inert gas washout and attenuates hypoxic and ischemic damage caused by bubbles in tissues (Arieli et al., 2009). Numerous studies have shown that HBO also provides delayed protection by mobilizing intrinsic protective mechanisms against a variety of harms (Camporesi and Bosco, 2014; Gonzales-Portillo et al., 2019). Previous studies from our team showed that 280-kPa-60-min HBO pretreatment significantly reduced DCS incidence and alleviated DCS spinal cord injury in rats (Fan et al., 2010; Ni et al., 2013). Further research found that the neuroprotection of HBO was strongly associated with heat shock protein 32 (HSP32) upregulation and a signaling pathway involving ROS/p38 MAPK was discovered (Huang et al., 2014, 2016). Interestingly, while upregulating the expression of HSP32 in spinal cord neurons, HBO also activated the MEK1/2-negative regulatory pathway to prevent HSP32 overexpression (Huang et al., 2016). As an important effector of HBO, moderately expressed HSP32 exerts antioxidative, anti-inflammatory, and antiapoptotic effects, while overexpressed HSP32 results in numerous inimical effects (Schipper et al., 2019).

Although HBO is a safe, economical, and efficient therapy, its application in practice may at times be logistically limited by the need for a hyperbaric chamber, trained operators, and physicians, any of which may be unavailable at diving sites, or during high-altitude flights, submarine escape, or extra-vehicular activity in space. Since MEK1/2 works as a negative regulator, it is speculated that HSP32 can be induced effectively by a lower pressure of oxygen when the role of MEK1/2 is inhibited. The purpose of this study was to observe the effects of combined pretreatment with pure oxygen in a normobaric environment (normobaric oxygen, NBO) and MEK1/2 inhibition (inducted by specific inhibitor U0126) on spinal cord HSP32 expression and to record the beneficial effects on spinal cord injury in a rat DCS model.

MATERIALS AND METHODS

Animals

A total of 194, 8-week-old adult male Sprague-Dawley (SD) rats weighing 300∼310 g were obtained from the Experimental Animal Center of the Naval Medical University (NMU). The animals were housed under a controlled light/dark cycle (12/12 h), temperature (24 ± 1°C), and relative humidity (54 ± 2%) and allowed to access a pelleted rodent diet and water *ad libitum* during the experiment.

Procedure and Design

Part I. Rats were treated by intraperitoneal injection with U0126 (20 mg/kg, Selleck, United States) dissolved in 100 μL DMSO (Beyotime, China) 30 min before NBO exposure. The expression of HSP32 in rat spinal cord tissue was determined at 6, 12, 18, and 24 h following combined treatment with NBO and U0126. NBO and U0126 treatment were settled alone at the HSP32 peak time point of 12 h following NBO/Air exposure, as factorial design to reveal the interaction between NBO and U0126 in HSP32 induction. Six rats were investigated in each group, for measurement of the expression of HSP32.

Part II. Another 152 rats were randomly divided into five groups, 35 each for four simulated air dive groups and 12 for a control group. The four simulated air dive groups received treatments as follows: (1) NBO-U0126: treated with NBO and U0126; (2) NBO: treated with NBO only; (3) U0126: treated with U0126 and a sham exposure with normobaric air instead of NBO; and (4) Air: a sham exposure with normobaric air. Simulated air diving occurred at 12 h after either NBO and/or U0126 treatment. Following rapid decompression, the rats were observed for 30 min for DCS diagnosis followed by a 3-min motor function evaluation. Surviving rats were anesthetized by intraperitoneal injection with 3% pentobarbital sodium (1.5 ml/kg) 2 h after decompression. Blood and spinal cord tissues were sampled for biochemical analysis. Control rats were similarly sampled without any treatments or simulated air diving.

Figure 1 shows the timeline of the experiments.

NBO Exposure

A 100-kPa-60-min NBO exposure was performed with rats inside a transparent hyperbaric rodent chamber (RDC 150-300-6, NMU, China). The rats were placed in the chamber, and it was flushed with pure oxygen for 5 min to replace the air inside, then it was continuously ventilated with pure oxygen for 60 min. The Air group and U0126 group were similarly exposed but with normobaric air instead of NBO.

Simulated Air Dive

Rats in four simulated air dive groups were compressed with air in a hyperbaric chamber (RDC 150-300-6) 10.5 h after either NBO-U0126 pretreatment or NBO/U0126/Air treatment, one rat at a time from each group. Compression to 700 kPa took 5 min and was maintained for 90 min. Decompression was linear to ambient pressure at 200 kPa/min in 3 min. During exposure, the chamber was continuously ventilated with air to minimize any decrease of oxygen and accumulation of carbon dioxide.

DCS Diagnosis

To standardize the activity level and facilitate DCS diagnosis, rats were subjected for 30 min to walk inside an electrically controlled cylindrical cage rotating at a perimeter speed of 3 m/min. During this time, two observers who were blinded to the treatments diagnosed DCS. According to previous studies from our team, DCS diagnosis was based on observation of any of the following symptoms: respiratory distress, walking difficulties, limb paralysis, rolling with cage rotation, convulsions, or death

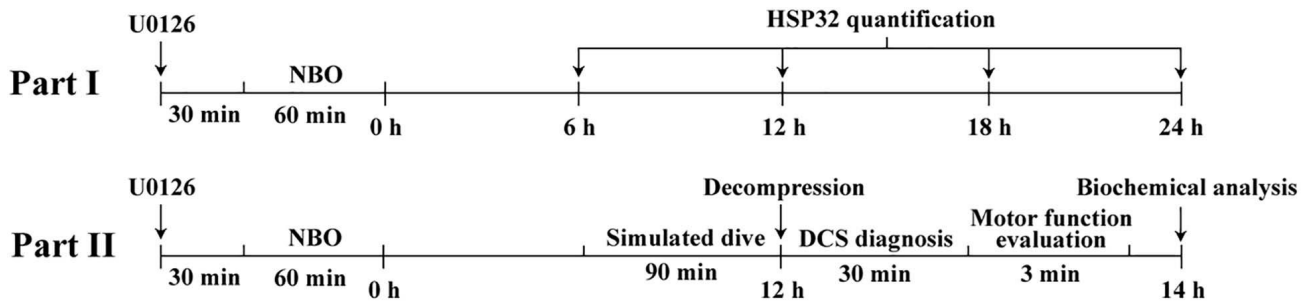

FIGURE 1 | The timeline and design of the study. Part I, NBO-U0126 treatment-induced HSP32 expression in rat spinal cord was determined at 6, 12, 18, and 24 h following NBO exposure. The separate NBO and U0126 treatment HSP32 samples were collected at 12 h following NBO exposure. Part II, rats in different treatment groups underwent simulated air dives, concluding that at the HSP32 peak time point of 12 h, DCS diagnosis, motor function evaluation, and sample collection for biochemical analysis were successively carried out.

(Fan et al., 2010; Ni et al., 2013; Zhang et al., 2015, 2016, 2017; Yu et al., 2020). A binary classification of "no-DCS" and "DCS" was recorded; whenever any symptoms described above were observed, the latency was also recorded.

Motor Function Evaluation

Immediately after a DCS diagnosis, the Basso–Beattie–Bresnahan (BBB) scale was used to evaluate the motor function of surviving rats. The score ranged from 0 to 21, with 0 indicating complete hindlimb disability and 21 indicating normal motor function; these scores are defined by the combinations of joint and limb movements, limb coordination, trunk stability, steps, paw placement, and tail position (Bhimani et al., 2017). Rats were allowed to walk freely for 3 min in an open field. Hindlimb movements and coordination were observed and scored by two experienced observers who were blinded to the treatments. All rats displayed normal motor function before the experiment.

HSP32 Quantification

Western blot analysis was performed to quantify spinal cord HSP32. In brief, 2 h after simulated air diving rats were euthanized by anesthesia overdose, then T10-L4 thoracolumbar spinal cords were removed and homogenated. Protein samples were collected and concentration determined with BCA Kits (Beyotime). The samples were electrophoresed and transferred to polyvinylidene fluoride membranes. Membranes were incubated with rabbit monoclonal primary antibodies directed against rat HSP32 (ab13243, Abcam, United Kingdom) and β-actin (4970, CST, United States). Proteins were visualized using infrared anti-rabbit IgG (5151, CST), and the intensity of each band was imaged in an Odyssey imaging system (Li-Cor Bioscience, United States). Ratios of HSP32 to β-actin were calculated.

Biochemical Analysis

Spinal cords were sampled in surviving rats 2 h after simulated air diving as described above. Venous blood was drawn from the postcava at the same time, then serum was collected after centrifuging. Spinal cord and serum levels of interleukin-1β (IL-1β), tumor necrosis factor-α (TNF-α), and neuron-specific enolase (NSE) were assayed by ELISA kits (Jiancheng Bioengineering Institute, China). Malondialdehyde (MDA) was detected by thiobarbituric acid colorimetric methods assay kits (Beyotime). Caspase-3 activity was determined by spectrophotometry assay kits (Jiancheng). All assays were performed following the respective manufacturer's instructions.

Histological Examination

T10-L4 thoracolumbar spinal cords were postfixed in 4% formaldehyde, embedded in paraffin, sectioned serially, and mounted on silane-covered slides. Immunohistochemical staining was performed in two rounds: firstly, using the Neun antibody (ab177487, Abcam) and TYR-488 regent (Ex/Em: 490/520 nm, Shanghai Rainbow, China), and secondly, performing Tunel staining using the Tunel-CY3 kit (Ex/Em: 550/570 nm, Shanghai Rainbow) with standard protocols. Antigen retrieval was preformed between each step. Finally, nuclei were labeled by DAPI (Ex/Em: 358/461 nm, Shanghai Rainbow), sections were examined at a magnification of ×400, and three fields were randomly chosen to determine Tunel-positive cells by using a computer image analysis system (DS-U3, NIKON, Japan).

Statistical Analysis

Preliminary experiments indicated that 73% vs. 40% of DCS incidence should be expected for Air and NBO-U0126 treatments, respectively, and 35 rats per group were estimated as adequate for 80% power to show a difference in the incidence of DCS, based on a two-tailed significance level of 0.05. All data are presented as mean ± SD, except mortality, DCS incidence, and BBB score. A chi-square test was conducted to compare mortality or DCS incidence between different groups. BBB scores were analyzed using a Mann–Whitney test. Continuous variables were tested for normal distribution with the Kolmogorov–Smirnov test and compared among groups by one-way ANOVA via a Student–Newman–Keuls test or *post hoc* Dunnett's test. The threshold for significance was accepted at $P < 0.05$. SPSS 22.0 (SPSS Inc., United States) was used for statistical analysis.

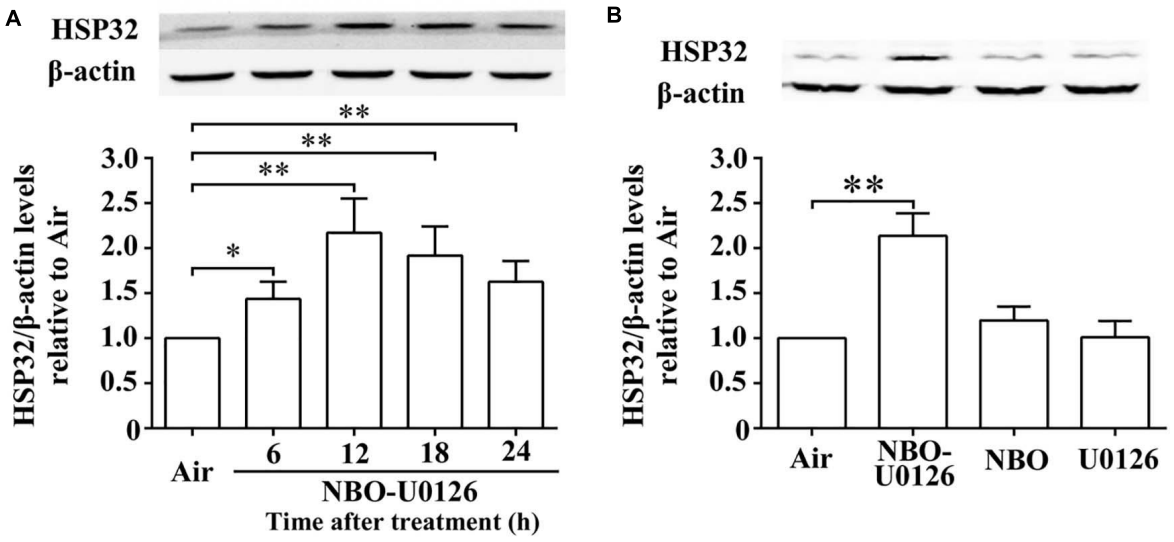

FIGURE 2 | Effects of NBO-U0126 on the expression of HSP32 in rat spinal cord. Rats were exposed with NBO and/or U0126, and spinal cord HSP32 was determined at designated times following treatment. **(A)** Time course expression of HSP32 ($n = 6$). **(B)** HSP32 expression at 12 h with different treatments ($n = 6$, the original image see in **Supplementary Material**). $^{*}P < 0.05$, $^{**}P < 0.01$.

RESULTS

Effects of NBO-U0126 on HSP32 Expression in Rat Spinal Cord

Western blot results showed that the expression of HSP32 in rat spinal cords increased significantly after NBO-U0126 treatment and peaked at 12 h ($P < 0.001$, **Figure 2A**). The factorial design analysis showed that neither NBO nor U0126 alone impacted on HSP32 expression ($P > 0.05$), but NBO and U0126 had a positive interaction on HSP32 upregulation in the NBO-U0126 treatment group ($P < 0.001$, **Figure 2B**).

Effects of NBO-U0126 on the Incidence and Mortality of DCS

The incidence of DCS in the NBO-U0126 group was significantly lower than in the Air group ($P = 0.029$, **Figure 3A**). Neither NBO nor U0126 alone had a significant impact on DCS incidence ($P > 0.05$), and no treatment made a significant difference to the latency or proportion of mortality in rats ($P > 0.05$).

Effects of NBO-U0126 on Motor Function and Spinal Cord Apoptosis After a Simulated Air Dive

BBB scores were markedly reduced after simulated diving, compared with controls ($P < 0.001$, **Figure 3B**). NBO-U0126 significantly increased the impaired scores in surviving rats ($P = 0.035$, **Figure 3B**). Tunel-positive cell numbers were markedly increased in DCS rats ($P < 0.001$, **Figure 4**), and NBO-U0126 reduced the impairment ($P = 0.001$, **Figure 4**).

Effects of NBO-U0126 on Spinal Cord and Serum Biomarkers After a Simulated Air Dive

After simulated air diving, all the spinal cord and serum injury biomarkers increased significantly ($P < 0.05$, **Figure 5**). NBO-U0126 reduced the deterioration of these parameters in surviving rats ($P < 0.05$, **Figure 5**).

DISCUSSION

DCS spinal cord injury is a critical medical concern in hyper-/hypo-baric exposures, which usually comes with severe symptoms and sequelae, and the pathogenesis is not fully clarified yet (Francis, 1998). Studies have found that decompression bubbles could induce spinal ischemia and inflammatory and oxidative stress, which may play important parts in the pathogenesis of DCS spinal cord injury (Hallenbeck et al., 1975; Francis, 1998). HSP32, also named heme oxygenase-1 (HO-1), has antioxidative, anti-inflammatory, and antiapoptotic properties by decomposing free heme and producing protective products including Fe^{2+}, carbon monoxide, and biliverdin (Gozzelino et al., 2010). Upregulation of HSP32 has been confirmed to alleviate a variety of central nervous system injuries including trauma, stroke, tumor, and neurodegeneration, especially in the spinal cord (Gozzelino et al., 2010; Sferrazzo et al., 2020).

Previous research from our team showed that a single exposure to 280 kPa HBO for 60 min reduced DCS spinal cord injury in rats (Ni et al., 2013), and ROS/p38 MAPK-mediated HSP32 upregulation was found to participate the process (Huang et al., 2014, 2016). Interestingly, a MEK1/2-mediated negative regulatory pathway was found to be simultaneously involved,

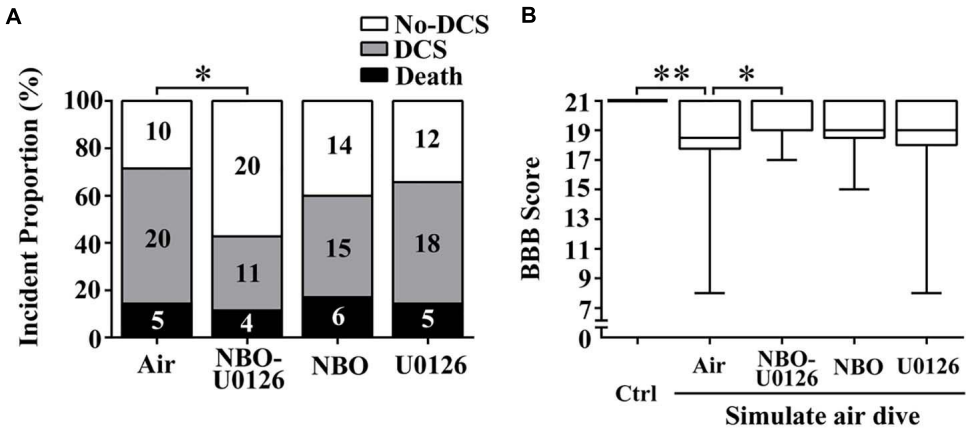

FIGURE 3 | Effects of NBO-U0126 on DCS incidence and motor function in rats. Rats were treated with NBO and/or U0126, 12 h prior to simulated air dives. The BBB scale was used to evaluate rat hindlimb motor function. **(A)** Incidence of DCS (n = 35, the numeric values in the bars are numbers of rats); **(B)** motor function scores in all surviving rats (Ctrl n = 12, Air n = 30, NBO-U0126 n = 31, NBO n = 29, U0126 n = 30). *P < 0.05, **P < 0.01.

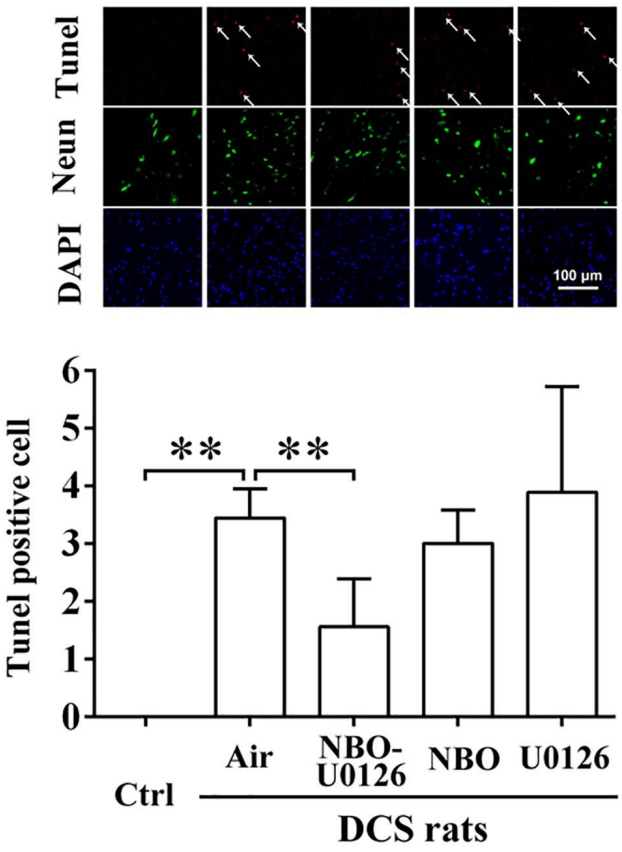

FIGURE 4 | Effect of NBO-U0126 on spinal cord apoptosis in DCS rats. Thoracolumbar spinal cords were sampled from surviving DCS rats at 2 h after simulated air dives, for Tunel/Neun immunohistochemistry to reveal cell apoptosis. Tunel-positive cells are labeled by arrows. **P < 0.01. (n = 6).

and inhibiting MEK1/2 led to overexpression of HSP32 (Huang et al., 2016). The results suggested that the 280-kPa-60-min HBO exposure may be excessive just for HSP32 expression, and a more moderate exposure regimen may be efficient in inducing HSP32 if the negative regulation is removed. The results in the present study verified this hypothesis, showing that the combined administration of NBO and MEK1/2 inhibitor U0126 achieved similar effects upon HSP32 expression as HBO did (Huang et al., 2014). Furthermore, NBO treatment alone showed only a non-significant slight increase in HSP32 expression, while U0126 alone had no effect.

Further observation identified that combined NBO-U0126 pretreatment markedly decreased the incidence of DCS from 71 to 43% in rats, which was not a simple overlay but a significant synergistic effect of the two treatments combined. The beneficial effect of NBO-U0126 upon DCS incidence was similar to that of the 280-kPa HBO treatment found in a previous study from our team (from 67 to 37%) (Ni et al., 2013).

Due to the abundance of lipids and lack of collateral circulation, the spinal cord is more prone to bubble damage (Francis, 1998; Huang et al., 2014). The current study again observed obvious signs and biomarker changes of spinal cord injury in all the simulated diving rats except those treated with NBO-U0126, in which group most of the deteriorated parameters were alleviated. Such effects were not observed among rats treated with NBO or U0126 alone. This appeared to be correlated with HSP32 expression, for neither NBO nor U0126 alone improved HSP32 expression in the spinal cord. By decomposing oxidative free heme and producing reductive biliverdin and Fe^{2+}, HSP32 enables antioxidation (Gozzelino, 2016). Carbon monoxide, another metabolin of HSP32, is able to mediate anti-apoptosis and anti-inflammation via the sGC pathway (Ryter, 2019). While oxidative stress, inflammation, and apoptosis are pivotal pathogenesis in DCS spinal cord injury, the beneficial outcomes from the NBO-U0126-treated rats suggest that HSP32 participates in the process of DCS spinal cord injury.

NBO-U0126 pretreatment had limited impact on the mortality in rats in the current study. This may be related to the rapid formation of bubbles and subsequent embolism

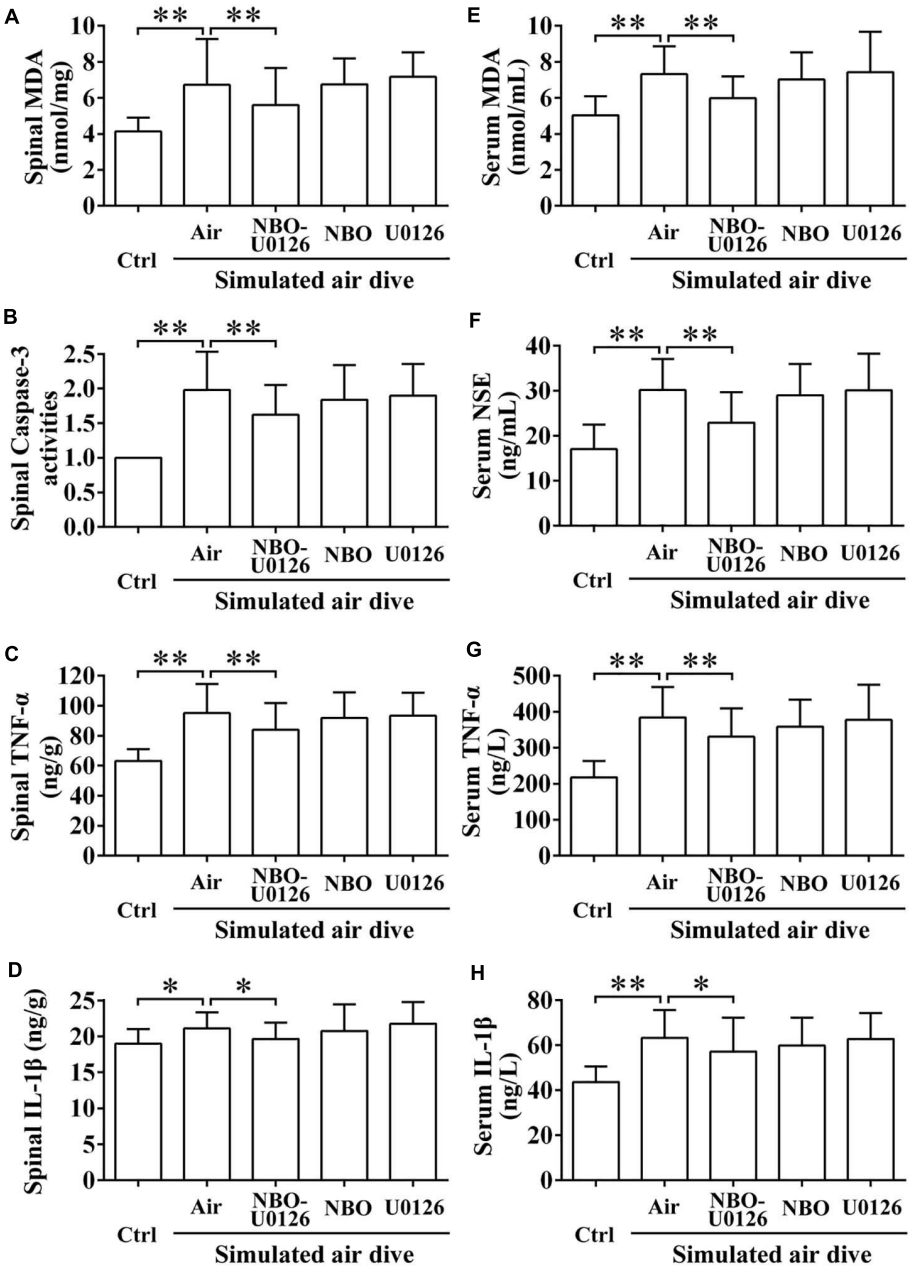

FIGURE 5 | Effects of NBO-U0126 on spinal cord and serum biomarkers after simulated air dive. Spinal cord and serum biomarkers were measured in all surviving rats 2 h after simulated air dive (Ctrl $n = 12$, Air $n = 30$, NBO-U0126 $n = 31$, NBO $n = 29$, U0126 $n = 30$). **(A–D)** Spinal cord biomarkers; **(E–H)** Serum biomarkers. $^{*}P < 0.05$, $^{**}P < 0.01$.

after decompression, leading to acute cardiopulmonary failure (Yount, 1979; Wisløff and Brubakk, 2001). Bubbles are likely the pathogenic factor for DCS, but in a previous study from our team, reducing bubble formation did not improve in the preventive effect of HBO pretreatment in rats (Ni et al., 2013). All mortal cases in this study occurred suddenly with respiratory distress or convulsions in seconds and were consistent with acute circulatory embolism (Yount, 1979; Wisløff and Brubakk, 2001).

Given the systemic effects of oxygen breathing and intraperitoneal administration of U0126, the protection of NBO-U0126 pretreatment upon DCS is possibly not limited to the spinal cord. The improvement of serum oxidative and inflammatory markers may be an indication of systemic protection. Although such improvements related to the alleviation of DCS spinal cord injury, the improvement of NSE may indicate reduced damage to the nervous system. Among the parameters investigated, the increase and improvement of IL-1β were more pronounced in serum than in spinal cord tissue. Given that serum IL-1β was reported responsible for

circulating microparticle-mediated DCS vascular injuries (Thom et al., 2018), our results support a potential systemic effect of NBO-U0126 pretreatment.

In summary, pretreatment with NBO and MEK1/2 inhibitor U0126 combined efficiently reduced the incidence of DCS and alleviated DCS spinal cord injury via the antioxidative, anti-inflammatory, and anti-apoptotic effects by HSP32 upregulation in the spinal cord. To our knowledge, this may be the first report that atmospheric pure oxygen can reduce DCS injury severity with greater effect using the synergism of a chemical agent. To fully realize the beneficial effects of hyperbaric treatment under atmospheric pressure, where a hyperbaric chamber is not available, the application of normobaric oxygen administration could be augmented in support of various hyper-/hypo-baric practices. Further research on the mechanisms underpinning these results is under way.

DATA AVAILABILITY STATEMENT

The raw data supporting the conclusions of this article will be made available by the authors, without undue reservation.

ETHICS STATEMENT

The animal study was reviewed and approved by the Ethics Committee for Animal Experiments of the Naval Medical University.

AUTHOR CONTRIBUTIONS

WX, GH, and QZ designed the experiments. QZ, XM, HY, and GH conducted the experiments. QZ, XM, JZ, and GH contributed to data analyses and interpretation of the results. QZ, XM, GH, KZ, and WX wrote the manuscript and prepared all the figures. All authors contributed to the article and approved the submitted version.

FUNDING

This work was supported by the National Natural Science Foundation of China (Nos. 81772014 and 81801868).

ACKNOWLEDGMENTS

We thank Dr. Peter Buzzacott for language polishing.

SUPPLEMENTARY MATERIAL

The Supplementary Material for this article can be found online at: https://www.frontiersin.org/articles/10.3389/fphys.2021.674430/full#supplementary-material

REFERENCES

Arieli, R., Boaron, E., and Abramovich, A. (2009). Combined effect of denucleation and denitrogenation on the risk of decompression sickness in rats. *J. Appl. Physiol.* 106, 1453–1458. doi: 10.1152/japplphysiol.91146.2008

Bhimani, A. D., Kheirkhah, P., Arnone, G. D., Nahhas, C. R., Kumar, P., Wonais, M., et al. (2017). Functional gait analysis in a spinal contusion rat model. *Neurosci. Biobehav. Rev.* 83, 540–546. doi: 10.1016/j.neubiorev.2017.09.007

Blatteau, J. E., Gempp, E., Simon, O., Coulange, M., Delafosse, B., Souday, V., et al. (2011). Prognostic factors of spinal cord decompression sickness in recreational diving: retrospective and multicentric analysis of 279 cases. *Neurocrit. Care* 15, 120–127. doi: 10.1007/s12028-010-9370-1

Camporesi, E. M., and Bosco, G. (2014). Hyperbaric oxygen pretreatment and preconditioning. *Undersea Hyperb. Med.* 41, 259–263.

Fan, D. F., Liu, K., Xu, W. G., Zhang, R. J., Liu, Y., Kang, Z. M., et al. (2010). Hyperbaric oxygen preconditioning reduces the incidence of decompression sickness in rats via nitric oxide. *Undersea Hyperb. Med.* 37, 173–180.

Francis, J. (1998). Mechanisms of spinal cord injury in DCI. *SPUMS J.* 28, 29–41.

Gonzales-Portillo, B., Lippert, T., Nguyen, H., Lee, J. Y., and Borlongan, C. V. (2019). Hyperbaric oxygen therapy: a new look on treating stroke and traumatic brain injury. *Brain Circ.* 5, 101–105. doi: 10.4103/bc.bc_31_19

Gozzelino, R. (2016). The pathophysiology of heme in the brain. *Curr. Alzheimer Res.* 13, 174–184. doi: 10.2174/1567205012666150921103304

Gozzelino, R., Jeney, V., and Soares, M. P. (2010). Mechanisms of cell protection by heme oxygenase-1. *Annu. Rev. Pharmacol. Toxicol.* 50, 323–354. doi: 10.1146/annurev.pharmtox.010909.105600

Hallenbeck, J. M., Bove, A. A., and Elliott, D. H. (1975). Mechanisms underlying spinal cord damage in decompression sickness. *Neurology* 25, 308–316. doi: 10.1212/wnl.25.4.308

Huang, G., Diao, J., Yi, H., Xu, L., Xu, J., and Xu, W. (2016). Signaling pathways involved in HSP32 induction by hyperbaric oxygen in rat spinal neurons. *Redox. Biol.* 10, 108–118. doi: 10.1016/j.redox.2016.09.011

Huang, G., Xu, J., Xu, L., Wang, S., Li, R., Liu, K., et al. (2014). Hyperbaric oxygen preconditioning induces tolerance against oxidative injury and oxygen-glucose deprivation by up-regulating heat shock protein 32 in rat spinal neurons. *PLoS One* 9:e85967. doi: 10.1371/journal.pone.0085967

Mahon, R. T., and Regis, D. P. (2014). Decompression and decompression sickness. *Compr. Physiol.* 4, 1157–1175. doi: 10.1002/cphy.c130039

Moon, R. E. (2014). Hyperbaric oxygen treatment for decompression sickness. *Undersea Hyperb. Med.* 41, 151–157.

Ni, X. X., Ni, M., Fan, D. F., Sun, Q., Kang, Z. M., Cai, Z. Y., et al. (2013). Heat-shock protein 70 is involved in hyperbaric oxygen preconditioning on decompression sickness in rats. *Exp. Biol. Med.* 238, 12–22. doi: 10.1258/ebm.2012.012101

Ryter, S. W. (2019). Heme oxygenase-1/carbon monoxide as modulators of autophagy and inflammation. *Arch. Biochem. Biophys.* 678:108186. doi: 10.1016/j.abb.2019.108186

Saadi, A., Ferenczi, E. A., and Reda, H. (2019). Spinal decompression sickness in an experienced scuba diver: a case report and review of literature. *Neurohospitalist* 9, 235–238. doi: 10.1177/1941874419828895

Schipper, H. M., Song, W., Tavitian, A., and Cressatti, M. (2019). The sinister face of heme oxygenase-1 in brain aging and disease. *Prog. Neurobiol.* 172, 40–70. doi: 10.1016/j.pneurobio.2018.06.008

Sferrazzo, G., Di Rosa, M., Barone, E., and Li Volti, G. (2020). Heme oxygenase-1 in central nervous system malignancies. *J. Clin. Med.* 9:1562. doi: 10.3390/jcm9051562

Thom, S. R., Bhopale, V. M., Yu, K., and Yang, M. (2018). Provocative decompression causes diffuse vascular injury in mice mediated by

microparticles containing interleukin-1β. *J. Appl. Physiol.* 125, 1339-1348. doi: 10.1152/japplphysiol.00620.2018

Vann, R. D., Butler, F. K., Mitchell, S. J., and Moon, R. E. (2011). Decompression illness. *Lancet* 377, 153–164. doi: 10.1016/s0140-6736(10)61085-9

Wisløff, U., and Brubakk, A. O. (2001). Aerobic endurance training reduces bubble formation and increases survival in rats exposed to hyperbaric pressure. *J. Physiol.* 537, 607–611. doi: 10.1111/j.1469-7793.2001.00607.x

Yount, D. E. (1979). Application of a bubble formation model to decompression sickness in rats and humans. *Aviat. Space Environ. Med.* 50, 44–50.

Yu, X., Xu, J., Liu, W., Zhang, Z., He, C., and Xu, W. (2020). Protective effects of pulmonary surfactant on decompression sickness in rats. *J. Appl. Physiol.* 130, 400–407. doi: 10.1152/japplphysiol.00807.2020

Zhang, K., Jiang, Z., Ning, X., Yu, X., Xu, J., Buzzacott, P., et al. (2017). Endothelia-targeting protection by escin in decompression sickness rats. *Sci. Rep.* 7:41288. doi: 10.1038/srep41288

Zhang, K., Wang, D., Jiang, Z., Ning, X., Buzzacott, P., and Xu, W. (2016). Endothelial dysfunction correlates with decompression bubbles in rats. *Sci. Rep.* 6:33390. doi: 10.1038/srep33390

Zhang, K., Wang, D., Xu, J., Li, R., Cai, Z., Liu, K., et al. (2015). Simvastatin decreases incidence of decompression sickness in rats. *Undersea Hyperb. Med.* 42, 115–123.

Conflict of Interest: The authors declare that the research was conducted in the absence of any commercial or financial relationships that could be construed as a potential conflict of interest.

frontiers in Physiology

ORIGINAL RESEARCH
published: 10 June 2021
doi: 10.3389/fphys.2021.660402

Acute Effects on the Human Peripheral Blood Transcriptome of Decompression Sickness Secondary to Scuba Diving

*Kurt Magri[1], Ingrid Eftedal[2,3], Vanessa Petroni Magri[4], Lyubisa Matity[1], Charles Paul Azzopardi[1], Stephen Muscat[1] and Nikolai Paul Pace[5]**

[1] Hyperbaric Unit, Department of Medicine, Mater Dei Hospital, Msida, Malta, [2] Department of Circulation and Medical Imaging, Faculty of Medicine and Health Sciences, NTNU Norwegian University of Science and Technology, Trondheim, Norway, [3] Faculty of Nursing and Health Sciences, Nord University, Bodø, Norway, [4] Department of Clinical Pharmacology and Therapeutics, Faculty of Medicine and Surgery, University of Malta, Msida, Malta, [5] Centre for Molecular Medicine and Biobanking, Faculty of Medicine and Surgery, University of Malta, Msida, Malta

Decompression sickness (DCS) develops due to inert gas bubble formation in bodily tissues and in the circulation, leading to a wide range of potentially serious clinical manifestations. Its pathophysiology remains incompletely understood. In this study, we aim to explore changes in the human leukocyte transcriptome in divers with DCS compared to closely matched unaffected controls after uneventful diving. Cases (n = 7) were divers developing the typical cutis marmorata rash after diving with a confirmed clinical diagnosis of DCS. Controls (n = 6) were healthy divers who surfaced from a ≥25 msw dive without decompression violation or evidence of DCS. Blood was sampled at two separate time points—within 8 h of dive completion and 40–44 h later. Transcriptome analysis by RNA-Sequencing followed by bioinformatic analysis was carried out to identify differentially expressed genes and relate their function to biological pathways. In DCS cases, we identified enrichment of transcripts involved in acute inflammation, activation of innate immunity and free radical scavenging pathways, with specific upregulation of transcripts related to neutrophil function and degranulation. DCS-induced transcriptomic events were reversed at the second time point following exposure to hyperbaric oxygen. The observed changes are consistent with findings from animal models of DCS and highlight a continuum between the responses elicited by uneventful diving and diving complicated by DCS. This study sheds light on the inflammatory pathophysiology of DCS and the associated immune response. Such data may potentially be valuable in the search for novel treatments targeting this disease.

Keywords: decompression sickness, decompression illness, scuba diving, transcriptome, leukocyte gene expression, myeloid cell, immediate early genes

OPEN ACCESS

Edited by:
Michael Bennett, University of New South Wales, Australia

Reviewed by:
Neal William Pollock, Laval University, Canada
Padhmanand Sudhakar, KU Leuven, Belgium

****Correspondence:***
Nikolai Paul Pace
nikolai.p.pace@um.edu.mt

Specialty section:
This article was submitted to Systems Biology Archive, a section of the journal Frontiers in Physiology

Received: *02 February 2021*
Accepted: *12 May 2021*
Published: *10 June 2021*

Citation:
Magri K, Eftedal I, Petroni Magri V, Matity L, Azzopardi CP, Muscat S and Pace NP (2021) Acute Effects on the Human Peripheral Blood Transcriptome of Decompression Sickness Secondary to Scuba Diving. Front. Physiol. 12:660402. doi: 10.3389/fphys.2021.660402

INTRODUCTION

Decompression sickness (DCS) is a potentially fatal condition usually observed after scuba diving. It involves bubble formation in blood and tissues from dissolved inert gas (usually nitrogen or helium), secondary to a decrease in ambient pressure (decompression). Its manifestations range from a mild illness to a rapidly life-threatening one. One subtype of DCS presents with

cutaneous manifestations, termed cutis marmorata. Cutis marmorata manifesting after diving is pathognomonic of DCS. It consists of a patchy, geographical rash usually crossing the midline, commonly involving fatty tissues such as the abdomen, breasts, buttocks, thighs, but also the torso and back. It is well-established that this subtype of DCS is associated with arterialization of bubbles via intracardiac right-to-left shunting of venous gas emboli, most commonly due to the presence of a patent foramen ovale (PFO) (Wilmshurst, 2015). Another potential mechanism is through right-to-left shunting via intrapulmonary arteriovenous anastomoses (IPAVA) (Madden et al., 2015). This subtype of DCS is therefore distinct from musculoskeletal DCS, which is thought to be due to the presence of *in situ* autochthonous bubble formation (Edmonds et al., 2015).

The standard treatment for DCS involves oxygen delivered at an elevated ambient pressure, hyperbaric oxygen (HBO). Following hyperbaric treatment, complete resolution of symptoms occurs in 80–90% of cases (Edmonds et al., 2015). Yet, victims may suffer from long-term sequelae. Of note, DCS involving the spinal cord is challenging to treat. It may result in permanent paraplegia or paraparesis, together with bladder dysfunction with or without incontinence and sexual dysfunction (Tournebise et al., 1995). The search for new treatments for DCS as adjuncts to HBO and fluid resuscitation has so far been largely unsuccessful, with only weak evidence encouraging the use of lidocaine and the non-steroidal anti-inflammatory drug tenoxicam (Bennett et al., 2012; Edmonds et al., 2015).

Transcriptomic studies provide an opportunity to explore the pathophysiologic pathways and the underlying transcriptional mechanisms that drive disease. Potentially, this can serve as a stepping-stone toward the identification of novel biomarkers or druggable targets. Gene expression studies in humans have focused on cohorts of divers completing uneventful free diving or scuba diving. Eftedal et al. (2013) characterized the peripheral blood leukocyte transcriptome in healthy, experienced human scuba divers, and demonstrated upregulation of transcripts associated with apoptosis, inflammation, and the innate immune responses. Diving-induced leukocyte-specific shifts in transcriptional patterns were described, with downregulation of genes expressed by CD8+ T-lymphocytes and natural killer cells, and upregulation of genes expressed by neutrophils, monocytes, and macrophages (Eftedal et al., 2013). Human studies have demonstrated increased expression of antioxidant enzymes in healthy uneventful scuba diving, including upregulation of catalase (*CAT*), superoxide dismutase 1 (*SOD1*), and glutathione synthetase (*GSS*) (Kiboub et al., 2018; Perović et al., 2018). Additionally, diving triggers the development of a systemic proinflammatory state through altered regulation of genes in immune pathways (Tillmans et al., 2019; Mrakic-Sposta et al., 2020). Similarly, freediving elicits changes in the leukocyte transcriptome, with an increase in neutrophil granulocytes and a decrease of cytotoxic lymphocytes possibly driven by hypoxia (Eftedal et al., 2016).

Animal models have also demonstrated upregulation of proinflammatory signaling molecules in DCS (Bigley et al., 2008; Liu et al., 2014; Wang H.T. et al., 2015). Both uneventful diving and DCS trigger changes in the peripheral blood transcriptome, and distinguishing physiological responses from pathological changes is a major challenge. To the best of our knowledge, no study has evaluated a DCS-induced transcriptomic signature in humans. In this study, we aim to explore the evolution of leukocyte gene expression in human subjects with DCS compared to closely matched divers after uneventful diving using a hypothesis-free RNA sequencing approach.

MATERIALS AND METHODS

Ethics Statement

This study was approved by the institutional ethics review board of the University of Malta (FRECMDS_1718_058). All subjects gave written informed consent for their participation in the study and for genetic analysis. The study protocol is in compliance with the Declaration of Helsinki.

Patient Selection and Inclusion Criteria

Recruitment of DCS cases ($n = 7$) and controls ($n = 6$) was carried out by a diving medicine physician. Details of specific inclusion and exclusion criteria are presented in **Supplementary Table 1**. Briefly, the control group consisted of scuba divers performing recreational diving with local diving clubs. Diving club members received an invitation to participate on a voluntary basis. Divers satisfying the inclusion and exclusion criteria were consented, recruited, and sampled at Mater Dei Hospital, Malta. DCS cases were included in this study if they presented with the typical cutis marmorata rash within 8 h of surfacing from an underwater dive. Control subjects were divers who surfaced from a deep dive ($\geq$25 msw) without dive table violation and without any symptoms suggestive of DCS as ascertained by a diving medicine physician. Specific exclusion criteria included (a) age $<$ 18 years (b) self-reported consumption of alcohol and/or strenuous physical activity before T2 (c) symptoms suggestive of delayed DCS presentation in controls at T2 d) acute life-threatening clinical complications or death within 72 h of surfacing. The Francis and Smith classification for dysbaric illness was recorded for each subject (Francis and Smith, 1991). All study subjects were unrelated and of Caucasian ethnicity, and none suffered from diabetes mellitus, hypertension, asthma, ischemic heart disease, or congestive heart failure at the time of sampling.

Hempleman's stress index ($Q = P\sqrt{t}$) was computed for each dive in both groups, where Q = exposure index (ATA.min$^{0.5}$), P = maximum depth in atmospheres absolute (ATA), and t = total dive time in minutes (Hempleman, 1952). This exposure index has been used to limit commercial diving in previous studies (Hugon et al., 2018). Additionally, the gas burden as per the Francis and Smith classification of dysbaric illness was recorded (Mathieu, 2006). According to this classification, gas burden is defined as—I. Low (e.g., within prescribed no decompression limits), II. Medium (e.g., a dive requiring decompression stops prior to surfacing) and III. High (e.g., violation of prescribed decompression requirements).

For both DCS cases and controls, whole blood was sampled at two time points, T1—within 8 h of surfacing from diving

and T2—at 40–44 h after surfacing. At T1, controls received instructions to follow with regards to behavior/lifestyle in the period prior to the second sampling time. This included fasting for 10 h prior to the second sampling time, avoiding caffeine and alcohol intake and avoiding strenuous exercise. Identical instructions were provided to recruited DCS cases to follow prior to T2. All DCS cases received emergency HBO as per United States Navy Treatment Table Six between T1 and T2.

Data Collection

For all participants, information on dive profile (maximum depth, bottom time, total time of dive, gas mix), the number of dives within the previous 7 days, and previous history of DCS was recorded. Additionally, age, gender, body mass index, smoking status, past medical history, drug history, illicit substance use, caffeine intake on the day of the dive and alcohol during the 24 h prior to the first dive of the day were also recorded.

Sample Processing and RNA Sequencing

For RNA isolation, 2.5 mL of whole blood was collected in a PAXgene® Blood RNA Tube (PreAnalytiX, Qiagen/BD) from DCS cases and controls at both T1 and T2. The samples were frozen within 24 h and stored at -80°C till further use. RNA was extracted using the PAXgene® blood kit (PreAnalytiX, Qiagen/BD) and quantified by 260/280 nm absorbance using UV-spectrophotometry (Nanodrop®, Thermo Fisher Scientific). The quality of RNA was evaluated by RNA Integrity Number (RIN) determination using the RNA6000 Nano protocol on an Agilent 2100 Bioanalyzer system (Agilent, United States). The RIN values for samples undergoing transcriptome analysis ranged from 7.8 to 9.3. Depletion of alpha and beta globin mRNA was carried out using the GLOBINclear^{TM} kit (Thermo Fisher Scientific). To minimize batch effects, all samples were processed simultaneously by the same investigator.

RNA samples were submitted for library generation and sequencing by the Beijing Genomics Institute (BGI-Shenzhen). Briefly, poly(A) mRNA was enriched using poly(T) oligo-attached magnetic beads, followed by fragmentation. First strand cDNA synthesis was carried out using random hexamer N6 primers and reverse transcriptase. Following adaptor ligation to cDNA fragments, PCR amplification and purification, single stranded DNA circles were generated in a final library. DNA nanoballs (DNBs) were subsequently generated by rolling circle replication, which underwent paired end sequencing (100 bp) on the BGI DNBseq platform.

Data Processing and Bioinformatic Analysis

Raw reads were filtered using SOAPnuke (BGI-Shenzhen) and clean reads mapped to the reference human genome (GRCh37) using HISAT2 (Li et al., 2009; Kim et al., 2019). Transcript counts were obtained using RSEM (RNA-Seq by Expectation Maximization) and normalized as FPKM (Fragments Per Kilobase of transcript per Million mapped reads (Li and Dewey, 2011). The DESeq2 algorithm was used to evaluate differentially expressed genes (DEGs) (Love et al., 2014). The *p*-values were adjusted for multiple comparisons by the Benjamini and Hochberg method, and differential expression of the genes was determined using a false discovery rate (FDR) cutoff of <0.05 (Benjamini and Hochberg, 1995). DESeq2 analysis was performed on normalized expression data to include only genes expressed at the level of 1 or higher using default parameters in iDEP. To select DEGs, a fold change of more than $\pm$ 2 (log2FC $>$ 1) was used, in view of the relatively low range of dispersion of log2FC values detected.

Principal component analysis (PCA) was used to explore the clustering of data and to characterize the inter-and intra-group variability. Gene expression heatmaps, k-means clustering of DEGs and analysis of tissue-specific co-expression patterns were explored using iDEP.91[1] and the TopFunn module of the TopGene Suite software (Division of Biomedical Informatics, Cincinnati Children's Hospital Medical Center, Cincinnati, OH) (Chen et al., 2009; Ge et al., 2018). This analysis relates the observed DEGs' patterns to specific tissues and cell types.

To gain insight into the functional attributes of DEGs, pathway analysis was carried out using iPathwayGuide (Advaita Bioinformatics, Michigan, United States) and Reactome (Ahsan and Drăghici, 2017; Jassal et al., 2020). iPathwayGuide implements an "Impact Analysis" approach that takes into consideration the direction and type of all signals on a pathway to identify putative mechanisms that can explain the measured gene expression changes (Donato et al., 2013). Pathways were analyzed in the context of data obtained from both Kyoto Encyclopedia of Genes and Genomes (KEGG) and Reactome databases, and ontology data was analyzed using the Gene Ontology Consortium database (Ashburner et al., 2000; Kanehisa and Goto, 2000). Functional analysis was carried out using both iPathwayGuide and Reactome in view of discrepancies in pathway resources between databases that limit interoperability and might influence results (Domingo-Fernández et al., 2018). DEGs were also evaluated by comparison to published datasets describing the acute effects of scuba diving on the peripheral blood transcriptome (Eftedal et al., 2013). Enrichr was used to explore transcriptional regulatory networks and to identify transcription factors (TFs) enriched for target genes using the gene set library from the ChIP-x Enrichment Analysis (ChEA) database (Lachmann et al., 2010; Chen et al., 2013).

Summary Sequencing Metrics

For all samples, sequencing generated approximately 6 Gbp of data, with Q20 scores over 98% and a median mapping ratio of 72% (IQR 1.5). Using DESeq2, we identified 159 DEGs in the comparison between uneventful diving controls at T1 and DCS cases at T1 (130 upregulated genes in DCS, 29 downregulated genes in DCS)—**Supplementary Tables 2, 3**. For the comparison of DCS cases at T1 with DCS cases at T2, 300 DEGs were identified (41 upregulated in DCS cases at T2, 259 downregulated in DCS cases at T2)—**Supplementary Tables 4, 5**. No transcripts exceeded significance thresholds for the comparison between controls at T1 vs. controls at T2. Pairwise comparison of controls

[1] http://bioinformatics.sdstate.edu/idep/

at T2 with DCS cases at T2 identified only three transcripts which were significantly upregulated in DCS—**Supplementary Table 6**.

qPCR Validation

Independent validation of RNA sequencing data was sought by evaluating the direction and magnitude of differential expression for selected genes using two-step reverse transcription—quantitative PCR (RT-qPCR). Five genes were randomly selected from the DEG pool (*PTGDR2*, *G0S2*, *AREG*, *IL5RA*, and *BMX*). Primers were designed using Primer3 and verified for specificity using NCBI-BLAST (Rozen and Skaletsky, 2000; Kent, 2002). Two hundred nanograms of RNA per subject was used for cDNA library synthesis using the GoScript™ Reverse Transcription System (Promega Corporation). The first-strand cDNA synthesis reaction was primed with oligo(dT) primers. Following reverse transcription, a 1:5 dilution of the cDNA library was used as a template for a quantitative PCR reaction. qPCR was carried out in triplicate using an EvaGreen® Master mix (Solis BioDyne, Estonia) and a BioRad CFX96 instrument. The relative expression of each gene was determined using the $2^{-\Delta\Delta CT}$ method. Glyceraldehyde-3-phosphate dehydrogenase (*GAPDH*) was used as housekeeping gene reference standard. Primer sequences are listed in the **Supplementary Material**. Expression patterns of the five selected transcripts matched the direction of expression observed from the RNA-Seq data (**Supplementary Material**).

Statistical Analysis

Analysis of clinical data was performed using IBM SPSS v26. The Kolmogorov-Smirnov and Shapiro-Wilk tests as well as visual inspection of Q-Q plots were used to assess the normality of distribution of quantitative variables. Since most variables showed a skewed, non-normal distribution, non-parametric statistics were used. Pairwise comparison between case and control groups was carried out using the Mann-Whitney *U* test for continuous and ordinal dependent variables. Categorical dependent variables were compared using Fisher's exact test. Numerical data is presented as medians (interquartile range) and categorical data is presented as percentages. A p-value of < 0.05 was considered statistically significant.

TABLE 1 | Clinical characteristics of the study group.

Characteristics	DCS cases (n = 7)	Controls (n = 6)	p-value
Age	35 (6)	40 (2)	0.133
Gender:			
Males n(%)	5 (71)	4 (67)	
Females n (%)	2 (29)	2 (33)	0.999
Body mass index (kg/m^2)	26.3 (4.0)	26.5 (1.9)	0.568
Previous DCS:			
Yes n (%)	1 (14)	1 (17)	
No n (%)	6 (86)	5 (83)	0.999
Allergy/inflammatory conditions requiring daily medication:			
Yes n (%)	1 (14)	2 (33)	
No n (%)	6 (86)	4 (67)	0.559
Drug history:			
Yes n (%)	1 (14)	3 (50)	
No n (%)	6 (86)	3 (50)	0.266
Illicit drug use within the previous 1 month:			
Yes n (%)	2 (29)	0 (0)	
No n (%)	5 (71)	6 (100)	0.462
Alcohol within 24 h of the first dive of the day:			
Yes n (%)	6 (86)	3 (50)	
No n (%)	1 (14)	3 (50)	0.266
Smoking Status:			
Current Smoker (%)	3 (43)	2 (33)	
Ex-smoker n (%)	0 (0)	1 (17)	
Non-smoker n (%)	4 (57)	3 (50)	0.999
Caffeine intake on the day of the dive:			
Energy drink n (%)	1 (14)	1 (16)	
Coffee n (%)	4 (57)	4 (67)	
Tea n (%)	0 (0)	0 (0)	
Nil n (%)	2 (29)	1 (16)	0.681

Numerical data is presented as medians with interquartile ranges, categorical data is described as percentages. The interquartile range represents the difference between the 75th and 25th percentiles. Column values are compared by Mann-Whitney U test for quantitative variables and by Fisher's exact test for categorical variables.

RESULTS

Clinical and Dive Characteristics of the Study Cohort

The baseline clinical characteristics of the seven divers with clinical DCS and six unaffected controls who met the inclusion criteria is shown in **Table 1**, and detailed dive characteristics in **Table 2**. No statistically significant differences in baseline demographics, dive characteristics and the Hempleman stress index between case and control subjects were present. No difference in median C-reactive protein (CRP) levels between cases and controls at T1 was detected (0.7 mg/L vs. 1.3 mg/L, p = 0.223). Cases at T2 had significantly higher CRP levels than cases at T1 [5.5 (5.45) mg/L vs. 0.7 (1.5) mg/L, p = 0.015]. In the DCS cases analyzed, the time from surfacing to onset of symptoms was ≤60 min, with a mean time of 26 min. On first review by the diving medicine physician at the accident and emergency department, all seven cases manifested the typical cutis marmorata rash together with typical history, confirming the diagnosis of DCS. In six cases, this was the first ever episode of DCS. Three cases demonstrated multisystem involvement, and two of these were neurological-type DCS (vestibulocochlear or cerebral). There was no evidence of spinal cord involvement in any of the DCS subjects. One subject presented with limb pain; however, this was not exclusive limb-pain DCS since it was accompanied by a typical cutis marmorata skin rash and preceded by dyspnea. Four cases were cutaneous-only type DCS. Further details according to the Francis and Smith classification for dysbaric illness are provided in **Supplementary Table 9**. Of

TABLE 2 | Detailed dive and sampling time characteristics.

Characteristics	Cases (n = 7)	Controls (n = 6)	p-value
Gas burden:			
Low n(%)	3 (43)	3 (50)	
Medium n(%)	4 (57)	3 (50)	
High n(%)	0 (0)	0 (0)	0.999
Hempleman's stress index (ATA.min$^{0.5}$)	29.9 (6.9)	31.6 (3.7)	0.589
Bottom time (mins)	25.0 (15.5)	21.5 (4.5)	0.385
Total dive time (mins)	55.0 (18.5)	59.5 (13.8)	0.830
Maximum depth (msw)	31.0 (3.8)	32.2 (2.4)	0.315
Time between surfacing and sampling time 1 (h)	2.7 (0.5)	3.8 (1.3)	0.475
Time between surfacing and sampling time 2 (h)	42.9 (2.5)	43.7 (2.6)	0.775

Quantitative variables are presented as medians with interquartile ranges. The interquartile range represents the difference between the 75th and 25th percentiles. Categorical data is presented as percentages. Column values are compared by Mann-Whitney U test for quantitative variables and by Fisher's exact test for categorical variables.

note, three cases required further hyperbaric treatments after their initial emergency DCS hyperbaric treatment.

DCS Cases and Diving Controls at T1

The molecular signature of the identified DEGs was interrogated using gene enrichment and pathway perturbation analysis. In the comparison of DCS cases vs. diving controls at T1, statistical enrichment of genes driving cell proliferation in the colorectal cancer and PI3K-AKT signaling pathways was detected. Additionally, significant enrichment for transcripts with immune function in malaria, rheumatoid arthritis, C-type lectin receptor signaling, and Toll-like receptor signaling pathways was observed (**Table 3**). The top upregulated transcripts in this group include *AREG* (Amphiregulin) and *EREG* (Epiregulin), *FOS* and *G0S2*. *AREG* and *EREG* are secreted peptide autocrine hormones and members of the epidermal growth factor (EGF) family of proteins. They are involved in a wide range of biological processes including inflammation, wound healing, and cell proliferation (Zaiss et al., 2015). The *FOS* gene encodes a leucine zipper protein that dimerizes with proteins of the JUN family, thus forming transcription factor complex AP-1. It regulates cell proliferation, differentiation, and transformation. Expression of the FOS has also been associated with apoptotic cell death and muscle injury (Preston et al., 2000). The phosphatidylinositol 3'-kinase (PI3K)-AKT signaling pathway is activated by many types of cellular stimuli or toxic insults and regulates fundamental cellular functions such as transcription, translation, proliferation, growth, and survival. AKT functions in the control of key cellular processes by phosphorylating substrates involved in apoptosis, protein synthesis, metabolism, and cell cycle. Additionally, early response genes were observed to be upregulated in this comparison.

Gene ontology (GO) category enrichment analysis showed statistical overrepresentation of transcripts involved in chemotaxis, cell surface receptor signaling and cytokine production (GO—Biological processes). PCA revealed a difference in transcriptome profile between DCS cases and controls at T1, with the first two principal components explaining 63% of the variability across the two biological groups. A greater heterogeneity in transcriptomic profiles amongst replicates in the DCS group was observed, which can potentially be attributed to clinical heterogeneity. No significant overlap in datapoints representing cases and controls occurs, indicating relative uniformity in gene expression signatures within cases and control groups (**Figure 1**).

Comparison DCS Cases at T1 and T2

The comparison of gene expression signatures between DCS cases at T1 and T2 revealed significant differences in several transcripts (**Figure 2**). Pathway analysis of the DEGs exceeding significance thresholds for the casesT1-casesT2 comparison revealed statistical enrichment of the neutrophil degranulation, signaling by interleukins, IL-10 signaling, IL-4 and IL-13 signaling, and immune system pathways (**Table 4**). Importantly, almost all transcripts in these pathways were observed to undergo significant downregulation at T2. Gene ontology category analysis revealed overrepresentation of transcripts involved in neutrophil activation and degranulation (GO-biological process), RAGE receptor binding (GO-molecular function), and secretory granules (GO-cellular components).

TABLE 3 | The top overrepresented pathways identified through impact analysis of DEGs in the casesT1-controlsT1 comparison.

Pathway	Pathway ID	No. of genes (DE/All)	p-value	Overrepresented genes on pathway
Colorectal cancer	KEGG–05210	3/85	2.593 e-4	*AREG*, *EREG*, *FOS*
PI3K-AKT signaling	KEGG–04151 Reactome–R-HSA-2219530	8/314	2.617 e-4	*AREG*, *THBS1*, *EREG*, *KITLG*, *ANGPT1*, *SGK2*, *TLR4*, *GNG2*
Malaria	KEGG–05144	4/48	0.002	*THBS1*, *CXCL8*, *SDC2*, *TLR4*
Rheumatoid arthritis	KEGG–05323	5/85	0.003	*CXCL8*, *ANGPT1*, *CCL3*, *TLR4*, *FOS*
C-type lectin receptor signaling	KEGG–0425	4/103	0.003	*EGR3*, *CLEC4D*, *CLEC4E*, *CLEC6A*
Toll-like receptor signaling	KEGG–04620	5/93	0.006	*CXCL8*, *CCL4*, *CCL3*, *TLR4*, *FOS*
Cytokine signaling in the immune system	Reactome–R-HSA-1280215	9/676	0.0155	*FOS*, *IRS2*, *IL1R2*, *MAPK8*, *LGALS9*, *BCL2*, *SERPINB2*, *CCL4*

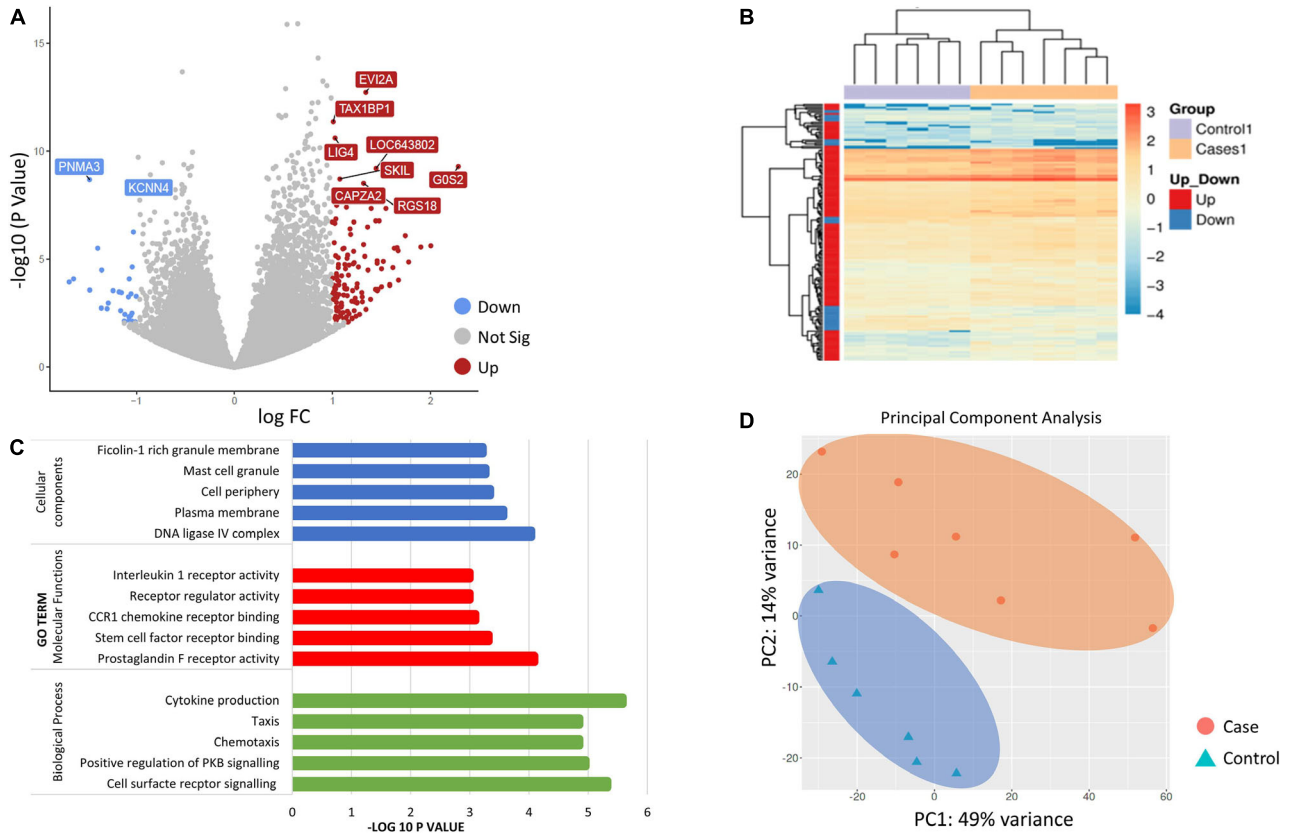

FIGURE 1 | (A) Volcano plot showing the top 10 significant differentially expressed genes (DEGs between controls and DCS cases at T1. The volcano plots distribution of log fold change (x-axis) and the negative log (base 10) of the *p*-values (y-axis). Upregulated genes are shown in of red while downregulated genes are shown in blue. **(B)** Heatmap of DEGs for the comparison of controls and cases at T1. Genes on heatmap are organized by hierarchical clustering based on the overall similarity in expression patterns. **(C)** Bar plots showing the top five enriched Gene Ontology terms. **(D)** Principal component analysis (PCA) depicting sample relationship based on dynamic gene expression. PCA identified two clusters in the data separated along the first and second principal components. The percentages on each axis represent the percentages of variation explained by the principal components. PC1 and PC2 define 49 and 14% of the variance, respectively. The distance between the points reflects the variance in gene expression between them. No significant overlap in datapoints representing cases and controls occurred, indicating relative uniformity in gene expression signatures between cases and controls.

To better characterize the time course of events following the initial DCS event, we evaluated similarities and differences with the DEGs arising from the case-control at T1 analysis. Ninety-six genes were exclusive to the comparison between casesT1-controlsT1, 237 genes were exclusive to the comparison between casesT1 and casesT2, and 63 genes were in common to both datasets, i.e., they were identified to be differentially expressed in both comparisons (**Figure 2**). Mechanistically, it is plausible to propose that the 96 genes which were exclusive to the casesT1-controlsT1 comparison represent the early phase of the response to DCS. Furthermore, the 237 genes which were exclusive to the casesT1-casesT2 comparison represent a combination of (a) the later (delayed) manifestations of DCS, (b) the pathophysiological response to DCS involving repair and recovery mechanisms, and/or (c) the physiological response to HBO. All DCS cases recruited in this study made complete clinical recovery by T2, hence it is unlikely that the 237 transcripts unique to the casesT1-casesT2 comparison reflect an ongoing or sustained response to DCS. Nevertheless, a prolonged subclinical pathophysiological reaction cannot be excluded.

To further relate the transcriptomic signature to the clinical resolution of DCS and the effects of HBO, we evaluated the direction of gene expression change in the DEG list at the intersection of the two datasets. These 63 transcripts exceeded statistical thresholds of significance in both the casesT1-controlsT1 and casesT1-casesT2 comparison, suggesting that their expression is causally related to the development and/or progression of DCS. Interestingly, for all the 63 genes, the direction of expression was completely reversed in cases at time point 2 compared to cases at time point 1, indicating that the resolution of DCS and the exposure to HBO significantly impacts on their expression. Pathway enrichment analysis applied to the 63 DEGs at the intersection of the two comparison reveals statistical overrepresentation of PI3K signaling ($p = 4.8 \times 10^{-3}$), consistent with earlier results demonstrating significant perturbation of the PI3K-AKT pathway in DCS cases compared to controls.

Exploratory PCA analysis was also applied to gene expression data from the four biological groups (DCS cases at T1 and T2, uneventful diving controls at T1 and T2 considered in

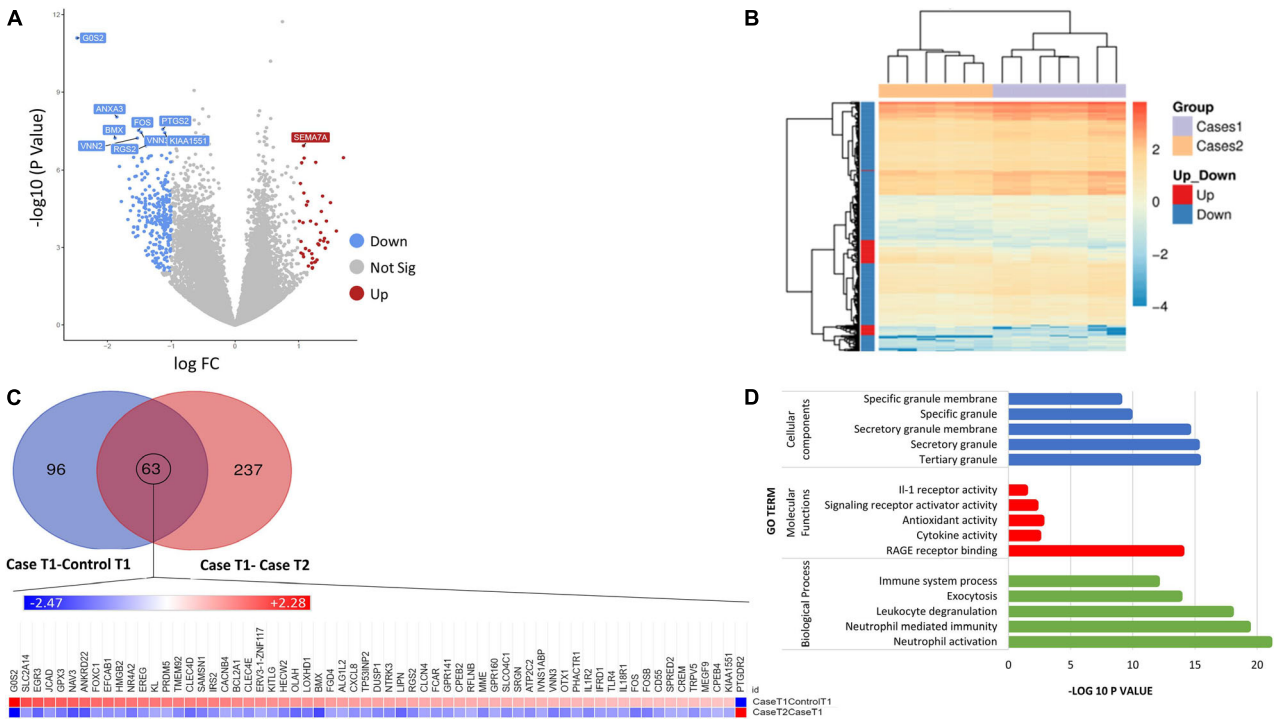

FIGURE 2 | (A) Volcano plot showing the top 10 significant DEGs between DCS cases at T1 and DCS at T2. Upregulated genes are shown in red while downregulated genes are shown in blue. **(B)** Heatmap of differentially expressed genes (DEGs) for the comparison of DCS cases at T1 vs. DCS cases at T2. Genes on heatmaps are organized by hierarchical clustering based on the overall similarity in expression patterns. The volcano plots distribution of log fold change (x-axis) and the negative log (base 10) of the *p*-values (y-axis). **(C)** Venn diagram illustrating DEG overlap between the caseT1-controlT1 and caseT2-controlT2 comparison. 63 transcripts at the intersection showed significance in differential expression across both comparisons. The heat map shows that the direction of expression of these transcripts is reversed at T2, suggesting that the resolution of DCS or the exposure to hyperbaric oxygen impacts on their expression. **(D)** Bar plots showing the top 5 enriched Gene Ontology terms for the caseT2-caseT1 comparison.

TABLE 4 | The top overrepresented pathways identified through impact analysis of DEGs in the casesT1-casesT2 comparison.

Pathway	Pathway ID	No. of genes (DE/All)	*p*-value	Overrepresented genes on pathway
Neutrophil degranulation	R-HSA-6798695	43/480	4.44 e-16	*CDA*, *ORM1*, *TNFAIP6*, *HP*, *SLC2A3*, *CXCL1*, *GPR84*
Signaling by interleukins	R-HSA-449147	33/639	9.88 e-7	*CXCL8*, *CEBPD*, *IL1R1*, *IL1R2*, *IL34*, *ALOX15*, *OSM*, *IL5RA*, *CXCL1*, *IRS2*, *FOS*
Il-4 and Il-13 signaling	R-HSA-6785807	16/211	8.33 e-6	*SOCS3*, *IL1A*, *CXCL8*, *CEBPD*, *BCL6*, *ALOX15*, *OSM*, *FOS*, *PTGS2*, *MMP9*
Immune system	R-HSA-168256	87/2,869	3.23 e-5	*CDA*, *ORM1*, *CXCL8*, *TNFAIP6*, *HP*, *IL5RA*, *SLC2A3*, *CXCL1*, *IRS2*, *PYGL*
Il-10 signaling	R-HSA-6783783	9/86	7.75 e-5	*IL1A*, *CXCL8*, *IL1R1*, *IL1R2*, *CXCL1*, *FPR2*, *PTGS2*
TNF signaling	KEGG–4668	7/110	0.0006	*MMP9*, *SOCS3*, *FOS*, *PTGS2*, *CXCL1*, *CREB6*, *IL18R1*

aggregate). PCA shows absence of separation between DCS cases at T2 and uneventful diving controls, while DCS cases at T1 demonstrated within-group heterogeneity and clustered differently from controls. Two distinct but broad clusters can be detected, largely defined by DCS cases at T1 and most of the controls (**Figure 3**). This analysis demonstrates that divers after uneventful diving demonstrate a relatively distinct gene expression signature from DCS cases. A greater heterogeneity in transcriptomic response can be observed in divers with DCS at times 1 and 2. It is plausible to propose that this heterogeneity in part reflects the combined effects of clinical treatment and varying resolution of the inflammatory stimulus.

K-Means Clustering and Analysis of Tissue-Specific Coexpression Patterns Reveals Leukocyte Subtype-Specific Gene Expression Signatures

K-means clustering was used to group gene expression signatures and to explore the GO terms enriched for each cluster. This unsupervised method enables the identification of transcripts that are co-functional and are coregulated. Based on the within-group sum of squares, $k = 4$ was chosen. The top 1,000 variable genes were included the analysis. K-means cluster analysis shows that genes in cluster A, strongly enriched for myeloid

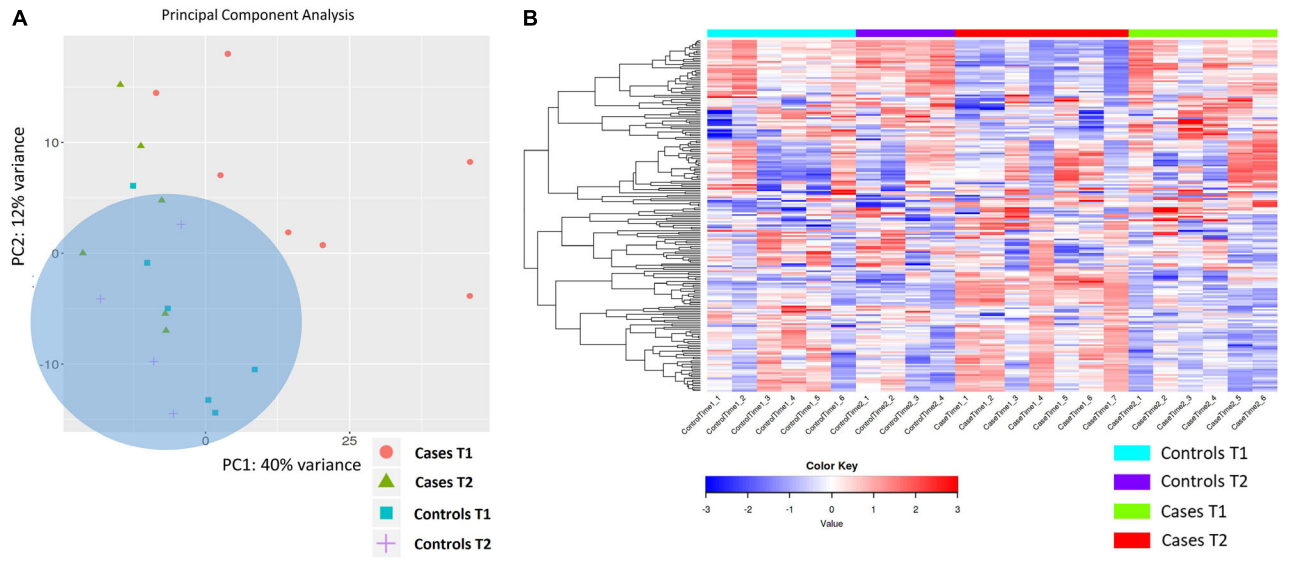

FIGURE 3 | (A) PCA analysis of gene expression across sequenced libraries repeated for DCS cases at T1 and T2 and uneventful diving controls at T1 and T2. PC1 and PC2 define 40 and 12% of the observed variance. A third component, PC3, defines 8% of the variance (not shown). Importantly, two distinct but broad clusters can be detected, largely defined by DCS cases at T1 and most of the controls in aggregate. **(B)** Heat map showing the top 200 DEGs across the four biological groups in this study. Genes on heatmap are organized by hierarchical clustering based on the overall similarity in expression patterns. Upregulated genes are shown in shades of red while downregulated genes are shown in shades of blue.

activation, neutrophil activation and leukocyte degranulation are upregulated in DCS cases at T1, while genes in cluster B, enriched for immune system processes, cell surface receptor signaling and lymphocyte activation were upregulated at T2 in DCS cases. Genes in clusters A and B showed opposing pattern of expression between DCS cases at T1 and T2, with expression patterns at T2 in DCS cases being largely similar to that observed in controls (**Figure 4**). To further relate the shift in gene expression patterns with specific leukocyte subtypes, we performed an analysis of tissue-specific patterns using ToppFun. The upregulated gene set in DCS cases at T1 are characteristic of myeloid cells, specifically CD11b + Ly6-G + neutrophils, monocytes, macrophages, and some dendritic cell subtypes (19/409 genes in annotation, $p = 2.029 \times 10^{-12}$). These cells produce Type I interferons and large quantities of reactive oxygen species (ROS). In keeping with K-means clustering analysis, the downregulated genes in DCS cases at T2 are again characteristic of myeloid cells.

Transcriptional Regulatory Networks

Transcriptional regulatory networks were explored using enrichment analysis of TF target gene sets. For the case T1-control T1 comparison, target genes of *SP1* (FDR = 5.9×10^{-2}), *GLIS2* (FDR = 1.1×10^{-2}) and *PAX5* (FDR = 1.5×10^{-1}) were overrepresented in down-regulated genes, while upregulated genes are enriched with target genes of *HLF* (FDR = 8.6×10^{-2}) and *FOXK1* (FDR = 1.3×10^{-1}). For the case T2-caseT1 comparison, target genes of *CEBPB* (FDR = 4.82×10^{-4}) and *SCL* (FDR = 1.73×10^{-3}) were overrepresented in upregulated genes, while downregulated genes were enriched for targets of *BACH1* (FDR = 2.984×10^{-7}) and *ZNF217* (FDR = 3.2×10^{-5}). *SP1*, *GLIS2*, *SCL*, and *FOXK1* play pivotal roles in cycle regulation. *PAX5* is a known regulator of B-cell development and *CEBPB* regulates the expression of genes involved in acute phase immune and inflammatory responses (Cobaleda et al., 2007, p. 5; Wang W. et al., 2015).

DISCUSSION

This study describes changes in the peripheral blood leukocyte transcriptome in divers with cutaneous DCS compared to matched controls after uneventful diving. It also evaluates the progression of these transcriptomic changes by comparison of gene expression at two discrete timepoints. We show that cutaneous DCS elicits the differential expression of several transcripts involved in leukocyte activity, inflammation, and cytokine production, with prominent perturbation of genes in the PI3K-AKT and TLR pathways. In fresh DCS cases within 8 h of surfacing from diving, upregulated transcripts are characteristic of the leukocyte myeloid lineage—specifically granulocytes. These show a significant downregulation when evaluated just under 48 h later. The reversal in the direction of expression of these transcripts is likely attributed to the effects of HBO and the clinical resolution of DCS. To the best of our knowledge, this is the first study that evaluates DCS-induced transcriptomic alterations in man.

DCS Triggers Activation of PI3K-Akt, TLR Pathways, and Immediate Early Genes

The findings from this study require meaningful interpretation in the context of existing knowledge on DCS. DCS is a systemic

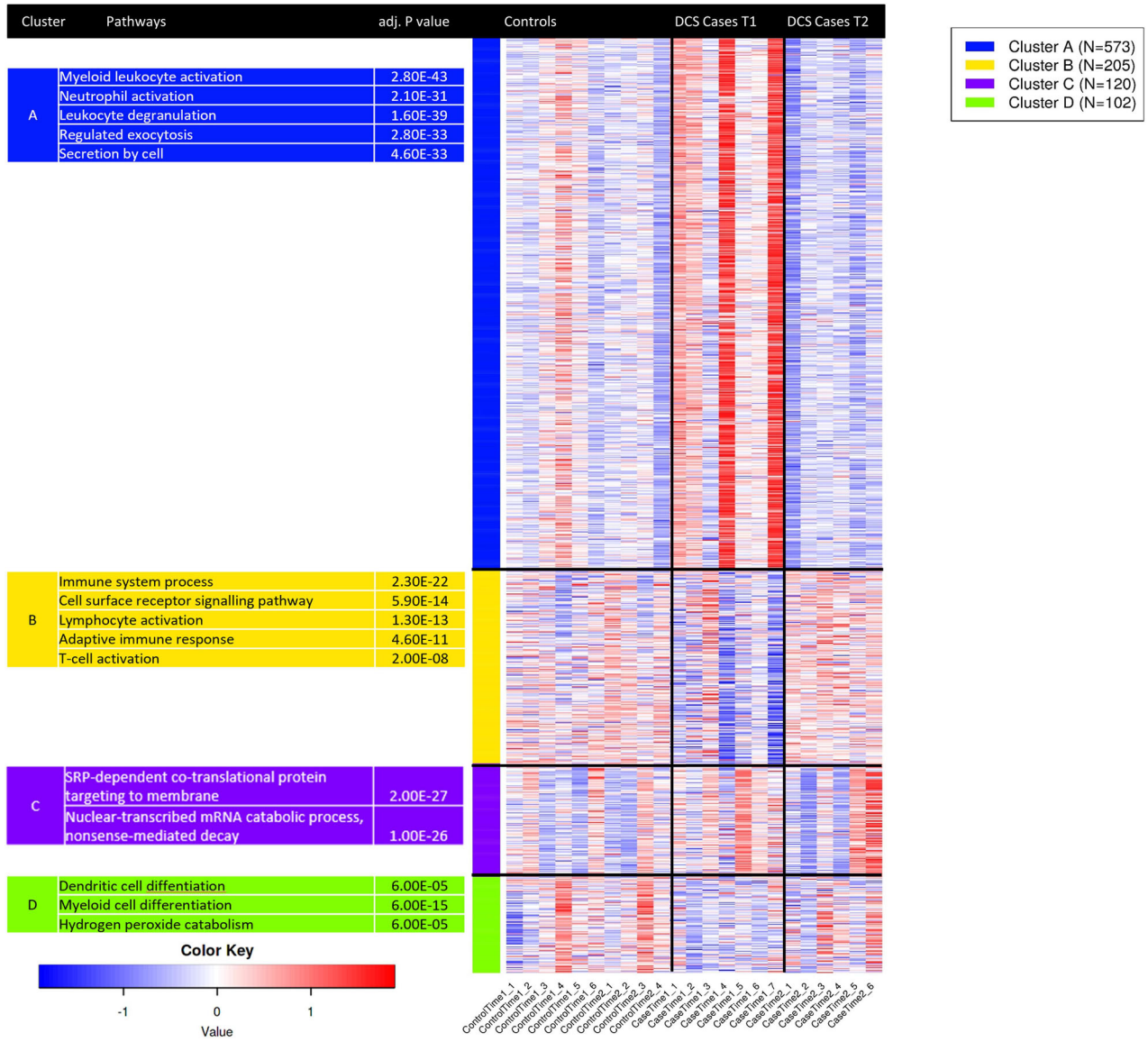

FIGURE 4 | K-means clustering analysis applied to the top 1,000 variable genes identifies co-regulated and co-functional transcripts. Genes in cluster A, strongly enriched for neutrophil activation, degranulation and myeloid activation are variably upregulated in DCS cases at T1. Genes in cluster B, strongly enriched for lymphocyte activation and T—cell activation are downregulated in DCS cases at T1. As GO terms are related or highly redundant, for each cluster the most significant terms are presented. Upregulated genes are shown in shades of red while downregulated genes are shown in shades of blue.

pathological process arising from the formation of inert gas bubbles in supersaturated tissues or blood following decreases in ambient pressure (Vann et al., 2011). Damage and dysfunction of the vascular endothelium following decompression has been reported in a number of animal studies (Nossum et al., 1999, 2002). Decompression-induced endothelial dysfunction correlates with bubble formation in rat models of DCS, an effect which is potentially attenuated by immunomodulatory drugs such as simvastatin or by NO donors (Møllerløkken et al., 2006; Zhang et al., 2015, 2016). In our study, acute phase DCS was accompanied by upregulation of genes involved in acute inflammation (*AREG*, *EREG*, *CXCL8*, *CCL4*, *EGR3*, *CLEC4E*, *CLEC6A*) and innate immunity (*TLR4*, *EGR3*). Amphiregulin (*AREG*) and epiregulin (*EREG*) are type II cytokines linked to a wide variety of inflammatory conditions, such as rheumatoid arthritis, chronic airway disease and glomerulonephritis (Yamane et al., 2008; Melderis et al., 2020). *AREG* skews monocytes and macrophages into a proinflammatory M1 phenotype, and the expression of *EREG* is induced by intermittent hypoxia (Kyotani et al., 2018). Toll-like receptors function in activation of the innate immune system, and *CXCL8* was the most strongly upregulated DEG for this pathway. *CXCL8* (IL-8) is a powerful chemoattractant involved in neutrophil recruitment and chemotaxis. *CXCL8* and other chemokines are consistently among the first signals to be expressed and released by the various cell types involved in inflammation (de Oliveira et al., 2013;

Torraca et al., 2017). Animal studies have demonstrated that acute DCS is accompanied by elevation of proinflammatory cytokines (TNF-α, IL-6, and IL-1) in both lung tissue and the circulation (Bigley et al., 2008; Chen et al., 2011). Thus, the proinflammatory gene expression signature of acute DCS described here is in keeping with evidence from previous *in vivo* animal studies. The acute-phase gene expression signature described in this report is significantly enriched for neutrophil and monocyte/macrophage-specific genes. Critically, this pattern is reversed at 40–44 h after surfacing from diving, following exposure to HBO. The role of neutrophil activation and vascular damage following microparticle release has been well-documented, with studies showing that exposure to inert gases at high pressure generates oxidative stress (Thom et al., 2011, 2014, 2015). Furthermore, uneventful diving triggers a similar shift in transcriptional pattern, with upregulation of genes expressed by myeloid cells and down regulation of CD8+ lymphocyte-expressed genes (Eftedal et al., 2013). Importantly, Eftedal et al. (2013) did not assess DCS or HBO exposures. The gene expression patterns described here are capturing the combined effect of three interrelated physiological stressors—diving, DCS and HBO exposure. At the two timepoints analyzed, these factors exert a varying effect on the magnitude and direction of the observed gene expression changes. It is likely that the diving-induced transcriptomic changes in the pathways observed by Eftedal et al. (2013) may have been obscured or possibly reversed in this study cohort. Furthermore, it is plausible to postulate that a direct continuum exists between the changes induced by uneventful diving and development of DCS, with the latter developing if the adverse physiological stimulus is in any way prolonged or sustained. Uneventful diving triggers a subclinical inflammatory response that can possibly progress to clinically overt DCS in susceptible individuals under extreme physiological conditions. In such a scenario, it is possible to hypothesize that the recruitment and activation of additional inflammatory pathways would potentially account for the observed clinical picture of DCS.

Pathway analysis in acute DCS demonstrates significant overrepresentation of PI3K-AKT and Toll-like receptor (TLR) signaling. The PI3K-AKT pathway has diverse cellular roles as it regulates proliferation, metabolism, survival, migration and tumor initiation (Cantley, 2002; Manning and Cantley, 2007). AKT positively regulates the production of reactive oxygen/nitrogen species (ROS/RNS) by modulating mitochondrial bioenergetics and activation of NADPH oxidases (Koundouros and Poulogiannis, 2018). TLR2 and TLR4 recognize pathogen-associated molecular patterns (PAMPs) on bacterial cell walls and activate innate immunity through NF-κB activity. TLR signaling augments activity of the PI3K-AKT pathway, and TLR2 or TLR4 activation on myeloid cells promotes the production of pro and anti-inflammatory cytokines (Weichhart et al., 2015). Recently, HBO therapy was shown to reverse AKT activity in a rat model of neuropathic pain (Liu et al., 2019). Importantly, Chen et al. (2011) showed that exposure to compression-decompression activates AKT signal transduction in the rat lung.

In addition, several other DEGs identified from the comparison of cases and controls within 8 h of surfacing from a dive are physiologically important. Of note, *EGR3* (Early Growth Response 3) was upregulated in DCS cases at T1. This transcription factor induces TGF-β, is a negative regulator of T-cell activation and is necessary for humoral immune tolerance (Morita et al., 2016). *JCAD* (Junctional Cadherin 5 Associated) is a junctional protein linked to proinflammatory changes and dysfunction of vascular endothelium (Shigeoka et al., 2020). *THBS1* (Thrombospondin 1) is a glycoprotein secreted by endothelium, where it participates in a broad array of functions related to vascular inflammation and cell-cell interactions (Liu Z. et al., 2015). *NR4A2* (Nuclear Receptor Subfamily 4 Group A Member 2) encodes an orphan nuclear receptor belonging to the steroid-thyroid hormone-retinoid receptor superfamily. *NR4A2* has also been shown to mediate acute inflammatory cascades (Doi et al., 2008). Members of the *NR4A* family are classified as "immediate early genes" (IEGs) induced by physiological and physical stimuli (Maxwell and Muscat, 2006). IEGs constitute a gateway to genomic responses, being rapidly and transiently activated in response to multiple stimuli. Their induction underlies acute inflammation (Wu et al., 2019). Gene expression studies following simulated diving in rats exposed to high bubble loads showed upregulation of *NR4A3*, a paralog of *NR4A2* (Eftedal et al., 2012). *G0S2* (G0/G1 switch gene 2) was significantly upregulated in DCS cases at T1. *G0S2* has disparate roles and is implicated in hypoxia-induced positive regulation of oxidative phosphorylation and induction of apoptosis by interaction with BCL2. *G0S2* is also an early response gene that is upregulated in autoimmune and inflammatory processes, and functions in the maintenance of T-cell quiescence (Yamada et al., 2011; Lee et al., 2015).

DCS Induces Activation of Antioxidant Defense Mechanisms

Our investigation also showed a significant upregulation of *GPX3* (Glutathione Peroxidase 3) in DCS cases at T1. This is an extracellular selenocysteine protein that plays a critical role in the scavenging of ROS. The upregulation of anti-oxidant pathways including *SOD2* and *GPX4* in diving has been described (Eftedal et al., 2013). In our study, *SOD2* was strongly expressed in both DCS cases and controls at T1, with a higher expression in DCS cases that, however, did not reach significance thresholds after adjustment for multiple testing. It is reasonable to postulate that *SOD2* was upregulated in response to diving in both DCS cases and controls, in keeping with previous studies. *SOD2* expression did not differ between controls at T1 and controls at T2. This is consistent with the findings of Perović et al. (2018) where the expression of *SOD2* normalized within 6 h post dive. In the casesT1-casesT2 comparison, nominal but significant downregulation of *SOD2* was observed at T2. Critically, extracellular superoxide activates neutrophils in a TLR4 dependent manner, and sub-lethal oxidative stress leads to selective activation of monocytes/macrophages through scavenger receptors (Lorne et al., 2008; Geiger-Maor et al., 2012).

Effect of HBO on the Peripheral Blood Transcriptome

The leukocyte gene expression patterns reported here are biologically meaningful. In acute DCS, the activation of inflammatory pathways playing critical roles in body defense is likely reflecting a physiological reaction triggered by a powerful exogenous stressor. However, the effect of HBO on gene expression is controversial and not fully ascertained. The transcriptomic changes in DCS cases at T2 are driven by the combined effects of clinical resolution of DCS and HBO therapy. This study was not designed to examine the relative contribution of each factor, and to the best of our knowledge the impact of HBO on the leukocyte transcriptome in man has not been reported. Limited inferences can be drawn from the literature. Godman et al. (2010) reported that hyperbaric exposure triggers the upregulation of antioxidant, cytoprotective, and IEGs in human microvascular endothelial cells, rendering them resistant to increased oxidative stress. Woo et al. (2020) showed that HBO alleviates exercise-induced inflammatory responses and muscle damage. Other investigators showed that a single HBO treatment significantly alters the expression of different inflammation and wound healing genes in endothelial cells at different timepoints (Kendall et al., 2012). HBO therapy is considered a useful anti-inflammatory adjunct in various pathologies (Novak et al., 2016; Hao et al., 2020). Conversely, HBO did not induce any pro-inflammatory, anti-inflammatory, or antioxidant effects in surgically induced inflammation in dogs (Gautier et al., 2019). Recently, a microarray transcriptome study showed that HBO does not exert significant effects on gene expression during surgical wound healing in rabbits (Tlapák et al., 2020). Critically, direct comparison of these studies is limited by differences in exposure, species, and the analytic methodology applied.

The DCS Transcriptome—Caveats and Challenges

The interpretation of transcriptomic signatures in DCS is challenging. Primarily, the DCS phenotype is clinically heterogenous, an effect which might account for within-group dispersion of gene expression. Additionally inter-subject and intra-subject variation in peripheral blood is well-recognized due to the dynamic nature of this tissue. In attempt to increase homogeneity in the DCS case cohort, we selected to only include divers exhibiting the cutis marmorata rash. This cutaneous manifestation is indicative of a systemic DCS pathology and an inflammatory response to nitrogen bubbles (Kalentzos, 2010). Cutis marmorata is not a universal feature of DCS and it is possible that the findings reported here are skewed toward one clinical subtype of DCS, and thus may not be generalizable to all forms of DCS. Secondly, acclimation to decompression has been described in rodent models (Montcalm-Smith et al., 2007, 2009). Chen et al. (2011) further show that repeated exposure to compression-decompression stress induces changes in EGR-1 and cytokine expression, although no acclimation-specific changes were detected. The physiological and molecular basis of acclimation are unknown, although reduced bubble load and attenuation of host responses have been suggested to play a role (Huang et al., 2003; Pontier et al., 2009). It is likely that the transcriptomic changes reported here are confounded to varying extents by interindividual differences in acclimation responses.

Are the Observed Transcriptomic Changes Confounded by Diving?

In view of the low incidence of DCS, this investigation was not designed to include pre-dive samples from DCS cases and controls. Pre-dive transcriptomic changes could thus not be directly investigated or considered as potential confounders. Furthermore, it is established that uneventful scuba diving triggers several acute gene-expression changes in blood sampled within 1 h of diving. Eftedal et al. (2013) characterized DEGs involved in apoptosis, immune responses, and inflammatory pathways that can be persistently deregulated in experienced divers. To increase the robustness and significance of this study, we sought to evaluate the DEG profile from the casesT1-controlsT1 comparison in this study to the dataset from Eftedal et al. (2013) showing acute blood transcriptomic changes after uneventful scuba diving. This analysis identified only seven DEGs at the intersection between the two datasets, of which five were consistently overexpressed in both datasets. This suggests that their expression is potentially modulated by the diving process itself rather than DCS. Conversely, two genes—*GZMB* and *ZFYVE16* showed an opposite direction of expression when the two datasets were compared. Interestingly, the magnitude of expression change was higher in DCS cases than in the Eftedal dataset. Eftedal et al. (2013) identified significant enrichment for the pathway containing *GZMB* (granzyme B) in response to uneventful diving, with *GZMB* and related genes undergoing transient change in expression and returning to predive levels between successive dives. In our dataset, *GZMB* underwent significant upregulation in DCS cases compared to diving controls. *GZMB* did not, however, exceed statistical significance thresholds when DCS cases at T2 were included in the comparison, implicating that upregulation of this gene may have persisted past 40–44 h from surfacing from the dive resulting in DCS. Although it cannot be fully evaluated in this study, its sustained upregulation provides evidence for a prolonged or persistent pro-inflammatory response. Similarly, *ZFYVE16* overlapped between the two datasets but showed an opposite direction of expression. The relevance of this locus to DCS biology is unknown. Comparison with the Eftedal dataset provides support for a minimal, yet relevant overlap between physiological responses elicited by uneventful diving and that of DCS. Furthermore, the absence of transcripts exceeding statistical significance thresholds between controls at T1 and controls at T2 reinforces the transient nature of transcriptomic changes, consistent with previous observations (Eftedal et al., 2013). We conclude that at the two sampling timepoints in this study, any gene expression changes induced by uneventful diving were reversed at T2.

Strengths and Limitations

Our investigation is strengthened by several factors. A unique human genomic signature of DCS has not been reported

previously. Here, a biologically agnostic high-throughput RNA sequencing approach is used. This method carries several advantages over microarray-based analysis, including low background noise and a large dynamic range (Hrdlickova et al., 2017). The RNA sequencing data was further validated using RT-qPCR. The selection of subjects followed stringent inclusion and exclusion criteria. To control for gene expression changes that arise due to diving, a comparably matched cohort of divers after uneventful diving was recruited. To ensure that the observed transcriptomic changes are a faithful representation of the DCS state, care was taken to minimize interindividual differences amongst the divers selected for this study. The peripheral blood transcriptome is known to broadly reflect the combined effects of pharmacotherapy, chronic disease, and environmental exposures such as smoking (Lampe et al., 2004; Liu Y. et al., 2015; Beretta et al., 2020; Ustinova et al., 2020). While these factors are integral components of many human studies, they can cause confounding in gene expression experiments.

This investigation carries a number of limitations. Primarily, the study was not designed to include pre-dive samples, hence the baseline stationary transcriptome could not be compared to the DCS changes at T1 and T2. DCS has a low incidence and is inherently unpredictable in nature, thus limiting prospective follow-up studies (Dardeau et al., 2012). Further investigations using simulated diving in animal models are necessary to clearly elucidate the transcriptomic effects of DCS and their time course. The small number of DCS cases meeting inclusion criteria necessitated the use of convenience sampling as opposed to random sampling, and selection bias cannot be fully excluded. In human subjects, the accurate quantification of decompression stress in uncontrolled environments is difficult. Despite our best efforts to ensure phenotypic homogeneity and comparability of the case and control cohorts, it is likely that uncontrolled factors persist. These may include differences in dive profiles and breathing gas composition that could modulate gene expression. The three-tier Francis and Smith classification and Hempleman's stress index may not fully capture the dynamic variation in dive characteristics or decompression profiles that could impact on the eventual clinical course. Additionally, we acknowledge that the unavailability of dive computer profile data and information on recent earlier diving is a significant limitation. Furthermore, gene expression data was not correlated to the quantitative determination of serum cytokine levels. A poor correlation between RNA expression and protein levels has been reported, in part due to variations in translational efficiency (Schwanhäusser et al., 2011; Cenik et al., 2015). Future research should also strive to evaluate the immunophenotype of peripheral blood leukocytes in response to DCS using flow cytometry to better define the inflammatory landscape in DCS.

Peripheral blood leukocytes were the primary source of RNA. These cells represent a highly heterogenous cell population, and dilution of biological effects due to the heterogenous cell population possibly accounts for the low range of log2FC (log2FC < 3) values detected in this study. In the targeted gene expression diving study by Chen et al. (2011) identically mild changes in cytokine gene expression were detected in rat lung. Of note, blood transcriptomic studies often apply arbitrary ranges of FC cut-offs (Greiner et al., 2013; Gaye et al., 2017; Dorsey et al., 2019; Ramsay et al., 2019). Furthermore, in many conditions, the magnitude of expression change in the global blood transcriptome may be subtle and generally lower than that observed in tissue-based experiments.

We also acknowledge that this investigation is limited by its small scale. While the findings from this pilot dataset offer insight into the transcriptomic responses to DCS, replication and independent validation in larger cohorts is warranted to enable robust and unbiased interpretation. Replication studies should also consider sampling at alternate time points to better elucidate the dynamics of the stress response elicited by DCS and its resolution. RNA-sequencing is, however, a powerful, precise tool in differential gene expression analysis and data robustness is dependent on the quality of each sample. This study is strengthened by the use of RNA exceeding the quality thresholds acceptable for a high throughput sequencing experiment. Quality control procedures following RNA extraction and bioinformatic analysis of sequencing data did not flag any outlier sample with poor quality issues.

Lastly, the paucity of human studies evaluating the DCS transcriptome limits comparison and interpretation of our findings. While comparison to various animal studies has been drawn, it must be emphasized that notable differences exist between rodents and man in the context of the genomic responses to acute inflammation (Osterburg et al., 2013; Seok et al., 2013). Metabolic differences between murine and human M1 macrophages have been described (Vijayan et al., 2019; Palmieri et al., 2020). Thom et al. (2014) showed that human and murine neutrophils exhibited similar responses to high pressure gases, however, murine cell microparticle production persisted even after decompression.

CONCLUSION

In this report we characterize the transcriptomic response elicited by DCS and its sequential progression in response to HBO therapy. This is a pilot investigation that provides a unique insight into the molecular etiology of this complex condition. DCS is accompanied by the dynamic regulation of several inflammatory and innate immune pathways, with a pronounced shift in transcriptional patterns characteristic of the myeloid lineage. Activation of free radical scavenging mechanisms is prominent in DCS. Our findings reinforce the role of acute inflammation in DCS and provide evidence for a continuum between the physiological response elicited by uneventful diving and diving complicated by DCS. Future studies with DCS cohorts are required to investigate the immunophenotype of peripheral blood leukocytes, as well as to enquire the epigenetic, metabolomics, and proteomic landscape of this disease.

DATA AVAILABILITY STATEMENT

The datasets presented in this study can be found in online repositories. The names of the repository/repositories and

accession number(s) can be found below: EMBL-EBI (www.ebi.ac.uk/arrayexpress) under accession number E-MTAB-10388. Intermediate analysis files have been uploaded on Dryad repository (doi: 10.5061/dryad.280gb5mpw).

ETHICS STATEMENT

The studies involving human participants were reviewed and approved by the Faculty Research Ethics Committee, University of Malta (FRECMDS_1718_058). The patients/participants provided their written informed consent to participate in this study.

AUTHOR CONTRIBUTIONS

KM, IE, LM, CA, SM, and NP: study conception and design. KM and VP: sample and data acquisition. KM, NP, IE, and VP: data analysis and drafting of the manuscript. IE and NP: project supervision. All authors contributed to the article and approved the submitted version.

FUNDING

This research was partly supported by Endeavour, which forms part of the European Union's European Social Fund—Operational Programme II—Cohesion Policy 2014–2020), by institutional funds of the University of Malta, and the Norwegian Research Council and Equinor on behalf of PRSI Pool (Petromaks2 Project No. 280425).

ACKNOWLEDGMENTS

We acknowledge the assistance of Anthony Fenech (Department of Clinical Pharmacology and Therapeutics, University of Malta) for his contribution to study design.

SUPPLEMENTARY MATERIAL

The Supplementary Material for this article can be found online at: https://www.frontiersin.org/articles/10.3389/fphys.2021.660402/full#supplementary-material

REFERENCES

Ahsan, S., and Drăghici, S. (2017). Identifying significantly impacted pathways and putative mechanisms with iPathwayGuide. *Curr. Protoc. Bioinformation* 57, 7.15.1–7.15.30.

Ashburner, M., Ball, C. A., Blake, J. A., Botstein, D., Butler, H., Cherry, J. M., et al. (2000). Gene ontology: tool for the unification of biology. the gene ontology consortium. *Nat. Genet.* 25, 25–29.

Benjamini, Y., and Hochberg, Y. (1995). Controlling the false discovery rate: a practical and powerful approach to multiple testing. *J. R. Stat. Soc. Ser. B Methodol.* 57, 289–300. doi: 10.1111/j.2517-6161.1995.tb02031.x

Bennett, M. H., Lehm, J. P., Mitchell, S. J., and Wasiak, J. (2012). Recompression and adjunctive therapy for decompression illness. *Cochrane Database Syst. Rev.* 2012:CD005277.

Beretta, L., Barturen, G., Vigone, B., Bellocchi, C., Hunzelmann, N., Langhe, E. D., et al. (2020). Genome-wide whole blood transcriptome profiling in a large European cohort of systemic sclerosis patients. *Ann. Rheum. Dis.* 79, 1218–1226. doi: 10.1136/annrheumdis-2020-217116

Bigley, N. J., Perymon, H., Bowman, G. C., Hull, B. E., Stills, H. F., and Henderson, R. A. (2008). Inflammatory cytokines and cell adhesion molecules in a rat model of decompression sickness. *J. Interferon Cytokine Res.* 28, 55–63. doi: 10.1089/jir.2007.0084

Cantley, L. C. (2002). The phosphoinositide 3-kinase pathway. *Science* 296, 1655–1657. doi: 10.1126/science.296.5573.1655

Cenik, C., Cenik, E. S., Byeon, G. W., Grubert, F., Candille, S. I., Spacek, D., et al. (2015). Integrative analysis of RNA, translation, and protein levels reveals distinct regulatory variation across humans. *Genome Res.* 25, 1610–1621. doi: 10.1101/gr.193342.115

Chen, E. Y., Tan, C. M., Kou, Y., Duan, Q., Wang, Z., Meirelles, G. V., et al. (2013). Enrichr: interactive and collaborative HTML5 gene list enrichment analysis tool. *BMC Bioinformatics* 14:128. doi: 10.1186/1471-2105-14-128

Chen, J., Bardes, E. E., Aronow, B. J., and Jegga, A. G. (2009). ToppGene suite for gene list enrichment analysis and candidate gene prioritization. *Nucleic Acids Res.* 37, W305–W311.

Chen, Y., Montcalm-Smith, E., Schlaerth, C., Auker, C., and McCarron, R. M. (2011). Acclimation to decompression: stress and cytokine gene expression in rat lungs. *J. Appl. Physiol.* 111, 1007–1013. doi: 10.1152/japplphysiol.01402.2010

Cobaleda, C., Schebesta, A., Delogu, A., and Busslinger, M. (2007). Pax5: the guardian of B cell identity and function. *Nat. Immunol.* 8, 463–470. doi: 10.1038/ni1454

Dardeau, M. R., Pollock, N. W., McDonald, C. M., and Lang, M. A. (2012). The incidence of decompression illness in 10 years of scientific diving. *Diving Hyperb. Med.* 42, 195–200. doi: 10.1016/b978-0-7216-9424-5.50016-2

de Oliveira, S., Reyes-Aldasoro, C. C., Candel, S., Renshaw, S. A., Mulero, V., and Calado, Â (2013). Cxcl8 (Interleukin-8) mediates neutrophil recruitment and behavior in the zebrafish inflammatory response. *J. Immunol.* 190, 4349–4359. doi: 10.4049/jimmunol.1203266

Doi, Y., Oki, S., Ozawa, T., Hohjoh, H., Miyake, S., and Yamamura, T. (2008). Orphan nuclear receptor NR4A2 expressed in T cells from multiple sclerosis mediates production of inflammatory cytokines. *Proc. Natl. Acad. Sci.* 105, 8381–8386. doi: 10.1073/pnas.0803454105

Domingo-Fernández, D., Hoyt, C. T., Bobis-Álvarez, C., Marín-Llaó, J., and Hofmann-Apitius, M. (2018). ComPath: an ecosystem for exploring, analyzing, and curating mappings across pathway databases. *Npj Syst. Biol. Appl.* 4:43.

Donato, M., Xu, Z., Tomoiaga, A., Granneman, J. G., MacKenzie, R. G., Bao, R., et al. (2013). Analysis and correction of crosstalk effects in pathway analysis. *Genome Res.* 23, 1885–1893. doi: 10.1101/gr.153551.112

Dorsey, S. G., Renn, C. L., Griffioen, M., Lassiter, C. B., Zhu, S., Huot-Creasy, H., et al. (2019). Whole blood transcriptomic profiles can differentiate vulnerability to chronic low back pain. *PLoS One* 14:e0216539. doi: 10.1371/journal.pone.0216539

Edmonds, C., Bennett, M., Lippmann, J., and Mitchell, S. (2015). *Diving and Subaquatic Medicin*, 5th Edition. Oakville: Apple Academic Press Inc.

Eftedal, I., Flatberg, A., Drvis, I., and Dujic, Z. (2016). Immune and inflammatory responses to freediving calculated from leukocyte gene expression profiles. *Physiol. Genomics* 48, 795–802. doi: 10.1152/physiolgenomics.00048.2016

Eftedal, I., Jørgensen, A., Røsbjørgen, R., Flatberg, A., and Brubakk, A. O. (2012). Early genetic responses in rat vascular tissue after simulated diving. *Physiol. Genomics* 44, 1201–1207. doi: 10.1152/physiolgenomics.00073.2012

Eftedal, I., Ljubkovic, M., Flatberg, A., Jørgensen, A., Brubakk, A. O., and Dujic, Z. (2013). Acute and potentially persistent effects of scuba diving on the blood transcriptome of experienced divers. *Physiol. Genomics* 45, 965–972. doi: 10.1152/physiolgenomics.00164.2012

Francis, T., and Smith, D. (eds). (1991). "Describing decompression illness," *Proceedings of the 42nd Workshop of the Undersea and Hyperbaric Medical Society* (Bethesda).

Gautier, A., Graff, E. C., Bacek, L., Fish, E. J., White, A., Palmer, L., et al. (2019). Effects of ovariohysterectomy and hyperbaric oxygen therapy on systemic inflammation and oxidation in dogs. *Front. Vet. Sci.* 6:506.

Gaye, A., Gibbons, G. H., Barry, C., Quarells, R., and Davis, S. K. (2017). Influence of socioeconomic status on the whole blood transcriptome in African Americans. *PLoS One* 12:e0187290. doi: 10.1371/journal.pone.0187290

Ge, S. X., Son, E. W., and Yao, R. (2018). iDEP: an integrated web application for differential expression and pathway analysis of RNA-Seq data. *BMC Bioinformatics* 19:534.

Geiger-Maor, A., Levi, I., Even-Ram, S., Smith, Y., Bowdish, D. M., Nussbaum, G., et al. (2012). Cells exposed to sublethal oxidative stress selectively attract monocytes/macrophages via scavenger receptors and MyD88-mediated signaling. *J. Immunol.* 188, 1234–1244. doi: 10.4049/jimmunol.1101740

Godman, C. A., Joshi, R., Giardina, C., Perdrizet, G., and Hightower, L. E. (2010). Hyperbaric oxygen treatment induces antioxidant gene expression. *Ann. N. Y. Acad. Sci.* 1197, 178–183. doi: 10.1111/j.1749-6632.2009.05393.x

Greiner, H. M., Horn, P. S., Holland, K., Collins, J., Hershey, A. D., and Glauser, T. A. (2013). mRNA blood expression patterns in new onset idiopathic pediatric epilepsy. *Epilepsia* 54, 272–279. doi: 10.1111/epi.12016

Hao, Y., Dong, X., Zhang, M., Liu, H., Zhu, L., and Wang, Y. (2020). Effects of hyperbaric oxygen therapy on the expression levels of the inflammatory factors interleukin-12p40, macrophage inflammatory protein-1β, platelet-derived growth factor-BB, and interleukin-1 receptor antagonist in keloids. *Medicine* 99:e19857. doi: 10.1097/md.0000000000019857

Hempleman, H. V. (1952). *Investigation into the Decompression Tables, Report III. Part A?: a New Theoretical Basis for the Calculation of Decompression Tables*. Available at: https://ci.nii.ac.jp/naid/10012835837/ (accessed April 8, 2021).

Hrdlickova, R., Toloue, M., and Tian, B. (2017). RNA-Seq methods for transcriptome analysis. *Wiley Interdiscip. Rev. RNA* 8:1364.

Huang, K. L., Wu, C. P., Chen, Y. L., Kang, B. H., and Lin, Y. C. (2003). Heat stress attenuates air bubble-induced acute lung injury: a novel mechanism of diving acclimatization. *J. Appl. Physiol.* 94, 1485–1490. doi: 10.1152/japplphysiol.00952.2002

Hugon, J., Metelkina, A., Barbaud, A., Nishi, R., Bouak, F., Blatteau, J.-E., et al. (2018). Reliability of venous gas embolism detection in the subclavian area for decompression stress assessment following scuba diving. *Diving Hyperb. Med.* 48, 132–140. doi: 10.28920/dhm48.3.132-140

Jassal, B., Matthews, L., Viteri, G., Gong, C., Lorente, P., Fabregat, A., et al. (2020). The reactome pathway knowledgebase. *Nucleic Acids Res.* 48, D498–D503.

Kalentzos, V. N. (2010). Cutis marmorata in decompression sickness. *Med. Hypotheses* 85, 863–869. doi: 10.1016/j.mehy.2015.09.022

Kanehisa, M., and Goto, S. (2000). KEGG: kyoto encyclopedia of genes and genomes. *Nucleic Acids Res.* 28, 27–30.

Kendall, A. C., Whatmore, J. L., Harries, L. W., Winyard, P. G., Smerdon, G. R., and Eggleton, P. (2012). Changes in inflammatory gene expression induced by hyperbaric oxygen treatment in human endothelial cells under chronic wound conditions. *Exp. Cell Res.* 318, 207–216. doi: 10.1016/j.yexcr.2011.10.014

Kent, W. J. (2002). BLAT–the BLAST-like alignment tool. *Genome Res.* 12, 656–664. doi: 10.1101/gr.229202.

Kiboub, F. Z., Møllerløkken, A., Hjelde, A., Flatberg, A., Loennechen, Ø, and Eftedal, I. (2018). Blood gene expression and vascular function biomarkers in professional saturation diving. *Front. Physiol.* 9:937.

Kim, D., Paggi, J. M., Park, C., Bennett, C., and Salzberg, S. L. (2019). Graph-based genome alignment and genotyping with HISAT2 and HISAT-genotype. *Nat. Biotechnol.* 37, 907–915. doi: 10.1038/s41587-019-0201-4

Koundouros, N., and Poulogiannis, G. (2018). Phosphoinositide 3-Kinase/Akt signaling and redox metabolism in cancer. *Front. Oncol.* 8:160.

Kyotani, Y., Itaya-Hironaka, A., Yamauchi, A., Sakuramoto-Tsuchida, S., Makino, M., Takasawa, S., et al. (2018). Intermittent hypoxia-induced epiregulin expression by IL-6 production in human coronary artery smooth muscle cells. *FEBS Open Bio* 8, 868–876. doi: 10.1002/2211-5463.12430

Lachmann, A., Xu, H., Krishnan, J., Berger, S. I., Mazloom, A. R., and Ma'ayan, A. (2010). ChEA: transcription factor regulation inferred from integrating genome-wide ChIP-X experiments. *Bioinformatics* 26, 2438–2444. doi: 10.1093/bioinformatics/btq466

Lampe, J. W., Stepaniants, S. B., Mao, M., Radich, J. P., Dai, H., Linsley, P. S., et al. (2004). Signatures of environmental exposures using peripheral leukocyte gene expression: tobacco smoke. *Cancer Epidemiol. Biomark. Prev.* 13, 445–453.

Lee, P.-H., Yamada, T., Park, C. S., Shen, Y., Puppi, M., and Lacorazza, H. D. (2015). G0S2 modulates homeostatic proliferation of naïve CD8+ T cells and inhibits oxidative phosphorylation in mitochondria. *Immunol. Cell Biol.* 93, 605–615. doi: 10.1038/icb.2015.9

Li, B., and Dewey, C. N. (2011). RSEM: accurate transcript quantification from RNA-Seq data with or without a reference genome. *BMC Bioinformatics* 12:323.

Li, R., Yu, C., Li, Y., Lam, T.-W., Yiu, S.-M., Kristiansen, K., et al. (2009). SOAP2: an improved ultrafast tool for short read alignment. *Bioinformatics* 25, 1966–1967. doi: 10.1093/bioinformatics/btp336

Liu, X., Cao, Y., Gao, G., Mao, R., Bi, L., and Geng, M. (2014). Gene expression profile of type II spinal cord decompression sickness. *Spinal Cord* 52, 606–610. doi: 10.1038/sc.2014.65

Liu, Y., Morley, M., Brandimarto, J., Hannenhalli, S., Hu, Y., Ashley, E. A., et al. (2015). RNA-Seq identifies novel myocardial gene expression signatures of heart failure. *Genomics* 105, 83–89. doi: 10.1016/j.ygeno.2014.12.002

Liu, Y.-D., Wang, Z.-B., Han, G., Jin, L., and Zhao, P. (2019). Hyperbaric oxygen relieves neuropathic pain through AKT/TSC2/mTOR pathway activity to induce autophagy. *J. Pain Res.* 12, 443–451. doi: 10.2147/jpr.s189353

Liu, Z., Morgan, S., Ren, J., Wang, Q., Annis, D. S., Mosher, D. F., et al. (2015). Thrombospondin-1 (TSP1) contributes to the development of vascular inflammation by regulating monocytic cell motility in mouse models of abdominal aortic aneurysm. *Circ. Res.* 117, 129–141. doi: 10.1161/circresaha.117.305262

Lorne, E., Zmijewski, J. W., Zhao, X., Liu, G., Tsuruta, Y., Park, Y.-J., et al. (2008). Role of extracellular superoxide in neutrophil activation: interactions between xanthine oxidase and TLR4 induce proinflammatory cytokine production. *Am. J. Physiol. Cell Physiol.* 294, C985–C993.

Love, M. I., Huber, W., and Anders, S. (2014). Moderated estimation of fold change and dispersion for RNA-seq data with DESeq2. *Genome Biol.* 15:550.

Madden, D., Ljubkovic, M., and Dujic, Z. (2015). Intrapulmonary shunt and SCUBA diving: another risk factor? *Echocardiography* 32(Suppl. 3), S205–S210.

Manning, B. D., and Cantley, L. C. (2007). AKT/PKB signaling: navigating downstream. *Cell* 129, 1261–1274. doi: 10.1016/j.cell.2007.06.009

Mathieu, D. (2006). *Handbook on Hyperbaric Medicine*. Berlin: Springer.

Maxwell, M. A., and Muscat, G. E. O. (2006). The NR4A subgroup: immediate early response genes with pleiotropic physiological roles. *Nucl. Recept. Signal.* 4:e002.

Melderis, S., Hagenstein, J., Warkotsch, M. T., Dang, J., Herrnstadt, G. R., Niehus, C. B., et al. (2020). Amphiregulin aggravates glomerulonephritis via recruitment and activation of myeloid cells. *J. Am. Soc. Nephrol.* 31, 1996–2012. doi: 10.1681/asn.2019111215

Møllerløkken, A., Berge, V. J., Jørgensen, A., Wisløff, U., and Brubakk, A. O. (2006). Effect of a short-acting NO donor on bubble formation from a saturation dive in pigs. *J. Appl. Physiol.* 101, 1541–1545. doi: 10.1152/japplphysiol.01191.2005

Montcalm-Smith, E. A., Caviness, J., Chen, Y., and McCarron, R. M. (2007). Stress biomarkers in a rat model of decompression sickness. *Aviat. Space Environ. Med.* 78, 87–93.

Montcalm-Smith, E. A., McCarron, R. M., Porter, W. R., Lillo, R. S., Thomas, J. T., and Auker, C. R. (2009). Acclimation to decompression sickness in rats. *J. Appl. Physiol.* 108, 596–603.

Morita, K., Okamura, T., Inoue, M., Komai, T., Teruya, S., Iwasaki, Y., et al. (2016). Egr2 and Egr3 in regulatory T cells cooperatively control systemic autoimmunity through Ltbp3-mediated TGF-β3 production. *Proc. Natl. Acad. Sci.* 113, E8131–E8140.

Mrakic-Sposta, S., Vezzoli, A., D'Alessandro, F., Paganini, M., Dellanoce, C., Cialoni, D., et al. (2020). Change in oxidative stress biomarkers during 30 days in saturation dive: a pilot study. *Int. J. Environ. Res. Public. Health* 17:7118. doi: 10.3390/ijerph17197118

Nossum, V., Hjelde, A., and Brubakk, A. O. (2002). Small amounts of venous gas embolism cause delayed impairment of endothelial function and increase polymorphonuclear neutrophil infiltration. *Eur. J. Appl. Physiol.* 86, 209–214. doi: 10.1007/s00421-001-0531-y

Nossum, V., Koteng, S., and Brubakk, A. O. (1999). Endothelial damage by bubbles in the pulmonary artery of the pig. *Undersea Hyperb. Med.* 26, 1–8.

Novak, S., Drenjancevic, I., Vukovic, R., Kellermayer, Z., Cosic, A., Tolusic Levak, M., et al. (2016). Anti-inflammatory effects of hyperbaric oxygenation during DSS-induced colitis in BALB/c mice include changes in gene expression of HIF-1α, proinflammatory cytokines, and antioxidative enzymes. *Mediators Inflamm.* 2016:e7141430.

Osterburg, A. R., Hexley, P., Supp, D. M., Robinson, C. T., Noel, G., Ogle, C., et al. (2013). Concerns over interspecies transcriptional comparisons in mice and humans after trauma. *Proc. Natl. Acad. Sci.* 110, E3370–E3370.

Palmieri, E. M., McGinity, C., Wink, D. A., and McVicar, D. W. (2020). Nitric oxide in macrophage immunometabolism: hiding in plain sight. *Metabolites* 10:429. doi: 10.3390/metabo10110429

Perović, A., Sobočanec, S., Dabelić, S., Balog, T., and Dumić, J. (2018). Effect of scuba diving on the oxidant/antioxidant status, SIRT1 and SIRT3 expression in recreational divers after a winter nondive period. *Free Radic. Res.* 52, 188–197. doi: 10.1080/10715762.2017.1422211

Pontier, J. M., Guerrero, F., and Castagna, O. (2009). Bubble formation and endothelial function before and after 3 months of dive training. *Aviat Space Environ. Med.* 80, 15–19. doi: 10.3357/asem.2347.2009

Preston, G. A., Srinivasan, D., and Barrett, J. C. (2000). Apoptotic response to growth factor deprivation involves cooperative interactions between c-Fos and p300. *Cell Death Differ.* 7, 215–226. doi: 10.1038/sj.cdd.4400637

Ramsay, L., Quillé, M.-L., Orset, C., de la Grange, P., Rousselet, E., Férec, C., et al. (2019). Blood transcriptomic biomarker as a surrogate of ischemic brain gene expression. *Ann. Clin. Transl. Neurol.* 6, 1681–1695. doi: 10.1002/acn3.50861

Rozen, S., and Skaletsky, H. (2000). Primer3 on the WWW for general users and for biologist programmers. *Methods Mol. Biol.* 132, 365–386. doi: 10.1385/1-59259-192-2:365

Schwanhäusser, B., Busse, D., Li, N., Dittmar, G., Schuchhardt, J., Wolf, J., et al. (2011). Global quantification of mammalian gene expression control. *Nature* 473, 337–342. doi: 10.1038/nature10098

Seok, J., Warren, H. S., Cuenca, A. G., Mindrinos, M. N., Baker, H. V., Xu, W., et al. (2013). Genomic responses in mouse models poorly mimic human inflammatory diseases. *Proc. Natl. Acad. Sci. U. S. A.* 112, 1167–1172.

Shigeoka, M., Arimoto, S., and Akashi, M. (2020). JCAD expression and localization in human blood endothelial cells. *Heliyon* 6:e05121. doi: 10.1016/j.heliyon.2020.e05121

Thom, S. R., Bennett, M., Banham, N. D., Chin, W., Blake, D. F., Rosen, A., et al. (2015). Association of microparticles and neutrophil activation with decompression sickness. *J. Appl. Physiol.* 119, 427–434. doi: 10.1152/japplphysiol.00380.2015

Thom, S. R., Bhopale, V. M., and Yang, M. (2014). Neutrophils generate microparticles during exposure to inert gases due to cytoskeletal oxidative stress. *J. Biol. Chem.* 289, 18831–18845. doi: 10.1074/jbc.m113.543702

Thom, S. R., Yang, M., Bhopale, V. M., Huang, S., and Milovanova, T. N. (2011). Microparticles initiate decompression-induced neutrophil activation and subsequent vascular injuries. *J. Appl. Physiol.* 110, 340–351. doi: 10.1152/japplphysiol.00811.2010

Tillmans, F., Sharghi, R., Noy, T., Kähler, W., Klapa, S., Sartisohn, S., et al. (2019). Effect of hyperoxia on the immune status of oxygen divers and endurance athletes. *Free Radic. Res.* 53, 522–534. doi: 10.1080/10715762.2019.1612890

Tlapák, J., Chmátal, P., Oniscenko, B., Pavlík, D., Páral, J., and Lochman, P. (2020). The effect of hyperbaric oxygen therapy on gene expression: microarray analysis on wound healing. *Undersea Hyperb. Med.* 47, 31–37.

Torraca, V., Otto, N. A., Tavakoli-Tameh, A., and Meijer, A. H. (2017). The inflammatory chemokine Cxcl18b exerts neutrophil-specific chemotaxis via the promiscuous chemokine receptor Cxcr2 in zebrafish. *Dev. Comp. Immunol.* 67, 57–65. doi: 10.1016/j.dci.2016.10.014

Tournebise, H., Boucand, M. H., Landi, J., and Theobald, X. (1995). Paraplegia and decompression sickness. *Paraplegia* 33, 636–639. doi: 10.1038/sc.1995.134

Ustinova, M., Ansone, L., Silamikelis, I., Rovite, V., Elbere, I., Silamikele, L., et al. (2020). Whole-blood transcriptome profiling reveals signatures of metformin and its therapeutic response. *PLoS One* 15:e0237400. doi: 10.1371/journal.pone.0237400

Vann, R. D., Butler, F. K., Mitchell, S. J., and Moon, R. E. (2011). Decompression illness. *Lancet Lond. Engl.* 377, 153–164.

Vijayan, V., Pradhan, P., Braud, L., Fuchs, H. R., Gueler, F., Motterlini, R., et al. (2019). Human and murine macrophages exhibit differential metabolic responses to lipopolysaccharide - a divergent role for glycolysis. *Redox Biol.* 22:101147. doi: 10.1016/j.redox.2019.101147

Wang, H.-T., Fang, Y.-Q., Bao, X.-C., Yuan, H.-R., Ma, J., Wang, F.-F., et al. (2015). Expression changes of TNF-α, IL-1β and IL-6 in the rat lung of decompression sickness induced by fast buoyancy ascent escape. *Undersea Hyperb. Med.* 42, 23–31.

Wang, W., Li, X., Lee, M., Jun, S., Aziz, K. E., Feng, L., et al. (2015). FOXKs promote Wnt/β-catenin signaling by translocating DVL into the nucleus. *Dev. Cell* 32, 707–718. doi: 10.1016/j.devcel.2015.01.031

Weichhart, T., Hengstschläger, M., and Linke, M. (2015). Regulation of innate immune cell function by mTOR. *Nat. Rev. Immunol.* 15, 599–614. doi: 10.1038/nri3901

Wilmshurst, P. T. (2015). The role of persistent foramen ovale and other shunts in decompression illness. *Diving Hyperb. Med.* 45, 98–104.

Woo, J., Min, J.-H., Lee, Y.-H., and Roh, H.-T. (2020). Effects of hyperbaric oxygen therapy on inflammation, oxidative/antioxidant balance, and muscle damage after acute exercise in normobaric, normoxic and hypobaric, hypoxic environments: a pilot study. *Int. J. Environ. Res. Public Health* 17:7377. doi: 10.3390/ijerph17207377

Wu, T.-H., Shi, L., Lowe, A. W., Nicolls, M. R., and Kao, P. N. (2019). Inducible expression of immediate early genes is regulated through dynamic chromatin association by NF45/ILF2 and NF90/NF110/ILF3. *PLoS One* 14:e0216042. doi: 10.1371/journal.pone.0216042

Yamada, T., Lee, P.-H., Burns, A., and Lacorazza, D. (2011). G0S2, an early response gene, regulates quiescence in naïve T cells (104.*10*). *J. Immunol.* 186:104.10.

Yamane, S., Ishida, S., Hanamoto, Y., Kumagai, K., Masuda, R., Tanaka, K., et al. (2008). Proinflammatory role of amphiregulin, an epidermal growth factor family member whose expression is augmented in rheumatoid arthritis patients. *J. Inflamm. Lond. Engl.* 5:5. doi: 10.1186/1476-9255-5-5

Zaiss, D. M. W., Gause, W. C., Osborne, L. C., and Artis, D. (2015). Emerging functions of amphiregulin in orchestrating immunity, inflammation and tissue repair. *Immunity* 42, 216–226. doi: 10.1016/j.immuni.2015.01.020

Zhang, K., Wang, D., Jiang, Z., Ning, X., Buzzacott, P., and Xu, W. (2016). Endothelial dysfunction correlates with decompression bubbles in rats. *Sci. Rep.* 6:33390.

Zhang, K., Wang, D., Xu, J., Li, R., Cai, Z., Liu, K., et al. (2015). Simvastatin decreases incidence of decompression sickness in rats. *Undersea Hyperb. Med.* 42, 115–123.

Conflict of Interest: The authors declare that the research was conducted in the absence of any commercial or financial relationships that could be construed as a potential conflict of interest.

frontiers in Physiology

ORIGINAL RESEARCH
published: 30 July 2021
doi: 10.3389/fphys.2021.695779

Treatment of Cardiovascular Dysfunction With PDE5-Inhibitors – Temperature Dependent Effects on Transport and Metabolism of cAMP and cGMP

*Anders L. Selli[1], Adrina K. Kuzmiszyn[1,2], Natalia Smaglyukova[1], Timofei V. Kondratiev[3], Ole-Martin Fuskevåg[4], Roy A. Lysså[1], Aina W. Ravna[1], Torkjel Tveita[2,3], Georg Sager[1] and Erik S. Dietrichs[1,5]**

[1] Experimental and Clinical Pharmacology, Department of Medical Biology, UiT – The Arctic University of Norway, Tromsø, Norway, [2] Division of Surgical Medicine and Intensive Care, University Hospital of North Norway, Tromsø, Norway, [3] Anesthesia and Critical Care Research Group, Department of Clinical Medicine, UiT – The Arctic University of Norway, Tromsø, Norway, [4] Department of Laboratory Medicine, Division of Diagnostic Services, University Hospital of North Norway, Tromsø, Norway, [5] Center for Psychopharmacology, Diakonhjemmet Hospital, Oslo, Norway

OPEN ACCESS

Edited by:
Gaetano Santulli,
Columbia University, United States

Reviewed by:
Rui Zhang,
Tongji University, China
Pasquale Mone,
University of Campania Luigi Vanvitelli, Italy

***Correspondence:**
Erik S. Dietrichs
erik.sveberg.dietrichs@uit.no

Specialty section:
This article was submitted to Clinical and Translational Physiology, a section of the journal Frontiers in Physiology

Received: 15 April 2021
Accepted: 09 July 2021
Published: 30 July 2021

Citation:
Selli AL, Kuzmiszyn AK, Smaglyukova N, Kondratiev TV, Fuskevåg O-M, Lysså RA, Ravna AW, Tveita T, Sager G and Dietrichs ES (2021) Treatment of Cardiovascular Dysfunction With PDE5-Inhibitors – Temperature Dependent Effects on Transport and Metabolism of cAMP and cGMP. Front. Physiol. 12:695779. doi: 10.3389/fphys.2021.695779

Introduction: Cardiovascular dysfunction is a potentially lethal complication of hypothermia. Due to a knowledge gap, pharmacological interventions are not recommended at core temperatures below 30°C. Yet, further cooling is induced in surgical procedures and survival of accidental hypothermia is reported after rewarming from below 15°C, advocating a need for evidence-based treatment guidelines. *In vivo* studies have proposed vasodilation and afterload reduction through arteriole smooth muscle cGMP-elevation as a favorable strategy to prevent cardiovascular dysfunction in hypothermia. Further development of treatment guidelines demand information about temperature-dependent changes in pharmacological effects of clinically relevant vasodilators.

Materials and Methods: Human phosphodiesterase-enzymes and inverted erythrocytes were utilized to evaluate how vasodilators sildenafil and vardenafil affected cellular efflux and enzymatic breakdown of cAMP and cGMP, at 37°C, 34°C, 32°C, 28°C, 24°C, and 20°C. The ability of both drugs to reach their cytosolic site of action was assessed at the same temperatures. IC_{50}- and K_i-values were calculated from dose–response curves at all temperatures, to evaluate temperature-dependent effects of both drugs.

Results: Both drugs were able to reach the intracellular space at all hypothermic temperatures, with no reduction compared to normothermia. Sildenafil IC_{50} and K_i-values increased during hypothermia for enzymatic breakdown of both cAMP (IC_{50}: 122 ± 18.9 μM at 37°C vs. 269 ± 14.7 μM at 20°C, $p < 0.05$) and cGMP (IC_{50}: 0.009 ± 0.000 μM at 37°C vs. 0.024 ± 0.004 μM at 32°C, $p < 0.05$), while no significant changes were detected for vardenafil. Neither of the drugs showed significant

hypothermia-induced changes in IC_{50} and K_{i}–values for inhibition of cellular cAMP and cGMP efflux.

Conclusion: Sildenafil and particularly vardenafil were able to inhibit elimination of cGMP down to 20°C. As the cellular effects of these drugs can cause afterload reduction, they show potential in treating cardiovascular dysfunction during hypothermia. As in normothermia, both drugs showed higher selectivity for inhibition of cGMP-elimination than cAMP-elimination at low core temperatures, indicating that risk for cardiotoxic side effects is not increased by hypothermia.

Keywords: hypothermia, PDE5-inhibitors, cyclic AMP, cyclic GMP, afterload reduction, cardiovascular dysfunction, HAPE, ECMO

INTRODUCTION

Accidental hypothermia is associated with a mortality rate up to 40% and is defined as involuntary drop of body core temperature below 35°C (Vassal et al., 2001). Hypothermia-induced cardiac dysfunction (HCD) contributes to the high mortality (Sessler Daniel, 2001; Kondratiev et al., 2006) and is recognized by decreased cardiac output (CO) as well as increased total peripheral resistance (TPR), during hypothermia and rewarming (Mann et al., 1992; Tveita, 2000; Dietrichs et al., 2015). Similarly, cardiovascular failure is associated with a negative outcome during therapeutic hypothermia (Bush et al., 1995). Other critical cardiovascular conditions, like high altitude pulmonary edema (HAPE), could occur in extreme conditions where exposure to low core temperatures are frequent, and evacuation of patients is difficult (Westensee et al., 2013). In such situations, knowledge about the temperature-dependent effect of relevant pharmacological strategies is paramount, to ensure optimal treatment.

Pharmacological manipulation of intracellular cyclic AMP (cAMP) and cyclic GMP (cGMP) levels is used to influence human cardiovascular function during normothermia. Both cAMP and cGMP are intracellular signal molecules with important function in the cardiovascular system. Intracellular levels of cAMP and cGMP are increased by stimulation of the β-receptor-AC-cAMP-PKA and NO-GC-cGMP-PKG pathways, respectively. Elimination is controlled by enzymatic breakdown and cellular extrusion (Subbotina et al., 2017). Elevated cardiomyocyte cAMP-levels are associated with increased cardiac inotropy and chronotropy, while elevation in peripheral smooth muscle cause relaxation and resulting vasodilation. Elevated levels of cGMP in smooth muscle is also associated with peripheral vasodilation, but in cardiomyocytes it has a slightly negative inotropic effect. cAMP degradation in human cardiomyocytes is largely caused by the phosphodiesterase-3A (PDE3A) enzyme. PDE5A is also present and active both in the healthy and failing human heart, as well as in human blood vessels, and is mainly responsible for cGMP degradation (Johnson et al., 2012). Elimination of cAMP and cGMP is also dependent on the activity of cellular efflux pumps. The ATP-binding cassette subfamily-C 4 (ABCC4) is mainly responsible for transporting cAMP out of cells, while cGMP is thought to be removed by ABCC5 (Jedlitschky et al., 2000; Sellers et al., 2012).

Inotropic effects of well-known adrenergic drugs, such as adrenaline and isoprenaline that elevate cAMP through β-receptor stimulation during normothermia, have been explored in rodent models. Hypothermia induced a paradoxical, negative inotropic effect and increased TPR during hypothermia (Dietrichs et al., 2015, 2016), worsening HCD. Several drugs with a different mechanistic approach to affect the β-receptor-AC-cAMP-PKA and NO-GC-cGMP-PKG pathways during hypothermia and rewarming have therefore been investigated *in vivo* (Tveita and Sieck, 2012; Dietrichs et al., 2014a, 2016; Håheim et al., 2017), with diverging hemodynamic effects. Administration of the potent vasodilator sodium nitroprusside lowered TPR, when administered in hypothermic rats. The results showed a positive effect on CO and prevented HCD (Håheim et al., 2017). Similar results were observed after administration of milrinone, a phosphodiesterase-3 (PDE3) inhibitor, impeding enzymatic breakdown of cAMP. In the hypothermic rat, milrinone-infusion resulted in decreased TPR and increased CO (Dietrichs et al., 2014b).

Total peripheral resistance-reduction therefore appears to be a favorable strategy to prevent HCD (Tveita and Sieck, 2012; Dietrichs et al., 2014a, 2018; Håheim et al., 2017). Elevation of cGMP through PDE5-inhibitors like sildenafil and vardenafil, is a potential pharmacological approach in hypothermic patients and a suggested treatment option in HAPE-patients (Luks et al., 2017). Drug specificity during hypothermic conditions is, however, unknown. Therefore, it is important to investigate the ability of sildenafil and vardenafil to reach their site of action and inhibit cGMP, as well as determining whether they also inhibit cAMP elimination at different stages of hypothermia, encountered in critically ill patients. Exploring the temperature-dependent properties of these clinically relevant drugs, could provide important information on their ability to help sustain cardiovascular functions, during hypothermia and rewarming.

MATERIALS AND METHODS

Three different experimental protocols were used to evaluate intracellular access, cellular efflux and phosphodiesterase activity, respectively.

Temperature

According to temperature-dependent clinical signs and physiological changes, The European Resuscitation Council has classified accidental hypothermia into mild hypothermia (35–32°C), moderate hypothermia (32–28°C) and severe hypothermia (below 28°C) (Truhlar et al., 2015). This classification was used in design of the present experiment, where we collected data at relevant temperatures for both accidental and therapeutic hypothermia. Accordingly, we assessed intracellular access of the drugs and pharmacological inhibition of cAMP- and cGMP-efflux, as well PDE3 and PDE5 at 37°C, 34°C, 32°C, 28°C, 24°C, and 20°C.

Pharmacological Substances

Sildenafil (Sigma-Aldrich, Schnelldorf, Germany) and vardenafil (Bayer Pharma AG, Wuppertal, Germany) were used in seven different concentrations increasing by a factor of 10, ranging from 1.00E-09 to 1.00E-03 M (1.00 nM to 1.00 mM), to test their potency at both inhibiting elimination of cAMP and cGMP through reducing cellular efflux and enzyme activity.

Intracellular Access

Both sildenafil and vardenafil are predominantly exerting their effects intracellularly. To estimate whether core temperature reduction would impede their ability to reach the site of action, both drugs were incubated at a concentration of 1.00 μM. The concentration is chosen from therapeutic serum concentrations and were obtained from a systematic literature review in PubMed with (sildenafil) OR (vardenafil) AND (intravenous) AND (plasma concentration) OR (serum concentration) (**Table 1**). References on intravenous administration was chosen due to patients suffering from hypothermia and HAPE often will have reduced consciousness, making oral administration difficult. Further, bioavailability of oral drugs during hypothermia is hard to predict and oral administration is not an alternative for gaining rapid pharmacological effects. The included reference articles had to report adult human data with a relevant cardiovascular topic. Relevant articles from references were also included. For vardenafil, concentrations from intravenous administration were not available and relevant articles for oral administration were included instead. As the aim for this experiment was to detect potential temperature-dependent effects on access through the cell membrane and potential for free fraction of drugs to increase during hypothermia, we chose a concentration of 1.00 μM for both drugs as this corresponded to the highest serum concentrations after intravenous administration of sildenafil.

Blood was provided by Blodbanken UNN (Department of Immunohematology and Transfusion Medicine, University Hospital of North Norway) where all participants (n = 18) were pre-screened and only admitted as donors if they were healthy. Each parallel only included blood from one donor. Experiments were initiated by washing and centrifuging recently (<24 h) drawn EDTA-blood three times with Krebs-Ringer-Phosphate-Buffer containing glucose (KRPB/G, pH∼7.4). The blood was added KRPB/G in a 2.5:1 relationship before measuring hematocrit (Hct) values. Depending on the values, calculations of amount KRPB/G to obtain a Hct of 0.44 were performed, which would later give Hct of 0.40 in the final incubate solution. To start the reaction, 500 μL blood suspension (Hct 0.44) was added to tubes containing 50 μL of either sildenafil, vardenafil or MQ-water (negative control). Each experiment contained triplicates of both drugs and control, and three experiments at each temperature were conducted – in total nine parallels. The reactions were stopped after 30 min (**Table 2**) by putting the tubes on ice and adding 4 mL ice cold KRPB/G. The reaction solutions were washed and centrifugated three times with ice cold KRPB/G. Fifty microliters of the remaining solution was then added to Eppendorf tubes along with 50 μL internal standard (IS), containing 250 nM IS-Sildenafil-d3 and 500 nM IS-Vardenfail-d5 (Toronto Research Chemicals, ON, Canada). Five samples contained 50 μL known concentrations of sildenafil and vardenafil, and 50 μL IS, and served as controls for accurate analysis. All samples were added 200 mL 0.1 M $ZnSO_4$, to lyse the erythrocytes, and then centrifugated. Thirty microliters was taken from Eppendorf tubes for measurements of protein concentration before adding 500 μL acetonitrile. One hundred microliters from each tube was collected for analysis using mass spectrometry (MS).

Cellular Efflux

Cellular extrusion was determined using the inside-out vesicle (IOV) method where erythrocytes from healthy, human donors were sampled. Donors were pre-screened and only admitted as donors by Blodbanken UNN (Department of Immunohematology and Transfusion Medicine, University Hospital of North Norway) if they were healthy. The erythrocytes were separated from plasma by centrifugation and washed. Inside-out vesicles were prepared according to Elin Orvoll et al. (2013) with minor modifications. The membrane vesiculation was initiated by adding hypertonic buffer to the cell suspension. After centrifugation, the suspension was forced through a syringe needle to enhance homogenization of the membranes. IOVs were separated from right side out vesicles (ROV) and unsealed erythrocyte membranes (ghosts) by ultracentrifugation overnight using a density gradient. The uppermost band was collected, washed, and resuspended. Percentage IOV was verified using acetylcholinesterase accessibility test (Ellman et al., 1961). Batches of IOVs used in the parallels were made eight times, including blood from a total of 35 healthy donors.

Inside-out vesicles were then incubated with or without 2 mM ATP and seven different concentrations of sildenafil or vardenafil. The incubation solutions also included radioactive labeled [^{3}H]-cGMP and [^{3}H]-cAMP (Perkin Elmer, Boston, MA, United States), at a concentration of, respectively, 2 μM and 20 μM. The assays were performed in triplicates at three different days: In total nine parallels were performed to calculate results for each concentration of both drugs at all temperatures. Incubation time of 60 min was chosen to ensure sufficient quality of the samples for each parallel (**Table 2**). The transport was stopped by adding ice cold buffer. The IOVs were then filtered through a nitrocellulose membrane (Bio-Rad Laboratories, Feldkirchen, Germany), and the membrane was dried. The dried membranes were

TABLE 1 | Therapeutic plasma concentrations from a literature review of sildenafil and vardenafil, administered for cardiovascular support.

Therapeutic plasma concentration	Calculated concentration in μM	Cardiovascular topic	References	Protein binding	References
Sildenafil	0.449 μM	Pulmonary hypertension	Vachiery et al. (2011)	94–96%	Walker (1999)
	0.101–0.768 μM	Cardiac surgery	Ring et al. (2017)	93–95%	Mehrotra et al. (2007)
Vardenafil	0.010 μM	Pulmonary hypertension	Henrohn et al. (2012)		
	0.044 μM	Pulmonary hypertension	Sandqvist et al. (2013)		

The search was performed in PubMed with (name of drug) AND (intravenous) AND (plasma concentration) OR (serum concentration). As no articles for intravenous vardenafil administration were found, studies conducted after oral administration were accepted instead.

TABLE 2 | Experimental protocol.

	Intracellular access			Enzyme inhibition						Cellular efflux inhibition					
Drug	**Sildenafil**	**Vardenafil**	**Control**	**Sildenafil**		**Vardenafil**		**Control**		**Sildenafil**		**Vardenafil**		**Control**	
Target	Human erythrocyte membranes			PDE3	PDE5	PDE3	PDE5	PDE3	PDE5	cAMP-efflux	cGMP-efflux	cAMP-efflux	cGMP-efflux	cAMP-efflux	cGMP-efflux
Incubation time	30 min			30 min						60 min					
Temperature	37°C–34°C–32°C–28°C–24°C–20°C														

Incubation time of 30 min was chosen for intracellular access and enzyme inhibition, while 60 min was necessary for cellular efflux inhibition to ensure good quality of samples.

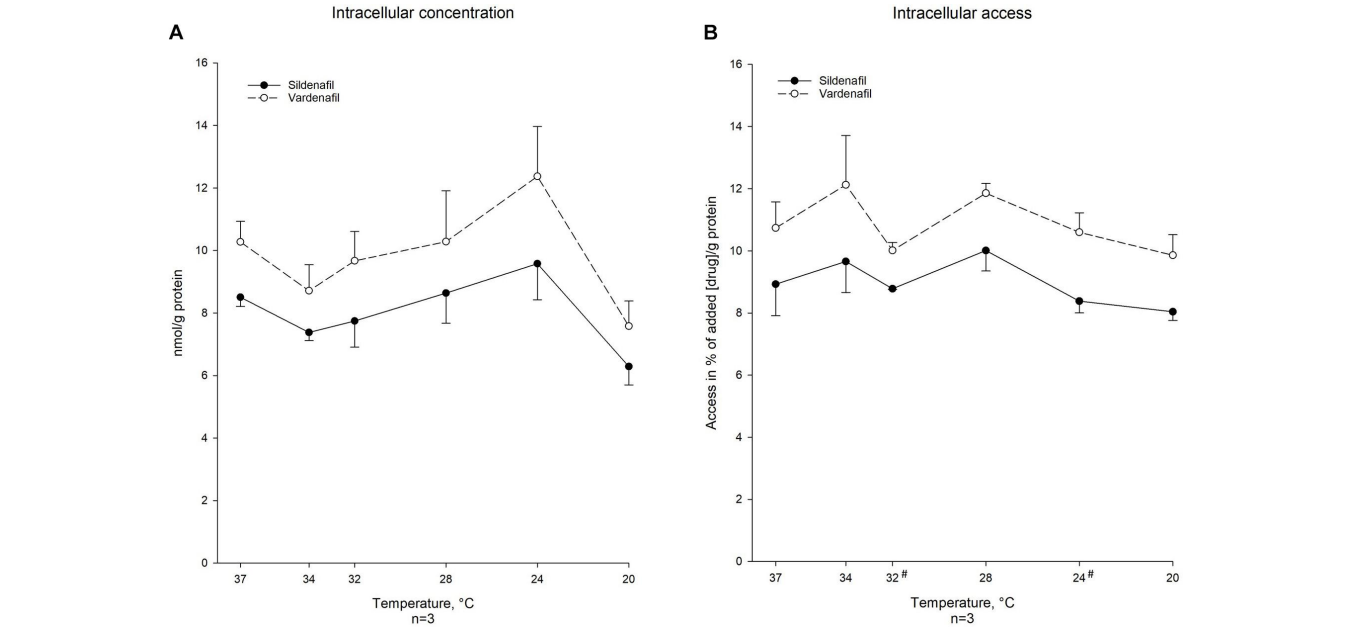

FIGURE 1 | Temperature-dependent intracellular concentration and protein-corrected access in % of added vardenafil and sildenafil. **(A)** Intracellular concentration of sildenafil and vardenafil in nmol/g protein at temperatures ranging from 37°C to 20°C calculated as means ± SEM. Values are calculated from concentration of drug and protein concentration in MS-sample. * Significant difference (*P*-value < 0.05) when nmol/g protein is different from normothermic value. # Significant difference (*P*-value < 0.05) between the two drugs concentrations at specific temperature. **(B)** Intracellular access of sildenafil and vardenafil in % of drug concentration per gram protein in MS-sample compared to drug concentration per gram protein in the incubation solution at temperatures ranging from 37°C to 20°C. Values are in means ś SEM. * Significant difference (*P*-value < 0.05) when % is different from normothermia. # Significant difference (*P*-value < 0.05) between the two drugs access (in %) at specific temperature.

later added scintillation fluid and radioactivity was measured using a Packard TopCount NXT (Packard, Downers Grove, IL, United States).

Experiments determined total ATP-dependent cellular efflux of cGMP or cAMP from IOVs. As described in previous studies, ABCC5 and ABCC4 are the dominant efflux pumps for cGMP and cAMP (Jedlitschky et al., 2000; Sellers et al., 2012), respectively.

Phosphodiesterase Activity

Ability of drugs to inhibit cAMP and cGMP hydrolysis by PDE3 and PDE5, respectively, was tested by incubating 5 μM cAMP

TABLE 3 | Linear regression analysis for intracellular access and inhibition of phosphodiesterase-5 (PDE5), phosphodiesterase-3 (PDE3), and inhibition of cAMP- and cGMP-efflux calculated at 37°C, 34°C, 32°C, 28°C, 24°C, and 20°C.

Regression analysis	**Intracellular access**		**PDE5-inhibition**		**PDE3-inhibition**		**Inhibition of cGMP-efflux**		**Inhibition of cAMP-efflux**	
Drug	**Sildenafil**	**Vardenafil**	**Sildenafil**	**Vardenafil**	**Sildenafil**	**Vardenafil**	**Sildenafil**	**Vardenafil**	**Sildenafil**	**Vardenafil**
Equation	$y = 7.14 + 0.063x$	$y = 9.14 + 0.059x$	$y = 0.064 - 0.002x$	$y = 0.039 - 0.001x$	$y = 367 - 7.90x$	$y = 131 - 3.09x$	$y = -2.07 + 19.2x$	$y = 9.64 - 0.098x$	$y = -7.13 + 0.363x$	$y = 26.4 - 0.545x$
Pearson's *r*	0.535	0.384	−0.906	−0.921	−0.751	−0.946	0.699	0.224	0.931	0.598
P-value	0.21	0.35	<0.01	<0.01	<0.01	<0.01	0.05	0.51	0.13	0.28

The y-value for the intracellular access equation is added [drug]/g protein and the y-value for inhibition equations are concentration of drug in μM. The x-value is temperature in degrees Celsius for all equation. Pearson's r is added to depict how well the regression fitted the observations.

or cGMP (Sigma-Aldrich, St. Louis, MO, United States) with the seven different concentrations of sildenafil and vardenafil. The assays were performed in triplicates at three different days. A total of nine parallels were used to calculate results for each concentration of both drugs at all temperatures. The reaction was started by adding either a solution containing 0.016 units/μg protein of PDE3 (Abcam, Cambridge United Kingdom), or 0.022 units/μg protein of PDE5 (Sigma-Aldrich, St. Louis, MO, United States), to the Eppendorf tubes. Parallels for cAMP-metabolism included PDE3 only and parallels for cGMP-metabolism included PDE5 only. Control samples were free of drug and was either with or without PDE3 or PDE5. This was done to assure that only the relevant PDE was responsible for breakdown of the cyclic nucleotide, as no other enzyme nor cellular material was added to the incubations. The incubation time was 30 min (see **Table 2**). Reaction was stopped by adding methanol to the tubes. Internal standard of cGMP/GMP or cAMP/AMP (Sigma-Aldrich, St. Louis, MO, United States, Germany and Toronto Research Chemicals Inc., Toronto, ON, Canada) were added to each sample. Five samples contained only known concentrations of cGMP/GMP or cAMP/AMP and served as calibrators. Samples were analyzed for cGMP/GMP and cAMP/AMP content, using MS.

Mass Spectrometry (MS) Analysis

Quantification of cAMP/AMP, cGMP/GMP, and PDE5-inhibitors in PDE- and intracellular access experiments were performed with liquid chromatography tandem mass spectrometry (LC-MS/MS). Preparation of samples for LC-MS/MS-analysis is described in the relevant paragraphs above. The method was found to be linear from 0.2 nM to at least 2000 nM ($r^2 > 0.998$) for cAMP, cGMP, and AMP. For GMP the method was linear from 2 nM to at least 2000 nM ($r^2 > 0.998$), and 10 nM to at least 5000 nM for the PDE5-inhibitors ($r^2 > 0.998$). Lower limit of quantification (LLOQ) was found to be 0.2 nM for cAMP, cGMP, and AMP, 2 nM for GMP and 10 nM for the PDE5-inhibitors (2 μl injection volume).

Data Analysis

The ability of drugs to inhibit cAMP-efflux, cGMP-efflux, PDE3, and PDE5 were determined by calculating IC_{50}- and K_i-values from inhibition plots. IC50 values were calculated according to Chou (1976) and data were transformed to K_i-values according to Cheng and Prusoff (1973). IC_{25} and IC_{75} values were estimated by polynomial, cubic regression, based on the inhibition curve of each experiment. Measurement of intracellular concentrations of drugs were adjusted for protein concentrations in each sample. The incubation concentrations were also adjusted for protein concentration in each sample to evaluate the access in percentage. Results are presented as mean ± standard error of mean (SEM). A one-way ANOVA with Holm–Sidak multiple comparisons *post hoc* test was used to compare the IC_{50} and K_i-values for the drugs, as well as intracellular concentrations of drugs, at each temperature with normothermic baseline (37°C). When results were not normally distributed, ANOVA on ranks was used with a Dunn *post hoc* test. Two-tailed *t*-tests were performed to compare IC_{50}-values, and adjusted

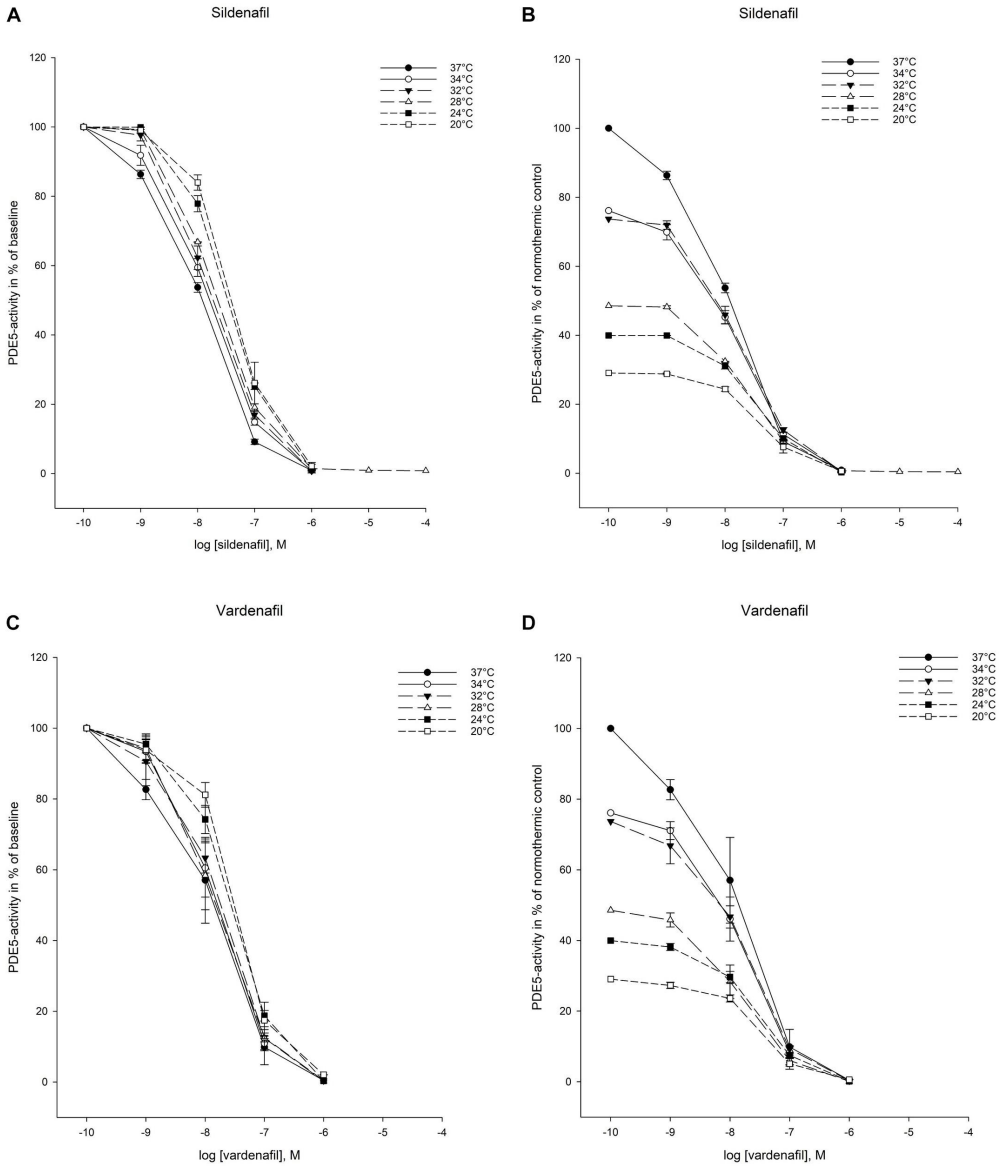

FIGURE 2 | Temperature-dependent inhibition of phosphodiesterase-5 (PDE5) by vardenafil and sildenafi. **(A)** Sildenafil inhibition curves for PDE5-activity at temperatures ranging from 37°C to 20°C. The doses of sildenafil are in logarithm of the concentration in mol/L. **(B)** Inhibition curves for PDE5-activity by sildenafil in % of normothermic inhibition curve at temperatures ranging from 37°C to 20°C. The doses of sildenafil are in logarithm of the concentration in mol/L. **(C)** Vardenafil inhibition curves for PDE5-activity at temperatures ranging from 37°C to 20°C. The doses of vardenafil are in logarithm of the concentration in mol/L. **(D)** Inhibition curves for PDE5-activity by vardenafil in % of normothermic inhibition curve at temperatures ranging from 37°C to 20°C. The doses of vardenafil are in logarithm of the concentration in mol/L.

intracellular concentrations, of sildenafil and vardenafil at each temperature. Regression analysis was performed to evaluate whether a linear relationship existed between IC_{50}-values and temperature for each drug at each elimination pathway of cAMP and cGMP. Regression analysis was also performed to evaluate if there was a linear relationship between intracellular access of the two drugs and temperature. Pearson's r was calculated for every regression analysis to evaluate how well the calculated lines fitted the observations. P-values < 0.05 were considered significant for our data analysis. All analysis were performed using SigmaPlot 14.0 (Systat Software, San Jose, CA, United States, RRID:SCR_003210).

RESULTS

Intracellular Access of Drugs During Hypothermia

Sildenafil and vardenafil, at incubate concentration of 1.00 μM, were able to reach the cytosol at all included temperatures from

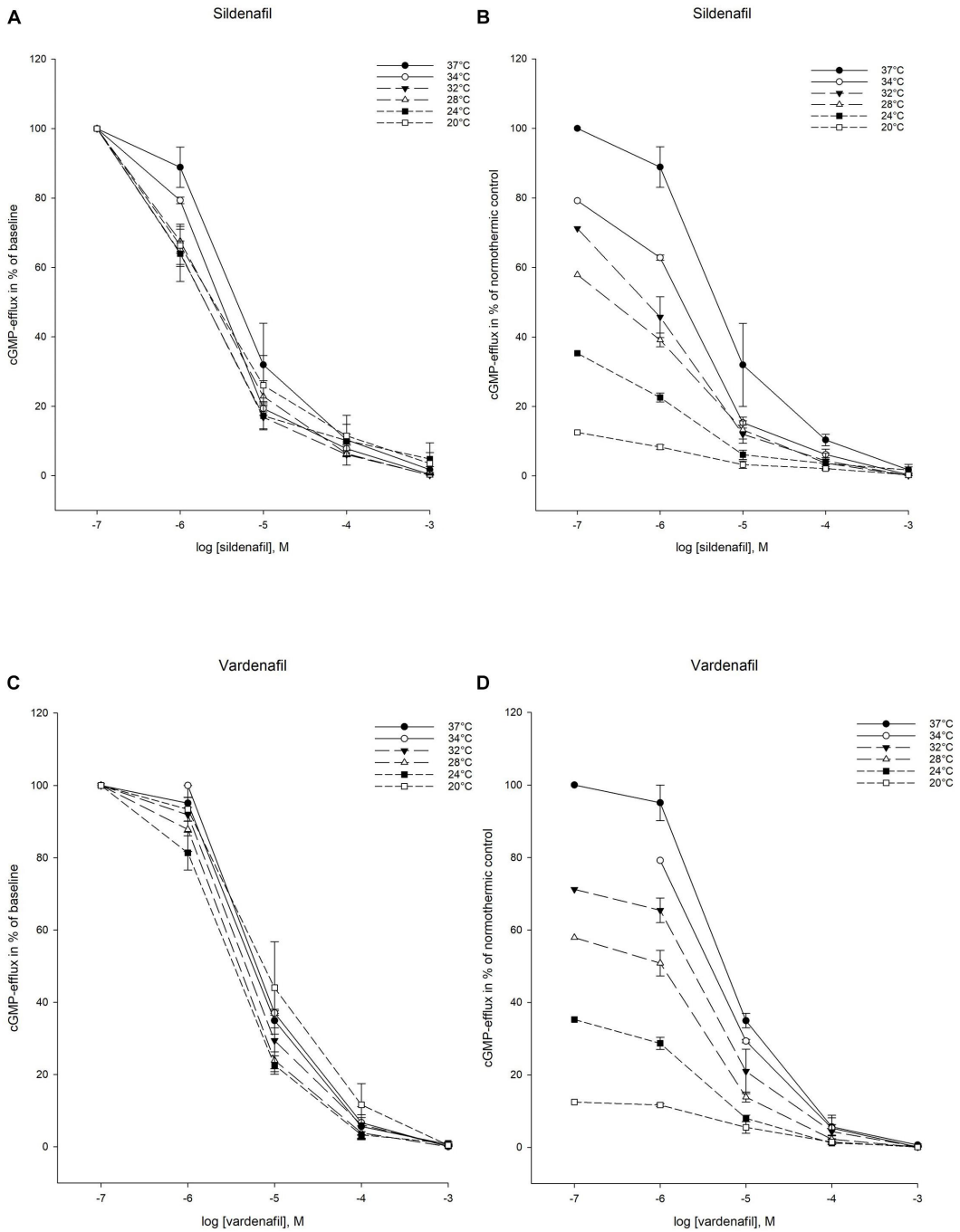

FIGURE 3 | Temperature-dependent inhibition of cGMP-efflux in inside-out vesicles (IOV). **(A)** Sildenafil inhibition curves for ABCC5-activity at temperatures ranging from 37°C to 20°C. The doses of sildenafil are in logarithm of the concentration in mol/L. **(B)** Inhibition curves for ABCC5-activity by sildenafil in % of normothermic inhibition curve at temperatures ranging from 37°C to 20°C. The doses of sildenafil are in logarithm of the concentration in mol/L. **(C)** Vardenafil inhibition curves for ABCC5-activity at temperatures ranging from 37°C to 20°C. The doses of vardenafil are in logarithm of the concentration in mol/L. **(D)** Inhibition curves for ABCC5-activity by vardenafil in % of normothermic inhibition curve at temperatures ranging from 37°C to 20°C. The doses of vardenafil are in logarithm of the concentration in mol/L.

37°C to 20°C after 30 min incubation (**Figure 1**). Decreased temperature did not affect the ability of either drug to reach their intracellular site of action. A significantly smaller percentage of sildenafil was able to reach the intracellular space compared to vardenafil at 32°C (% of drug: 8.78 ± 0.027 vs. 10.0 ± 0.257, $p < 0.05$) and at 24°C (% of drug: 8.38 ± 0.381 vs. 10.6 ± 0.625, $p < 0.05$). Regression analysis showed no significant linear relationship between access, neither when looking at total

amount nor percentage that reached cytosol, and temperature for any of the drugs (**Table 3**).

Cellular Elimination of cGMP

Both sildenafil and vardenafil were able to inhibit cellular elimination of cGMP by PDE5 and efflux pumps at all temperatures (**Figures 2, 3**).

Intracellular Elimination by PDE5

IC_{50}- and K_i -values for PDE5 inhibition were significantly increased compared to normothermic baseline at 32°C for sildenafil (IC_{50}: 0.024 ± 0.004 vs. 0.009 ± 0.000 μM, $p < 0.05$) and remained elevated down to 20°C, with exception of measurements at 28°C (**Tables 4, 5**). For vardenafil, IC_{50}-values did not significantly differ from normothermic control at any temperatures. When comparing IC_{50}- and K_i-values of sildenafil and vardenafil at different temperatures, sildenafil had significantly higher IC_{50}- and K_i -values at 20°C (IC_{50}: 0.037 ± 0.003 vs. 0.023 ± 0.002 μM, $p < 0.05$). The IC_{25}–IC_{75} interval was significantly increased for sildenafil compared to normothermic baseline at 24°C (IC_{25}–IC_{75}: 0.098 ± 0.012 μM vs. 0.038 ± 0.000 μM, $p < 0.05$) and 20°C (IC_{25}–IC_{75}: 0.132 ± 0.048 μM 20°C vs. 0.038 ± 0.000 μM, $p < 0.05$) (**Table 6**).

The temperature-dependent increase in IC_{50} for both sildenafil and vardenafil appeared to follow a linear pattern (**Table 3**). Regression analysis provided the equation for calculating sildenafil IC_{50} values during hypothermia: $y = 0.064 - 0.002x$ μM, with x being the temperature in Celsius. The R-value was −0.906 ($p < 0.05$). For vardenafil the calculated equation was $y = 0.039 - 0.001x$ μM, with $R = -0.921$ ($p < 0.01$).

Cellular Efflux

For ABBC5 inhibition, there were no statistically significant difference in IC_{50}- and K_i-values for either sildenafil or vardenafil when compared to 37°C (**Tables 4, 5**). Only at 32°C there was a significant lower IC_{50}- and K_i-value for sildenafil than vardenafil (IC_{50}: 3.68 ± 0.416 vs. 9.40 ± 0.762 μM, $p < 0.05$). The IC_{25}–IC_{75} interval remained stable for both drugs during hypothermia.

Regression analysis showed that neither sildenafil nor vardenafil inhibition of cGMP-efflux followed a linear pattern during temperature reduction (**Table 3**).

Cellular Elimination of cAMP

PDE3-mediated elimination of cAMP was inhibited by both sildenafil and vardenafil at all temperatures in the experimental protocol (**Figure 4**). Inhibition of cAMP-efflux was however only achieved down to 28°C (**Figure 5**). At the two lowest temperatures, 24°C and 20°C, neither of the drugs were able to inhibit cAMP-efflux. These temperatures are therefore excluded from IC_{50} and K_i calculations.

Intracellular Elimination by PDE3

IC_{50}- and K_i-values for PDE3-inhibition was substantially increased for sildenafil at 20°C compared to normothermic control (IC_{50}: 269 ± 14.7 vs. 122 ± 18.9 μM, $p < 0.05$). For vardenafil, there were no significant differences compared to normothermia. Differences in IC_{50}- and K_i-values between drugs, $p < 0.05$, were observed at all temperatures except 24°C (**Tables 4, 5**). The IC_{25}–IC_{75} interval was significantly increased for both sildenafil and vardenafil compared to normothermic baseline at 20°C (IC_{25}–IC_{75} sildenafil: 697 ± 22.5 μM vs. 460 ± 38.8 μM, $p < 0.05$. IC_{25}–IC_{75} vardenafil: 790 ± 105 μM vs. 61.0 ± 14.3 μM, $p < 0.05$) (**Table 6**).

Regression analysis showed significant correlation ($p < 0.05$) between IC_{50} values and temperature for sildenafil with $y = 367 - 7.90x$ μM, $R = -0.751$. For vardenafil, there was a significant correlation ($p < 0.05$) with $R = -0.946$, providing the equation $y = 131 - 3.09x$ μ M (**Table 3**).

Cellular Efflux

The IC_{50}- and K_i-values for inhibition of cAMP-efflux by sildenafil and vardenafil at hypothermic temperatures, showed no significant difference when compared to normothermic control. When comparing drugs however, IC_{50}- and K_i-values for sildenafil were significantly lower than vardenafil at 32°C (IC_{50}: 4.66 ± 1.37 vs. 13.0 ± 1.69 μM, $p < 0.05$) (**Tables 4, 5**). The IC_{25}–IC_{75} interval remained stable for both drugs during hypothermia.

Regression analysis showed no significant correlation for IC_{50} pattern with temperature for neither of the drugs (**Table 3**).

Drug Selectivity

Phosphodiesterase Enzymes

As expected, calculated ratios between IC_{50} values showed that the sildenafil concentration needed to inhibit PDE3 was higher (by a factor of 14400) than the dose needed to achieve PDE5-inhibition during normothermic conditions (37°C). Vardenafil was less selective, with a PDE3/PDE5-inhibiting ratio of 1960. Hypothermia appeared to reduce PDE5-selectivity of sildenafil, with a PDE3/PDE5-inhibiting ratio of 7270 at 20°C and increase PDE5-selectivity of vardenafil, as the PDE3/PDE5-inhibiting ratio was increased to 3230 at 20°C (**Table 7**).

Efflux Pumps

The normothermic cAMP-efflux/cGMP-efflux IC_{50}-ratio for sildenafil (0.832) and vardenafil (1.11) indicate that both drugs inhibit cAMP and cGMP efflux at similar concentrations. The tendency for both drugs is a modest increase in selectivity for cGMP-efflux during hypothermia, with a sildenafil-ratio of 0.917 and vardenafil-ratio of 1.95 at 20°C (**Table 7**).

cGMP Elimination

During normothermic conditions, the predominant inhibition of cGMP-elimination by sildenafil and vardenafil, is through PDE5-inhibition, as the cGMP-efflux/PDE5 inhibition-ratio was 815 and 625, respectively. For both drugs the ratios decreased during hypothermia

TABLE 4 | IC_{50}-values for inhibition of phosphodiesterase-5 (PDE5), phosphodiesterase-3 (PDE3), and inhibition of cAMP- and cGMP-efflux at temperatures ranging from 37°C to 20°C.

IC_{50}	PDE5		PDE3		cGMP-efflux		cAMP-efflux	
Temperature	**Sildenafil (μM)**	**Vardenafil (μM)**	**Sildenafil (μM)**	**Vardenafil (μM)**	**Sildenafil (μM)**	**Vardenafil (μM)**	**Sildenafil (μM)**	**Vardenafil (μM)**
37°C	0.009 ± 0.000	0.008 ± 0.003	122 ± 18.9#	16.5 ± 6.08#	6.96 ± 2.58	5.26 ± 1.46	5.79 ± 1.73	5.85 ± 0.51
34°C	0.014 ± 0.002	0.015 ± 0.005	91.9 ± 12.6#	24.9 ± 5.73#	3.68 ± 0.416#	9.40 ± 0.762#	5.91 ± 2.22	5.82 ± 0.685
32°C	0.024 ± 0.004*	0.015 ± 0.004	103 ± 14.1#	40.5 ± 3.78#	2.53 ± 0.878	6.50 ± 1.20	4.66 ± 1.37#	13.0 ± 1.69#
28°C	0.017 ± 0.003	0.015 ± 0.003	95.7 ± 16.1#	32.7 ± 11.0#	2.98 ± 0.304	4.94 ± 0.891	2.73 ± 0.382	9.63 ± 5.79
24°C	0.028 ± 0.005*	0.022 ± 0.003	143 ± 44.8	55.5 ± 4.75	2.21 ± 0.434	3.75 ± 0.926	–	–
20°C	0.037 ± 0.003*#	0.023 ± 0.002#	269 ± 14.7*#	73.4 ± 26.3#	2.76 ± 1.27	10.9 ± 4.79	–	–

Values are mean ± SEM and given in ±M.
**Significant difference (P-value < 0.05), when compared to normothermic control.*
#Significant difference (P-value < 0.05) when IC_{50} values of sildenafil and vardenafil are compared at same temperature. Neither of the drugs inhibited ABCC4-activity below 28°C.

TABLE 5 | K_i-values for inhibition of phosphodiesterase-5 (PDE5), phosphodiesterase-3 (PDE3), and inhibition of cAMP- and cGMP-efflux at temperatures ranging from 37°C to 20°C.

K_i	PDE5-inhibition		PDE3-inhibition		cGMP-efflux		cAMP-efflux	
Temperature	**Sildenafil (μM)**	**Vardenafil (μM)**	**Sildenafil (μM)**	**Vardenafil (μM)**	**Sildenafil (μM)**	**Vardenafil (μM)**	**Sildenafil (μM)**	**Vardenafil (μM)**
37°C	0.002 ± 0.000	0.002 ± 0.001	5.61 ± 0.865#	0.757 ± 0.276#	3.93 ± 1.46	2.97 ± 0.823	3.51 ± 1.05	3.55 ± 0.311
34°C	0.004 ± 0.000	0.004 ± 0.001	4.21 ± 0.579#	1.14 ± 0.263#	2.08 ± 0.235#	5.31 ± 0.431#	3.59 ± 1.35	3.53 ± 0.415
32°C	0.006 ± 0.001*	0.004 ± 0.001	4.66 ± 0.647#	1.85 ± 0.173#	1.43 ± 0.497	3.67 ± 1.13	2.83 ± 0.828#	7.86 ± 1.02#
28°C	0.004 ± 0.001	0.004 ± 0.001	4.38 ± 0.739#	1.50 ± 0.505#	1.68 ± 0.172	2.79 ± 0.504	1.66 ± 0.232	5.84 ± 3.51
24°C	0.007 ± 0.001*	0.006 ± 0.001	6.49 ± 2.05	2.54 ± 0.218	1.25 ± 0.245	2.12 ± 0.523	–	–
20°C	0.009 ± 0.001*#	0.006 ± 0.000#	12.3 ± 0.675*#	3.36 ± 1.21#	1.56 ± 0.718	6.17 ± 2.71	–	–

Values are mean ± SEM and given in μ M.
**Significant difference (P-value < 0.05) when compared to normothermic control.*
#Significant difference (P-value < 0.05) when IC50 values of sildenafil and vardenafil are compared at same temperature. Neither of the drugs inhibited cAMP-efflux below 28°C.

TABLE 6 | IC_{25}–IC_{75} intervals, describing the concentration needed to increase inhibition of phosphodiesterase-5 (PDE5), phosphodiesterase-3 (PDE3), and inhibition of cAMP- and cGMP-efflux from 25% to 75%, at temperatures ranging from 37°C to 20°C.

IC_{25}–IC_{75}	PDE5		PDE3		cGMP-efflux		cAMP-efflux	
Temperature	**Sildenafil (μM)**	**Vardenafil (μM)**	**Sildenafil (μM)**	**Vardenafil (μM)**	**Sildenafil (μM)**	**Vardenafil (μM)**	**Sildenafil (μM)**	**Vardenafil (μM)**
37°C	0.038 ± 0.000	0.059 ± 0.029	460 ± 38.8	61.0 ± 14.3	23.6 ± 9.08	12.6 ± 3.89	27.1 ± 9.36	30.9 ± 6.82
34°C	0.055 ± 0.004	0.028 ± 0.012	411 ± 40.4	72.1 ± 3.24	13.5 ± 1.74	19.2 ± 3.16	19.8 ± 1.82	19.9 ± 0.967
32°C	0.060 ± 0.006	0.062 ± 0.016	485 ± 32.4	107 ± 27.0	9.76 ± 3.99	18.0 ± 4.12	20.0 ± 4.27	27.3 ± 6.19
28°C	0.083 ± 0.008	0.049 ± 0.016	450 ± 35.9	128 ± 35.9	12.0 ± 1.96	10.6 ± 2.75	13.8 ± 3.85	17.3 ± 6.59
24°C	0.098 ± 0.012*	0.074 ± 0.005	584 ± 55.0	148 ± 31.9	11.4 ± 4.73	13.0 ± 1.74	–	–
20°C	0.132 ± 0.048*	0.103 ± 0.027	697 ± 22.5*	709 ± 105*	19.2 ± 8.45	28.1 ± 14.6	–	–

Values are mean ± SEM given in μ M.
**Significant difference (P-value < 0.05) when compared to normothermic control. Neither of the drugs inhibited cAMP-efflux below 28°C.*

to 170 for vardenafil at 24°C and 74.5 for sildenafil at 20°C (**Table 7**).

cAMP Elimination

Both sildenafil and vardenafil are more efficient inhibitors of cAMP efflux than PDE3-mediated elimination in normothermic conditions, with an cAMP-efflux/PDE3 inhibition-ratio of 0.047 for sildenafil and 0.354 for vardenafil. Values decreased with reduced temperature. At 28°C the inhibition-ratios for sildenafil was 0.029, and 0.294 for vardenafil (**Table 7**).

DISCUSSION

Temperature reduction does not affect the ability of PDE5-inhibitors sildenafil and vardenafil to reach their cytosolic site of action. Our results show that both drugs inhibit

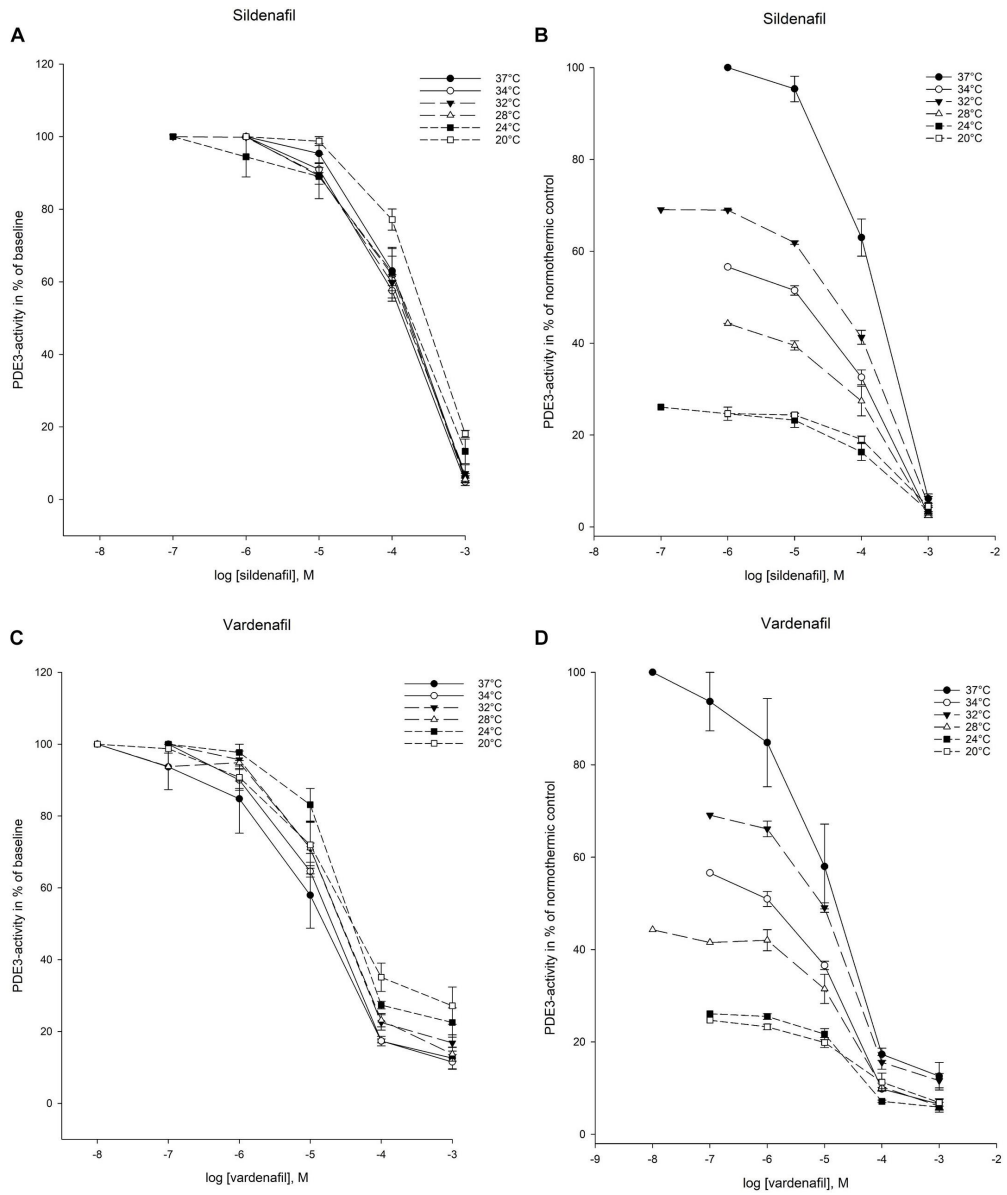

FIGURE 4 | Temperature-dependent inhibition of phosphodiesterase-3 (PDE3) by vardenafil and sildenafil. **(A)** Sildenafil inhibition curves for PDE3-activity at temperatures ranging from 37°C to 20°C. The doses of sildenafil are in logarithm of the concentration in mol/L. **(B)** Inhibition curves for PDE3-activity by sildenafil in % of normothermic inhibition curve at temperatures ranging from 37°C to 20°C. The doses of sildenafil are in logarithm of the concentration in mol/L. **(C)** Vardenafil inhibition curves for PDE3-activity at temperatures ranging from 37°C to 20°C. The doses of vardenafil are in logarithm of the concentration in mol/L. **(D)** Inhibition curves for PDE3-activity by vardenafil in % of normothermic inhibition curve at temperatures ranging from 37°C to 20°C. The doses of vardenafil are in logarithm of the concentration in mol/L.

elimination of cGMP, as well as cAMP, at temperatures down to 20°C. The concentration of sildenafil needed to inhibit PDE-enzymes is increased with temperature reduction, while there is a tendency toward increased sensitivity of efflux pumps to sildenafil-inhibition. Vardenafil concentrations needed to inhibit all elimination pathways remain unchanged during temperature reduction. Establishing the pharmacodynamic properties of these PDE5-inhibitors is crucial in the process of developing better treatment-guidelines for cardiovascular complications in accidental and therapeutic hypothermia.

Accidental hypothermia guidelines recommend to avoid pharmacological treatment until a body core temperature of minimum 30°C is reached (No Author, 2000; Truhlar et al., 2015). Subsequently, use of vasopressors are listed as the preferred drugs for cardiovascular support, despite the benefits being unclear (Paal et al., 2016). There are indications that this strategy might be unfavorable. In experimental hypothermia and rewarming, increased afterload is associated with HCD and a poor outcome (Dietrichs et al., 2014a, 2015; Håheim et al., 2017). Contradictory to current recommendations, pharmacologically induced vasodilation emerge as a promising strategy to prevent

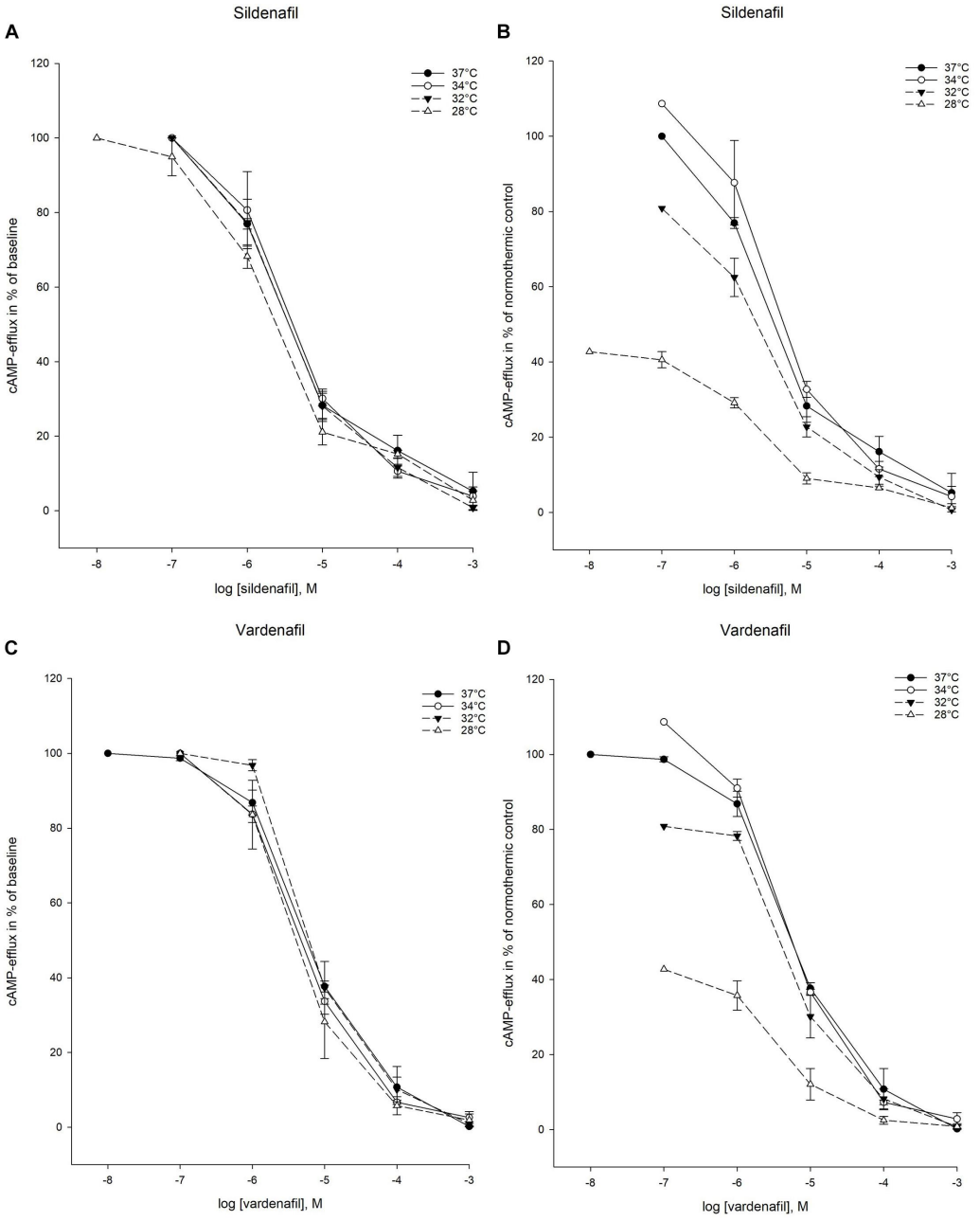

FIGURE 5 | Temperature-dependent inhibition of cAMP-efflux in inside-out vesicles (IOV). **(A)** Sildenafil inhibition curves for ABCC4-activity at temperatures ranging from 37°C to 28°C. The doses of sildenafil are in logarithm of the concentration in mol/L. **(B)** Inhibition curves for ABCC4-activity by sildenafil in % of normothermic inhibition curve at temperatures ranging from 37°C to 28°C. The doses of sildenafil are in logarithm of the concentration in mol/L. **(C)** Vardenafil inhibition curves for ABCC4-activity at temperatures ranging from 37°C to 28°C. The doses of vardenafil are in logarithm of the concentration in mol/L. **(D)** Inhibition curves for ABCC4-activity by vardenafil in % of normothermic inhibition curve at temperatures ranging from 37°C to 28°C. The doses of vardenafil are in logarithm of the concentration in mol/L.

HCD and elevate organ blood flood during rewarming (Håheim et al., 2017, 2020). cGMP elevation is a central mechanism for vasodilation that remains intact during severe hypothermia and rewarming (Håheim et al., 2017, 2020). Pharmacological cGMP-increase is achieved either through stimulating intracellular production, or through reducing elimination. At low core temperatures, it is apparent that drug-induced cGMP production, through stimulating the NO-GC-cGMP-PKG-pathway, is a challenging strategy. Doses of nitroprusside giving favorable effects in normothermia proved harmful in severe hypothermia, due to elevated potency, while doses adjusted to effect on mean arterial pressure (MAP) reduction were favorable (Håheim et al., 2017). In this context, elevating intracellular cGMP through inhibiting elimination, could prove a physiological approach

TABLE 7 | Drug selectivity for sildenafil and vardenafil at temperatures ranging from 37°C to 20°C.

Drug selectivity [IC_{50}]/[IC_{50}]	[PDE3-inhibition]/[PDE5-inhibition]		[cAMP-efflux-inhibition]/[cGMP-efflux-inhibition]		[cGMP-efflux-inhibition]/[PDE5-inhibition]		[cAMP-efflux-inhibition]/[PDE3-inhibition]	
Temperature	**Sildenafil**	**Vardenafil**	**Sildenafil**	**Vardenafil**	**Sildenafil**	**Vardenafil**	**Sildenafil**	**Vardenafil**
37°C	14400	1960	0.832	1.11	815	625	0.047	0.354
34°C	6730	1650	1.61	0.620	269	622	0.064	0.234
32°C	4240	2630	1.84	1.99	105	422	0.046	0.320
28°C	5780	2220	0.917	1.95	180	335	0.029	0.294
24°C	5110	2510	–	–	79.7	170	–	–
20°C	7270	3230	–	–	74.5	480	–	–

Values are ratios between IC_{50}-values for different elimination ways of cAMP and cGMP. Neither of the drugs inhibited cAMP-efflux below 28°C.

to achieve reduction of afterload, without causing uncontrolled reduction of MAP.

Our findings demonstrate that the difference between IC_{50}-values for cGMP-efflux-inhibition and PDE5-inhibition decreases during cooling, indicating that the elimination of cGMP during hypothermia is more dependent on cGMP-efflux. IC_{25}–IC_{75} intervals were calculated to estimate a pharmacodynamic window of effect for both drugs on all elimination pathways. No decrease was detected during hypothermia. Targeting cGMP-efflux, in addition to PDE5, therefore appears to be a relevant strategy for cardiovascular support during rewarming from hypothermia. We show that sildenafil and vardenafil are both able to inhibit these cGMP-elimination pathways at low core temperatures, and that they therefore show potential for treatment of hypothermic patients.

There is consensus of venoarterial extra corporeal membrane oxygenation (VA-ECMO) being the preferred treatment of hemodynamically unstable hypothermic patients (No Author, 2000; Brown et al., 2012; Truhlar et al., 2015; Saczkowski et al., 2018). During such treatment, cardiovascular complications are common (Rao et al., 2018; Choi et al., 2019). Left ventricle (LV) dysfunction can appear as not all of the circulating blood is directed through the VA-ECMO device. Some will still pass through the pulmonary circulation. Since MAP is increased by VA-ECMO, the LV has to overcome increased afterload to maintain ejection fraction. Failure could lead to LV-distention and elevated pressure, with a backward failure giving increased pulmonary pressure and edema (Lo Coco et al., 2018; Rao et al., 2018). Risk is higher if the patient has an underlying LV-dysfunction, like HCD (Dietrichs et al., 2018). Pharmacological afterload reduction is a suggested treatment strategy to alleviate backward failure during VA-ECMO-treatment, but it is important to avoid systemic hypotension (Rao et al., 2018). In the present experiment, inhibition of cGMP-efflux is achieved at supratherapeutic concentrations during both normothermia and hypothermia, while PDE5 inhibition by sildenafil or vardenafil, appears a promising strategy to achieve physiologically balanced afterload reduction, and prevent pulmonary edema in hypothermic VA-ECMO patients (Lo Coco et al., 2018).

In addition to afterload reduction, inotropic support could also be favorable during VA-ECMO-treatment (Rao et al., 2018). Inotropes are administered to help overcome the increased afterload and maintain LV ejection fraction (Rao et al., 2018). We show that sildenafil and vardenafil inhibit elimination of cAMP during hypothermia. Earlier studies have shown positive inotropic effect of PDE3-inhibition *in vivo* (Dietrichs et al., 2014a, 2018). IC_{50}-values for PDE5-inhibition by sildenafil and vardenafil are in the nM-range, while IC_{50}-values for PDE3 and inhibition of cAMP-efflux are in the μM-range. These concentrations are supratherapeutic during normothermia (**Tables 4, 5**). In order to provide evidence-based inotropic support during VA-ECMO-treatment in hypothermic patients, further studies on drugs that target inhibition of cAMP-elimination are needed as sildenafil and vardenafil appears to be ineffective in therapeutic doses.

Treatment of hemodynamically unstable hypothermic patients, face some of the same challenges as pre-hospital HAPE-treatment, when evacuation is difficult, and the patient is exposed to low temperatures. Sildenafil has been proposed as treatment, as it can be administered when oxygen treatment and rapid decent is impossible (Bates et al., 2007). The strong linear correlation between IC_{50}-value and decreasing temperature may serve as a helpful tool in low ambient temperatures, as effect is decided according to measured core temperature. Further investigation of pharmacokinetic data could complement this finding and help develop evidence-based guidelines, with pinpointed dose recommendations for cardiovascular support in hypothermic patients. Although sildenafil and tadalafil are the only PDE5-inhibitors suggested in the treatment of HAPE (Maggiorini et al., 2006; Bates et al., 2007), vardenafil may now be suggested as a candidate drug. Our findings show little pharmacodynamic change, meaning that clinicians only need to account for the impact of hypothermia on pharmacokinetic properties, when calculating adequate vardenafil dosage.

Metabolism of sildenafil and vardenafil is performed in the liver mainly by CYP3A4 but also CYP2C9 and CYP3A5 (Huang and Lie, 2013). Enzyme affinity is decreased with reduction of core temperature, impeding elimination (Tortorici et al., 2006; van den Broek et al., 2010). CYP3A4, the main metabolizing enzyme of both sildenafil and vardenafil is shown to have an activity of 48% at 26°C and 68% at 32°C (Fritz et al., 2005). Sildenafil and vardenafil are both metabolized to active metabolites that are less potent

than the parent compounds (Hyland et al., 2001; Bischoff, 2004b). These metabolites are largely eliminated through biliary excretion (Mehrotra et al., 2007), which also is impaired during hypothermia (van den Broek et al., 2010). Decreased activity of CYP-enzymes and biliary excretion during hypothermia, alongside changed plasma protein binding (van den Broek et al., 2010), will lead to slower metabolism of the PDE5-inhibitors, slower production of active metabolites, reduced excretion, altered free fraction and thus, unpredictable therapeutic effect and increased risk of toxicity. In order to safely introduce the use of PDE5-inhibitors in treatment of cardiovascular complications during hypothermia and rewarming, these pharmacokinetic aspects need to be addressed through further experiments.

Although PDE3 and PDE5 are the main targets for pharmacological agents aiming to treat cardiovascular conditions through PDE-inhibition, other PDEs could also be affected by sildenafil and vardenafil administration. None have been investigated during hypothermia. In therapeutic concentrations of the PDE5-inhibitors, the isoenzyme closest in IC_{50}-value, and of cardiovascular relevance, is PDE1 (Bischoff, 2004a; Levy et al., 2011). PDE2, PDE4, PDE6 and PDE9 may also influence cardiovascular functions by inhibition of metabolism of cAMP, cGMP or both. However, these PDEs have much higher IC_{50}-values for sildenafil and vardenafil during normothermia (Adderley et al., 2010; Kim and Kass, 2017). Studies on other PDEs were excluded from our experiment due to PDE5 being the main target for afterload reduction by vascular smooth muscle and PDE3 being the target for inotropic support in cardiac muscle. Our results show that sildenafil and vardenafil largely remain specific for PDE5. Further studies looking at other relevant PDEs in our hypothermic model would provide a better overall description on possible inhibition of other PDEs by sildenafil and vardenafil. PDEs are also known to interact when present in the same tissue or experimental solutions (Zhao et al., 2015). Assessing these different aspects could provide more information about potential effects and side effects of the drugs during hypothermia and therefore remains to be studied in future studies in our model.

CONCLUSION

Sildenafil and vardenafil are able to reach cytosol and IC_{50}-values for cGMP-elimination remain intact or predictable at temperatures down to 20°C. As the cellular effects of these drugs can cause afterload reduction, they show potential in treating cardiovascular dysfunction during hypothermia. Our findings lay foundation for *in vivo* studies and further development of evidence-based, pharmacological treatment guidelines in both accidental and therapeutic hypothermia, as well as in HAPE-patients.

DATA AVAILABILITY STATEMENT

The raw data supporting the conclusions of this article will be made available by the authors, without undue reservation.

ETHICS STATEMENT

Ethical review and approval was not required for the study on human participants in accordance with the local legislation and institutional requirements. The patients/participants provided their written informed consent to participate in this study.

AUTHOR CONTRIBUTIONS

AS, AK, NS, and TK conducted the experiments in the lab. RL helped with technical issues and theoretical questions during experiments. O-MF analyzed the results using mass-spectrometry. AS and ED interpreted the results and performed the statistics. AR, TT, GS, and ED planned the research project. AS, ED, O-MF, NS, and GS contributed to the manuscript. All authors read and approved the manuscript.

FUNDING

The project was funded by a grant from the medical research student program (Forskerlinjen) at UiT – The Arctic University of Tromsø awarded AS, a grant from Stiftelsen Norsk Luftambulanse awarded AK and a grant from the Northern Norwegian Health Authority [HNF1337–17] awarded ED.

ACKNOWLEDGMENTS

We thank the Department of Immunohematology and Transfusion Medicine, University Hospital of North Norway for the contribution of blood used in the experiments.

REFERENCES

Adderley, S. P., Sprague, R. S., Stephenson, A. H., and Hanson, M. S. (2010). Regulation of cAMP by phosphodiesterases in erythrocytes. *Pharmacol. Rep.* 62, 475–482. doi: 10.1016/s1734-1140(10)70303-0

Bates, M. G., Thompson, A. A., and Baillie, J. K. (2007). Phosphodiesterase type 5 inhibitors in the treatment and prevention of high altitude pulmonary edema. *Curr. Opin. Investig. Drugs* 8, 226–231.

Bischoff, E. (2004a). Potency, selectivity, and consequences of nonselectivity of PDE inhibition. *Int. J. Impot. Res.* 16, S11–S14.

Bischoff, E. (2004b). Vardenafil preclinical trial data: potency, pharmacodynamics, pharmacokinetics, and adverse events. *Int. J. Impotence Res.* 16, S34–S37.

Brown, D. J. A., Brugger, H., Boyd, J., and Paal, P. (2012). Accidental Hypothermia. *N. Engl. J. Med.* 367, 1930–1938.

Bush, H. L., Hydo, L. J., Fischer, E., Fantini, G. A., Silane, M. F., and Barie, P. S. (1995). Hypothermia during elective abdominal aortic aneurysm repair: the high price of avoidable morbidity. *J. Vasc. Surg.* 21, 392–400. doi: 10.1016/s0741-5214(95)70281-4

Cheng, Y., and Prusoff, W. H. (1973). Relationship between the inhibition constant (K1) and the concentration of inhibitor which causes 50 per cent inhibition

(I50) of an enzymatic reaction. *Biochem. Pharmacol.* 22, 3099–3108. doi: 10.1016/0006-2952(73)90196-2

Choi, M. S., Sung, K., and Cho, Y. H. (2019). Clinical Pearls of Venoarterial Extracorporeal Membrane Oxygenation for Cardiogenic Shock. *Kor. Circulat. J.* 49, 657–677. doi: 10.4070/kcj.2019.0188

Chou, T. C. (1976). Derivation and properties of Michaelis-Menten type and Hill type equations for reference ligands. *J. Theor. Biol.* 59, 253–276. doi: 10.1016/0022-5193(76)90169-7

Dietrichs, E. S., Håheim, B., Kondratiev, T., Sieck, G. C., and Tveita, T. (2014a). Cardiovascular effects of levosimendan during rewarming from hypothermia in rat. *Cryobiology* 69, 402–410. doi: 10.1016/j.cryobiol.2014.09.007

Dietrichs, E. S., Håheim, B., Kondratiev, T., Traasdahl, E., and Tveita, T. (2018). Effects of hypothermia and rewarming on cardiovascular autonomic control in vivo. *J. Appl. Physiol.* 124, 850–859. doi: 10.1152/japplphysiol.00317.2017

Dietrichs, E. S., Kondratiev, T., and Tveita, T. (2014b). Milrinone ameliorates cardiac mechanical dysfunction after hypothermia in an intact rat model. *Cryobiology* 69, 361–366. doi: 10.1016/j.cryobiol.2014.09.002

Dietrichs, E. S., Sager, G., and Tveita, T. (2016). Altered pharmacological effects of adrenergic agonists during hypothermia. *Scandinav. J. Trauma Resuscitat. Emerg. Med.* 24:143.

Dietrichs, E. S., Schanche, T., Kondratiev, T., Gaustad, S. E., Sager, G., and Tveita, T. (2015). Negative inotropic effects of epinephrine in the presence of increased β-adrenoceptor sensitivity during hypothermia in a rat model. *Cryobiology* 70, 9–16. doi: 10.1016/j.cryobiol.2014.10.012

Elin Orvoll, R. A. L., Ravna, A. W., and Sager, G. (2013). Misoprostol and the Sildenafil Analog (PHAR-0099048) Modulate Cellular Efflux of cAMP and cGMP Differently. *Pharmacol. Pharm.* 2013, 104–109. doi: 10.4236/pp.2013.41015

Ellman, G. L., Courtney, K. D., Andres, V. Jr., and Feather-Stone, R. M. (1961). A new and rapid colorimetric determination of acetylcholinesterase activity. *Biochem. Pharmacol.* 7, 88–95. doi: 10.1016/0006-2952(61)90145-9

Fritz, H. G., Holzmayr, M., Walter, B., Moeritz, K.-U., Lupp, A., and Bauer, R. (2005). The Effect of Mild Hypothermia on Plasma Fentanyl Concentration and Biotransformation in Juvenile Pigs. *Anesthesia Analgesia* 100, 996–1002. doi: 10.1213/01.ane.0000146517.17910.54

Håheim, B., Kondratiev, T., Dietrichs, E. S., and Tveita, T. (2017). The beneficial hemodynamic effects of afterload reduction by sodium nitroprusside during rewarming from experimental hypothermia. *Cryobiology* 77, 75–81. doi: 10.1016/j.cryobiol.2017.05.002

Håheim, B., Kondratiev, T., Dietrichs, E. S., and Tveita, T. (2020). Comparison Between Two Pharmacologic Strategies to Alleviate Rewarming Shock: Vasodilation vs. Inodilation. *Front. Med.* 7:566388. doi: 10.3389/fmed.2020.566388

Henrohn, D., Sandqvist, A., Hedeland, M., Egeröd, H., Bondesson, U., and Wikström, G. (2012). Acute haemodynamic response in relation to plasma vardenafil concentrations in patients with pulmonary hypertension. *Br. J. Clin. Pharmacol.* 74, 990–998. doi: 10.1111/j.1365-2125.2012.04303.x

Huang, S. A., and Lie, J. D. (2013). Phosphodiesterase-5 (PDE5) Inhibitors In the Management of Erectile Dysfunction. *P T Peer Rev. J. Formul. Manage.* 38, 407–419.

Hyland, R., Roe, E. G., Jones, B. C., and Smith, D. A. (2001). Identification of the cytochrome P450 enzymes involved in the N-demethylation of sildenafil. *Br. J. Clin. Pharmacol.* 51, 239–248. doi: 10.1046/j.1365-2125.2001.00318.x

Jedlitschky, G., Burchell, B., and Keppler, D. (2000). The multidrug resistance protein 5 functions as an ATP-dependent export pump for cyclic nucleotides. *J. Biol. Chem.* 275, 30069–30074. doi: 10.1074/jbc.m005463200

Johnson, W. B., Katugampola, S., Able, S., Napier, C., and Harding, S. E. (2012). Profiling of cAMP and cGMP phosphodiesterases in isolated ventricular cardiomyocytes from human hearts: Comparison with rat and guinea pig. *Life Sci.* 90, 328–336. doi: 10.1016/j.lfs.2011.11.016

Kim, G. E., and Kass, D. A. (2017). Cardiac Phosphodiesterases and Their Modulation for Treating Heart Disease. *Handb. Exp. Pharmacol.* 243, 249–269. doi: 10.1007/164_2016_82

Kondratiev, T. V., Flemming, K., Myhre, E. S. P., Sovershaev, M. A., and Tveita, T. (2006). Is oxygen supply a limiting factor for survival during rewarming from profound hypothermia? *Am. J. Physiol. Heart Circulat. Physiol.* 291, H441–H450.

Levy, I., Horvath, A., Azevedo, M., de Alexandre, R. B., and Stratakis, C. A. (2011). Phosphodiesterase function and endocrine cells: links to human disease and roles in tumor development and treatment. *Curr. Opin. Pharmacol.* 11, 689–697. doi: 10.1016/j.coph.2011.10.003

Lo Coco, V., Lorusso, R., Raffa, G. M., Malvindi, P. G., Pilato, M., Martucci, G., et al. (2018). Clinical complications during veno-arterial extracorporeal membrane oxigenation in post-cardiotomy and non post-cardiotomy shock: still the achille's heel. *J. Thoracic Dis.* 10, 6993–7004. doi: 10.21037/jtd.2018.11.103

Luks, A. M., Swenson, E. R., and Bärtsch, P. (2017). Acute high-altitude sickness. *Eur. Respirat. Rev.* 26:160096.

Maggiorini, M., Brunner-La Rocca, H. P., Peth, S., Fischler, M., Böhm, T., Bernheim, A., et al. (2006). Both tadalafil and dexamethasone may reduce the incidence of high-altitude pulmonary edema: a randomized trial. *Ann. Intern. Med.* 145, 497–506. doi: 10.7326/0003-4819-145-7-200610030-00007

Mann, D. L., Kent, R. L., Parsons, B., and Cooper, G. T. (1992). Adrenergic effects on the biology of the adult mammalian cardiocyte. *Circulation* 85, 790–804. doi: 10.1161/01.cir.85.2.790

Mehrotra, N., Gupta, M., Kovar, A., and Meibohm, B. (2007). The role of pharmacokinetics and pharmacodynamics in phosphodiesterase-5 inhibitor therapy. *Int. J. Impot. Res.* 19, 253–264. doi: 10.1038/sj.ijir.3901522

No Author. (2000). Part 8: Advanced Challenges in Resuscitation. *Circulation* 102(Suppl._1), I–229–I–52. doi: 10.1016/s0300-9572(00)00286-0

Paal, P., Gordon, L., Strapazzon, G., Brodmann Maeder, M., Putzer, G., Walpoth, B., et al. (2016). Accidental hypothermia–an update. *Scand. J. Trauma Resuscitat. Emerg. Med.* 24:111. doi: 10.1016/0300-9572(96)00983-5

Rao, P., Khalpey, Z., Smith, R., Burkhoff, D., and Kociol, R. D. (2018). Venoarterial Extracorporeal Membrane Oxygenation for Cardiogenic Shock and Cardiac Arrest. *Circulat. Heart Failure* 11:e004905.

Ring, A., Morris, T., Wozniak, M., Sullo, N., Dott, W., Verheyden, V., et al. (2017). A Phase I study to determine the pharmacokinetic profile, safety and tolerability of sildenafil (Revatio(§)) in cardiac surgery: the REVAKI-1 study. *Br. J. Clin. Pharmacol.* 83, 709–720. doi: 10.1111/bcp.13162

Saczkowski, R. S., Brown, D. J. A., Abu-Laban, R. B., Fradet, G., Schulze, C. J., and Kuzak, N. D. (2018). Prediction and risk stratification of survival in accidental hypothermia requiring extracorporeal life support: An individual patient data meta-analysis. *Resuscitation* 127, 51–57. doi: 10.1016/j.resuscitation.2018.03.028

Sandqvist, A. M., Henrohn, D., Schneede, J., Hedeland, M., Egeröd, H. C., Bondesson, U. G., et al. (2013). High inter-individual variability of vardenafil pharmacokinetics in patients with pulmonary hypertension. *Eur. J. Clin. Pharmacol.* 69, 197–207. doi: 10.1007/s00228-012-1323-5

Sellers, Z. M., Naren, A. P., Xiang, Y., and Best, P. M. (2012). MRP4 and CFTR in the regulation of cAMP and β-adrenergic contraction in cardiac myocytes. *Eur. J. Pharmacol.* 681, 80–87. doi: 10.1016/j.ejphar.2012.02.018

Sessler Daniel, I. (2001). Complications and Treatment of Mild Hypothermia. *Anesthesiology* 95, 531–543. doi: 10.1097/00000542-200108000-00040

Subbotina, A., Ravna, A. W., Lysaa, R. A., Abagyan, R., Bugno, R., and Sager, G. (2017). Inhibition of PDE5A1 guanosine cyclic monophosphate (cGMP) hydrolysing activity by sildenafil analogues that inhibit cellular cGMP efflux. *J. Pharmacy Pharmacol.* 69, 675–683. doi: 10.1111/jphp.12693

Tortorici, M. A., Kochanek, P. M., Bies, R. R., and Poloyac, S. M. (2006). Therapeutic hypothermia-induced pharmacokinetic alterations on CYP2E1 chlorzoxazone-mediated metabolism in a cardiac arrest rat model. *Crit. Care Med.* 34, 785–791. doi: 10.1097/01.ccm.0000201899.52739.4f

Truhlar, A., Deakin, C. D., Soar, J., Khalifa, G. E., Alfonzo, A., Bierens, J. J., et al. (2015). European Resuscitation Council Guidelines for Resuscitation 2015: Section 4. Cardiac arrest in special circumstances. *Resuscitation* 95, 148–201.

Tveita, T. (2000). Rewarming from hypothermia. Newer aspects on the pathophysiology of rewarming shock. *Int. J. Circumpol. Health* 59, 260–266.

Tveita, T., and Sieck, G. C. (2012). Effects of milrinone on left ventricular cardiac function during cooling in an intact animal model. *Cryobiology* 65, 27–32. doi: 10.1016/j.cryobiol.2012.03.007

Vachiery, J.-L., Huez, S., Gillies, H., Layton, G., Hayashi, N., Gao, X., et al. (2011). Safety, tolerability and pharmacokinetics of an intravenous bolus of sildenafil in patients with pulmonary arterial hypertension. *Br. J. Clin. Pharmacol.* 71, 289–292. doi: 10.1111/j.1365-2125.2010.03831.x

van den Broek, M. P. H., Groenendaal, F., Egberts, A. C. G., and Rademaker, C. M. A. (2010). Effects of Hypothermia on Pharmacokinetics and Pharmacodynamics. *Clin. Pharmacokinet.* 49, 277–294. doi: 10.2165/11319360-000000000-00000

Vassal, T., Benoit-Gonin, B., Carrat, F., Guidet, B., Maury, E., and Offenstadt, G. (2001). Severe accidental hypothermia treated in an ICU: prognosis and outcome. *Chest* 120, 1998–2003. doi: 10.1378/chest.120.6.1998

Walker, D. K. (1999). Pharmacokinetics and metabolism of sildenafil in mouse, rat, rabbit, dog and man. *Xenobiotica* 29, 297–310. doi: 10.1080/004982599238687

Westensee, J., Rogé, I., Van, Roo JD, Pesce, C., Batzli, S., Courtney, D. M., et al. (2013). Mountaineering Fatalities on Aconcagua: 2001–2012. *High Altitude Med. Biol.* 14, 298–303. doi: 10.1089/ham.2013.1018

Zhao, C. Y., Greenstein, J. L., and Winslow, R. L. (2015). Interaction between phosphodiesterases in the regulation of the cardiac β-adrenergic pathway. *J. Mol. Cell Cardiol.* 88, 29–38. doi: 10.1016/j.yjmcc.2015.09.011

Conflict of Interest: The authors declare that the research was conducted in the absence of any commercial or financial relationships that could be construed as a potential conflict of interest.

Publisher's Note: All claims expressed in this article are solely those of the authors and do not necessarily represent those of their affiliated organizations, or those of the publisher, the editors and the reviewers. Any product that may be evaluated in this article, or claim that may be made by its manufacturer, is not guaranteed or endorsed by the publisher.

frontiers in Physiology

ORIGINAL RESEARCH
published: 06 September 2021
doi: 10.3389/fphys.2021.718667

Cardiovascular Effects of Epinephrine During Experimental Hypothermia (32°C) With Spontaneous Circulation in an Intact Porcine Model

*Rizwan Mohyuddin[1], Erik Sveberg Dietrichs[2,3], Predip Sundaram[1], Timofey Kondratiev[1], Marie Fjellanger Figenschou[1,4], Gary C. Sieck[5] and Torkjel Tveita[1,4,5]**

[1]Anesthesia and Critical Care Research Group, Department of Clinical Medicine, UiT, The Arctic University of Norway, Tromsø, Norway, [2]Experimental and Clinical Pharmacology Research Group, Department of Medical Biology, UiT, The Arctic University of Norway, Tromsø, Norway, [3]Center for Psychopharmacology, Diakonhjemmet Hospital, Oslo, Norway, [4]Division of Surgical Medicine and Intensive Care, University Hospital of North Norway, Tromsø, Norway, [5]Department of Physiology and Biomedical Engineering, Mayo Clinic, Rochester, MI, United States

OPEN ACCESS

Edited by:
Bruno Moreira Silva, Federal University of São Paulo, Brazil

Reviewed by:
Raphael Briot, Centre Hospitalier Universitaire de Grenoble, France
Paweł Podsiadło, Jan Kochanowski University, Poland

***Correspondence:**
Torkjel Tveita
torkjel.tveita@uit.no

Specialty section:
This article was submitted to Clinical and Translational Physiology, a section of the journal Frontiers in Physiology

Received: *01 June 2021*
Accepted: *25 June 2021*
Published: *06 September 2021*

Citation:
Mohyuddin R, Dietrichs ES, Sundaram P, Kondratiev T, Figenschou MF, Sieck GC and Tveita T (2021) Cardiovascular Effects of Epinephrine During Experimental Hypothermia (32°C) With Spontaneous Circulation in an Intact Porcine Model. Front. Physiol. 12:718667. doi: 10.3389/fphys.2021.718667

Aims: Rewarming from accidental hypothermia and therapeutic temperature management could be complicated by cardiac dysfunction. Although pharmacologic support is often applied when rewarming these patients, updated treatment recommendations are lacking. There is an underlying deficiency of clinical and experimental data to support such interventions and this prevents the development of clinical guidelines. Accordingly, we explored the clinical effects of epinephrine during hypothermic conditions.

Materials and methods: Anesthetized pigs were immersion cooled to 32°C. Predetermined variables were compared at temperature/time-point baseline, after receiving 30 ng/kg/min and 90 ng/kg/min epinephrine infusions: (1) before and during hypothermia at 32°C, and after rewarming to 38°C (n = 7) and (2) a time-matched (5 h) normothermic control group (n = 5).

Results: At 32°C, both stroke volume and cardiac output were elevated after 30 ng/kg/min administration, while systemic vascular resistance was reduced after 90 ng/kg/min. Epinephrine infusion did not alter blood flow in observed organs, except small intestine flow, and global O_2 extraction rate was significantly reduced in response to 90 ng/kg/min infusion. Electrocardiographic measurements were unaffected by epinephrine infusion.

Conclusion: Administration of both 30 ng/kg/min and 90 ng/kg/min at 32°C had a positive inotropic effect and reduced afterload. We found no evidence of increased pro-arrhythmic activity after epinephrine infusion in hypothermic pigs. Our experiment therefore suggests that β_1-receptor stimulation with epinephrine could be a favorable strategy for providing cardiovascular support in hypothermic patients, at core temperatures >32°C.

Keywords: cardiovascular dysfunction, vasopressor, targeted temperature management, rewarming, electrophysiology, ventricular arrhythmias

INTRODUCTION

Guidelines for targeted temperature management (TTM) and therapeutic hypothermia recommend reducing core temperatures to 36–32°C for neuroprotection in comatose patients after resuscitation from sudden cardiac arrest (Nolan et al., 2015). However, after return of spontaneous circulation, these patients often suffer acute heart failure and need inotropic drugs to support inadequate circulatory function (Bernard et al., 2002; Safar and Kochanek, 2002).

Temperatures similar to those used in TTM are regularly observed in victims of accidental hypothermia. These patients often display hypothermia-induced cardiac dysfunction (HCD), associated with reduced cardiac output (CO) during rewarming. In order to elevate low CO, epinephrine has been used in experimental treatment of HCD (Kondratiev and Tveita, 2006; Tveita and Sieck, 2011). Despite its frequent use as an inotropic agent, little is known about the clinical effects of epinephrine (Epi) in TTM patients and victims of accidental hypothermia. Accordingly, guidelines describing the use of inotropic drugs to support cardiovascular function at low core temperatures are lacking evidence-based information. Thus, it is vital to acquire more translational data to understand the pharmacological properties of Epi at low core temperatures.

During normal core temperatures, Epi works as a β-receptor agonist and increases cardiac contractility *via* a G protein – protein kinase A (PKA) signaling pathway, by increasing cyclic adenosine monophosphate (cAMP). In low concentrations, Epi causes peripheral vasodilation, through β_2-stimulation and elevated cAMP in smooth muscle. At higher concentrations β-adrenergic selectivity is lost, with increasing α-receptor stimulation, causing vasoconstriction (Dietrichs et al., 2016). Several of our *in vivo* rat studies have shown that Epi failed to elevate stroke volume (SV) and cardiac out (CO) during hypothermia and after rewarming. Moreover, it has been reported that inotropic effect of Epi decreases below 34°C, due to relative higher α-receptor than β-receptor response, shown through elevated total peripheral resistance (Kondratiev and Tveita, 2006; Tveita and Sieck, 2011; Dietrichs et al., 2016). We found that low dose (0.125 μg/min) Epi compared to high dose (1.25 μg/min) gave positive inotropic effect during hypothermia (28°C; Tveita and Sieck, 2011). These results in a rat model indicate that hypothermia exerts a negative impact on cardiac inotropy, mediated by the β_1-receptor pathway, causing a reduced therapeutic interval for beneficial effects of Epi (Dietrichs et al., 2016).

Fundamental species-dependent differences exist in physiology and metabolism, including pharmacokinetics and pharmacodynamics of different drugs (Toutain et al., 2010). In this study, a pig model was chosen due to its close morphologic and physiologic relationship with humans, giving a higher translational potential than previous findings in rodents (Swindle, 1998). Accordingly, the present study aimed to assess whether a low (30 ng/kg/min) and a high (90 ng/kg/min) doses of Epi provide inotropic support at low core temperatures, relevant in TTM and accidental hypothermia. For this purpose, we monitored global O_2 delivery (DO_2), O_2 consumption (VO_2), and organ blood flow, as well as cardiac electrophysiology during hypothermia (32°C) and rewarming to 38°C, using an intact porcine model with spontaneous circulation throughout the experiment.

MATERIALS AND METHODS

Ethical Approval

The Norwegian National Animal Research Authority approved the experimental protocol. The experiments were conducted in accordance with the Norwegian Regulation on Animal Experimentation and the European Contention for the Protection of Vertebrate Animals used for Experimental and Other Scientific Purposes (European Council, ETS no. 170). The animals received humane care in accordance to the Norwegian Animal Welfare Act.

Experimental Animals

Fourteen castrated juvenile male NOROC stock pigs weighing 27 ± 5 kg were acclimated to the animal department for 3–5 days before experiments. Two pigs were used for pilot experiments to determine expedient dose of Epi.

Anesthesia and Instrumentation

Methods for anesthesia, instrumentation, monitoring, sampling, data analysis, and calculations used in the porcine animal model for this study were previously described in detail (Valkov et al., 2019). Briefly, after an overnight fast, the pigs were premedicated by *i.m.* injections of 20 mg/kg ketamine, 30 mg midazolam, and 1 mg of atropine. Anesthesia was induced by intravenous injection of pentobarbital 10 mg/kg and fentanyl 0.01 mg/kg. The pigs were tracheostomized and intubated with a 7.0 mm Portex tracheal tube. They were ventilated with end-expiratory pressure of 0 cm H_2O, FiO_2 0.21 (Siemens Servo 900D, Solna, Sweden). Arterial, central venous, mixed venous, and cerebral venous were sampled and analyzed (ABL800 FLEX, Radiometer medical, Copenhagen, Denmark) to confirm adequate ventilation and calculate global and cerebral O_2 transport. Anesthesia was maintained by continuous intravenous infusion of pentobarbital 4 mg/kg/h, fentanyl 0.02 mg/kg/h, and midazolam 0.3 mg/kg/h along with infusion of 9 ml/kg/h Ringer-acetate throughout the experiment. Euthanasia was performed by *i.v.* injection of 1 g pentobarbital and 20 ml KCl (1 mmol/ml) at the end of experiment. Medical infusions were provided through an 18 Ga central venous line in the right jugular vein. Cerebral venous blood gases were obtained from a retrograde 18 Ga central venous line in the jugular bulb, introduced through the left internal jugular vein (7–10 cm). Pulmonary artery pressure, central venous pressure (CVP), core temperature, and CO measurements were enabled *via* a 7.5 Fr Swan-Ganz catheter (Edwards Lifesciences, Irvine, United States) in the pulmonary trunk through an 8.5 Fr Intro-Flex introducer (Intro-Flex, Edwards Lifesciences, Irvine, United States) in the left femoral vein. CO was

measured by thermodilution using a CO-monitor (Vigilance, Edwards Lifesciences, Irvine, United States). For preload reduction, a 7 Fr Fogarty catheter (Edwards Lifesciences, Irvine, United States) was placed in the inferior vena cava *via* an 8.5 Fr introducer in the right femoral vein. A 7 Fr pressure-volume (PV) catheter (Ventri-Cath-507, Millar Instruments, Huston, TX, United States) was placed in the left ventricle *via* a 10 Fr Super Arrow-Flex introducer (Arrow, Reading, United States) in the right carotid artery. A 7.5 Fr Swan-Ganz catheter was lead through an 8 Fr introducer (Super Arrow-Flex PSI Set, Arrow, Reading, United States) in the left femoral artery and positioned in the aortic arch for measurement of blood pressure, sampling of blood for arterial blood gases and microspheres reference sampling. Injections of stable isotope labeled microspheres were performed *via* a 6 Fr pigtail catheter (Cordis Corporation, Miami, FL, United States) positioned in the left ventricle *via* an 8 Fr introducer through the right femoral artery. All animals received 5000 IU heparin after instrumentation. A 16 Fr Foley catheter (Teleflex Medical, Perak, Malaysia) was introduced *via* a lower abdominal incision for continuous monitoring of urinary output.

Experimental Protocol

Following surgery, animals were allowed to rest for 30 min before experiments started. To assess the appropriate dose of Epi, a pilot experiment was performed using two pigs. One pig received Epi infusions at normothermia in doses of 15, 30, 45, 60, 75, 90, 105, and 120 ng/kg/min, while monitoring HR, MAP, CVP, and CO. A 25–30% increase in CO was determined as a target for the first Epi dose (E1), whereas the target for the second Epi dose (E2) was inducing a maximal increase of CO. The selected doses were administered again after the initial tests to test the reproducibility of the results. The second pig was cooled to 32°C, and Epi doses of 30, 75, and 90 ng/kg/min were administered to test effect on CO. From these pilot experiments, Epi doses of 30 and 90 ng/kg/min were chosen.

Twelve animals were divided into two groups: normothermic (NT group, n = 5) and hypothermic (HT group, n = 7). Sample size was calculated using power analysis. In both groups, data were assessed at three different time points. For the NT group recordings were performed at baseline after initial stabilization, and then after 3 h and 5 h at 38°C (**Figure 1**). For the HT group, recordings were performed at 38°C baseline, and then after 30 min and 3?? at 32°C (3 h) and also following rewarming to 38°C (5 h). At each time period, three samples were obtained as: baseline before starting Epi infusion (E0), during 30 ng/kg/min Epi infusion (E1), and during 90 ng/kg/min Epi infusion (E2). Each Epi infusion continued for at least 5 min before recording was started, and lasted 15–20 min. All hemodynamic data were recorded using a digital acquisition system (PowerLab 16/35, ADInstruments, Bella Vista, Australia and MPVS Ultra PV unit, Millar Instruments, Huston, TX, United States) and were analyzed using Lab Chart Pro 8 software (ADInstruments, Bella Vista, Australia).

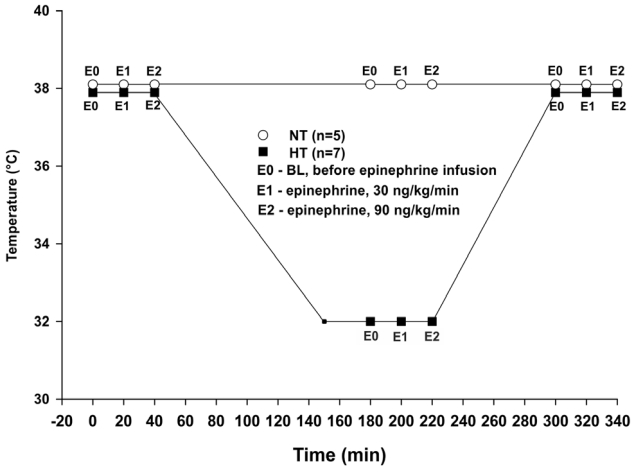

FIGURE 1 | Experimental protocol. NT – time-matched normothermic group, kept at 38°C for 5 h (n = 5); HT – hypothermic group, cooled to 32°C and rewarmed back to 38°C (n = 7); E0 – no epinephrine; E1 – epinephrine, 30 ng/kg/min; and E2 – epinephrine, 90 ng/kg/min.

Temperature Regulation

Core body temperature was monitored *via* a thermistor positioned at the tip of the thermodilution catheter positioned in the pulmonary artery. Animals in the HT group were cooled by circulating iced water in a reservoir mounted to the top of the operating table with the animals placed in a supine position, leaving the dorsal 2/3 of the body submerged. As blood temperature reached 32°C, water was drained from the reservoir and temperature stabilized at 32 ± 1°C, which was chosen due to this temperature being the lower end of therapeutic temperature management in comatose survivors of cardiac arrest. For rewarming, the reservoir was circulated with tap water at a temperature of 38–40°C.

Regional Blood Flow

Regional blood flow was estimated using method of neutron activation of stable isotope labeled microspheres (BioPAL Inc., Worchester, MA, United States) proposed by Reinhardt et al. (2001) as a high-sensitive and reliable method for measuring of regional blood flow in intact tissue. This method was refined to use in our animal model as described in detail by Valkov et al. (2019).

At every data sampling time point an injection of ∼ 10^6 microspheres, of different specificity, was given through a fluid-filled pigtail catheter placed in the left ventricle. At the same time, a reference blood sample was drawn from the aortic arch using a withdrawal pump set at a fixed sample rate (5 ml min^{-1}) for 2 min (New Era Pump Systems, Inc., Farmingdale, NY, United States). Each reference blood sample, with the predetermined type of microsphere in accordance with the data collection point, was collected in 20 ml sample vials. The syringe was rinsed with "sansSaLine" medium (BioPAL, Inc.) to secure removal of microspheres attached to the wall. Reference blood samples were centrifuged twice with "sansSaLine"

to remove sodium and chloride together with the supernatant to improve the signal-to-noise ratio of the sample. After the end of the experiment, animals were killed, and organ tissue samples were taken from the same locations in all animals and rinsed with "sansSaLine" to remove surface blood and other potential contaminants. Both reference blood samples and organ tissue samples were dried in an oven (70°C overnight). After processing, reference blood samples and tissue samples were analyzed at the BioPAL laboratory for specific activity. Tissue samples for evaluation of regional blood flow were taken from the heart, brain, kidneys, liver, stomach, and small intestine. Determination of regional tissue blood flow (expressed in milliliters per minute per gram) was calculated using the following equation: $Q = \left(\mathrm{Tis_{dpm}} \times \mathrm{Q_{ref}}\right) / \left(\mathrm{Ref_{dpm}} \times \mathrm{g}\right)$, where Q is blood flow in milliliters per minute, $\mathrm{Tis_{dpm}}$ is the number of radioactive decays in the tissue sample in decays per minute, Q_{ref} is the reference flow rate in milliliters per minute, $\mathrm{Ref_{dpm}}$ is the number of radioactive decays in the reference blood sample in decays per minute, and g is weight of the tissue sample in grams (Valkov et al., 2019).

Hemodynamic Variables, Global and Cerebral O_2 Transport, and O_2 Extraction Rate

Left ventricular pressure was measured by a pressure transducer on the tip of the PV catheter. Left ventricular contractility was assessed by occluding the inferior vena cava with an inflatable balloon. At each data sampling point, the balloon was inflated to obtain different levels of mechanical work. To relate the raw measurement to an estimate of actual volume, transthoracic echocardiographic measurements (parasternal short axis view) of end diastolic diameter and end systolic diameter were obtained at all data sampling points. Using the Teichholz formula $\left(\mathrm{EDV} = \left[\frac{7}{2.4 + \mathrm{EDD}}\right] \times \mathrm{EDD}^3\right)$, left ventricular end diastolic volume (EDV) and end systolic volume were calculated. The same operator conducted all echocardiographic measurements.

CO values were obtained from thermodilution data. Stroke volume (SV) was calculated as: SV = CO/HR. O_2 content ($ContO_2$) values in arterial, mixed venous, and jugular bulb samples were calculated according to the formula: $\mathrm{ContO_2} = \left(\mathrm{sO_2} \times \mathrm{Hb} \times \left(1.34 \times 10^{-2}\right)\right) + \left(\mathrm{pO_2} \times 0.023\right)$, where sO_2 is blood O_2 saturation (%) and Hb is hemoglobin (ml/dl). Global DO_2 was calculated as the product of CO and arterial $ContO_2$ per kg body weight. Global VO_2 was calculated as the product of CO and the difference between arterial and mixed venous $ContO_2$ per kg body weight. Cerebral DO_2 was calculated as a product of arterial $ContO_2$ and cerebral blood flow (CBF). CBF was estimated using the average flow of the five cerebral samples (right and left temporal, right and left cerebellum, and hippocampus) using the regional blood flow estimation technique. Cerebral VO_2 was calculated as a product of difference between arterial and jugular bulb $ContO_2$ and CBF. Global and cerebral O_2 extraction rate (O_2 ER) was calculated as the ratio of corresponding VO_2 to DO_2 values.

Electrocardiogram

Internal resultant ECG signals from the conductance catheter were used. The first 4–5 beats in steady state at each recording point were averaged and analyzed using Lab Chart Pro 8 software. QT interval was corrected for HR using Bazett's formula (QTc). QRS/QTc was calculated according to a recent publication relating this parameter to risk for hypothermia-induced cardiac arrest (Dietrichs et al., 2020a,b).

Statistics

Sample size was calculated using power analysis. The results for blood flow and O_2 transport are presented as means ± SD. The results for hemodynamic variables and ECG intervals are presented as median and percentiles. Data distribution was assessed using Shapiro-Wilk test. Dependent on data distribution, one-way RM ANOVA for normal distributed data or RM ANOVA on ranks for non-normal distributed data, was used to compare values within groups. If the F value was greater than critical, *post-hoc* tests were used to obtain p values. *Tukey's* test was used for pairwise multiple comparison of corresponding values before and during epinephrine infusions within groups. *Dunnett's* test was used to compare baseline values at 38°C to baseline values before Epi infusion after 3–5 h (NT group) and at 32–38°C after rewarming (HT group). The values of $p < 0.05$ were considered statistically significant.

RESULTS

Cooling and Rewarming Rates

All animals survived the experimental protocol. Cooling from 38°C to 32°C was carried out with a cooling rate of 4°C/h, while the rewarming rate was 4.5°C/h.

Responses to Epi Infusion in NT and HT Groups at 38°C Baseline

Hemodynamics

Compared to baseline values (before Epi infusion), hemodynamic responses were identical in the two groups (**Figures 2–4**). A significant increase in HR was observed only in response to 90 ng/kg/min, while SV and CO increased significantly in response to 30 ng/kg/mg. MAP and left ventricular systolic pressure (LVSP) remained unchanged, whereas SVR was significantly reduced in response to 30 ng/kg/min. Both maximum rate of LV pressure rise (dP/dt_{max}) and preload recruitable stroke work (PRSW) increased in response to 90 ng/kg/min.

O_2 Transport

A similar increase in global DO_2 was measured in both groups (**Figure 5**). Global DO_2 increased in response to 30 ng/kg/min and was further increased by 90 ng/kg/min. Global VO_2

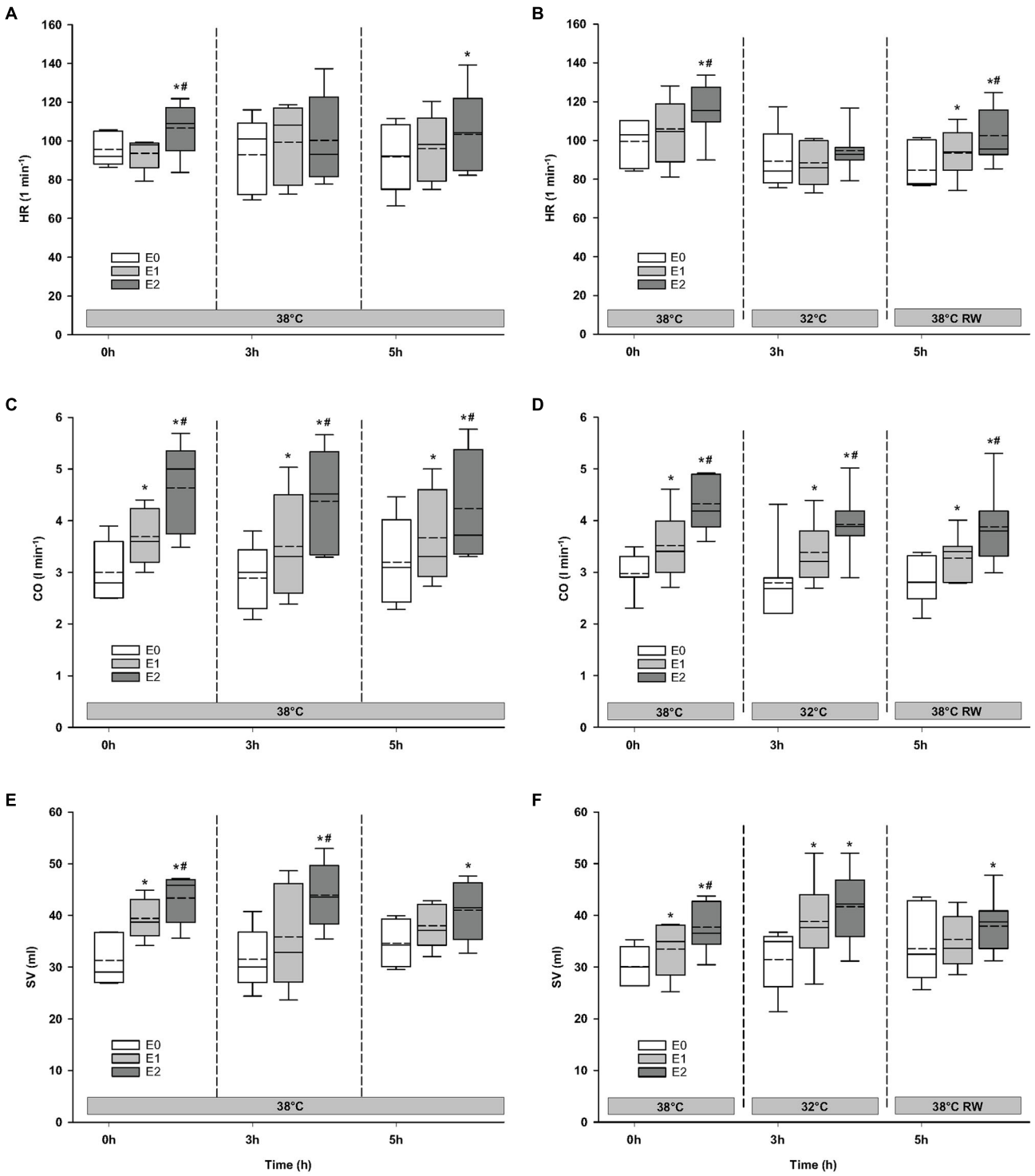

FIGURE 2 | Hemodynamic variables. **(A,B)** HR, heart rate; **(C,D)** CO, cardiac output; and **(E,F)** SV, stroke volume. $N = 5$ (NT group, left column) and $n = 7$ (HT group, right column). E0 – before epinephrine infusion, E1 – epinephrine infusion 30 ng/kg/min, E2 – epinephrine infusion 90 ng/kg/min, and RW – rewarming. Data are presented as vertical boxes with median (solid line), mean (dashed line), and interquartile range with 10th and 90th percentile error bars. Significance is indicated by: * – compared with corresponding E0 and # – compared with corresponding E1 (30 ng/kg/min). Level of significance: $p < 0.05$.

remained unchanged. Global O_2 ER was well below the critical value (0.7). A significant reduction was observed in response to 90 ng/kg/min.

Organ Blood Flow

Epi infusion did not result in any significant changes in regional blood flow in temporal lobes, liver, and gastro-intestinal

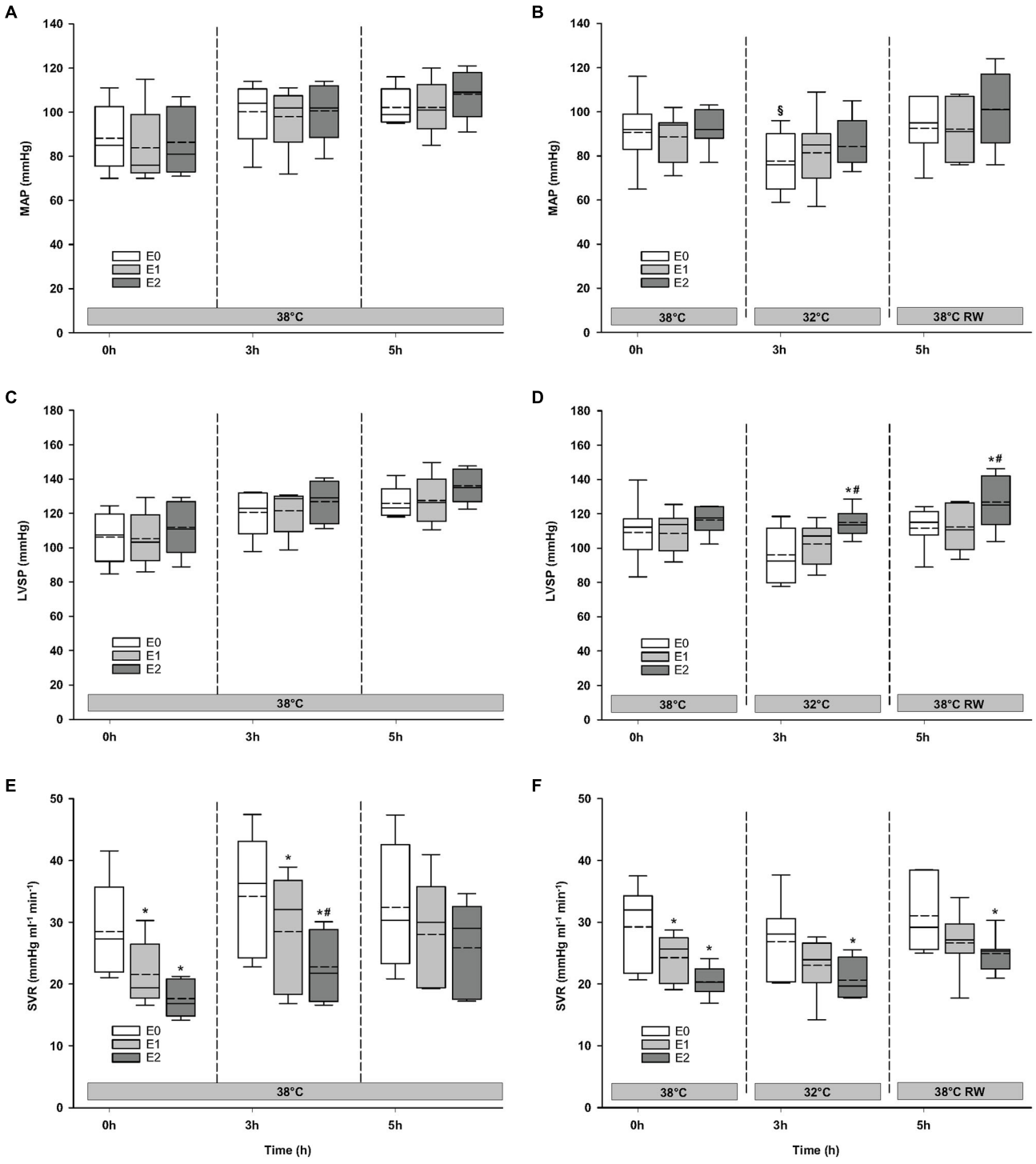

FIGURE 3 | Hemodynamic variables (cont.). **(A,B)** MAP, mean arterial pressure; **(C,D)** LVSP, left ventricular systolic pressure; and **(E,F)** SVR, systemic vascular resistance. $N = 5$ (NT group, left column) and $n = 7$ (HT group, right column). E0 – before epinephrine infusion, E1 – epinephrine infusion 30 ng/kg/min, E2 – epinephrine infusion 90 ng/kg/min, and RW – rewarming. Data are presented as vertical boxes with median (solid line), mean (dashed line), and interquartile range with 10th and 90th percentile error bars. Significance is indicated by: * – compared with corresponding E0, # – compared with corresponding E1 (30 ng/kg/min), and § – compared with absolute (0 h) baseline (E0). Level of significance: $p < 0.05$.

organs, except small intestine flow at 32°C (not shown; **Figures 6, 7**). Some blood flow changes occurred in the cerebellum, hippocampus, and heart in response to Epi infusion. These occurred irregularly and were not always in a dose-dependent pattern. Importantly, blood flow in these organs was not reduced during Epi

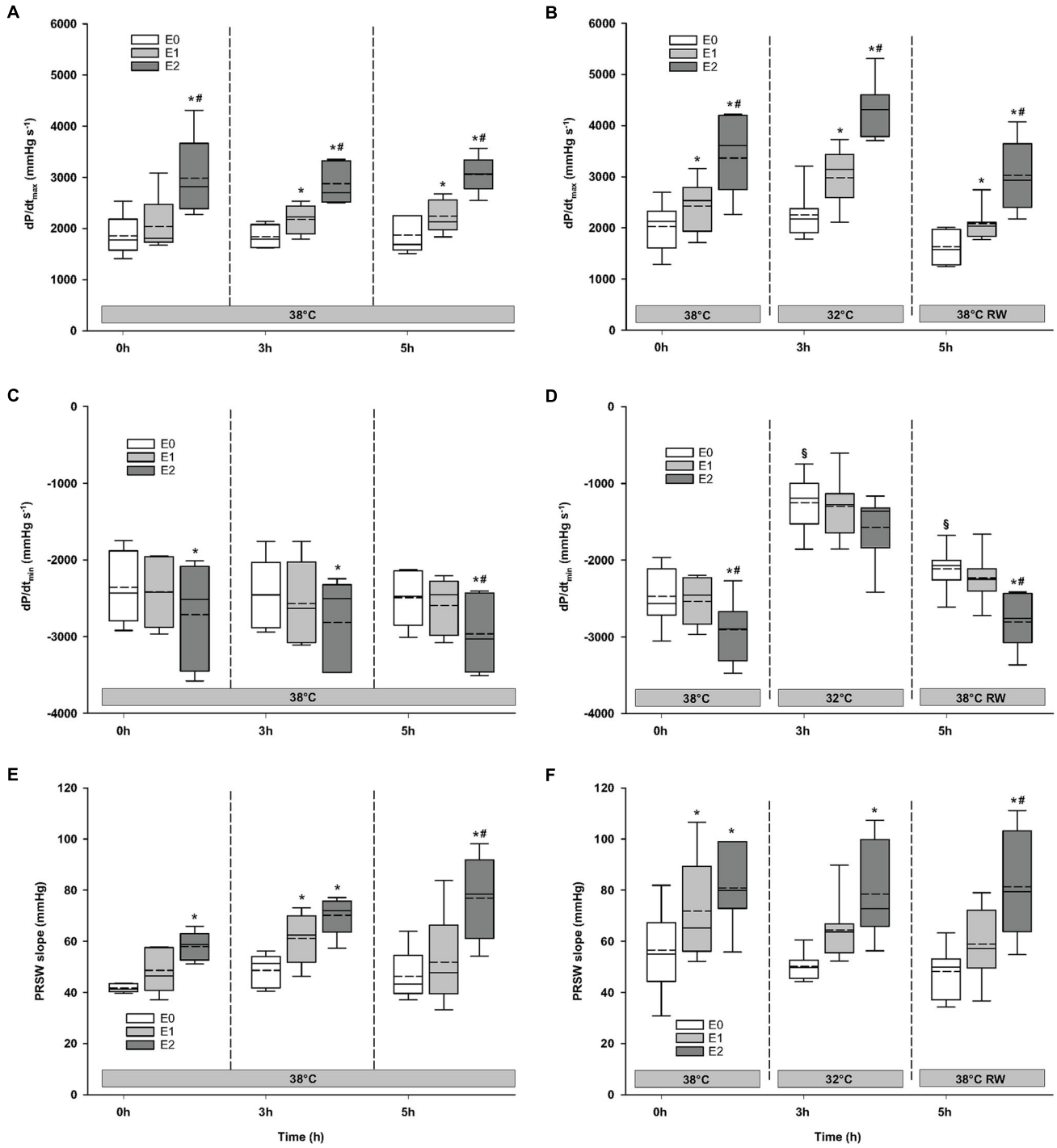

FIGURE 4 | Hemodynamic variables (cont.). **(A,B)** dP/dt_{max}, maximum rate of LV pressure rise; **(C,D)** dP/dt_{min}, maximum rate of LV pressure decline; and **(E,F)** PRSW, preload recruitable stroke work. $N = 5$ (NT group, left column) and $n = 7$ (HT group, right column). E0 – before epinephrine infusion, E1 – epinephrine infusion 30 ng/kg/min, E2 – epinephrine infusion 90 ng/kg/min, and RW – rewarming. Data are presented as vertical boxes with median (solid line), mean (dashed line), and interquartile range with 10th and 90th percentile error bars. Significance is indicated by: * – compared with corresponding E0, # – compared with corresponding E1 (30 ng/kg/min), and § – compared with absolute (0 h) baseline (E0). Level of significance: $p < 0.05$.

infusion, except for hippocampal blood flow was reduced in the NT group in response to 90 ng/kg/min compared to 30 ng/kg/min. Kidney blood flow was increased after 90 ng/kg/min.

Electrocardiogram

Epi infusions did not change duration of QTc intervals, or QRS/QTc ratio (**Figure 8**). QRS interval increased in the HT group in response to 90 ng/kg/min.

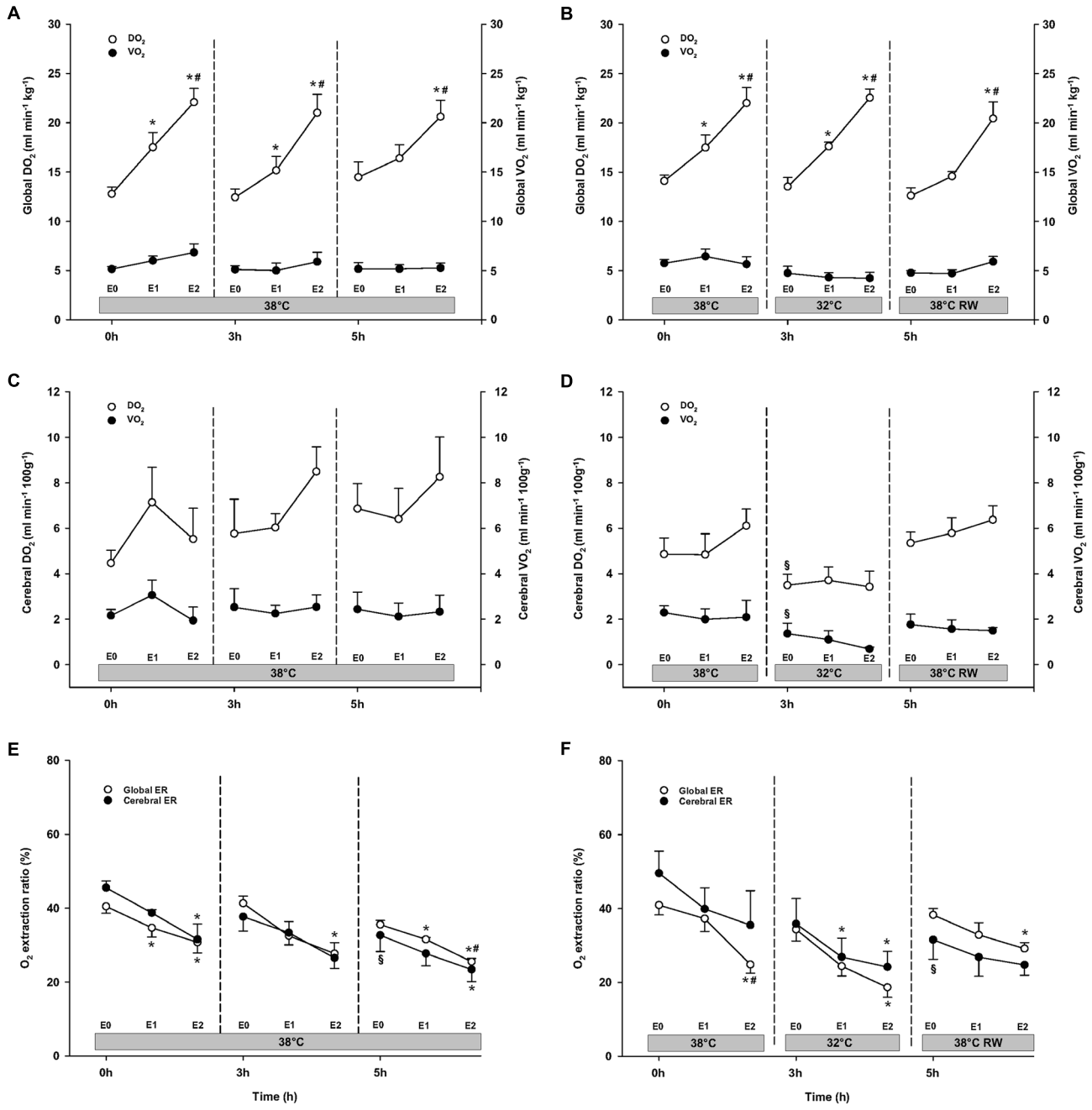

FIGURE 5 | Oxygen transport. **(A,B)** Global oxygen delivery, DO_2 and consumption, VO_2; **(C,D)** cerebral oxygen delivery, DO_2 and consumption, VO_2; and **(E,F)** global and cerebral O_2 extraction ratio, O_2 ER. $N = 5$ (NT group, left column) and $n = 7$ (HT group, right column). E0 – before epinephrine infusion, E1 – epinephrine infusion 30 ng/kg/min, E2 – epinephrine infusion 90 ng/kg/min, and RW – rewarming. Data are presented as means and standard deviation. Significance is indicated by: * – compared with corresponding E0, # – compared with corresponding E1 (30 ng/kg/min), and § – compared with absolute (0 h) baseline (E0). Level of significance: $p < 0.05$.

Responses to Epi Infusion in NT Group at 38°C After 3 h and HT Group at 32°C After 3 h

Hemodynamic Variables

For the majority of hemodynamic variables, cooling did not induce significant changes between NT baseline and 32°C (**Figures 2–4**). Exceptions were MAP and dP/dt_{min}. Neither HR nor MAP was responsive to Epi infusion. In the HT group, LVSP increased during 90 ng/kg/min and CO was elevated in response to 30 ng/kg/min. SV was increased by 30 ng/kg/min in the HT group but only by 90 ng/kg/min in the NT group. Likewise, Epi dose-dependent reduction of SVR was observed in NT group, while in the HT group, SVR was only reduced in response

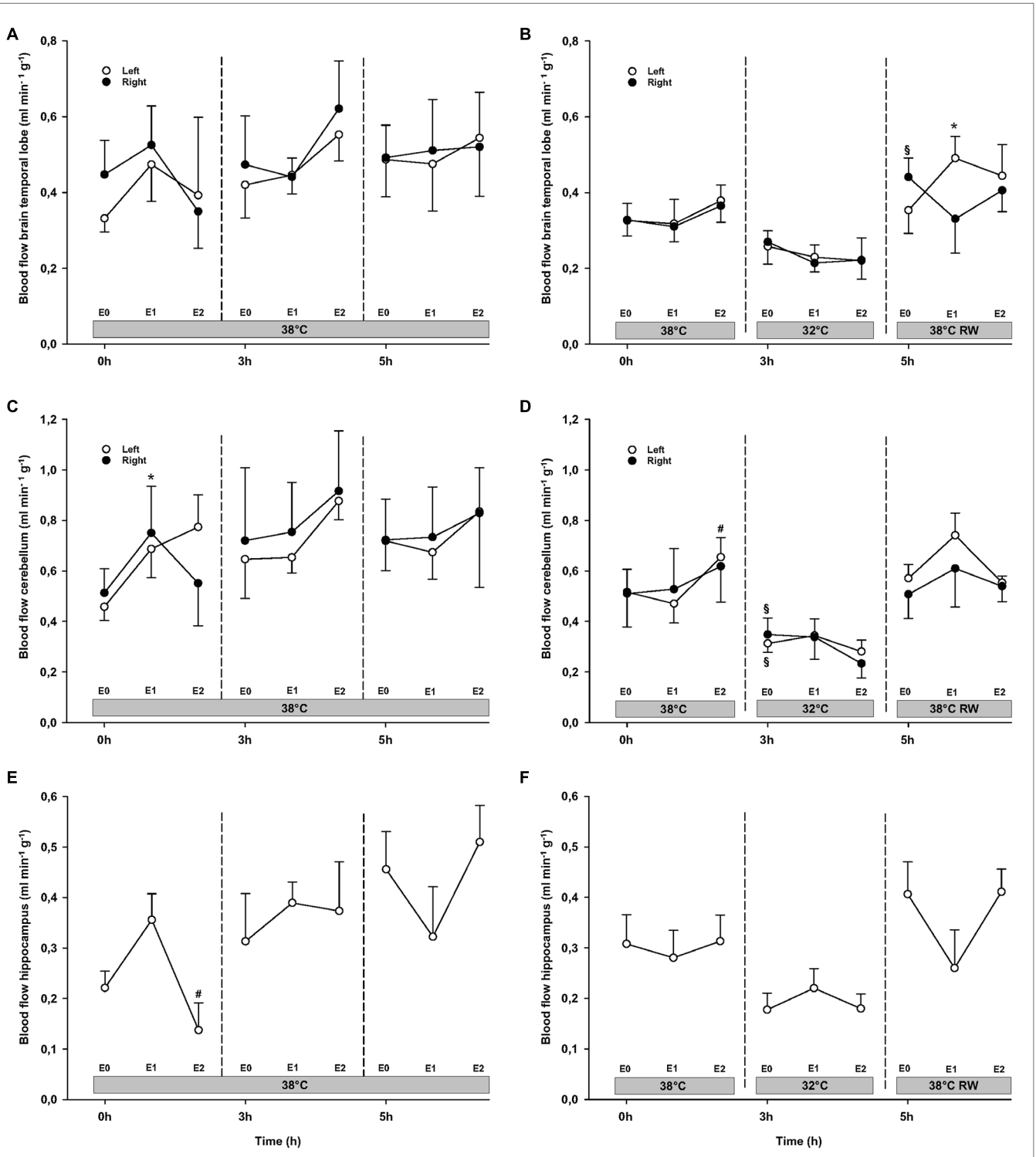

FIGURE 6 | Organ blood flow. **(A,B)** Brain temporal lobe, **(C,D)** cerebellum, and **(E,F)** hippocampus. $N = 5$ (NT group, left column) and $n = 7$ (HT group, right column). E0 – before epinephrine infusion, E1 – epinephrine infusion 30 ng/kg/min, E2 – epinephrine infusion 90 ng/kg/min, and RW – rewarming. Data are presented as means and standard deviation. Significance is indicated by: * – compared with corresponding E0, # – compared with corresponding E1 (30 ng/kg/min), and § – compared with absolute (0 h) baseline (E0). Level of significance: $p < 0.05$.

to 90 ng/kg/min. Effect of Epi infusion on dP/dt_{max} was similar in both groups, with increase in response to 30 ng/kg/min. dP/dt_{min} was changed only in the NT group after 90 ng/kg/min. PRSW increased in response to 30 ng/kg/min in the NT group, while only elevated by 90 ng/kg/min in the HT group.

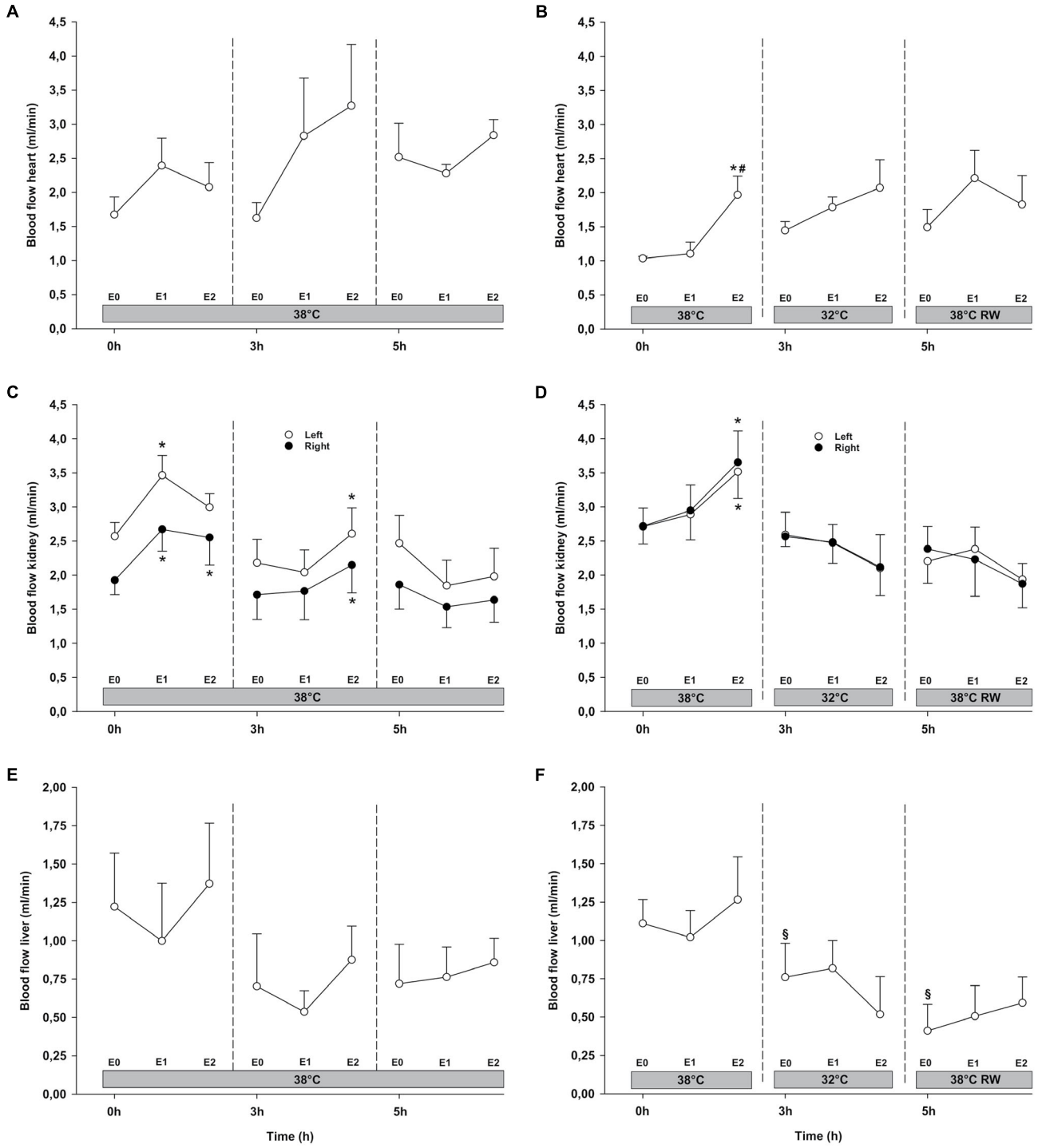

FIGURE 7 | Organ blood flow (cont.). **(A,B)** Heart, **(C,D)** kidneys, and **(E,F)** liver. *N* = 5 (NT group, left column) and *n* = 7 (HT group, right column). E0 – before epinephrine infusion, E1 – epinephrine infusion 30 ng/kg/min, E2 – epinephrine infusion 90 ng/kg/min, and RW – rewarming. Data are presented as means and standard deviation. Significance is indicated by: * – compared with corresponding E0, # – compared with corresponding E1 (30 ng/kg/min), and § – compared with absolute (0 h) baseline (E0). Level of significance: $p < 0.05$.

O_2 Transport

DO_2, VO_2, and O_2 ER remained unchanged at baseline in the NT group after 3 h (**Figure 5**). In the HT group, both cerebral DO_2 and VO_2 were reduced compared to prehypothermic baseline. Both groups showed dose-dependent increase in global DO_2 during Epi infusion. However, cerebral O_2 transport (cerebral DO_2 and VO_2) and global VO_2 were not affected by Epi infusion. Global O_2 ER was significantly reduced in

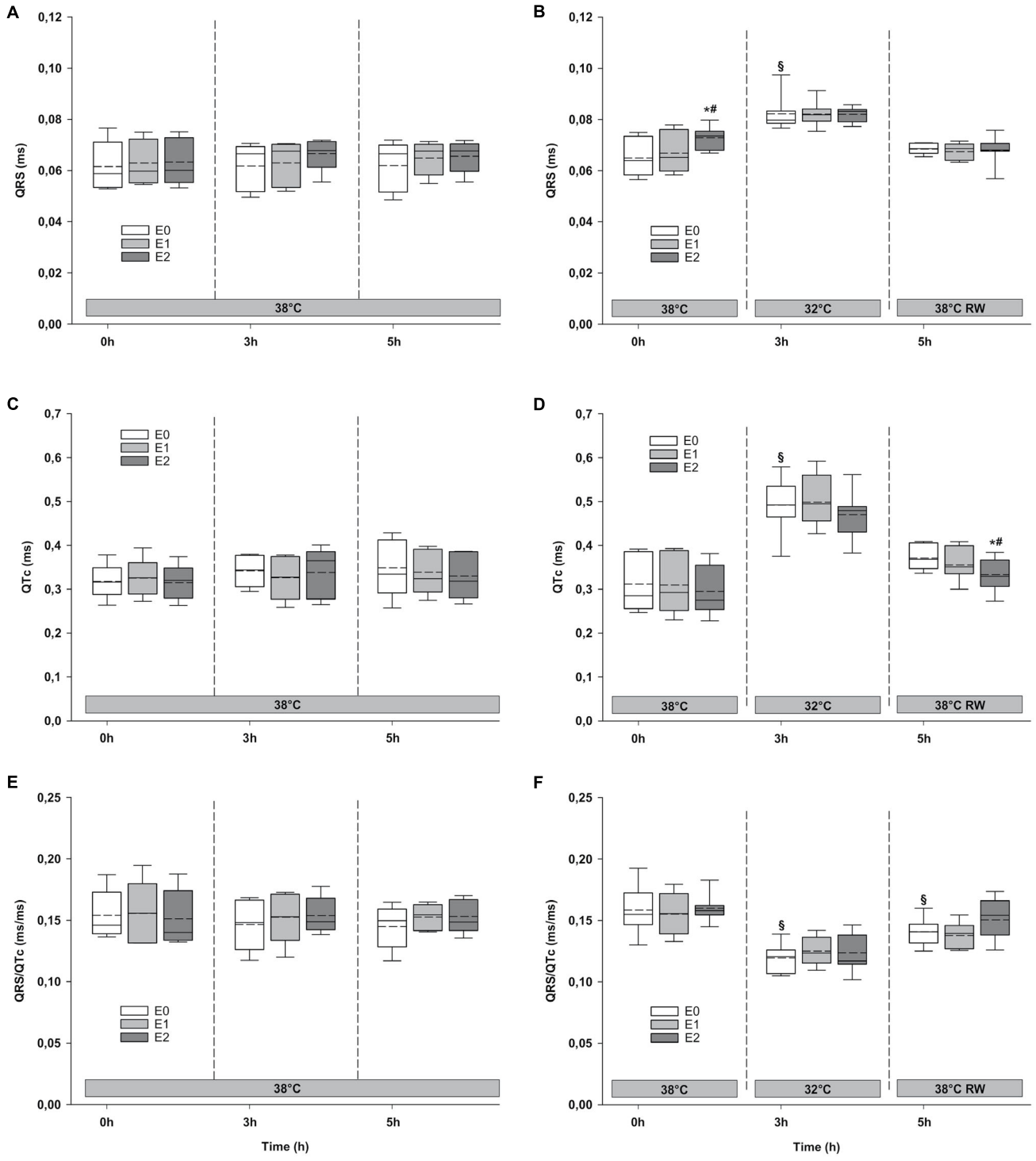

FIGURE 8 | ECG. **(A,B)** QRS interval, **(C,D)** QTc interval, and **(E,F)** QRS/QTc ratio. *N* = 5 (NT group, left column) and *n* = 7 (HT group, right column). E0 – before epinephrine infusion, E1 – epinephrine infusion 30 ng/kg/min, E2 – epinephrine infusion 90 ng/kg/min, and RW – rewarming. Data are presented as vertical boxes with median (solid line), mean (dashed line), and interquartile range with 10th and 90th percentile error bars. Significance is indicated by: * – compared with corresponding E0, # – compared with corresponding E1 (30 ng/kg/min), and § – compared with absolute (0 h) baseline (E0). Level of significance: $p < 0.05$.

both groups in response to 90 ng/kg/min. Cerebral O_2 ER was reduced only in the HT group, after 30 ng/kg/min administration.

Organ Blood Flow

Cerebellar and liver blood flow was reduced at 32°C in the HT group, compared to prehypothermic baseline (**Figures 6, 7**).

Epi infusion did not induce effects on blood flow, except for increased kidney blood flow after 90 ng/kg/min in the NT group, and reduced small intestine blood flow after 90 ng/kg/min in the HT group.

Electrocardiogram

Cooling resulted in prolongation of QRS and QTc intervals at baseline, while QRS/QTc decreased (**Figure 8**). Epi infusion did not have any effect on these variables.

Responses to Epi Infusion in NT Group at 38°C After 5 h and HT Group After Rewarming

Hemodynamic Variables

Only dP/dt_{min} in the HT group changed (decreased) compared to its prehypothermic value (**Figures 2–4**). In the NT group, HR increased in response to 90 ng/kg/min, whereas in the HT group, Epi elevated HR after 30 ng/kg/min. CO increased in a dose-dependent manner from 30 ng/kg/min in both groups, while SV only increased in response to 90 ng/kg/min. MAP remained unresponsive to Epi in both groups. LVSP was unaffected of Epi infusion in NT group only but increased after 90 ng/kg/min in the HT group. SVR reduction in response to Epi occurred only in the HT group during 90 ng/kg/min. In both groups, dP/dt_{max} increased after 30 ng/kg/min, while dP/dt_{min} and PRSW were increased only after 90 ng/kg/min.

O_2 Transport

Compared to their baseline values, cerebral O_2 ER after 5 h baseline values was significantly reduced in both groups (**Figure 5**). All other O_2 transport variables were unchanged. In both groups, 90 ng/kg/min caused an increase in global DO_2, while global VO_2, as well as cerebral DO_2 and VO_2 remained unaltered by Epi infusion. Global O_2 ER was reduced in response to 30 ng/kg/min in the NT group, whereas only after 90 ng/kg/min in the HT group. Cerebral O_2 ER was reduced in response to 90 ng/kg/min in the NT group and remained unchanged in the HT group.

Organ Blood Flow

Except for increased baseline blood flow in the right temporal lobe and reduced liver blood flow of the HT group, no changes occurred from baseline (**Figures 6, 7**). Epi infusions did not alter blood flow in any organ, except for the left temporal lobe in the HT group, where it was increased in response to 30 ng/kg/min.

Electrocardiogram

Only QRS/QTc ratio in the HT group was significantly reduced after rewarming compared to prehypothermic baseline (**Figure 8**). Epi infusion did not affect ECG parameters in the NT group. In the HT group, Epi infusion shortened the QTc intervals in response to 90 ng/kg/min. QRS interval and QRS/QTc ratio remained unaffected by Epi.

DISCUSSION

This study demonstrated that low- (30 ng/kg/min) and high- (90 ng/kg/min) dose Epi infusion provided positive inotropic effects, both after cooling to 32°C and subsequent rewarming to 38°C. We did not find any indication that Epi infusion increased risk for ventricular arrhythmias during hypothermia.

Our previous studies using an intact rodent model have indicated that the beneficial hemodynamic effects of Epi are lost during cooling to 34°C, as administration gave a detrimental elevation of SVR during hypothermia (Kondratiev and Tveita, 2006; Tveita and Sieck, 2011; Dietrichs et al., 2016). Accordingly, a pharmacodynamic shift toward increased α-receptor-mediated vasoconstriction, over the β-receptor mediated vasodilation and positive inotropic effects observed in normothermic controls, seems to exist in hypothermic rodents, even when administering low doses of Epi. These changes were found at core temperatures regularly observed in victims of accidental hypothermia and as induced in TTM-treated patients. Rewarming from accidental hypothermia is often complicated by HCD, while TTM-patients often suffer acute heart failure and need pharmacological support of cardiovascular function (Bernard et al., 2002; Safar and Kochanek, 2002). In such patients, isolated α-receptor agonist effect of Epi infusion could be treacherous, as afterload increases without simultaneous support of a failing heart. In the present experiment, however, both doses of Epi reduced SVR and had no significant effect on MAP, indicating that the cardiac and peripheral β-adrenergic effects were dominant of these doses, even during hypothermia. This study therefore provides vital information, indicating that the translational potential of earlier rodent findings is limited and that Epi treatment could be suitable in hypothermic patients at core temperatures ≥32°C. As the pigs in the current study were not cooled to temperatures associated with HCD and did not have underlying cardiac disease, the present result advocates further studies exploring the effects of Epi during such pathophysiological conditions in pig.

In the present experiment, Epi infusion induced a dose-dependent increase in PRSW, CO, and SV, both at 32°C and after rewarming. This indicates an intact effect of increasing cardiac inotropy through stimulating the β_1-receptor – adenyl cyclase (AC) – cyclic AMP (cAMP) – PKA pathway during hypothermia. In rat studies, we found myocardial Ca^{2+} overload and increased cardiac troponin I phosphorylation in relation to HCD (Wold et al., 2013; Schaible et al., 2016). In a failing heart, PKA-mediated phosphorylation of regulatory proteins would expectedly enhance both findings and have a negative impact on cardiac function. The present experiment shows that cardiomyocytes of pigs cooled to 32°C instead have a beneficial response to stimulation of the β_1-receptor pathway, similar to normothermic animals. Moreover, we find no indication of a pharmacodynamic shift toward an increased peripheral α-receptor response and vasoconstriction, over smooth muscle β_2-receptor stimulation and vasodilation. The dose-dependent Epi-induced reduction in SVR during hypothermia and

rewarming is similar to that in normothermic controls. Accordingly, high-dose Epi infusion did not increase afterload, in stark contrast to rodent findings during deep hypothermia (Dietrichs et al., 2015).

TTM and therapeutic hypothermia are used in different patient groups for neuroprotection after a hypoxic insult, or prior to surgery with reduced cerebral perfusion (Fawaz and Tutunji, 1960; Dietrichs and Dietrichs, 2015). Increased VO_2 is a well-known effect of Epi infusion (Fawaz and Tutunji, 1960) and could therefore be hypothesized to have a negative impact in hypothermic patients. However, there is no indication that hypoxia is part of the pathophysiology underlying HCD (Kondratiev et al., 2006). Still, Epi infusion could be anticipated to alter organ blood flow, through unbalanced stimulation of peripheral α- and β_2-receptors in arterioles. Yet, neither hippocampal, cerebellar nor temporal lobe blood flow is changed by Epi infusion during hypothermia. This is accompanied by absence of increased O_2 demand during drug infusion at 32°C. High-dose Epi increased global DO_2 in presence of unaltered global VO_2, both during hypothermia and after rewarming, causing global as well as cerebral O_2 ER to decrease with Epi infusion during hypothermia. Accordingly, Epi infusion had a positive impact on the ratio between cerebral supply and demand of O_2 at 32°C. Our findings therefore indicate that use of Epi to support cardiovascular function is suitable during TTM or hypothermia, as there is no suggestion of negative impact of Epi on the neuroprotective effect of core temperature reduction.

Reduction of core temperature is associated with changes in cardiac electrophysiology that increase risk for ventricular arrhythmias, which together with HCD contribute to high mortality of accidental hypothermia (van der Ploeg et al., 2010). The pathophysiological mechanism is disputed with much emphasis on observed J-waves that do not appear to be pathognomonic for hypothermia-induced cardiac arrest (Dietrichs et al., 2019, 2020a). Recent studies find that dispersion of repolarization and a depolarization/repolarization mismatch is associated with increased risk for ventricular fibrillation at 31–32°C (Piktel et al., 2010; Dietrichs et al., 2020a). These pro-arrhythmic changes can be detected by low values of a novel ECG marker for hypothermia-induced cardiac arrest; QRS/QTc (Dietrichs et al., 2020b, 2021; Ref). Hypothermic pigs in the present study were cooled to the same temperature and given β_1-receptor stimulating Epi infusions.

Due to risk for ventricular arrhythmias, Epi is considered to be unfavorable in repolarization disturbances like long-QT syndrome (Tan et al., 2014), which is a similar to the observed effects of hypothermia on cardiac electrophysiology. In the present experiment, we observed a pronounced prolongation of the QTc interval and a parallel reduction in QRS/QTc values, indicating that cooling had a heterogenic effect on repolarization and depolarization. In rabbit hearts cooled to 31°C, a similar reduction in QRS/QTc values correlated with a 2-fold increase in risk for induction of ventricular fibrillation (Dietrichs et al., 2020a,b). In the present experiment, pigs were probably at a higher risk for developing ventricular arrhythmias at 32°C, compared to at 38°C before Epi infusion. Interestingly, neither low- or high-dose Epi appeared to increase risk for hypothermia-induced arrhythmias, as QRS/QTc values remained stable throughout infusions at 32°C. Thus, the electrophysiological effects of Epi do not appear to prevent utilization of the positive hemodynamic properties of drug infusion during hypothermia and rewarming, as shown in this study.

CONCLUSION

Administration of both 30 ng/kg/min and 90 ng/kg/min Epi infusion during hypothermia (32°C) produced a positive inotropic effect and reduced afterload in a porcine model of hypothermia and rewarming. The observed hemodynamic response corresponded with findings in the normothermic control group, and are different from earlier reports, reporting negative hemodynamic impact of catecholamine administration in hypothermic rodents. Further, we find no evidence of increased pro-arrhythmic activity after Epi infusion in hypothermic pigs. The results of these experiments therefore suggest that β_1-receptor stimulation with epinephrine is a favorable strategy for providing cardiovascular support in hypothermic patients, at core temperatures >32°C.

DATA AVAILABILITY STATEMENT

The raw data supporting the conclusions of this article will be made available by the authors, without undue reservation.

ETHICS STATEMENT

The animal study was reviewed and approved by the Norwegian National Animal Research Authority.

AUTHOR CONTRIBUTIONS

TT, GS, RM, ED, and TK contributed to the conception and design, the data analysis and interpretation, and revision of the manuscript. RM, PS, TK, and ED contributed to the completion of experiments and collection of the data. TT, GS, RM, ED, TK, MF, and PS contributed to drafting of the manuscript for intellectual content. All authors contributed to the article and approved the submitted version.

FUNDING

This work was generously supported by grants from the Norwegian Research Council (Petromax2) and the Norwegian Ministry of Foreign Affairs (Barents 2020).

REFERENCES

Bernard, S. A., Gray, T. W., Buist, M. D., Jones, B. M., Silvester, W., Gutteridge, G., et al. (2002). Treatment of comatose survivors of out-of-hospital cardiac arrest with induced hypothermia. *N. Engl. J. Med.* 346, 557–563. doi: 10.1056/NEJMoa003289

Dietrichs, E. S., and Dietrichs, E. (2015). Neuroprotective effects of hypothermia. *Tidsskr. Nor. Laegeforen.* 135, 1646–1651. doi: 10.4045/tidsskr.14.1250

Dietrichs, E. S., McGlynn, K., Allan, A., Connolly, A., Bishop, M., Burton, F., et al. (2020a). Moderate but not severe hypothermia causes pro-arrhythmic changes in cardiac electrophysiology. *Cardiovasc. Res.* 116, 2081–2090. doi: 10.1093/cvr/cvz309

Dietrichs, E. S., Sager, G., and Tveita, T. (2016). Altered pharmacological effects of adrenergic agonists during hypothermia. *Scand. J. Trauma Resusc. Emerg. Med.* 24:143. doi: 10.1186/s13049-016-0339-8

Dietrichs, E. S., Schanche, T., Kondratiev, T., Gaustad, S. E., Sager, G., and Tveita, T. (2015). Negative inotropic effects of epinephrine in the presence of increased β-adrenoceptor sensitivity during hypothermia in a rat model. *Cryobiology* 70, 9–16. doi: 10.1016/j.cryobiol.2014.10.012

Dietrichs, E. S., Selli, A. L., Kondratiev, T., McGlynn, K., Smith, G., and Tveita, T. (2021). Resistance to ventricular fibrillation predicted by the QRS/QTc - ratio in an intact rat model of hypothermia/rewarming. *Cryobiology* 98, 33–38. doi: 10.1016/j.cryobiol.2021.01.003

Dietrichs, E. S., Tveita, T., Myles, R., Smith, G., Torkjel, T., Myles, R., et al. (2020b). A novel ECG-biomarker for cardiac arrest during hypothermia. *Scand. J. Trauma Resusc. Emerg. Med.* 28:27. doi: 10.1186/s13049-020-00721-0

Dietrichs, E. S., Tveita, T., and Smith, G. (2019). Hypothermia and cardiac electrophysiology: a systematic review of clinical and experimental data. *Cardiovasc. Res.* 115, 501–509. doi: 10.1093/cvr/cvy305

Fawaz, G., and Tutunji, B. (1960). The effects of adrenaline and noradrenaline on the metabolism and performance of the isolated dog heart. *Br. J. Pharmacol. Chemother.* 15, 389–395. doi: 10.1111/j.1476-5381.1960.tb01261.x

Kondratiev, T. V., Flemming, K., Myhre, E. S. P., Sovershaev, M. A., and Tveita, T. (2006). Is oxygen supply a limiting factor for survival during rewarming from profound hypothermia? *Am. J. Physiol. Heart Circ. Physiol.* 291, H441–H450. doi: 10.1152/ajpheart.01229.2005

Kondratiev, T. V., and Tveita, T. (2006). Effects of sympathetic stimulation during cooling on hypothermic as well as posthypothermic hemodynamic function. *Can. J. Physiol. Pharmacol.* 84, 985–991. doi: 10.1139/y06-051

Nolan, J. P., Soar, J., Cariou, A., Cronberg, T., Moulaert, V. R. M., Deakin, C. D., et al. (2015). European Resuscitation Council and European Society of Intensive Care Medicine guidelines for post-resuscitation care 2015. Section 5 of the European Resuscitation Council guidelines for resuscitation 2015. *Resuscitation* 95, 202–222. doi: 10.1016/j.resuscitation.2015.07.018

Piktel, J. S., Jeyaraj, D., Said, T. H., Rosenbaum, D. S., and Wilson, L. D. (2010). Enhanced dispersion of repolarization explains increased arrhythmogenesis in severe versus therapeutic hypothermia. *Circ. Arrhythm. Electrophysiol.* 4, 79–86. doi: 10.1161/CIRCEP.110.958355

Reinhardt, C. P., Dalhberg, S., Tries, M. A., Marcel, R., and Leppo, J. A. (2001). Stable labeled microspheres to measure perfusion: validation of a neutron activation assay technique. *Am. J. Physiol. Heart Circ. Physiol.* 280, H108–H116. doi: 10.1152/ajpheart.2001.280.1.H108

Safar, P. J., and Kochanek, P. M. (2002). Therapeutic hypothermia after cardiac arrest. *N. Engl. J. Med.* 346, 612–613. doi: 10.1056/NEJM200202213460811

Schaible, N., Han, Y.-S., Hoang, T., Arteaga, G., Tveita, T., and Sieck, G. (2016). Hypothermia/rewarming disrupts excitation-contraction coupling in cardiomyocytes. *Am. J. Physiol. Heart Circ. Physiol.* 310, H1533–H1540. doi: 10.1152/ajpheart.00840.2015

Swindle, M. M. (1998). Comparative anatomy and physiology of the pig. *Scand. J. Lab. Anim. Sci.* 25, 11–21.

Tan, V. H., Duff, H., Kuriachan, V., and Gerull, B. (2014). Congenital long QT syndrome: severe torsades de pointes provoked by epinephrine in a digenic mutation carrier. *Heart Lung* 43, 541–545. doi: 10.1016/j.hrtlng.2014.07.004

Toutain, P. L., Ferran, A., and Bousquet-Mélou, A. (2010). Species differences in pharmacokinetics and pharmacodynamics. *Handb. Exp. Pharmacol.* 199, 19–48. doi: 10.1007/978-3-642-10324-7_2

Tveita, T., and Sieck, G. C. (2011). The physiologic responses to epinephrine during cooling and after rewarming *in vivo*. *Crit. Care* 15:R225. doi: 10.1186/cc10465

Valkov, S., Mohyuddin, R., Nilsen, J. H., Schanche, T., Kondratiev, T. V., Sieck, G. C., et al. (2019). Organ blood flow and O_2 transport during hypothermia (27°C) and rewarming in a pig model. *Exp. Physiol.* 104, 50–60. doi: 10.1113/EP087205

van der Ploeg, G.-J., Goslings, J. C., Walpoth, B. H., and Bierens, J. J. L. M. (2010). Accidental hypothermia: rewarming treatments, complications and outcomes from one university medical centre. *Resuscitation* 81, 1550–1555. doi: 10.1016/j.resuscitation.2010.05.023

Wold, R. M., Kondratiev, T., and Tveita, T. (2013). Myocardial calcium overload during graded hypothermia and after rewarming in an *in vivo* rat model. *Acta Physiol.* 207, 460–469. doi: 10.1111/apha.12003

Conflict of Interest: The authors declare that the research was conducted in the absence of any commercial or financial relationships that could be construed as a potential conflict of interest.

frontiers in Physiology

ORIGINAL RESEARCH
published: 29 September 2021
doi: 10.3389/fphys.2021.741241

Rewarming With Closed Thoracic Lavage Following 3-h CPR at 27°C Failed to Reestablish a Perfusing Rhythm

*Joar O. Nivfors[1], Rizwan Mohyuddin[1], Torstein Schanche[1,2], Jan Harald Nilsen[1,3,4], Sergei Valkov[1], Timofei V. Kondratiev[1], Gary C. Sieck[2] and Torkjel Tveita[1,2,3]**

[1] Anesthesia and Critical Care Research Group, Department of Clinical Medicine, UiT-The Arctic University of Norway, Tromsø, Norway, [2] Department of Physiology and Biomedical Engineering, Mayo Clinic, Rochester, MN, United States, [3] Division of Surgical Medicine and Intensive Care, University Hospital of North Norway, Tromsø, Norway, [4] Department of Research and Education, Norwegian Air Ambulance Foundation, Drøbak, Norway

OPEN ACCESS

Edited by:
George Grant,
University of Aberdeen,
United Kingdom

Reviewed by:
Samuel Tisherman,
University of Maryland, Baltimore,
United States
Sylweriusz Kosinski,
Jagiellonian University Medical College, Poland
Tomasz Darocha,
Medical University of Silesia, Poland

***Correspondence:**
Torkjel Tveita
torkjel.tveita@uit.no

Specialty section:
This article was submitted to Clinical and Translational Physiology, a section of the journal Frontiers in Physiology

Received: 14 July 2021
Accepted: 30 August 2021
Published: 29 September 2021

Citation:
Nivfors JO, Mohyuddin R, Schanche T, Nilsen JH, Valkov S, Kondratiev TV, Sieck GC and Tveita T (2021) Rewarming With Closed Thoracic Lavage Following 3-h CPR at 27°C Failed to Reestablish a Perfusing Rhythm. Front. Physiol. 12:741241. doi: 10.3389/fphys.2021.741241

Introduction: Previously, we showed that the cardiopulmonary resuscitation (CPR) for hypothermic cardiac arrest (HCA) maintained cardiac output (CO) and mean arterial pressure (MAP) to the same reduced level during normothermia (38°C) vs. hypothermia (27°C). In addition, at 27°C, the CPR for 3-h provided global O_2 delivery (DO_2) to support aerobic metabolism. The present study investigated if rewarming with closed thoracic lavage induces a perfusing rhythm after 3-h continuous CPR at 27°C.

Materials and Methods: Eight male pigs were anesthetized, and immersion-cooled. At 27°C, HCA was electrically induced, CPR was started and continued for a 3-h period. Thereafter, the animals were rewarmed by combining closed thoracic lavage and continued CPR. Organ blood flow was measured using microspheres.

Results: After cooling with spontaneous circulation to 27°C, MAP and CO were initially reduced by 37 and 58% from baseline, respectively. By 15 min after the onset of CPR, MAP, and CO were further reduced by 58 and 77% from baseline, respectively, which remained unchanged throughout the rest of the 3-h period of CPR. During CPR at 27°C, DO_2 and O_2 extraction rate (VO_2) fell to critically low levels, but the simultaneous small increase in lactate and a modest reduction in pH, indicated the presence of maintained aerobic metabolism. During rewarming with closed thoracic lavage, all animals displayed ventricular fibrillation, but only one animal could be electro-converted to restore a short-lived perfusing rhythm. Rewarming ended in circulatory collapse in all the animals at 38°C.

Conclusion: The CPR for 3-h at 27°C managed to sustain lower levels of CO and MAP sufficient to support global DO_2. Rewarming accidental hypothermia patients following prolonged CPR for HCA with closed thoracic lavage is not an alternative to rewarming by extra-corporeal life support as these patients are often in need of massive cardio-pulmonary support during as well as after rewarming.

Keywords: accidental hypothermia, hypothermic cardiac arrest, organ blood flow, reperfusion, cardiopulmonary resuscitation

INTRODUCTION

Accidental hypothermia is defined as an involuntary drop in core body temperature to <35°C. Mild (35–32°C) hypothermia is common involving no serious medical concerns (Danzl and Pozos, 1994; Walpoth et al., 2017). However, a severe (28–24°C) accidental hypothermia has been termed an "orphan disease," since it is uncommon and can be life-threatening. In the United States, accidental hypothermia causes 1,500 deaths per year, approximating to 0.5 death per 100,000 inhabitants per year (Brown et al., 2012).

During exposure to low temperature, the thermogenesis and behavioral responses serve to minimize heat loss but these can be overwhelmed by the cold stress, and the core body temperature will continue to fall unless homeostasis is restored. During hypothermia, the coordinated thermoregulatory systems begin to fail, resulting in further heat loss (Danzl and Pozos, 1994; Zafren et al., 2014). The marked reduction in metabolism hypothermia is the main reason why successful resuscitation can be achieved after the prolonged periods in hypothermic cardiac arrest (HCA) (Weiss et al., 2012; Hilmo et al., 2014). As core body temperature decreases, HCA eventually occurs and is the main cause of the high mortality seen in severe and profound (<24°C) hypothermia (Lloyd, 1996). In mild hypothermia, thermoregulatory mechanisms are preserved. Thus, shivering is triggered to elevate the metabolic thermogenesis in the early phases of cooling and during mild hypothermia. However, at moderate hypothermia thermoregulatory mechanisms are lost (Giesbrecht, 2001). As core body temperature drops below 28°C, the risk of HCA increases substantially (Danzl and Pozos, 1994). The decreased sensitivity of central CO_2-receptors leads to hypoventilation and respiratory acidosis (Zafren et al., 2014). However, the hypoxic respiratory drive is preserved until ∼25°C when apnea eventually occurs (Young et al., 1995). At some point, irreversible hypothermia occurs (Lloyd, 1996), but survival and full neurological recovery have been reported in cases where core body temperature was as low as 11.8°C (Mroczek et al., 2020).

The current gold standard for rewarming hypothermic patients with unstable circulation or in HCA is by use of extra-corporeal life support (ECLS), applying any form of cardio-pulmonary bypass, and there is clinical consensus that these patients should be transported to a ECLS-facility for rewarming (Brown et al., 2012; Brugger et al., 2013; Zafren et al., 2014). The rationale for active internal (or central) rewarming is that it is more effective (Lloyd, 1996) and may reduce the risk of severe rewarming shock, i.e., decline in systemic vascular resistance not associated with an increase in cardiac output (CO) (Brunette et al., 1987). In 2014, a systematic review evaluated ECLS used to rewarm hypothermia in HCA and revealed a 67.7% survival to discharge and a 61.5% rate of good neurological recovery (Dunne et al., 2014). However, there are limited data available for comparison of patients with profound or severe hypothermia in cardiac arrest that were not treated with ECLS (Brown et al., 2012).

Our University Hospital of Northern Norway, situated at the 69.65° N latitude, has a large hospital catchment area though it mostly covers rural lands and is the only institution north of 63.43° N equipped with ECLS for rewarming. There are <500,000 inhabitants of which most are spread out in small communities along an intricate coastline of islands and fjords. Thus, the transport time for accidental hypothermia patients is sometimes substantial, which makes evacuation and transportation time typically 3–4 h for patients with HCA in need of in-hospital rewarming. When transport to our ECLS facility is impossible, mostly due to weather conditions, the local guidelines from 2014 suggest some form of thoracic lavage rewarming as an alternative option. This is recommended in a much-sited review of accidental hypothermia from 2012 (Brown et al., 2012), as well as in the American Heart Association guidelines (Nichol et al., 2010; Perkins et al., 2015). Closed thoracic (pleural) lavage may be instituted by the physicians in any local hospital (Brunette et al., 1987; Plaisier, 2005), utilizing the pleural cavity for infusion of warm saline, or tap water, to rewarm the heart and blood in central blood vessels by means of conduction and convection. However, the efficacy of closed thoracic lavage in rewarming accidental hypothermia patients is not explored experimentally.

In a porcine model of accidental hypothermia, we recently documented (Scientific Reports in press) that rewarming with ECLS following a 3-h period of continuous CPR for HCA at 27°C, took over global hemodynamic function, restored blood flow to the heart and the brain, and created a "shockable" cardiac rhythm. In the present study, we used the same experimental protocol to rewarm animals following a 3-h period of continuous CPR for HCA at 27°C by use of continuous closed thoracic lavage.

MATERIALS AND METHODS

The Norwegian Food Safety Authority approved the study (ID 5748, internal reference: 33/13). In this study, 11 castrated male pigs (wt. 26 ± 4 kg, age 3 months) from NOROC stock were used. On arrival, the animals were acclimated for 2–5 days before the terminal experiment. The animals were fed two times daily, always had free access to water, and received humane care in accordance with the Norwegian Animal Welfare Act.

Anesthesia and Instrumentation

We previously reported the detailed methods for hemodynamic monitoring, immersion cooling, and blood flow measurements using the porcine animal model (Valkov et al., 2019). Briefly, after fasting the animals overnight, premedication was induced by an intramuscular bolus of ketamine hydrochloride (20 mg kg^{-1}), midazolam (30 mg), and atropine (1 mg), and anesthesia was induced by a bolus infusion of fentanyl (10 μg kg^{-1}) and pentobarbital-sodium (10 mg kg^{-1}) in an ear vein. After tracheotomy and intubation, the animals were connected to a respirator (Siemens Servo 900D, Solna, Sweden), adjusted to maintain PaO_2 > 10 kPa and $PaCO_2$ at 4.5–6.0 kPa uncorrected for temperature (α-stat management). During the ventricular fibrillation and CPR, FiO_2 was set to 1.0, infusion of fentanyl (20 μg kg^{-1} h^{-1}) and midazolam (0.3 μg kg^{-1} h^{-1}). Pentobarbital-sodium (4 mg kg^{-1} h^{-1}) was continued *via* a femoral vein catheter. Anesthesia was discontinued during cooling at 27°C and re-instituted at the start of rewarming.

The microspheres were injected into the left ventricle through a 6F fluid-filled pigtail catheter, (Cordis Corporation, Miami, FL, USA). The core temperature, CO, and venous and mixed venous blood gases were measured *via* a 7F pulmonary artery thermodilution catheter (Edwards Lifesciences LLC, Irvine, CA, USA) positioned in the pulmonary trunk. Thermodilution is described as the gold standard for measuring CO during CPR (Carretero et al., 2010). The tip of another 7F pulmonary artery thermodilution catheter was positioned in the aortic arch *via* the left femoral artery to monitor the arterial blood gas and mean arterial pressure (MAP) and to collect the reference blood samples for the microsphere technique. A 3.5F pressure catheter (SPR-524, Millar Instruments Inc., Huston, TX, USA) for monitoring of intracranial pressure (ICP) was placed in the brain parenchyma just below the dura mater through a 2 mm cranial hole drilled 1 cm to the right of the sagittal suture and 1 cm dorsal to the coronal suture. The urinary output was followed by a 14F urinary bladder catheter introduced *via* a lower abdominal incision. For rewarming, two PVC tubes were placed in the left pleural space, one (16F) in the mid-clavicular line in the second intercostal space, the other (24F) in the mid-axillary line in the sixth intercostal space. The animals were given 5,000 IE Heparin and allowed to stabilize for 45 min before the start of the experimental protocol.

Regional Blood Flow Measurements

To determine organ blood flow, at each sampling point, ∼10 million 15μm microspheres labeled with different stable isotopes (BioPAL Inc., Worcester, MA, USA) were injected into the left ventricle (Reinhardt et al., 2001). The reference blood samples were drawn from the aortic arch (5ml min^{-1}, 2min) simultaneously with microsphere injections to calculate the regional blood flow. Blood flow was determined in the tissue samples from the brain (temporal lobes and cerebellum), kidneys, liver, heart, small intestine, spleen, and stomach based on a technique of neutron activation to analyze the microsphere content as already described in detail (Valkov et al., 2019).

Experimental Protocol

The animals were immersion-cooled in ice water to a blood temperature of 27°C, and ventricular fibrillation was induced by stimulating the epicardial surface using an alternating current (5–20 mA, 6 Hz, and 30 V) delivered *via* a 15-cm-long needle electrode (**Figure 1**). The needle was inserted in the epigastric area, pointed toward the heart apex. Correct needle placement was confirmed when aspirating arterial blood from the left ventricle. Cardiac arrest was defined as asystole or ventricular fibrillation observed by ECG with an associated absence of fluctuation in arterial pressure. After 90 s of cardiac arrest, an automated chest compression device (LUCAS chest compression system, Physio-Control Inc., Lund, Sweden) was started. The piston on this compression device was equipped with a suction cup to ensure active decompression with a continuous mode compression/decompression duty cycle of 50 ± 5% at a rate of 100 ± 5 compressions/min and compression depth was 4–5 cm. For rewarming to 38°C after a 3-h period of CPR at 27°C, *via* tubing, the upper (inlet) pleural tube was connected to a roller pump circulating water at 40–42°C from the reservoir, whereas drainage was obtained *via* the outlet tube by gravity. Care was taken to keep the flow rate <500 ml min^{-1} to avoid a potential tension hydrothorax (Barr et al., 1988), with close attention to the water temperature and water level in the reservoir. Based on the previous observation of multiple costae and sternal fractures during a 3-h period of CPR using the LUCAS chest compression system (Nilsen et al., 2020), if cardioversion was unsuccessful after the three shocks at 30°C, a sternotomy was made to evacuate extravascular blood, followed by internal defibrillation (5–15 J). The experiment was concluded after core body temperature reached 38°C and the animals were euthanized.

Rewarming With Closed Thoracic Lavage

During continuous CPR above 30°C, the appearance of spontaneous "shockable rhythms" in the ECG would initiate attempts with cardioversion, precipitated by intra-cardiac bolus injections of epinephrine (0.05–0.25 mg) to maintain MAP above 35 mmHg. If there was no cardioversion at 30°C after three repeated attempts at 50, 100, and 150 J, the procedure was repeated when core body temperature reached 31–32°C or 33–34°C. In the case of persistent arrhythmias, amiodarone (100–150 mg) was injected through intravenous (IV) followed by up to three additional cardioversion attempts (at 100 J).

A perfusing rhythm was defined following the cardioversion attempts at >30°C as the appearance of spontaneous pulsations in the arterial pressure wave with a MAP >35 mmHg lasting >10 min, accompanied by a sinus rhythm in the ECG. Epinephrine infusion was instituted to maintain MAP > 35 mmHg during rewarming.

Measurements and Sampling Rates

The mean arterial pressure (MAP), left ventricular pressure, heart rate (HR), intracranial pressure (ICP), central venous pressure (CVP), were recorded using PowerLAB 16/35 and LabChart software (ADInstruments, Dunedine, New Zealand). CO was measured by thermodilution using 10 ml cold saline injected into the PA-catheter and recorded on a Vigilance monitor (Edwards Lifesciences, Irvine, CA, USA). All the measurements were obtained at three core body temperatures: baseline 38°C, during cooling at 32°, and at 27°C. The measurements were also obtained during CPR after 15, 60, 120, and 180 min, and during rewarming at 32° and 38°C.

Statistics

The statistical analyses were performed using Sigma Plot statistical software version 13 [Systat Software Inc. (SSI), Richmond, CA, USA]. A Sample size was calculated using power analysis. Normal distribution was assessed using the Shapiro–Wilk test. Intragroup comparisons were performed by one-way repeated measures ANOVA for normally distributed variables, and Friedman's repeated measures ANOVA on ranks for non-normally distributed variables. Where significant differences were found, Dunnett's test was used to compare the values within group vs. baseline. The level of significance was set at $p < 0.05$. Data are presented as means and SD.

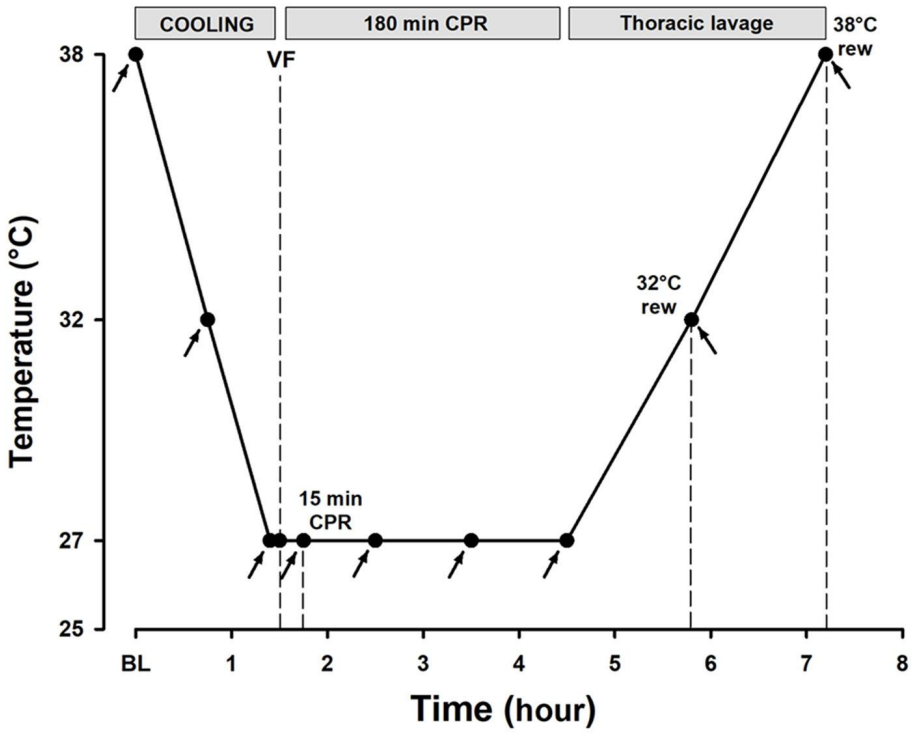

FIGURE 1 | Experimental timeline. Arrows depict the time points for hemodynamic measurements, blood sampling, and microsphere administration.

RESULTS

At the start of the experimental protocol, three animals died within the first 90 min of CPR due to physical damage to the atria by the tip of the lavage catheters causing hemothorax. After careful placement of the lavage catheters further out of reach for the piston on the automated chest compression device, this problem was eliminated, and as per protocol, only data from the other eight animals are included.

Immersion Cooling and 3-h Period of CPR at 27°C

Hemodynamic Changes

All statistical comparisons are reported in reference to the individual baseline (38°C) values (**Figures 2A,B**). Cooling reduced MAP (**Figure 2B**, **Table 1**) significantly from 78 ± 5 to 49 ± 6 mmHg at 27°C (−37%). After 15 min of CPR, MAP fell further to 33 ± 17 mmHg (−58%) and remained at this reduced level throughout the remaining 3-h period of CPR. Similarly, after cooling to 27°C, CO (**Figure 2A**, **Table 1**) fell significantly from 3.1 ± 0.5 to 1.3 ± 0.3 L min^{-1} (−58%). After 15 min of CPR, CO fell even further to 0.7 ± 0.2 L min^{-1} (−77%) and remained at this reduced level during the remaining 3-h period of CPR.

O_2 Transport and Extraction

Global DO_2 (**Figure 3A**) was reduced significantly during cooling to 27°C from 13.8 ± 1.5 to 5.7 ± 1.4 ml min^{-1} kg^{-1} (−59%). Similarly, VO_2 (**Figure 3A**) decreased during cooling to 27°C from 5.6 ± 1.1 to 1.9 ± 0.3 ml min^{-1} kg^{-1} (−66%). After 15 min of CPR, DO_2 was further reduced to 3.0 ± 0.9 (−78%), and VO_2 was reduced to 1.7 ± 0.5 (−70%) ml min^{-1} kg^{-1}, and both DO_2 and VO_2 remained at these reduced levels throughout the remaining 3-h period of CPR. Global O_2 extraction ratio (DO_2/VO_2) (**Figure 3C**) was significantly reduced by cooling to 27°C, and after 60 min of CPR, the extraction ratio reached 0.69 ± 0.07, the reported critical extraction ratio (ER_{crit}) necessary to provide aerobic metabolism (Fairley et al., 1957). Due to the stable CO throughout the 3-h period of CPR period, the extraction ratio remained at this elevated level. Cerebral DO_2 (**Figure 3B**) was reduced significantly during cooling to 27°C from 4.7 ± 1.7 to 1.9 ± 0.6 ml min^{-1} $(100\,g)^{-1}$ (−60%). Cerebral VO_2 (**Figure 3B**) decreased significantly during cooling to 27°C from 1.8 ± 1.4 to 0.4 ± 0.3 ml min^{-1} $(100\,g)^{-1}$ (−78%). After 15 min of CPR, cerebral DO_2 remained at the same level as at cooling 27°C, while cerebral VO_2 increased to 0.9 ± 0.8 ml/min/100 g. Both the cerebral DO_2 and VO_2 remained significantly reduced throughout the 3-h period of CPR.

Arterial Lactate, pH, and Central Venous O_2 Saturation (SvO_2)

Cooling to 27°C and the 3-h period of CPR caused an almost linear reduction in pH (**Table 2**) from 7.53 ± 0.05 to 7.26 ± 0.08, simultaneously with an increase in serum lactate (**Table 2**) from 0.8 ± 0.2 to 5.0 ± 1.8 mmol L^{-1}. These relatively modest changes in pH and lactate took place while SvO_2 (**Table 2**) fell from 59 ± 8 to 31 ± 10%.

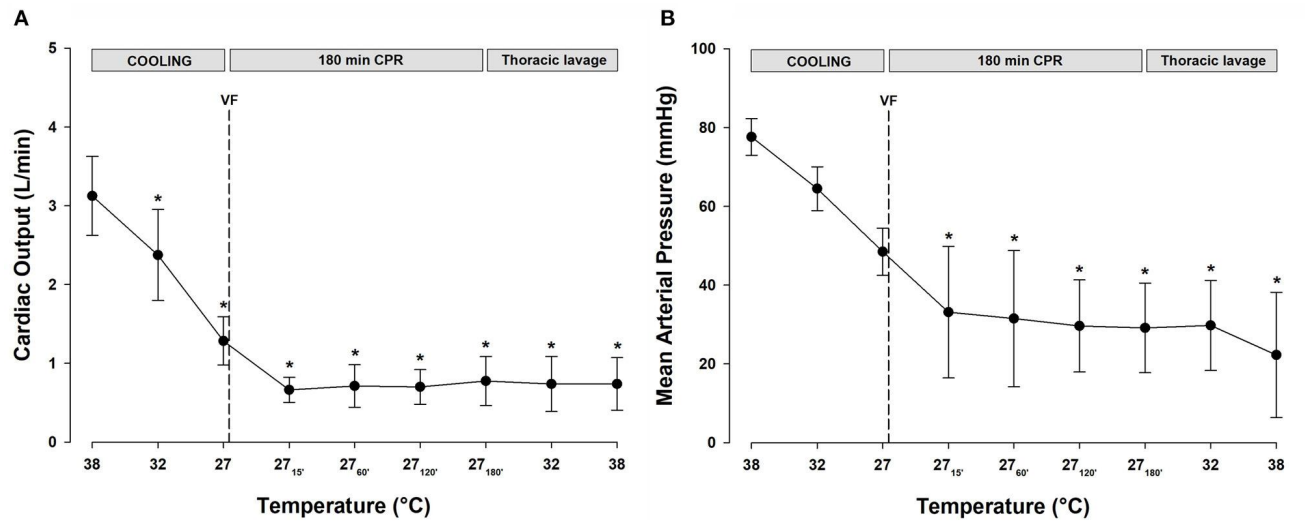

FIGURE 2 | (A) Cardiac output. **(B)** Mean arterial pressure. $n = 8$, values are mean ± SD. *$p < 0.05$ statistically significantly different from the baseline value.

TABLE 1 | Hemodynamic variables and values for cerebral pressures.

	38°C	27°C	27°C$_{15\ min}$	27°C$_{3\text{-}h}$	RW 32°C	RW 38°C
MAP, mmHg	78 ± 5	49 ± 6*	33 ± 17*	29 ± 11*	30 ± 11*	22 ± 16*
PAP, mmHg	18 ± 3	20 ± 4	42 ± 22*	41 ± 15*	30 ± 12	29 ± 9
LVSP, mmHg	114 ± 10	68 ± 10*	108 ± 59	119 ± 46	84 ± 44	73 ± 33
CVP, mmHg	5 ± 2	5 ± 2	37 ± 27*	30 ± 18*	23 ± 14*	23 ± 15*
ICP, mmHg	13 ± 3	13 ± 5	16 ± 3	16 ± 5	17 ± 4*	19 ± 2*
CPP, mmHg	64 ± 6	26 ± 18*	17 ± 15*	15 ± 10*	14 ± 10*	6 ± 14*
HR, 1/min	98 ± 14	62 ± 16*	100 ± 0	100 ± 0	100 ± 0	100 ± 0
CO, L/min	3 ± 1 , 0,5	1,3 ± 0,3*	0,7 ± 0,2*	0,8 ± 0,3*	0,7 ± 0,4*	0,7 ± 0,3*
SV, ml	32 ± 5	21 ± 3*	7 ± 2*	8 ± 3*	7 ± 4*	7 ± 3*
TPR, mmHg/L/min	25 ± 3	39 ± 9	54 ± 35*	43 ± 23	45 ± 22	32 ± 15

*MAP, mean arterial pressure; PAP, pulmonary arterial pressure; LVSP, left ventricular systolic pressure; CVP, central venous pressure; ICP, intracranial pressure; CPP, cerebral perfusion pressure (CPP = MAP – ICP); HR, heart rate; CO, cardiac output; SV, stroke volume (SV = CO/HR); TPR, total peripheral resistance (TPR = MAP/CO). n = 8, values are mean and SD. *p < 0.05 statistically significantly different from the baseline value.*

Organ Blood Flow

After ventricular fibrillation and 15 min CPR at 27°C, myocardial blood flow (**Figure 4A**) was significantly reduced compared with the baseline (−86%) and remained at this reduced level during the remaining 3-h period of CPR. After cooling to 27°C, blood flow in the temporal lobes (**Figure 4B**) was significantly reduced (left lobe −54%, and right lobe −61%). Compared with the baseline, after 15 min of CPR, blood flow to the left and right temporal lobe remained reduced, by −46 and −38%, respectively, but after the 3-h of CPR, blood flow to the left and the right temporal lobes were further reduced to −75 and −77% of baseline, respectively. Cooling to 27°C significantly reduced the blood flow to the left (−65%) and right (−64%) cerebellar hemispheres (**Figure 4C**). Initially, after 15 min of CPR, there was no further reduction in the cerebellar blood flow, but after 3-h of CPR, blood flow to the left (−78%) and the right (−75%) cerebellar hemispheres was further reduced. The abdominal organs (**Figures 4D-F**) showed a varying reduction in the blood flow during cooling, as well as during a 3-h period of CPR. Cooling to 27°C significantly reduced the blood flow to the left (−55%) and right (−48%) kidneys (**Figure 4E**), and renal blood flow was almost completely shut off after 3-h of CPR (-97%, both). Liver blood flow (**Figure 4F**) was unaltered after cooling to 27°C, whereas blood flow to the spleen (**Figure 4F**) was reduced (−79%). Both the organs had severely impaired blood flow during CPR, and after 3-h, the blood flow was reduced by −98% in the liver and −99% in the spleen compared with baseline at 38°C. After cooling to 27°C, the blood flow to the stomach and small intestine (**Figure 4D**) remained statistically unchanged. However, after 3-h of CPR, blood flow to the stomach and small intestine was severely reduced by −95 and −88% of baseline, respectively.

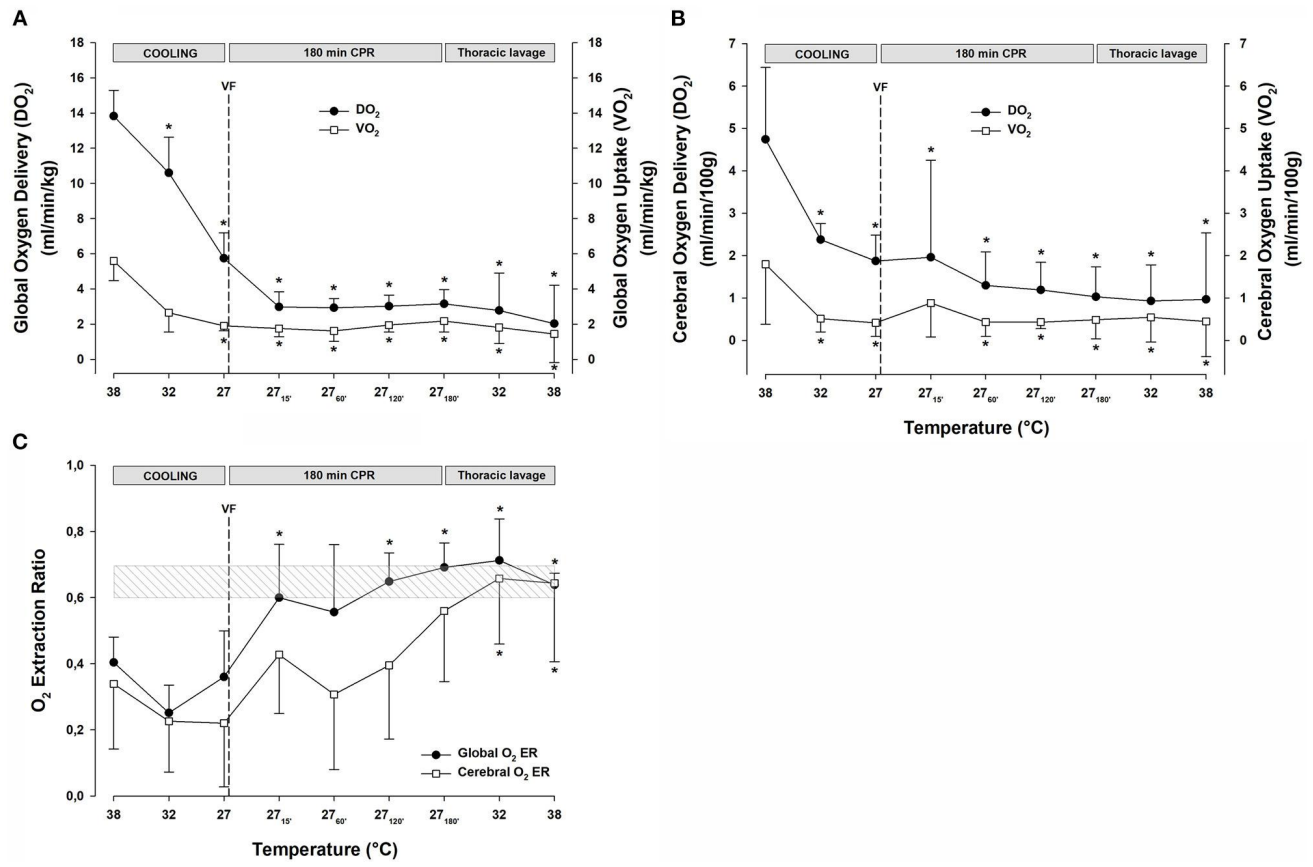

FIGURE 3 | (A) Global oxygen delivery, and global oxygen uptake (VO_2). **(B)** Cerebral oxygen delivery, and cerebral oxygen uptake (VO_2). **(C)** Global and cerebral oxygen extraction ratio. $n = 8$, values are mean ± SD. *$p < 0.05$ statistically significantly different from the baseline value. Striated area indicates a critical level of extraction ratio.

TABLE 2 | Blood gases and biochemical variables.

	38°C	27°C	27°C$_{15\ min}$	27°C$_{3\text{-}h}$	RW 32°C	RW 38°C
pH	7.53 ± 0.05	7.45 ± 0.02*	7.4 ± 0.04*	7.26 ± 0.08*	7.15 ± 0.08*	6.97 ± 0.17*
Hb (g/dL)	8.4 ± 0.3	8.8 ± 0.5	8.5 ± 0.6	8.6 ± 0.7	8.8 ± 0.7	7.6 ± 1.7
Hct (%)	26 ± 1	27 ± 2	26 ± 2	27 ± 2	28 ± 3	24 ± 5
Lactate (mmol/l)	0.8 ± 0.2	0.8 ± 0.7	1.7 ± 1.0*	5.0 ± 1.8*	8.1 ± 2.2*	10.0 ± 3.9*
BE (mmol/l)	4.7 ± 2.0	4.1 ± 1.6	−0.6 ± 2.9*	−6.6 ± 2.2*	−12.9 ± 4.1*	−18.6 ± 5.9*
HCO_3- (mmol/l)	29 ± 2	28 ± 1	24 ± 3*	19 ± 2*	14 ± 3*	10 ± 5*
K^+ (mmol/l)	3.3 ± 0.4	2.7 ± 0.5	3.1 ± 0.8	4.9 ± 1.3*	6.0 ± 1.7*	7.4 ± 2.8*
PaO_2 (kPa)	15 ± 7	18 ± 2	25 ± 23	19 ± 18	16 ± 20	10 ± 9
$PaCO_2$ (kPa)	4.5 ± 0.5	5.4 ± 0.5	5.0 ± 0.9	6.0 ± 1.4	5.7 ± 1.5	6.5 ± 2.2
SaO_2 (%)	99 ± 2	99 ± 1	95 ± 6	91 ± 8	76 ± 21*	57 ± 26*
SvO_2 (%)	59 ± 8	67 ± 15	41 ± 18*	31 ± 10*	24 ± 15*	17 ± 9*
SvO_2 jug.bulb (%)	65 ± 15	87 ± 12*	57 ± 16	41 ± 20*	21 ± 15*	18 ± 15*

*Hct, hematocrit; BE, base excess; HCO_3-, bicarbonate; P_aO_2, arterial partial O_2 pressure; P_aCO_2, arterial partial CO_2 pressure; SaO_2, arterial O_2 saturation; SvO_2, mixed venous O_2 saturation; SvO_2 jug.bulb., jugular bulb venous O_2 saturation. $n = 8$, values are mean and SD. *$p < 0.05$ statistically significantly different from the baseline value.*

Rewarming With Closed Thoracic Lavage

Lavage rewarming gave a mean rewarming rate of 3.8°C h^{-1} (max 12°C h^{-1} and min 1.6°C h^{-1}). The total volume of IV Ringer infused was 1.7 ± 0.4 l.

Attempts to Achieve a Perfusing Rhythm

Based on continuous ECG monitoring, all the animals had ventricular fibrillations during CPR and CPR/rewarming. At 30°C, attempts to achieve a perfusing rhythm were made by

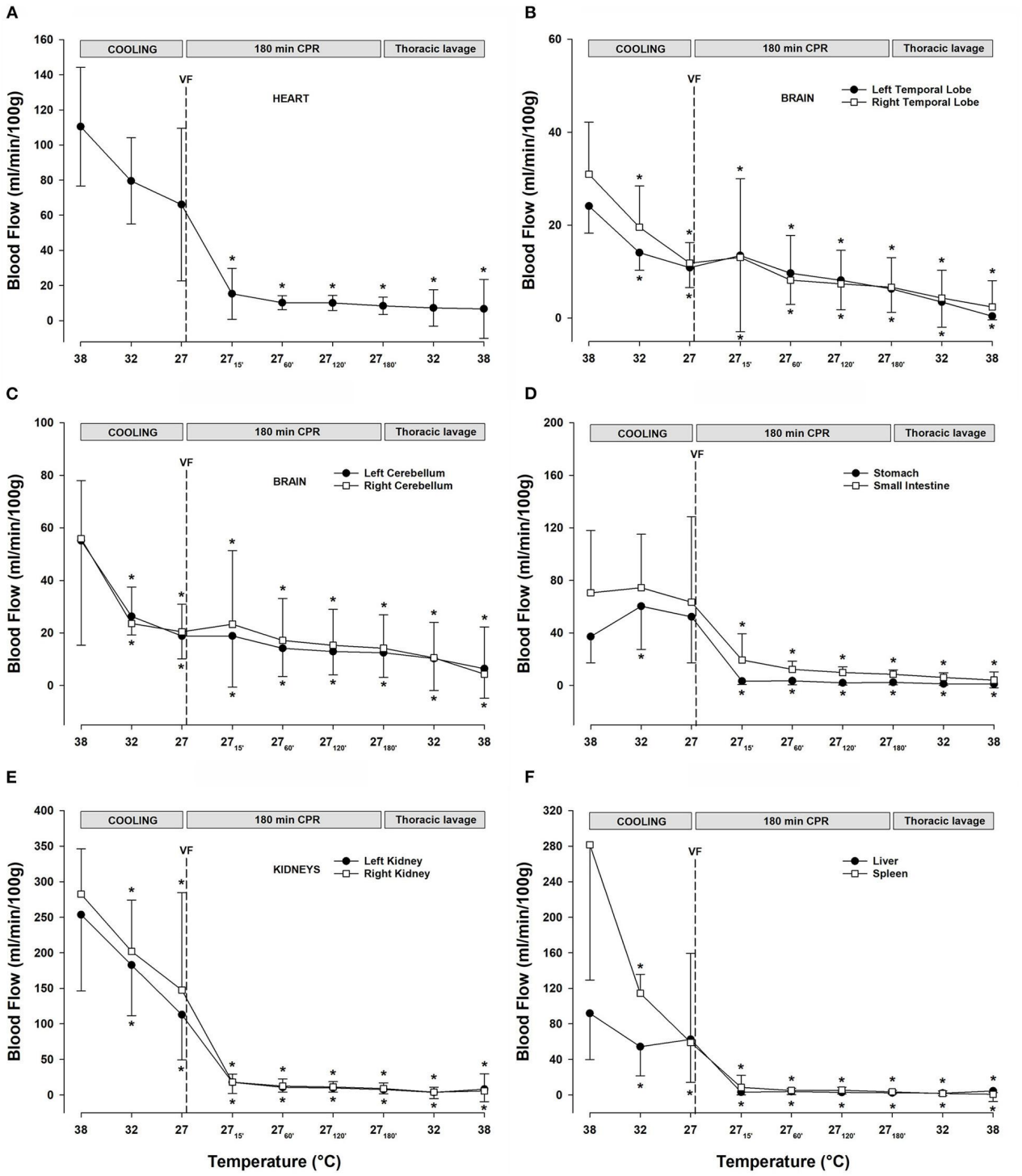

FIGURE 4 | (A) Myocardial blood flow. **(B)** Blood flow in the left and right temporal lobes. **(C)** Blood flow in the left and right cerebellar hemispheres. **(D)** Blood flow in the stomach and small intestine. **(E)** Renal blood flow. **(F)** Blood flow in the liver and the spleen. $n = 8$, values are mean ± SD. *$p < 0.05$ statistically significantly different from baseline value.

cardioversion of ventricular fibrillation to sinus rhythm. In only one out of eight animals, a perfusing rhythm (sinus rhythm, MAP between 49 and 60 mmHg) was achieved at 31°C after the two cardioversion attempts (50 and 100 J), and a single bolus of 0.1 mg epinephrine. The three animals had a spontaneous conversion from ventricular fibrillation to

ventricular tachycardia during rewarming above 30°C and were treated with repeated IV injections of amiodarone (100–150 mg) followed by unsuccessful cardioversion attempts (100 J, up to three times). In the remaining four animals, the repeated attempts to convert the ventricular fibrillation were unsuccessful at all predetermined temperatures.

Hemodynamic Function

Throughout the period of lavage rewarming and continuous CPR, CO, and SV (**Table 1**) remained lowered at 27°C, and after rewarming they remained reduced at −80 and −79%, respectively, when compared with the baseline values at 38°C. In the single animal where a perfusing rhythm was established under continuous epinephrine infusion, MAP remained at 50–60 mmHg, whereas CO was reduced, −77%, when compared with its baseline value.

O_2 Transport and Extraction

The continuous CPR and closed thoracic lavage rewarming did not change global DO_2 (**Figure 3A**), and at 38°C, it was significantly reduced compared with the baseline [15.2 ± 4.4 vs. 9.4 ± 3.0 ml min^{-1} $(100\,g)^{-1}$; −38%]. Likewise, global VO_2 (**Figure 3A**) remained unchanged during the closed thoracic lavage rewarming, and at 38°C, it was significantly reduced compared with the baseline [6.8 ± 2.5 vs. 4.3 ± 1.1 ml min^{-1} $(100\,g)^{-1}$; −34%].

During rewarming, the cerebral DO_2 and VO_2 (**Figure 3B**) remained unaltered but the difference between them appeared practically vanished at 38°C, and they were both significantly reduced when compared with the baseline (DO_2: 4.41 ± 2.14 vs. 2.11 ± 2.23; −50% and VO_2: 2.08 ± 1.17 vs. 0.85 ± 0.87 ml min^{-1} $(100\,g)^{-1}$; −56%). Both the global and cerebral extraction ratios (**Figure 3C**) increased to values ∼0.7 during rewarming and at 38°C, they were significantly elevated compared with the baseline values.

During rewarming at 32 and 38°C, a substantial reduction in arterial pH (**Table 2**) from 7.15 ± 0.08 to 6.97 ± 0.17, respectively, was measured, and both the values were significantly reduced compared with the 38°C baseline pH value of 7.53 ± 0.05. The reduced pH occurred simultaneously with a significant increase in serum lactate (**Table 2**) from the baseline 38°C value of 0.8 ± 0.2 to 10.0 ± 3.9 mmol L^{-1} after rewarming, a significant reduction of HCO_3^- (**Table 2**) from 29 ±2 to 10 ± 5 mmol L^{-1}, and a fall in S_vO_2 (**Table 2**) from 59 ± 8 to 17 ± 9%.

Organ Blood Flow

Lavage rewarming did not lead to any change in the already reduced blood flow (**Figures 4A-F**) measured during CPR at 27°C in all organs investigated.

DISCUSSION

In the present study, a porcine experimental animal model was used to mimic the condition of prehospital accidental hypothermia with HCA and CPR for a 3-h period at 27°C. Specifically, we explored if rewarming by closed thoracic lavage could be used to establish a spontaneous "shockable" cardiac rhythm and reestablish a perfusing rhythm. The potential translational value of this experiment was to provide evidence supporting (or not) the use of closed thoracic lavage rewarming after long-lasting CPR in the accidental hypothermia patients in a local hospital as an alternative to continued CPR and transportation to a medical center equipped for rewarming with ECLS. The safe time limits for hypothermic CPR are yet not documented, whereas it is well-documented that during normothermic CPR, it is vital to establish a perfusing rhythm within 20 min. The present study demonstrated that the continuous CPR at 27°C maintained CO, MAP, and blood flow to the vital organs at the same reduced level for 3-h and supported global aerobic metabolism. However, the ensuing rewarming using closed thoracic lavage and continued CPR failed to establish an adequate perfusing rhythm in any animal.

All the animals in this study had ventricular fibrillation during rewarming and attempts to establish a perfusing rhythm were started at 30°C by cardioversion. We were able to establish a sinus rhythm in only one out of eight animals during rewarming, but due to electro-mechanic dissociation, it was out of reach to establish a perfusing rhythm. In all animals, the attempts to establish a perfusing rhythm were under continuous epinephrine support, which re-established MAP (50–60 mmHg) but failed to elevate CO that remained seriously reduced (−77%). After rewarming by closed thoracic lavage, the reduced CO was unable to elevate the organ blood flow or DO_2 over the corresponding values measured during CPR at 27°C. During the period of rewarming by closed thoracic lavage, all the animals had seriously reduced organ blood flow and simultaneously worsening metabolic acidosis. The failure to re-establish perfusion ended in circulatory collapse at 38°C. In a previous report, we documented that the level of CO produced by CPR during 38°C remained unchanged after cooling to 27°C (Nilsen et al., 2020). The results from the present experiment support this observation, and consequently, the low CO produced by continuous CPR must be converted to a perfusing rhythm during rewarming at 30–32°C to make closed thoracic lavage an alternative to ECLS as a rewarming technique. Further, in the single animal where ventricular fibrillation was converted to a perfusing rhythm, the CO remained low despite pharmacologic support. This observation is consistent with the existence of hypothermia-induced, left ventricular dysfunction (Bigelow et al., 1950; Fairley et al., 1957; Tveita et al., 1994, 1998; Filseth et al., 2010), which may necessitate massive cardiac support, making ECLS the only therapeutic alternative. So far, the longest period of HCA before successful resuscitation and rewarming with ECLS has been reported after 6.5 h of continuous CPR (Lexow, 1991). In the porcine model, we recently documented (Scientific Reports in press) successful rewarming by ECLS after a 3-h period of continuous CPR using an extracorporeal membrane oxygenator (ECMO), which restored the blood flow to the heart and the brain. After the period of CPR and rewarming by ECLS, we were able to convert the spontaneous ventricular fibrillation to a sinus rhythm

in all the animals. Successful rewarming by ECLS after long-lasting CPR for HCA has been documented (Brown et al., 2012), but after rewarming, these patients often need cardio-respiratory support for days, a fact in favor of using ECMO-rewarming (Ruttmann et al., 2007). In fact, ECMO rewarming has been suggested to be superior to other ECLS techniques (Silfvast and Pettila, 2003). By using the ECMO technique for rewarming, the survival and neurologic outcome of accidental hypothermia patients with HCA has improved significantly (Debaty et al., 2017; Bjertnaes et al., 2021).

Thoracic Lavage

Technically, the thoracic lavage is applicable as open or closed. Open thoracic lavage involves a thoracic incision big enough to enable manipulation of the heart and other mediastinal structures, while directly pouring warm liquid on the heart (Linton and Ledingham, 1966; Althaus et al., 1982; Best et al., 1985; Brunette et al., 1992). Closed thoracic lavage, as used in this experiment, involves small incisions to enable the insertion of one or more pleural drains in one or both thoracic cavities. This procedure is often performed by inserting one "inlet" drain and one "outlet" drain in the left thoracic cavity (Hall and Syverud, 1990; Iversen et al., 1990; Kornberger et al., 2001; Schwarz et al., 2002), and the procedure can be performed by a variety of hospital physicians (Brunette et al., 1987; Plaisier, 2005). With closed thoracic lavage, external chest compressions can be performed throughout the resuscitation. This may be beneficial as it preserves the thoracic pump mechanism (Plaisier, 2005), one of the key factors for a favorable outcome during CPR, linked to the recognition of chest wall recoil and negative thoracic pressure as mechanisms for venous blood return, as well as for cerebral- and coronary blood flow in the decompression phase (Georgiou et al., 2014). However, a feared consequence of the closed thoracic lavage is an increase in intrathoracic pressure. This unwanted side effect is most often brought about by a mismatch between inlet and outlet volumes leading to the retention of water and subsequent increase in pressure inside the thoracic cavity. Any increase in thoracic pressure may cause dramatic consequences on the hemodynamic function during spontaneous circulation, as well as during CPR (Aufderheide et al., 2008; Metzger et al., 2012; Kill et al., 2014).

There are only a few human reports (Winegard, 1997; Plaisier, 2005; Kjaergaard and Bach, 2006; Turtiainen et al., 2014) and animal studies (Brunette et al., 1987; Barr et al., 1988; Otto and Metzler, 1988), utilizing closed thoracic lavage in the context of rewarming from hypothermia and HCA, with no conclusions regarding the superiority of one rewarming technique over the other. Further, the longest period of HCA before successful resuscitation and rewarming with closed thoracic lavage so far is 3 h and 13 min (Winegard, 1997). Thoracic lavage is independent of an intact circulation to effectively warm the heart and is, except for ECLS, probably among the fastest active internal rewarming techniques (Brown et al., 2012) to facilitate defibrillation and to establish a perfusing rhythm in a patient with HCA (Plaisier, 2005). In addition, in hypothermic patients with unstable circulation, direct rewarming of the heart with this method may be protective against ventricular fibrillation (Barr et al., 1988).

Despite many unanswered questions related to using closed thoracic lavage, the introduction of its use in humans took only a couple of years as described in a case report (Hall and Syverud, 1990). ECLS is not always available for rewarming patients in HCA; thus, closed thoracic lavage was suggested as an alternative method that appears to be both efficient and safe when applied by competent physicians (Winegard, 1997; Plaisier, 2005; Kjaergaard and Bach, 2006; Turtiainen et al., 2014). However, to recommend this method as an alternative to ECLS for a variety of physicians to rewarm accidental hypothermia patients in any local hospital (Brunette et al., 1987; Plaisier, 2005), it is essential that evidence of its utility must be demonstrated as documenting any potential negative side effects. Unfortunately, the evidence base for the application of closed thoracic lavage as an alternative to ECLS was never provided.

In this study model, it often appeared challenging to combine the use of closed thoracic lavage with ongoing CPR. The practical challenges were many, such as maintaining constant inflow temperature and constant tap water flow, maintaining a closed circuit, and preventing a build-up in intrathoracic pressure. We previously have documented challenges related to the use of closed thoracic lavage for rewarming during spontaneous circulation (Valkov et al., 2019), without simultaneous CPR. In sum, the spread in rewarming rate using closed thoracic lavage documented in the present experiment may be taken as the consequence of all these practical issues.

Continuous CPR

In addition to the factors described above, it is possible that prolonged CPR causes trauma to the heart. However, in the 82 retrospective cases of CPR for 20–230 min, only 10 patients were treated for HCA and only seven cases had reduced ejection fraction. Of these seven cases, one patient had aortic valve deformity, and there were no other cardiac CPR-related complications reported (Youness et al., 2016).

CONCLUSION

Anecdotal case reports have suggested that the accidental hypothermia patients can be successfully rewarmed with thoracic lavage, but with little if any documentation. Our animal experiment, evaluating the effects of rewarming by closed thoracic lavage after a 3-h period of continuous CPR for HCA at 27°C, found that the critical element of the successful use of this method, reestablishment of a perfusing rhythm during the early part (30–32°C) of rewarming, could not be demonstrated. Thus, the results of this experiment do not support the use of closed thoracic lavage as an alternative to ECLS for rewarming accidental hypothermia patients after long-lasting CPR for HCA.

DATA AVAILABILITY STATEMENT

The raw data supporting the conclusions of this article will be made available by the authors, without undue reservation.

ETHICS STATEMENT

The animal study was reviewed and approved by The Norwegian Food Safety Authority.

AUTHOR CONTRIBUTIONS

TT, GS, JN, RM, and TK contributed to the conception and design, data analysis and interpretation, and drafting the manuscript for intellectual content. JN, RM, TS, JN, SV, and TK contributed to the completion of experiments and collection of data. JN, RM, TS, JN, SV, TK, GS, and TT contributed to the revision of the manuscript. All authors contributed to the article and approved the submitted version.

FUNDING

This work was generously supported by grants from the Norwegian Research Council (Petromax2) and the Norwegian Ministry of Foreign Affairs (Barents 2020).

REFERENCES

Althaus, U., Aeberhard, P., Schupbach, P., Nachbur, B. H., and Muhlemann, W. (1982). Management of profound accidental hypothermia with cardiorespiratory arrest. *Ann. Surg.* 195, 492–495. doi: 10.1097/00000658-198204000-00018

Aufderheide, T. P., Alexander, C., Lick, C., Myers, B., Romig, L., Vartanian, L., et al. (2008). From laboratory science to six emergency medical services systems: new understanding of the physiology of cardiopulmonary resuscitation increases survival rates after cardiac arrest. *Crit. Care Med.* 36(11 Suppl), S397–S404. doi: 10.1097/CCM.0b013e31818a7e56

Barr, G. L., Halvorsen, L. O., and Donovan, A. J. (1988). Correction of hypothermia by continuous pleural perfusion. *Surgery* 103, 553–557.

Best, R., Syverud, S., and Nowak, R. M. (1985). Trauma and hypothermia. *Am. J. Emerg. Med.* 3, 48–55. doi: 10.1016/0735-6757(85)90013-0

Bigelow, W. G., Lindsay, W. K., and Greenwood, W. F. (1950). Hypothermia. its possible role in cardiac surgery: an investigation of factors governing survival in dogs at low body temperatures. *Ann. Surg.* 132, 849–864. doi: 10.1097/00000658-195011000-00001

Bjertnaes, L. J., Hindberg, K., Naesheim, T. O., Suborov, E. V., Reierth, E., Kirov, M. Y., et al. (2021). Rewarming from hypothermic cardiac arrest applying extracorporeal life support: a systematic review and meta-analysis. *Front. Med.* 8:641633. doi: 10.3389/fmed.2021.641633

Brown, D. J., Brugger, H., Boyd, J., and Paal, P. (2012). Accidental hypothermia. *N. Engl. J. Med.* 367, 1930–1938. doi: 10.1056/NEJMra1114208

Brugger, H., Durrer, B., Elsensohn, F., Paal, P., Strapazzon, G., Winterberger, E., et al. (2013). Resuscitation of avalanche victims: Evidence-based guidelines of the international commission for mountain emergency medicine (ICAR MEDCOM): intended for physicians and other advanced life support personnel. *Resuscitation* 84, 539–546. doi: 10.1016/j.resuscitation.2012.10.020

Brunette, D. D., Biros, M., Mlinek, E. J., Erlandson, C., and Ruiz, E. (1992). Internal cardiac massage and mediastinal irrigation in hypothermic cardiac arrest. *Am. J. Emerg. Med.* 10, 32–34. doi: 10.1016/0735-6757(92)90121-D

Brunette, D. D., Sterner, S., Robinson, E. P., and Ruiz, E. (1987). Comparison of gastric lavage and thoracic cavity lavage in the treatment of severe hypothermia in dogs. *Ann. Emerg. Med.* 16, 1222–1227. doi: 10.1016/S0196-0644(87)80227-5

Carretero, M. J., Fontanals, J., Agusti, M., Arguis, M. J., Martinez-Ocon, J., Ruiz, A., et al. (2010). Monitoring in resuscitation: comparison of cardiac output measurement between pulmonary artery catheter and NICO. *Resuscitation* 81, 404–409. doi: 10.1016/j.resuscitation.2009.12.021

Danzl, D. F., and Pozos, R. S. (1994). Accidental hypothermia. *N. Engl. J. Med.* 331, 1756–1760. doi: 10.1056/NEJM199412293312607

Debaty, G., Babaz, V., Durand, M., Gaide-Chevronnay, L., Fournel, E., Blancher, M., et al. (2017). Prognostic factors for extracorporeal cardiopulmonary resuscitation recipients following out-of-hospital refractory cardiac arrest. a systematic review and meta-analysis. *Resuscitation* 112, 1–10. doi: 10.1016/j.resuscitation.2016.12.011

Dunne, B., Christou, E., Duff, O., and Merry, C. (2014). Extracorporeal-assisted rewarming in the management of accidental deep hypothermic cardiac arrest: a systematic review of the literature. *Heart Lung Circ.* 23, 1029–1035. doi: 10.1016/j.hlc.2014.06.011

Fairley, H. B., Waddell, W. G., and Bigelow, W. G. (1957). Hypothermia for cardiovascular surgery: acidosis in the rewarming period. *Br. J. Anaesth.* 29, 310–318. doi: 10.1093/bja/29.7.310

Filseth, O. M., How, O. J., Kondratiev, T., Gamst, T. M., and Tveita, T. (2010). Post-hypothermic cardiac left ventricular systolic dysfunction after rewarming in an intact pig model. *Crit. Care* 14:R211. doi: 10.1186/cc9334

Georgiou, M., Papathanassoglou, E., and Xanthos, T. (2014). Systematic review of the mechanisms driving effective blood flow during adult CPR. *Resuscitation* 85, 1586–1593. doi: 10.1016/j.resuscitation.2014.08.032

Giesbrecht, G. G. (2001). Emergency treatment of hypothermia. *Emerg. Med.* 13, 9–16. doi: 10.1046/j.1442-2026.2001.00172.x

Hall, K. N., and Syverud, S. A. (1990). Closed thoracic cavity lavage in the treatment of severe hypothermia in human beings. *Ann. Emerg. Med.* 19, 204–206. doi: 10.1016/S0196-0644(05)81810-4

Hilmo, J., Naesheim, T., and Gilbert, M. (2014). "Nobody is dead until warm and dead": prolonged resuscitation is warranted in arrested hypothermic victims also in remote areas–a retrospective study from northern Norway. *Resuscitation* 85, 1204–1211. doi: 10.1016/j.resuscitation.2014.04.029

Iversen, R. J., Atkin, S. H., Jaker, M. A., Quadrel, M. A., Tortella, B. J., and Odom, J. W. (1990). Successful CPR in a severely hypothermic patient using continuous thoracostomy lavage. *Ann. Emerg. Med.* 19, 1335–1337. doi: 10.1016/S0196-0644(05)82300-5

Kill, C., Hahn, O., Dietz, F., Neuhaus, C., Schwarz, S., Mahling, R., et al. (2014). Mechanical ventilation during cardiopulmonary resuscitation with intermittent positive-pressure ventilation, bilevel ventilation, or chest compression synchronized ventilation in a pig model. *Crit. Care Med.* 42, e89–e95. doi: 10.1097/CCM.0b013e3182a63fa0

Kjaergaard, B., and Bach, P. (2006). Warming of patients with accidental hypothermia using warm water pleural lavage. *Resuscitation* 68, 203–207. doi: 10.1016/j.resuscitation.2005.06.019

Kornberger, E., Lindner, K. H., Mayr, V. D., Schwarz, B., Rackwitz, K. S., Wenzel, V., et al. (2001). Effects of epinephrine in a pig model of hypothermic cardiac arrest and closed-chest cardiopulmonary resuscitation combined with active rewarming. *Resuscitation* 50, 301–308. doi: 10.1016/S0300-9572(01)00353-7

Lexow, K. (1991). Severe accidental hypothermia: survival after 6 hours 30 minutes of cardiopulmonary resuscitation. *Arctic. Med. Res.* 50(Suppl. 6), 112–114.

Linton, A. L., and Ledingham, I. M. (1966). Severe hypothermia with barbiturate intoxication. *Lancet* 1, 24–26. doi: 10.1016/S0140-6736(66)90009-2

Lloyd, E. L. (1996). Accidental hypothermia. *Resuscitation* 32, 111–124. doi: 10.1016/0300-9572(96)00983-5

Metzger, A. K., Herman, M., McKnite, S., Tang, W., and Yannopoulos, D. (2012). Improved cerebral perfusion pressures and 24-hr neurological survival in a porcine model of cardiac arrest with active compression-decompression cardiopulmonary resuscitation and augmentation of negative intrathoracic pressure. *Crit. Care Med.* 40, 1851–1856. doi: 10.1097/CCM.0b013e318246b9ad

Mroczek, T., Gladki, M., and Skalski, J. (2020). Successful resuscitation from accidental hypothermia of 11.8 degrees C: where is the lower bound for human beings? *Eur. J. Cardiothorac. Surg.* 58, 1091–1092. doi: 10.1093/ejcts/ezaa159

Nichol, G., Aufderheide, T. P., Eigel, B., Neumar, R. W., Lurie, K. G., Bufalino, V. J., et al. (2010). Regional systems of care for out-of-hospital cardiac arrest: a policy statement from the American Heart Association. *Circulation* 121, 709–729. doi: 10.1161/CIR.0b013e3181cdb7db

Nilsen, J. H., Valkov, S., Mohyuddin, R., Schanche, T., Kondratiev, T. V., Naesheim, T., et al. (2020). Study of the effects of 3 h of continuous cardiopulmonary resuscitation at 27°C on Global oxygen transport and organ blood flow. *Front. Physiol.* 11:213. doi: 10.3389/fphys.2020.00213

Otto, R. J., and Metzler, M. H. (1988). Rewarming from experimental hypothermia: comparison of heated aerosol inhalation, peritoneal lavage, and pleural lavage. *Crit. Care Med.* 16, 869–875. doi: 10.1097/00003246-198809000-00010

Perkins, G. D., Jacobs, I. G., Nadkarni, V. M., Berg, R. A., Bhanji, F., Biarent, D., et al. (2015). Cardiac arrest and cardiopulmonary resuscitation outcome reports: update of the Utstein Resuscitation Registry Templates for Out-of-Hospital Cardiac Arrest: a statement for healthcare professionals from a task force of the International Liaison Committee on Resuscitation (American Heart Association, European Resuscitation Council, Australian and New Zealand Council on Resuscitation, Heart and Stroke Foundation of Canada, InterAmerican Heart Foundation, Resuscitation Council of Southern Africa, Resuscitation Council of Asia); and the American Heart Association Emergency Cardiovascular Care Committee and the Council on Cardiopulmonary, Critical Care, Perioperative and Resuscitation. *Circulation* 132, 1286–1300. doi: 10.1161/CIR.0000000000000144

Plaisier, B. R. (2005). Thoracic lavage in accidental hypothermia with cardiac arrest–report of a case and review of the literature. *Resuscitation* 66, 99–104. doi: 10.1016/j.resuscitation.2004.12.024

Reinhardt, C. P., Dalhberg, S., Tries, M. A., Marcel, R., and Leppo, J. A. (2001). Stable labeled microspheres to measure perfusion: validation of a neutron activation assay technique. *Am. J. Physiol. Heart Circ. Physiol.* 280, H108–H16. doi: 10.1152/ajpheart.2001.280.1.H108

Ruttmann, E., Weissenbacher, A., Ulmer, H., Muller, L., Hofer, D., Kilo, J., et al. (2007). Prolonged extracorporeal membrane oxygenation-assisted support provides improved survival in hypothermic patients with cardiocirculatory arrest. *J. Thorac. Cardiovasc. Surg.* 134, 594–600. doi: 10.1016/j.jtcvs.2007.03.049

Schwarz, B., Mair, P., Raedler, C., Deckert, D., Wenzel, V., and Lindner, K. H. (2002). Vasopressin improves survival in a pig model of hypothermic cardiopulmonary resuscitation. *Crit. Care Med.* 30, 1311–1314. doi: 10.1097/00003246-200206000-00027

Silfvast, T., and Pettila, V. (2003). Outcome from severe accidental hypothermia in Southern Finland–a 10-year review. *Resuscitation* 59, 285–290. doi: 10.1016/S0300-9572(03)00237-5

Turtiainen, J., Halonen, J., Syvaoja, S., and Hakala, T. (2014). Rewarming a patient with accidental hypothermia and cardiac arrest using thoracic lavage. *Ann. Thorac. Surg.* 97, 2165–2166. doi: 10.1016/j.athoracsur.2013.08.028

Tveita, T., Mortensen, E., Hevrøy, O., Refsum, H., and Ytrehus, K. (1994). Experimental hypothermia: effects of core cooling and rewarming on hemodynamics, coronary blood flow and myocardial metabolism in dogs. *Anesth. Analg.* 79, 212–218. doi: 10.1213/00000539-199408000-00002

Tveita, T., Ytrehus, K., Myhre, E. S., and Hevroy, O. (1998). Left ventricular dysfunction following rewarming from experimental hypothermia. *J. Appl. Physiol.* 85, 2135–2139. doi: 10.1152/jappl.1998.85.6.2135

Valkov, S., Mohyuddin, R., Nilsen, J. H., Schanche, T., Kondratiev, T. V., Sieck, G. C., et al. (2019). Organ blood flow and O2 transport during hypothermia (27 degrees C) and rewarming in a pig model. *Exp. Physiol.* 104, 50–60. doi: 10.1113/EP087205

Walpoth, B. H., Meyer, M., Gaudet-Blavignac, C., Baumann, P., Gilquin, P., and Lovis, C. (2017). The International Hypothermia Registry (IHR): Dieter's ESAO Winter schools and beat's international hypothermia registry. *Int. J. Artif. Organs.* 40:40–42. doi: 10.5301/ijao.5000574

Weiss, A. J., Pawale, A., Griepp, R. B., and Di, L. G. (2012). Deep versus mild hypothermia during thoracoabdominal aortic surgery. *Ann. Cardiothorac. Surg.* 1, 329–333. doi: 10.1016/j.jtcvs.2011.07.020

Winegard, C. (1997). Successful treatment of severe hypothermia and prolonged cardiac arrest with closed thoracic cavity lavage. *J. Emerg. Med.* 15, 629–632. doi: 10.1016/S0736-4679(97)00139-X

Youness, H., Al, H. T., Hussein, H., Awab, A., Jones, K., and Keddissi, J. (2016). Review and outcome of prolonged cardiopulmonary resuscitation. *Crit. Care Res. Pract.* 2016:7384649. doi: 10.1155/2016/7384649

Young, A. J., Sawka, M. N., Levine, L., Burgoon, P. W., Latzka, W. A., Gonzalez, R. R., et al. (1995). Metabolic and thermal adaptations from endurance training in hot or cold water. *J. Appl. Physiol.* 78, 793–801. doi: 10.1152/jappl.1995.78.3.793

Zafren, K., Giesbrecht, G. G., Danzl, D. F., Brugger, H., Sagalyn, E. B., Walpoth, B., et al. (2014). Wilderness Medical Society practice guidelines for the out-of-hospital evaluation and treatment of accidental hypothermia: 2014 update. *Wilderness Environ. Med.* 25(4 Suppl), S66–S85. doi: 10.1016/j.wem.2014.10.010

Conflict of Interest: The authors declare that the research was conducted in the absence of any commercial or financial relationships that could be construed as a potential conflict of interest.

Publisher's Note: All claims expressed in this article are solely those of the authors and do not necessarily represent those of their affiliated organizations, or those of the publisher, the editors and the reviewers. Any product that may be evaluated in this article, or claim that may be made by its manufacturer, is not guaranteed or endorsed by the publisher.

frontiers in Physiology

ORIGINAL RESEARCH
published: 03 November 2021
doi: 10.3389/fphys.2021.763975

Effects of Cold Decompression on Hemodynamic Function and Decompression Sickness Risk in a Dry Diving Rat Model

Svein E. Gaustad[1,2,3], Timofei V. Kondratiev[3], Ingrid Eftedal[2,4] and Torkjel Tveita[3,5]*

[1]Møreforsking AS, Volda, Norway, [2]Department of Circulation and Medical Imaging, Norwegian University of Science and Technology, Trondheim, Norway, [3]Anesthesia and Critical Care Research Group, Department of Clinical Medicine, UiT, The Arctic University of Norway, Tromsø, Norway, [4]Faculty of Nursing and Health Sciences, Nord University, Bodø, Norway, [5]Division of Surgical Medicine and Intensive Care, University Hospital of North Norway, Tromsø, Norway

OPEN ACCESS

Edited by:
Airong Qian, Northwestern Polytechnical University, China

Reviewed by:
Costantino Balestra, Haute École Bruxelles-Brabant (HE2B), Belgium
Danilo Cialoni, Dan Europe Foundation, Italy

***Correspondence:**
Ingrid Eftedal
ingrid.eftedal@ntnu.no

Specialty section:
This article was submitted to Environmental, Aviation and Space Physiology, a section of the journal Frontiers in Physiology

Received: *24 August 2021*
Accepted: *05 October 2021*
Published: *03 November 2021*

Citation:
Gaustad SE, Kondratiev TV, Eftedal I and Tveita T (2021) Effects of Cold Decompression on Hemodynamic Function and Decompression Sickness Risk in a Dry Diving Rat Model. Front. Physiol. 12:763975. doi: 10.3389/fphys.2021.763975

Background: Diving in cold water is thought to increase the risk of decompression sickness (DCS), especially if the diver is cold during decompression. In this study, we investigated hemodynamic function and DCS risk in an animal model, where cold decompression was followed by rewarming at the surface.

Methods: Nine female Sprague Dawley rats had pressure-volume catheters inserted into their left heart ventricle and femoral artery before they were exposed to dry air dives in which their core temperature was normothermic during the bottom phase, cold (35°C) during decompression, and normothermic after the dive. Data from an earlier study were used as controls. The rats were compressed in air to 600 kPa, maintained at pressure for 45 min, and decompressed at 50 kPa/min. Hemodynamic data were recorded before, during, and 60 min after decompression. Venous gas bubbles were recorded in the right heart ventricle and pulmonary artery for 60 min after the dive.

Results and Conclusion: During decompression, cardiac output (CO), and stroke volume (SV) decreased equally in cold rats and controls. CO and SV were temporarily re-established at the surface, before falling again in the cold rats. There was no difference in post-dive venous bubble grades. However, as the post-dive fall in CO and SV could be a sign of gas emboli obstructing the pulmonary circulation, we cannot conclude whether the DCS risk was increased. More sensitive bubble detection methods are needed to elucidate this point.

Keywords: diving, hemodynamic function, temperature, cold diving, left ventricle, venous gas bubbles

INTRODUCTION

DCS risk after diving is thought to be temperature dependent, although causal relationships are undetermined (Dunford and Hayward, 1981; Mekjavić and Kakitsuba, 1989; Leffler, 2001; Fahlman and Kayar, 2006). Empirical and experimental data indicate that cold water diving is associated with more DCS, especially if the diver is cold during decompression (Toner and Ball, 2004). United States Navy procedures require longer decompression times when divers are "exceptionally cold" (Commander, 1999).

DCS is a multifaceted disease triggered by inert gas bubbles released from supersaturated tissues during decompression. The uptake and removal of inert gas is determined primarily by tissue perfusion (Ohta et al., 1978), which is regulated by temperature sensitive mechanisms (Barcroft and Edholm, 1943; Caldwell et al., 2016). It follows that a diver who is cold during the bottom phase and warm during decompression would desaturate more efficiently and therefore may have lower DCS risk compared to one who is warm at the bottom, cold during decompression, and rewarmed at the surface (Dunford and Hayward, 1981; Mack and Lin, 1986; Mekjavić and Kakitsuba, 1989; Gerth et al., 2007). In addition to temperature, tissue perfusion depends on the solubility and diffusion capacity of the breathing gas (Lango et al., 1996), and the picture is further complicated by other factors, which contribute to DCS risk, including immersion, BMI/fat mass, age, gender, and work load/activity levels before, during, and after the dive (Dujic et al., 2006, 2008; Cialoni et al., 2017). In this complex picture, there is a need for controlled experiments that focus on thermal effects.

In this comparative study, we examined whether a core temperature reduction to 35°C during decompression followed by rewarming to 37°C at the surface would increase the risk of DCS. We employed a previously established diving rat model designed to measure hemodynamic function (Gaustad et al., 2020), to which we added core temperature control and used post-decompression venous gas bubble formation as a proxy measure for DCS.

MATERIALS AND METHODS

Ethics

The study protocol was approved in advance by the Norwegian Council for Animal Research (approval ID 2111). All procedures were consistent with the European Convention for the Protection of Vertebrate Animals used for Experimental and Other Scientific Purposes. In partial fulfillment of the requirement to minimize the number of animals, the control rats referred to in this experiment are the same individuals as previously described (Gaustad et al., 2020).

Animals

Female Sprague Dawley rats (259.0 ± 5.4 g) were obtained from Charles River Laboratories (Charles River Laboratories Inc., Sulzfeld, Germany). To limit stress to the animals prior to the dives, they were kept at an approved animal facility in which they had *ad libitum* access to a standard rodent chow and water and were handled by a dedicated technician. As rats are nocturnal, the light in the facility was controlled at a 12-h dark-12 h cycle with the dark cycle coinciding with human daytime. The experimental dives were performed during the rat's wake (dark) cycle.

Pre-dive Procedures

Prior to the experiment the rats were anesthetized by sodium pentobarbital. A 13 Gauge metal tube was inserted into the trachea to establish a patent airway. For hemodynamic monitoring, two microtip pressure-volume (P-V) catheters (SPR-838, 2.0 F, Millar Instruments; Houston, TX, United States) were used, one was inserted into the left ventricle (LV) to obtain LV volumes and LV pressure and another one was placed into the femoral artery to obtain MAP as previously described (Gaustad et al., 2020). The rats rested for 60 min to regain hemodynamic stability and were placed in the supine position and kept under anesthesia while breathing spontaneously until the end of the experiment.

Conductance Measurement Calibration for Hypothermia

The principle for adjustment of conductance catheter readings for different temperatures was previously described in detail by Han et al. (2008). In short, for assessment of the left ventricular volume, the cuvette calibration was used to adjust for temperature-dependent changes in blood viscosity. Plexiglas calibration cuvettes (910–1048, Millar Instruments, Houston, TX, United States) with wells of known volumes from 28 to 346 µl were filled with heparinized blood from the rat and immersed in a temperature-controlled water bath to adjust blood temperature to 37, 36, and 35°C during catheter calibration. The P-V catheter was sequentially placed into wells, and the conductance values were recorded for each well at each temperature mentioned above. Linear regression between conductance values and corresponding wells' volumes was plotted for each temperature. Slopes and y-intercepts obtained at the above temperatures were applied to the analysis software (PVAN 3.6, Millar Instruments, Houston, TX, United States) to convert conductance units to true volumes in µl. Ideally, measurements should be corrected for parallel conductance induced by the alternating current passing from the catheter through the blood and into the surrounding LV wall or inter-ventricular septum. Parallel conductance is usually measured by a saline bolus injection at the end of experiment (Georgakopoulos and Kass, 2000). However, we did not consider this method suitable to our experimental protocol, which required the measurements of left ventricular volume at different temperatures. Considering temperature-dependent changes in viscosity of blood, a bolus injection performed at the end of experiment (37°C) would not represent the true parallel conductance at lower core temperature, and injection of hypertonic saline (30% NaCl) in animals positioned inside the

chamber was not possible. In addition, repeated injections might harm the animal. Therefore, parallel conductance correction was not included in our volume measurements.

Core Temperature Control

An electric heat pad was used to control the rats' core temperature throughout the experiment. For temperature monitoring, we used a digital thermometer (Thermoalert, Columbus Instruments, OH, United States) connected to a thermocouple wire with its tip positioned in the lower 1/3 of the rat's esophagus. During the simulated diving exposure, the thermometer was placed inside the pressure chamber and observed through a porthole.

Simulated Diving

The protocol for simulated diving has been described in detail elsewhere (Gaustad et al., 2020). In short, rats ($n = 9$) were exposed one at a time to hyperbaric air in a pressure chamber (Sira Engineering, Trondheim, NO). Compression was done at 200 kPa/min to a pressure of 600 kPa, corresponding to a water depth of 50 m. This pressure was maintained during a 45-min bottom phase before the animals were decompressed back to surface at 50 kPa/min over 10 min. The dive was followed by a 60-min post-dive observation. During the bottom phase, the rats were kept at a normothermic core temperature (37°C). They were cooled to 35.1 ± 0.2°C during the decompression, before they were gently rewarmed to normothermia for the 60 min post-dive observation (**Figure 1**).

Hemodynamic Data Recording and Analysis

The following data were obtained during the experiment: mean arterial pressure (MAP), heart rate (HR), maximal LV systolic pressure, LV end-diastolic pressure, maximal slope of LV systolic pressure increment (LV dP/dtmax), stroke volume (SV), LV end-diastolic volume (LVEDV), LV end-systolic volume (LVESV), CO, and stroke work (SW). Preload recruitable stroke work (PRSW) was measured before and after the simulated diving. During the bottom phase of the dive, recordings were done at 1, 2, 3, and 5 min, and further repeated every 10 min. During the decompression, recordings were done every 2 min, and during the post-dive observation, recordings were done after 2 min, 5 min, and then repeated every 10 min until the end of the experiment after 60 min. The data were recorded using ADInstruments LabChart DAQ software (AD Instruments, Hastings, United Kingdom) and analyzed in a cardiac P-V analysis program (PVAN 3.6, Millar Instruments, Houston, TX, United States).

Post-decompression Venous Gas Bubbles

Venous gas bubbles were detected by insonating the rat's pulmonary artery and aorta using a GE Vingmed Vivid-i ultrasonic scanner with a 10-MHz transducer to record as previously described (Wisloff and Brubakk, 2001). Bubbles were recorded at 10-min intervals up to 60 min, at which time the animals were sacrificed. Ultrasound images were used to grade bubble loads by the Eftedal and Brubakk scale (Eftedal and Brubakk, 1997).

Statistics

Hemodynamic data were assessed by one-way repeated measures ANOVA. In cases where the F value was greater than critical, Dunnett's test was used to evaluate differences between baseline and later measurements. Mann–Whitney U test was used to evaluate differences in bubble grades. Effects were considered significant for $p < 0.05$. Results are shown as mean ± SEM.

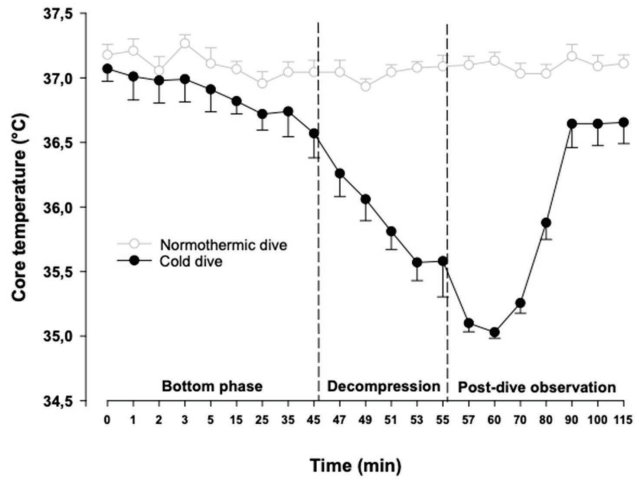

FIGURE 1 | Body core temperature. The cold dive group was normothermic during the bottom phase, cooled to 35°C during the decompression and rewarmed to 37°C after the dive. Temperatures are mean ± SEM. $N = 9$ in both groups. Data for the normothermic control dive group are adapted from Gaustad et al. (2020).

RESULTS

Hemodynamics

During the bottom phase of the dive, LV end-systolic volume and pressure increased significantly after 2 min, peaked after 5 min (+21 and +40%, respectively), returned to pre-dive levels during decompression, and remained unchanged during the post-dive observation period (**Figures 2A,B**). Simultaneously, a significant decrease in CO and SV (−26 and −232%, respectively) took place, returned to control during decompression, but unlike all other cardiac variables a significant reduction of both CO and SV re-emerged during the final part of the 60 min post-dive observation period after the animals had been rewarmed to normothermia (**Figures 2C,D**). Whereas LV end-diastolic volume was significantly elevated during the dive for the short period when LV-systolic pressure peaked, LV end-diastolic volume remained unchanged (**Figures 3A,B**). The changes in LV – functional variables took place in parallel with a significant increase in MAP and TPR, which returned to control during decompression (**Figures 3C,D**). LVdP/dt_{max}, which was continuously monitored (**Figure 4A**), showed increase

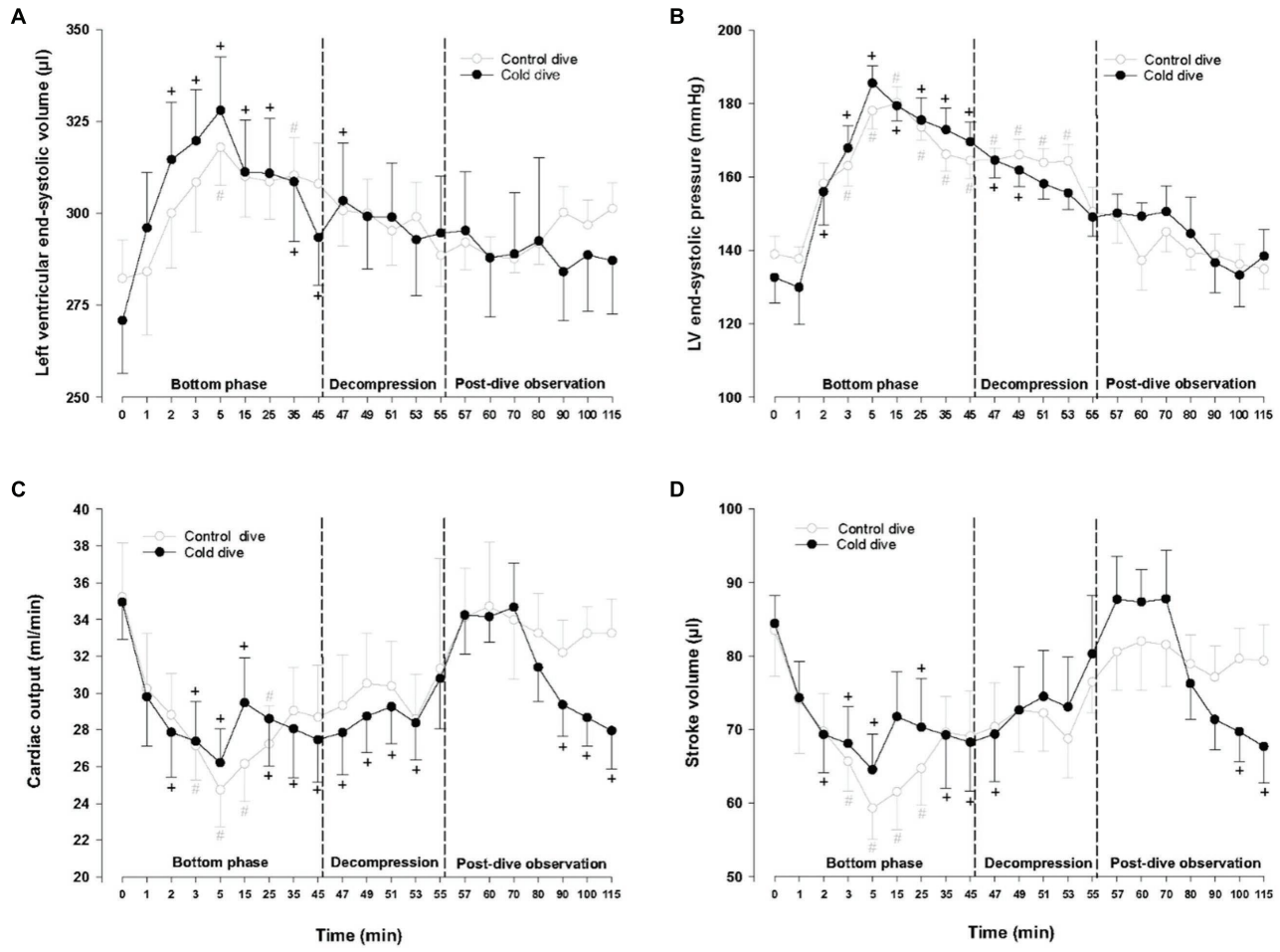

FIGURE 2 | Hemodynamic variables. **(A)** Left ventricular end-systolic volume (LVESV), **(B)** left ventricular end-systolic pressure (LVESP), **(C)** cardiac output (CO), and **(D)** stroke volume (SV). Data are mean ± SEM. $N = 9$ in both groups. $^{*}p < 0.05$ compared to baseline in the cold dive group. $^{\#}p < 0.05$ compared to baseline in the control dive group. Data for the control dive group are adapted from Gaustad et al. (2020).

in LV-contractility during the last period of decompression and the early part of the post-dive observation; whereas PRSW, which was measured before the dive and at the end of the experiment, showed no change in contractility (**Figure 4B**). HR and SW were unaltered relative to control throughout the experiment (**Figures 4C,D**).

Venous Gas Bubbles

There were no differences in venous bubble grades after decompression when the cold diving rats in this study were compared to normothermic diving rats from Gaustad et al. (2020) (**Table 1**).

DISCUSSION

In this study, we used P-V catheterized and temperature-controlled rats to investigate hemodynamic function and DCS risk in response to a 2°C core temperature reduction during decompression from a simulated dive followed by rewarming at the surface. To control for specific effects of cooling, the hemodynamic data were controlled against our previously reported data on normothermic animals (Gaustad et al., 2020). Like in the normothermic controls, the rats in the present study experienced a physiologic reduction in CO and SV during the dive, caused by an abrupt increase in LV afterload induced by the hyperbaric environment. Ultrasound insonation with a 10 MHz probe revealed no changes in bubble grades to indicate increased DCS risk. However, after the animals in the current study were rewarmed at the surface, they experienced a second fall in CO and SV that was not present in the controls.

Why did CO and SV fall after the animals were rewarmed? The post-dive reduction in SV cannot have been caused by reduced LV mechanical function. On the contrary, the absence of change in the indexes of cardiac contractility, dP/dt_{max} and PRSW, makes it unlikely that the reduction in SV and CO were caused by myocardial dysfunction. Neither is it likely that the outcome was triggered by the changes in core temperature: a significant reduction in CO after rewarming

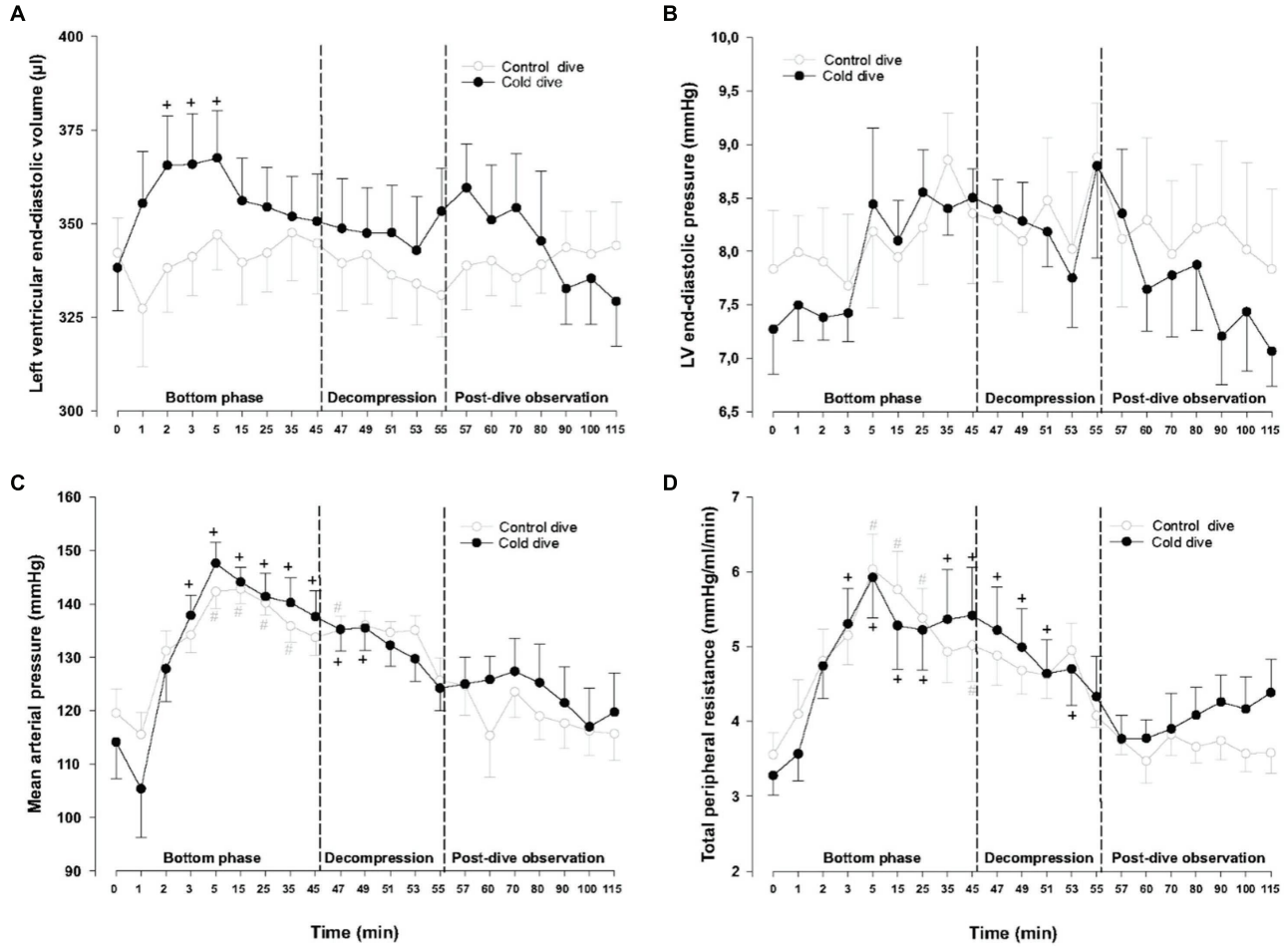

FIGURE 3 | Hemodynamic variables (cont.). **(A)** Left ventricular end-diastolic volume (LVEDV), **(B)** left ventricular end-diastolic pressure (LVEDP), **(C)** mean arterial pressure (MAP), and **(D)** total peripheral resistance (TPR). Data are mean ± SEM. $N = 9$ in both groups. $^{+}p < 0.05$ compared to baseline in the cold dive group. $^{\#}p < 0.05$ compared to baseline in the control dive group. Data for the control dive group are adapted from Gaustad et al. (2020).

has been reported in animals after rewarming from profound hypothermia to 15°C (Kondratiev et al., 2006), but the modest 2°C temperature reduction in our study is above the threshold at which changes in hemodynamic function have been reported (Reuler, 1978; Danzl and Pozos, 1994).

One possible explanation is that the post-dive fall in CO and SV is the consequence of an abrupt increase in pulmonary resistance and subsequent reduced LV volume load. This is supported by a concurrent, albeit non-significant, trend toward the reduction of both LV end-diastolic pressure and volume (**Figures 3B, 4B**). Gas emboli can cause increased pulmonary resistance (Mélot and Naeije, 2011). Pulmonary capillaries have diameters <20–25 µm, with sizes down to 3 µm in rats (Townsley, 2012), and the ultrasonic insonation method we used detects bubbles with diameters >35 µm. Capillaries could thus be blocked by emboli that are smaller than the detection threshold in our experiment. A more sensitive contrast ultrasound method that detect bubbles <10 µm in diameter (Le et al., 2021) is needed to further elucidate this point. It is also possible that "frame based" bubble counting would uncover differences in bubble loads that was not picked up by our scoring system (Germonpré et al., 2014).

Additionally, a tendency towards an increase in TPR took place after decompression, indicating the presence of an autonomic compensatory response to the abrupt fall in CO. One may speculate whether there was a reduction of blood volume due to vascular escape, pooling of blood in capillaries, or hypercapnia-induced vascular smooth muscle relaxation during compression and hypothermia (Brickner et al., 1956; Suzuki and Penn, 1965; Tveita et al., 1996). These are changes which cannot be immediately reversed during rewarming (Kondratiev et al., 2006).

There was no indication of cold-induced vasoconstriction during the bottom phase and decompression in our animals, since MAP and TPR were similar in cold rats and controls. It thus appears that the perfusion was unaltered, which is in contrast to a previous report in which wake mildly hypothermic rats (33°C) had reduced nitrogen elimination and washout rate constant (Mack and Lin, 1986). However, the animals in our study were anesthetized, and the effects of anesthesia on

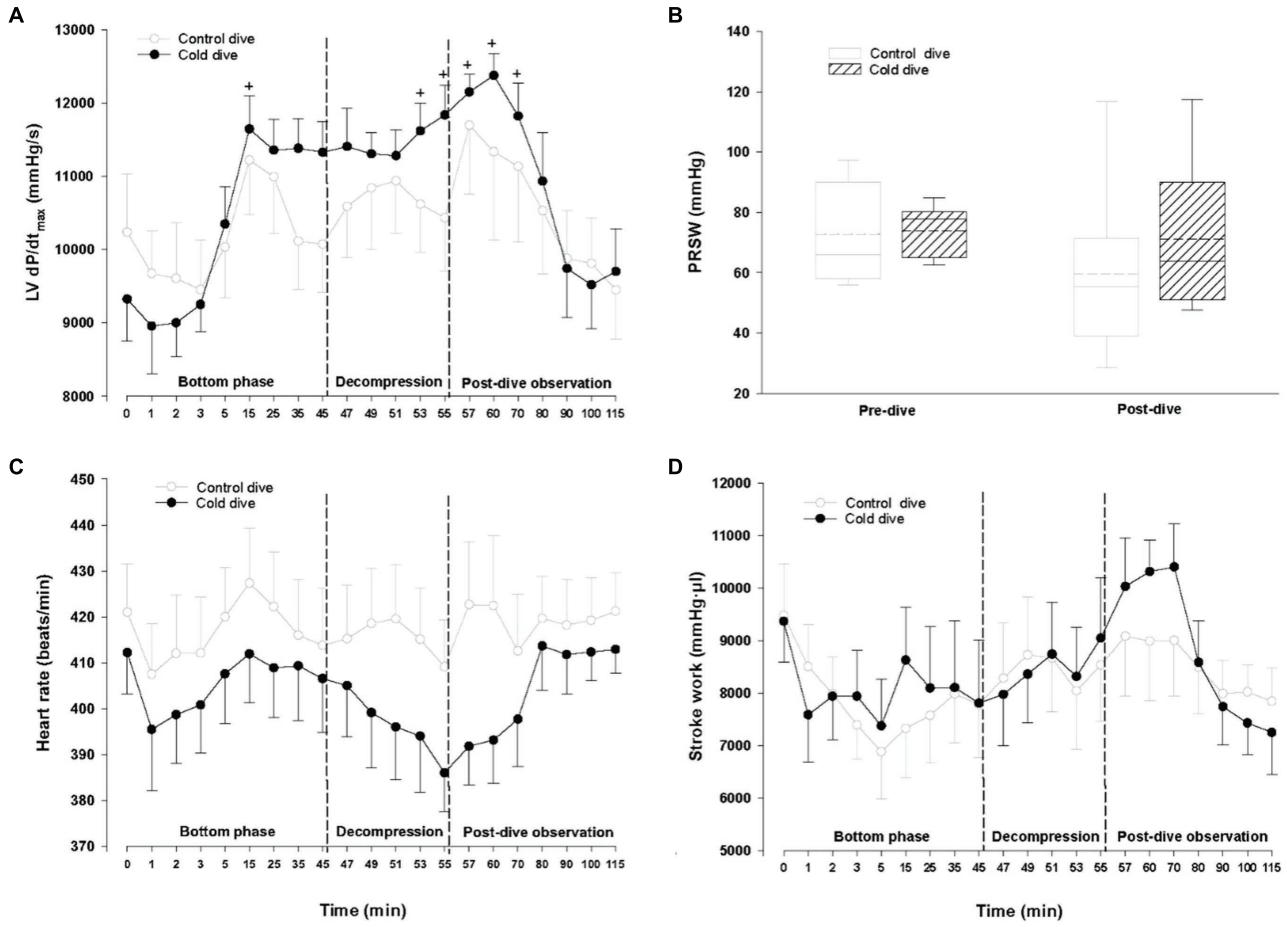

FIGURE 4 | Hemodynamic variables (cont.). **(A)** Maximal slope of systolic pressure increment (LV dP/dt_{max}), **(B)** preload recruitable stroke work (PRSW), **(C)** heart rate (HR), and **(D)** Stroke work (SW). Data presented as mean ± SEM for **(A,C)**, and **(D)**. Data are presented as vertical boxes with median (solid line), mean (dashed line) and interquartile range with 10th and 90th percentile error bars for **(B)**. $N = 9$ in both groups. $^{+}p < 0.05$ compared to baseline in the cold dive group. $^{\#}p < 0.05$. Data for the control dive group are adapted from Gaustad et al. (2020).

TABLE 1 | Minimal core temperature during decompression vs. maximal bubble grades observed post-dive in rats exposed to simulated diving.

Group	Minimal core temperature (°C)	Bubble grades
*Normothermic	37.2 ± 0.3	0 (0–2)
Cold decompression	35.1 ± 0.2	0 (0–3)

Minimal core temperatures are mean ± SEM, bubble grades are median and range. N = 9 in both groups.
**Data for the normothermic group are from Gaustad et al. (2020).*

vascular tone may explain this apparent discrepancy (Akata and Warltier, 2007).

When the results from this study are interpreted, it should be noted that laboratory animals are not perfect models for human responses (Shanks et al., 2009). While the cardiovascular system of humans and rats are largely similar structurally and functionally (Buetow and Laflamme, 2018), the rodents' relatively larger body surface area and higher metabolic rate cause them to respond differently from humans to changes in ambient temperature (Maloney et al., 2014). Also, dry diving affects cardiovascular function to a lesser degree than water immersion does (Gaustad et al., 2010), and diving-naïve rats, as the ones in the present study, display different vascular responses than rats that have been exposed to diving regularly (Berenji Ardestani et al., 2019, 2020). Finally, epidemiological data from human divers as well as pre-clinical models show that DCS development is dictated by more factors than bubbles (Cialoni et al., 2017; Lautridou et al., 2017). Additionally, as CO and SV were still falling at the time our experiment was terminated, we do not know how large the final decrease might be had the experiment been extended. Considering these limitations, additional studies that include water immersion, and a longer post-dive observation period, as well as a more severe temperature reduction ("exceptionally cold dives") are required to identify causal links between cold decompression and DCS.

In conclusion, while a 2°C core temperature reduction during decompression caused CO and SV to fall after dry air diving, no changes were observed in venous bubble grades. However, while we cannot conclude from our data that the DCS risk increased, the post-dive fall in CO and SV could be explained

by a fall in LV pre-load secondary to embolic occlusion of pulmonary capillaries. More sensitive bubble detection methods are needed to determine whether there is increased production of smaller gas bubbles (< 35 µm) when the body is rewarmed after cold decompression.

DATA AVAILABILITY STATEMENT

The raw data supporting the conclusions of this article will be made available by the authors, without undue reservation.

ETHICS STATEMENT

The animal study was reviewed and approved by the Norwegian Council for Animal Research.

AUTHOR CONTRIBUTIONS

SG and TT designed the study. SG and TK did the experimental work. IE contributed to the manuscript. All authors contributed to the article and approved the submitted version.

FUNDING

The study was supported by the Norwegian Petroleum Directorate, Statoil (now Equinor), ExxonMobil, and Gassco under the Competence Program Diving (NUI No. 4600002328) and the Research Council of Norway's Large-scale Programme for Petroleum Research (Petromaks2 No. 280425). The funders were not involved in the study design, collection, analysis, interpretation of data, writing, or the decision to submit this article for publication.

REFERENCES

Akata, T., and Warltier, D. C. (2007). General anesthetics and vascular smooth muscle: direct actions of general anesthetics on cellular mechanisms regulating vascular tone. *Anesthesiology* 106, 365–391. doi: 10.1097/00000542-200702000-00026

Barcroft, H., and Edholm, O. G. (1943). The effect of temperature on blood flow and deep temperature in the human forearm. *J. Physiol.* 102, 5–20. doi: 10.1113/jphysiol.1943.sp004009

Berenji Ardestani, S., Matchkov, V. V., Eftedal, I., and Pedersen, M. (2019). A single simulated heliox dive modifies endothelial function in the vascular wall of ApoE knockout male rats more than females. *Front. Physiol.* 10:1342. doi: 10.3389/fphys.2019.01342

Berenji Ardestani, S., Matchkov, V. V., Hansen, K., Jespersen, N. R., Pedersen, M., and Eftedal, I. (2020). Extensive simulated diving aggravates endothelial dysfunction in male pro-atherosclerotic ApoE knockout rats. *Front. Physiol.* 11:611208. doi: 10.3389/fphys.2020.611208

Brickner, E. W., Dowds, E. G., Willitts, B., and Selkurt, E. E. (1956). Mesenteric blood flow as influenced by progressive hypercapnia. *Am. J. Phys.* 184, 275–281. doi: 10.1152/ajplegacy.1956.184.2.275

Buetow, B. S., and Laflamme, M. A. (2018). "Chapter 10 – cardiovascular," in *Comparative Anatomy and Histology*. eds. P. M. Treuting, S. M. Dintzis and K. S. Montine. *2nd edn*. (San Diego: Academic Press), 163–189.

Caldwell, J. N., Matsuda-Nakamura, M., and Taylor, N. A. (2016). Interactions of mean body and local skin temperatures in the modulation of human forearm and calf blood flows: a three-dimensional description. *Eur. J. Appl. Physiol.* 116, 343–352. doi: 10.1007/s00421-015-3288-4

Cialoni, D., Pieri, M., Balestra, C., and Marroni, A. (2017). Dive risk factors, gas bubble formation, and decompression illness in recreational SCUBA diving: analysis of DAN Europe DSL data base. *Front. Psychol.* 8:1587. doi: 10.3389/fpsyg.2017.01587

Commander, N.S.S.C. (1999). "U.S. Navy Diving Manual, Revison 4". (Arlington, VA: NAVSEA Publication SS521-AG-PRO-010).

Danzl, D. F., and Pozos, R. S. (1994). Accidental hypothermia. *N. Engl. J. Med.* 331, 1756–1760.

Dujic, Z., Palada, I., Valic, Z., Duplancic, D., Obad, A., Wisloff, U., et al. (2006). Exogenous nitric oxide and bubble formation in divers. *Med. Sci. Sports Exerc.* 38, 1432–1435. doi: 10.1249/01.mss.0000228936.78916.23

Dujic, Z., Valic, Z., and Brubakk, A. O. (2008). Beneficial role of exercise on scuba diving. *Exerc. Sport Sci. Rev.* 36, 38–42. doi: 10.1097/jes.0b013e31815ddb02

Dunford, R., and Hayward, J. (1981). Venous gas bubble production following cold stress during a no-decompression dive. *Undersea Biomed. Res.* 8, 41–49.

Eftedal, O., and Brubakk, A. O. (1997). Agreement between trained and untrained observers in grading intravascular bubble signals in ultrasonic images. *Undersea Hyperb. Med.* 24, 293–299.

Fahlman, A., and Kayar, S. R. (2006). Nitrogen load in rats exposed to 8 ATA from 10-35 degrees C does not influence decompression sickness risk. *Aviat. Space Environ. Med.* 77, 795–800.

Gaustad, S. E., Brubakk, A. O., Høydal, M., Catalucci, D., Condorelli, G., Dujic, Z., et al. (2010). Immersion before dry simulated dive reduces cardiomyocyte function and increases mortality after decompression. *J. Appl. Physiol.* 1985, 109, 752–757. doi: 10.1152/japplphysiol.01257.2009

Gaustad, S. E., Kondratiev, T. V., Eftedal, I., and Tveita, T. (2020). Continuous hemodynamic monitoring in an intact rat model of simulated diving. *Front. Physiol.* 10:1597. doi: 10.3389/fphys.2019.01597

Georgakopoulos, D., and Kass, D. A. (2000). Estimation of parallel conductance by dual-frequency conductance catheter in mice. *Am. J. Physiol. Heart Circ. Physiol.* 279, H443–H450. doi: 10.1152/ajpheart.2000.279.1.H443

Germonpré, P., Papadopoulou, V., Hemelryck, W., Obeid, G., Lafère, P., Eckersley, R. J., et al. (2014). The use of portable 2D echocardiography and 'frame-based' bubble counting as a tool to evaluate diving decompression stress. *Diving Hyperb. Med.* 44, 5–13.

Gerth, W. A., Ruterbusch, V. L., and Long, E. T. (2007). The influence of thermal exposure on diver susceptibility to decompression sickness. Navy Experimental Diving UNIT, NEDU TR, Panama City, FL, 6–7.

Han, Y. S., Tveita, T., Kondratiev, T. V., Prakash, Y. S., and Sieck, G. C. (2008). Changes in cardiovascular beta-adrenoceptor responses during hypothermia. *Cryobiology* 57, 246–250. doi: 10.1016/j.cryobiol.2008.09.006

Kondratiev, T. V., Flemming, K., Myhre, E. S., Sovershaev, M. A., and Tveita, T. (2006). Is oxygen supply a limiting factor for survival during rewarming from profound hypothermia? *Am. J. Physiol. Heart Circ. Physiol.* 291, H441–H450. doi: 10.1152/ajpheart.01229.2005

Lango, T., Morland, T., and Brubakk, A. O. (1996). Diffusion coefficients and solubility coefficients for gases in biological fluids and tissues: a review. *Undersea Hyperb. Med.* 23, 247–272.

Lautridou, J., Buzzacott, P., Belhomme, M., Dugrenot, E., Lafère, P., Balestra, C., et al. (2017). Evidence of heritable determinants of decompression sickness in rats. *Med. Sci. Sports Exerc.* 49, 2433–2438. doi: 10.1249/mss.0000000000001385

Le, D. Q., Dayton, P. A., Tillmans, F., Freiberger, J. J., Moon, R. E., Denoble, P., et al. (2021). Ultrasound in decompression research: fundamentals, considerations, and future technologies. *Undersea Hyperb. Med.* 48, 59–72.

Leffler, C. T. (2001). Effect of ambient temperature on the risk of decompression sickness in surface decompression divers. *Aviat. Space Environ. Med.* 72, 477–483.

Mack, G. W., and Lin, Y. C. (1986). Hypothermia impairs but hyperthermia does not promote inert gas elimination in the rat. *Undersea Biomed. Res.* 13, 133–145.

Maloney, S. K., Fuller, A., Mitchell, D., Gordon, C., and Overton, J. M. (2014). Translating animal model research: does it matter that our rodents are cold? *Physiology* 29, 413–420. doi: 10.1152/physiol.00029.2014

Mekjavić, I. B., and Kakitsuba, N. (1989). Effect of peripheral temperature on the formation of venous gas bubbles. *Undersea Biomed. Res.* 16, 391–401.

Mélot, C., and Naeije, R. (2011). "Pulmonary vascular diseases," in *Comprehensive Physiology*. ed. R. Terjung (United States: John Wiley & Sons), 593–619.

Ohta, Y., Song, S. H., Groom, A. C., and Farhi, L. E. (1978). Is inert gas washout from the tissues limited by diffusion? *J. Appl. Physiol.* 45, 903–907. doi: 10.1152/jappl.1978.45.6.903

Reuler, J. B. (1978). Hypothermia: pathophysiology, clinical settings, and management. *Ann. Intern. Med.* 89, 519–527. doi: 10.7326/0003-4819-89-4-519

Shanks, N., Greek, R., and Greek, J. (2009). Are animal models predictive for humans? *Philos. Ethics Humanit. Med.* 4:2. doi: 10.1186/1747-5341-4-2

Suzuki, M., and Penn, I. (1965). A reappraisal of the microcirculation during general hypothermia. *Surgery* 58, 1049–1060.

Toner, C., and Ball, R. (2004). *The Effect of Temperature on Decompression and Decompression Sickness Risk: A Critical Review.* Bethesda: Naval Medical Research Center.

Townsley, M. I. (2012). "Structure and composition of pulmonary arteries, capillaries, and veins," in *Comprehensive Physiology*. ed. R. Terjung (United States: John Wiley & Sons), 675–709.

Tveita, T., Ytrehus, K., Skandfer, M., Oian, P., Helset, E., Myhre, E. S., et al. (1996). Changes in blood flow distribution and capillary function after deep hypothermia in rat. *Can. J. Physiol. Pharmacol.* 74, 376–381.

Wisloff, U., and Brubakk, A. O. (2001). Aerobic endurance training reduces bubble formation and increases survival in rats exposed to hyperbaric pressure. *J. Physiol.* 537, 607–611.

Conflict of Interest: SG was employed by the company Møreforsking AS.

The remaining authors declare that the research was conducted in the absence of any commercial or financial relationships that could be construed as a potential conflict of interest.

Publisher's Note: All claims expressed in this article are solely those of the authors and do not necessarily represent those of their affiliated organizations, or those of the publisher, the editors and the reviewers. Any product that may be evaluated in this article, or claim that may be made by its manufacturer, is not guaranteed or endorsed by the publisher.

frontiers in Physiology

BRIEF RESEARCH REPORT
published: 03 December 2021
doi: 10.3389/fphys.2021.768517

Cognitive Performance During Night Work in the Cold

Hilde Færevik[1], Jakob Hønborg Hansen[2], Øystein Wiggen[1] and Mariann Sandsund[1]*

[1] SINTEF Digital, Department of Health Research, Trondheim, Norway, [2] Wood Group, Sandefjord, Norway

Objective: The objective of this study was to investigate how night work at low ambient temperatures affects cognitive performance (short-term memory and reaction time), skin- and core temperature, thermal comfort, sleepiness, and cortisol. We hypothesized that cognitive performance is reduced at night compared with daytime and worsened when exposed to low ambient temperatures.

Method: Eleven male subjects were recruited to perform three tests in a climatic chamber at night and daytime: Night –2°C, Night 23°C and Day 23°C. Each test lasted 6 h. Cognitive performance (short-term memory and reaction time), skin- and core temperature, thermal sensation and comfort, cortisol levels and sleepiness were measured during the tests.

Results: A lower mean skin temperature and corresponding lower thermal sensation were observed at Night –2°C compared to Day 23°C and Night 23°C. Night work caused increased sleepiness and lower cortisol levels, but was not affected by changes in ambient temperatures, thermal comfort, or skin temperatures. There was no effect of either day/night work nor ambient temperature on the short-term memory or reaction time test.

Conclusion: Lower skin- and core temperature were observed at night when exposed to low ambient temperature (–2°C), but there was no effect on short-term memory or reaction time. Increased sleepiness and lower cortisol levels were observed at night compared to daytime and was not influenced by low ambient temperature at night. The result from this study suggests that cognitive performance (short-term memory and reaction time) is not adversely affected by night work when exposed to low ambient temperatures if adequate protective clothing is worn.

Keywords: day/night work, cold environment, cognitive performance, temperature regulation, sleepiness, cortisol, protective clothing

OPEN ACCESS

Edited by:
Torkjel Tveita,
Arctic University of Norway, Norway

Reviewed by:
Jaromir Myslivecek,
Charles University, Czechia
Phyllis Kravet Stein,
Washington University in St. Louis, United States

****Correspondence:***
Hilde Færevik
hilde.ferevik@sintef.no

Specialty section:
This article was submitted to Clinical and Translational Physiology, a section of the journal Frontiers in Physiology

Received: *31 August 2021*
Accepted: *12 November 2021*
Published: *03 December 2021*

Citation:
Færevik H, Hansen JH, Wiggen Ø and Sandsund M (2021) Cognitive Performance During Night Work in the Cold. Front. Physiol. 12:768517. doi: 10.3389/fphys.2021.768517

INTRODUCTION

Cold exposure is experienced in many occupational and leisure settings and humans exhibit a range of physiological responses when exposed to cold environments. This includes changes in skin- and core- body temperature inducing e.g., cutaneous vasoconstriction to decrease heat loss and shivering thermogenesis which increase metabolic heat production to maintain thermal balance (Castellani and Young, 2016). Exposure to low ambient temperatures may also be associated

with declines in cognitive functioning. Both increase and decrease in accuracy and efficiency on cognitive tests assessing vigilance, reasoning and memory have been found in laboratory settings (Palinkas, 2001; Pilcher et al., 2002; Hancock et al., 2007). The few observational studies that have examined the association between and cognition report a "U" shaped relationship of temperature and performance (Ramsey, 1995; Dai et al., 2016). The decline in cognitive functioning in the cold have been explained by the discomfort caused by the cold exposure, resulting in difficulties in concentration. This "distraction theory" have been proposed by Muller et al. (2012), and later supported by studies of Taylor et al. (2015). Other studies have suggested that acute cold exposure may reduce levels of catecholamines or thyroid hormones, which in turn is associated with worse cognitive functioning (Shurtleff et al., 1994; Leppäluoto et al., 2005). Moderate cold exposure affects cognition function negatively through the mechanisms of distraction and both positively and negatively through the mechanism of arousal (increased vigilance in the cold) (Mäkinen, 2007). The study by Mäkinen (2007) proposes that especially simple cognitive tasks are adversely affected by cold, while more complex tasks may even improve in mild or moderate cold.

Occupations that require outdoor work in cold environments (Naesgaard et al., 2017) in combination with night- work face a combination of several interacting occupational health risk factors. Both night- and shift work are known to affect cognitive functioning and sleep negatively (Friborg et al., 2014). Shift workers commonly report poor sleep and decreased sleep quality (Harris, 2011). This increases the risk of human error (Akerstedt et al., 2007; Akerstedt, 2007) and can be a concurrent factor in explaining why many critical accidents are more prevalent at night (Mitler et al., 1988). The natural circadian rhythm in core body temperature results from the heat gain and heat loss mechanisms caused by the suprachiasmatic nuclei (SCN) in the hypothalamus, and regulates the natural lowering of core temperature at night (Panda, 2016). Working at night, when the body naturally regulates metabolism and temperature to a lower level, may be a contributing factor to the decline in cognitive functioning and especially vigilance at night.

To our knowledge no studies have previously investigated the combination of work at low ambient temperatures during night and the possible negative impact this may have on cognitive performance.

The objective of this study was to investigate night work at low ambient temperatures, and to what extent this will affect cognitive performance (short-term memory and reaction time), skin- and core temperature, thermal comfort, sleepiness, and cortisol. We hypothesized that cognitive performance is reduced at night compared with daytime and worsened when exposed to low ambient temperatures at night.

METHODS

Test Subjects

Eleven male volunteer subjects were recruited into the study (age, 23 ± 2 years; mass, 81.4 ± 5.5 kg; height, 1.85 ± 0.04 cm; body mass index, 23.5 ± 2.1 kg · m^{-2}; and body fat, 13.7 ± 3.2%). The subjects were non-smokers, had no sleep disturbances and had not flown between time zones in the week that preceded the trial. The subjects had a normal night's sleep before the test and did not have any coffee, tea, cola soft drink or chocolate in the 2 h that preceded the test, or alcohol or tobacco 24 h before the test. All participants were informed about the aim of the study, the test protocol, and their rights to terminate their participation at any time in accordance with the 2013 Declaration of Helsinki before they provided written consent. All subjects underwent a doctor's medical check-up in advance of the study. The exclusion criteria were previous cold-related injuries or Raynaud's syndrome. The study was approved by the Committee for Medical and Health Research Ethics, Central Norway.

Experimental Protocol

To familiarize themselves with the cognitive test battery and prevent a learning effect, the participants performed five pre-tests before participating in the tests. The participants then performed three main tests in a climatic chamber in the Work Physiology Laboratory at the Department of Health Research at SINTEF, Trondheim, Norway, in January and February 2017. Each test had a duration of 6 h and were performed during the night at −2 and 23°C ambient temperature and a control series at 23°C at daytime. The three series was fully randomized, and each participant accomplished the different tests and was their own control.

Upon arrival at the laboratory, the subjects were equipped with thermistors, a rectal probe and a heart-rate recorder. They were dressed in underwear and rested in a room with temperature of 22–23°C outside the climatic chamber. Two test subjects participated in each test. The subjects were allowed to drink water (2 cups *ad libitum*) and eat a banana or apple at 03:00 am (night test) or 11:00 am (day test). They were dressed in woolen underwear and protective outdoor work clothing and moved into the climatic chamber, where they performed identical repeated activities as follows; Time at day/night trials; 08:00/00:00 and every second hour; cognitive test, 08:00/00:00 and every hour; subjective score, 08:30/00:30 and every hour; treadmill (6 min, 4 km/h); 12:00/04:00 cortisol test.

Measurements

Upon arrival at the laboratory, the height and weight (IDI; Mettler-Toledo, Albstadt, Germany) of the participants were recorded and the fat percentage was measured using a skinfold pinch (Harpenden Skinfold Caliper; Baty, United Kingdom). The amount of subcutaneous fat was measured on m. Biceps brachii, m. Triceps brachii, m. Subscapularis and the supra-iliac skinfold and calculated based on the formula given by Durnin and Womersley (1974).

To measure the body's heat content and detect changes in body heat, continuous measurements of core and skin temperatures were performed using a rectal probe and thermistors (YSI 400; Yellow Springs Instruments, Yellow Springs, OH, United States), respectively, with an accuracy of ±0.15°C. The rectal probe was inserted to a depth of 10 cm from the spinal cord. Average

skin temperature was calculated from the formula given by Ramanathan (1964), based on measurements from the chest, upper arm, thigh and leg.

The subjects were asked to evaluate their own thermal comfort and temperature sensation during the experiment. Thermal sensation was evaluated on a scale from –5 to 5 (extremely cold to extremely hot) and thermal comfort was evaluated on a scale of 1–4 (comfortable to very uncomfortable) (Nielsen et al., 1989).

Sleepiness was evaluated using the 9-step Karolinska Sleepiness Scale (KSS), which is based on a scoring from 1 = very awake to 9 = sleepy (fighting against sleep) (Akerstedt and Gillberg, 1990).

To test cognitive function (reaction time and short-term memory), the iPad-based system CANTAB Connect from Cambridge Cognition (Cambridge, United Kingdom) was used. The paired associates learning (PAL) and reaction time (RT) cognitive tests were performed. In the PAL test, boxes appear on the screen and are "opened" in a random order. One or more boxes contain a pattern. The patterns are then displayed at the center of the screen one at a time and the participant must select the box in which the pattern was originally placed. If the participant makes a mistake, the boxes are reordered, to remind the participant of the placement of the patterns. In the RT test, the subject holds a response button at the bottom of the screen. A series of five circular figures is presented above, and a yellow dot appears in one of the circles. The respondent must respond as quickly as possible and release the response button at the bottom of the screen and select the circle in which the dot appears. The test measures the average time required (in ms) for a subject to release the response button and select the yellow stimulus presented on the screen.

The cortisol test was administered at 4:00 am and at 12:00 pm on the respective night and day trials. All saliva analyses required at least 1 ml of saliva, which was collected in a test tube. Saliva production was not stimulated; rather, it formed naturally. No food was consumed during the 30 min that preceded sampling. Samples were stored immediately at –20°C. The number and time of samplings of the test subjects were recorded. The samples were analyzed by the Department of Medical Biochemistry, Laboratory Centre at St. Olav's Hospital, Trondheim, Norway.

During the experiments, the following clothing was worn. Low ambient temperature (–2°C): woolen sweater, long underpants, wool jacket and pants, parka and trousers, headgear, balaclava and hood, winter shoes, gloves and wool socks. High ambient temperature (23°C): underwear, woolen sweater, long underpants, and wool socks.

Statistical Analysis

Statistical analyses were performed using SPSS for Windows (v. 18.0; SPSS Inc., Chicago, IL, United States) and Microsoft Excel 2010 (Microsoft Corp., Redmond, WA, United States). Data were checked for normality using Kolmogorov–Smirnoff tests. The difference in cognitive performance response under the different ambient conditions was assessed by two-way analyses of variance (ANOVA) for repeated measures as previously done by Faerevik and Reinertsen (2003) A within group study design was used and all subjects were their own control. All cognitive performance data were tested for effects of time, ambient condition, and the interaction between these two. Time-dependent changes in rectal temperature and mean skin temperatures were also evaluated by two-way analyses of variance (ANOVA) for repeated measures. When ANOVA revealed a significant main effect, a contrast test was used as a *post hoc* test to locate the significant differences between the temperatures. Temperature data were analyzed every 10 min and cognitive measurements had four data points in the analysis. Subjective measurements were analyzed using Friedman's non-parametric test for repeated measurements. Subjective measurements had seven data points in the analysis. Data are presented as the average and standard deviation. Significance was set at $P < 0.05$.

RESULTS

There was a significantly greater reduction in core temperature in the night trial performed at –2°C (from 37.4 to 36.2°C) compared with that performed at 23°C at night (from 37.5 to 36.5°C) (Anova GLM analysis within subjects' effects: Temp × tid ($p = 0.026$, $df = 6{,}224$, $F = 2{,}585$) (**Figure 1**). In the day trial in the warm condition (23°C), a stable core temperature was maintained throughout the test, with a change from 37.0°C at the start to 36.9°C toward the end of the test. Both night trials (–2 and 23°C) had a significant greater reduction in core temperature compared to the day trial in 23°C [Anova GLM analysis within subjects effects: Night –2°C vs. Day 23°C: Temp × time ($p = 0.001$, $df = 4{,}705$, $F = 29{,}728$), Night23°C vs. Day 23°C: Temp × time ($p = 0.001$, $df = 4{,}631$, $F = 20{,}389$)].

The average skin temperature was significantly lower after exposure to –2°C compared with 23°C during both the night and day tests (**Figure 1**). The skin temperature was 33.4°C at the start of the night test and 32.5°C at the start of the day test, regardless of ambient temperature. The skin temperature was relatively stable throughout both tests at 23°C, but fell to 31.8°C in the night test at –2°C. During all trials, small variations (less than 0.5°C) in the average skin temperature were observed which is due to the variation between rest and easy work. The repeated work periods included in the test did not significantly affect core temperature. Thermal sensation of the body, feet, hands, and head showed that the subjects were significantly colder and more uncomfortable when exposed to –2°C compared with 23°C, regardless of whether it was night or day. There were no significant differences in thermal sensation or comfort during the night or day exposure to 23°C. There were no significant effects of either ambient temperature or day/night on reaction time or short-term memory during the experiments (**Table 1**). Sleepiness increased significantly throughout the night at both –2 and 23°C. During the day trial, there was significant less decrease in sleepiness over time compared with night trials (**Figure 2**). Cortisol levels were significantly lower during both the night trials compared with the daytime trial; however, there was no effect of ambient temperature on cortisol level at night (**Figure 3**).

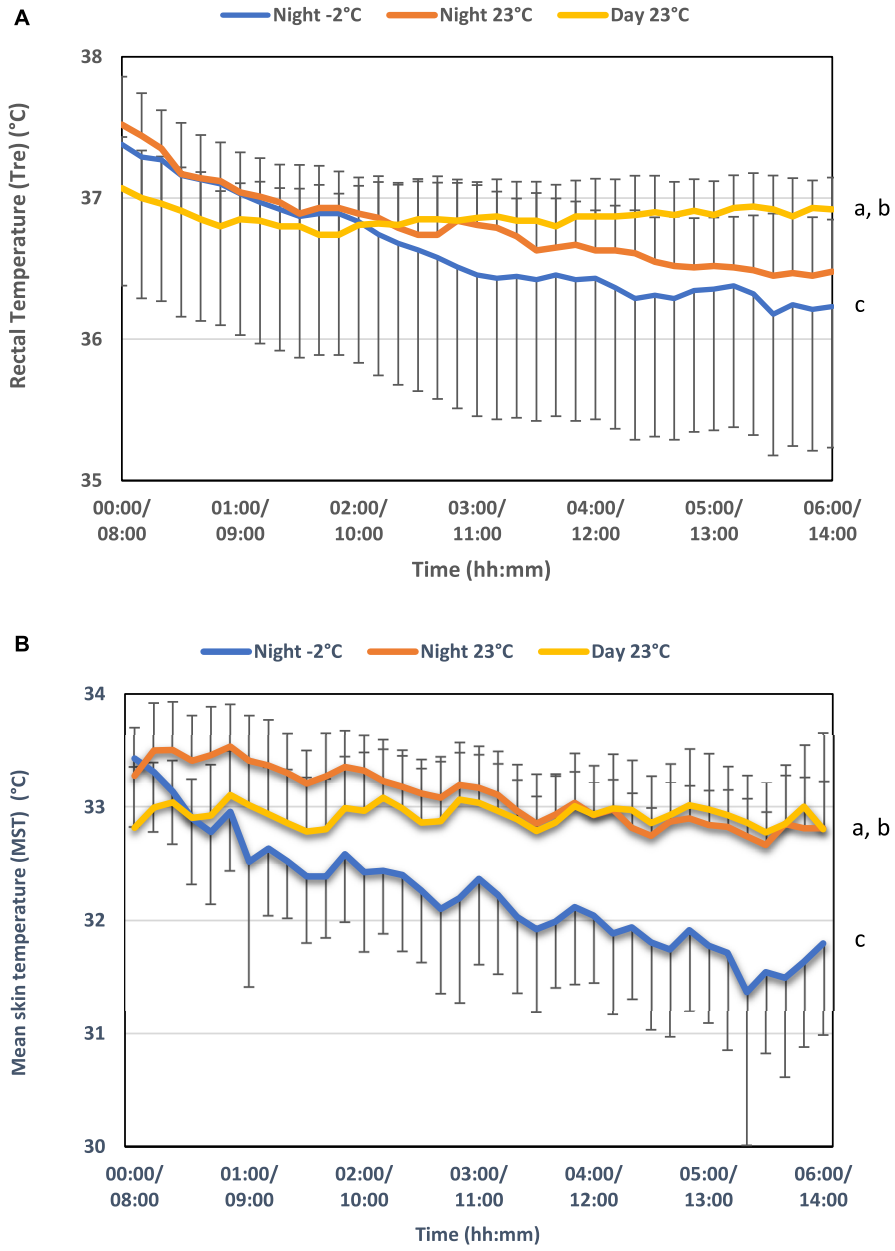

FIGURE 1 | (A) Rectal temperature (T_{re}) and **(B)** mean skin temperature (MST) for all exposures. a. A significant difference in the time dependent development of temperature between Night –2°C and Day 23°C for T_{re} ($p = 0.001$) and MST ($p = 0.001$). b. A significant difference in the time dependent development of temperature between Day 23°C and Night 23°C for T_{re} ($p = 0.001$) and MST ($p = 0.001$). c. A significant difference in the time dependent development of temperature between Night –2°C and Night 23°C for T_{re} ($p = 0.026$) and MST ($p = 0.001$). Data are presented as means ± SD ($n = 11$ for MST, $n = 10$ for T_{re}, missing data for one person).

DISCUSSION

The objective of this study was to investigate the effect of night work at low ambient temperatures, and to what extent this will affect cognitive performance (short-term memory and reaction time), skin- and core temperature, thermal comfort, sleepiness, and cortisol. A control series was performed at day at 23°C.

The results for this study demonstrates a natural lowering of core temperature at night, as reported by Kräuchi (2002). During both night studies performed at –2 and 23°C, the core temperature were higher in the afternoon when arriving to the laboratory and decreased gradually during night, which is a well-known physiological response (Wright et al., 2002). A slight increase in heat production was attributed to the preparation performed before the experiment, followed by a return of the core temperature to normal levels as reported earlier (Wiggen et al., 2011). The change in skin temperature was also dependent on whether it was night or day, which can be explained by the natural

diurnal variation in core temperature. Sleep usually occurs in the descending part of the core temperature curve, when the heat loss from the body is maximal (Kräuchi et al., 2000). This indicates a close relationship between sleeping and heat loss from the body. However, in this study the participants were not allowed to sleep, and this may have influenced the normal regulation of core temperature during night. A lower core- and skin temperature was observed at −2°C at night compared to 23°C (both night and daytime) with corresponding lower thermal sensation and comfort of the body, especially the hands and feet in −2°C.

Several studies have demonstrated impairment in cognitive performance (e.g., reaction time and short-term memory) upon exposure to low ambient temperatures (Stang and Wiener, 1970; Coleshaw et al., 1983; Palinkas, 2001). Physiological parameters, such as skin- and core temperature, are often used as indicators of reduction in cognitive performance. Reaction time is also among the parameters that are most affected during a simulated heat stress in pilots (Faerevik and Reinertsen, 2003). Thermal comfort can have a greater impact on cognitive performance compared to physiological parameters (Pilcher et al., 2002) since the discomfort by freezing will be able to distract the person and in this way reduce the reaction time and precision of the given the task (distraction theory). The results of our study suggest that neither low ambient temperatures nor night work influences short-term memory or reaction time. This is in contrasts with other studies in cold environments and must be considered in relation to the degree of thermal stress and that the subjects were protected by the clothing worn in the test. Muller et al. (2012) showed that several cognitive functions were reduced even at an ambient temperature of 10°C and that the reduced functions remained impaired over a heating period. The major difference between that study and our work was the clothing; Muller et al. (2012) dressed their subjects in shorts only before exposure to an ambient temperature of 10°C. This led to a significantly greater reduction in average skin temperature and thermal comfort compared with our study. Muller et al. (2012) reported an average skin temperature of about 22–23°C and a thermal sensation of cold. They emphasized that the exact physiological mechanisms that explain the reduction in cognitive performance observed during acute cold exposure is unclear but suggested that acute adaptations in the blood vessels in the brain caused by cold exposure could lead to cognitive dysfunction. Vasoconstriction has been detected in several parts of the circulatory system during cold exposure, but the specific relationship between skin cooling and the effect on the brain remains unclear (Muller et al., 2012). Adequate clothing will limit the acute effect of exposure to low ambient temperature, which minimizes the risk of decreased cognitive performance during work. Optimized clothing is one important factor for maintaining cognitive performance in cold environments (Taylor et al., 2015). In our study the subjects were exposed to significant ambient cold stress at night; but they did

TABLE 1 | Cognitive parameters.

	00:00/08:00	02:00/10:00	04:00/12:00	06:00/14:00
(1a) Reaction time in milliseconds				
Night 23°C	141 ± 27	140 ± 22	136 ± 30	139 ± 20
Night −2°C	143 ± 21	150 ± 29	142 ± 24	141 ± 19
Day 23°C	141 ± 21	138 ± 22	137 ± 22	142 ± 24
(1b) Short term memory for every other hour for all exposures.				
Night 23°C	3.6 ± 2.8	3.4 ± 2.1	2.3 ± 2,0	3.8 ± 3.8
Night −2°C	2.9 ± 4.2	3.9 ± 4.2	4.5 ± 4.0	4.1 ± 4.9
Day 23°C	3.9 ± 3.2	2.5 ± 2.3	4.1 ± 4.2	2.5 ± 2.6

Data are presented as means ± SD (n = 11).

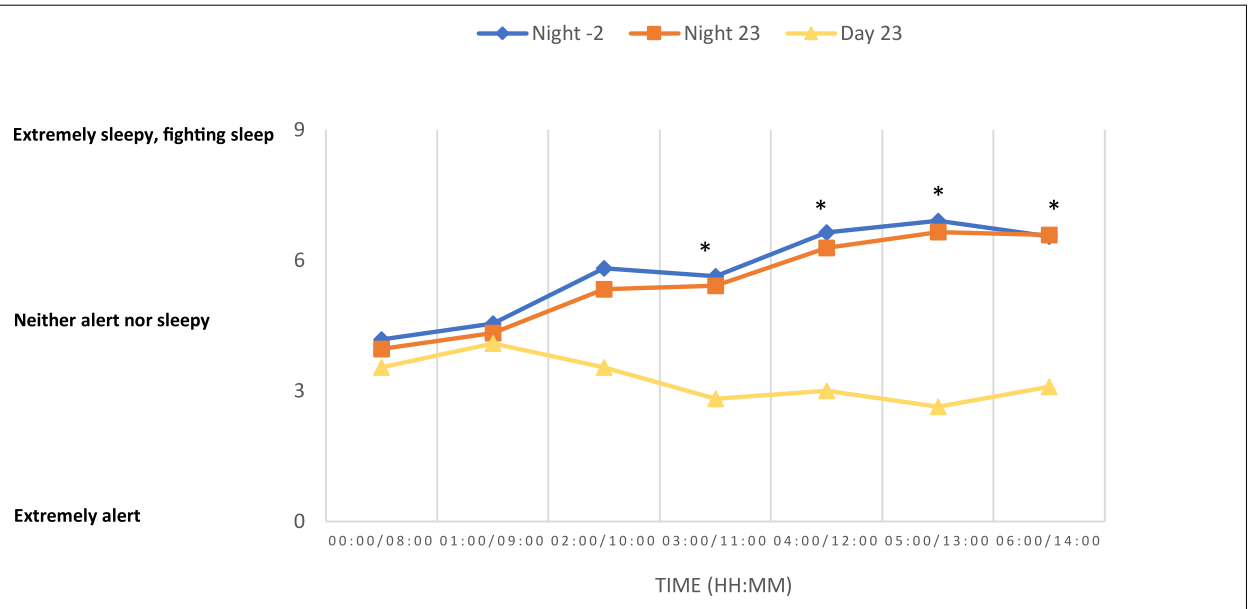

FIGURE 2 | Sleepiness (Karolinska Sleepiness Scale). *Significant increase in sleepiness at night compared to and day at both temperatures (Night −2°C and Night 23°C). Data are presented as means (*n* = 11).

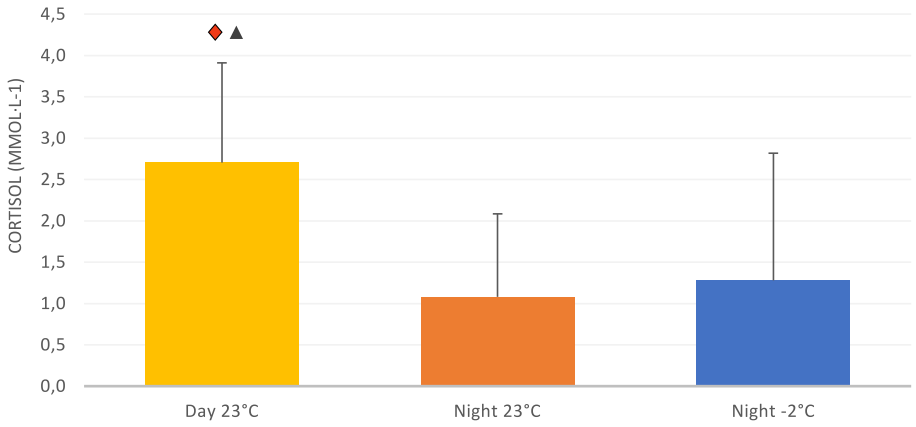

FIGURE 3 | Cortisol in saliva at 04:00 am and at 12:00 pm under all exposures. (♦) A significant difference between Day 23°C and Night 23°C and (▲) significant difference between Day 23°C and Night –2°C. Data are presented as means ± SD (n = 11).

not experience any critically low skin temperatures (below 10°C) and subjective thermal comfort was between neutral and slightly cool throughout the test. The lack of more severe cold stress is partly explained by the protective clothing worn.

Sleepiness is commonly affected by exposure to night shifts and gradually increases beyond the night. In our laboratory study the subjects experienced significant sleepiness at the night trials, but we did not find any effect of sleepiness on cognitive parameters. This is in contrast to field studies that have demonstrated reduced cognitive performance at the end of 12 h night and day shifts (Kazemi et al., 2016). This study also showed that cognitive performance was reduced to a greater extent at night compared with day, as assessed using reaction time as a measurement parameter. Our findings did not support this study, one reason may be that our study only had a duration of 6 h. The subjects of Kazemi et al.'s (2016) study were all familiar with night work and reported being less sleepy (score of 5 on the KSS) than the participants in our study (score of 7 on the KSS), who were not used to night work. Our study simulated the first night of a nightshift, with an absence of adaptation to night work. In real-world working conditions, the daily rhythm will gradually adapt to the new work situation. A study from 2010 documented this adaptation over 7 days of 12 h shifts (Hansen et al., 2010). That study was performed on supply vessels in the North Sea, where vessel movements, noise and vibration also play a role and probably reduce the ability to adapt. In studies performed on oil platforms in the North Sea (Gibbs et al., 2002, 2007) similar adjustments were observed for 12 h shift work.

The level of cortisol measured in the saliva was significantly higher during daytime (at 12:00 pm) compared with night (at 4:00 am), but no effect of ambient temperature on cortisol levels was found. Day-to-day cortisol variations, as shown in this study, are well-documented in the literature, showing that the level of cortisol in the blood (and in the urine and saliva) usually rises and decreases in line with the daily rhythm. The cortisol level is highest at rising time (˜8:00 am). This value then decreases somewhat and remains relatively stable throughout the day. In the evening, the values drop and reach a minimum around midnight (Turek and Zee, 1999). However, this pattern may change if a person is working irregularly (e.g., night shift) and sleeps at different times of the day. The participants in our study were recruited from a normal population and were informed before the study to sleep as normal as possible. Therefore, we consider that the cortisol level of the participants followed a normal daily variation.

Cortisol is secreted in response to various stressful situations and studies of the effects of short-term cold exposure have yielded conflicting results. In our study, no effect of ambient temperature on cortisol was found. This agrees with the conclusion of a study reported by Granberg (1995), which showed that cold stress does not increase cortisol secretion. However, other studies have found increased cortisol secretion after exposure to low ambient temperatures. A 2 h exposure to low temperatures (5–15°C) increased cortisol levels (Wagner et al., 1987), and the addition of physical stress and cold showers increased these levels further (Tikuisis et al., 1999). Some studies have also reported reduced (Wittert et al., 1992) or unchanged (Gerra et al., 1992) cortisol levels in response to cold exposure. As discussed earlier, the participants were dressed in warm winter clothes throughout the experiment and reported being comfortable or a little cool throughout the test period in the low ambient temperature at night. Probably, the exposure to low ambient temperatures was insufficient to increase cortisol secretion due to the protection provided by the clothing worn. Several other factors may affect the secretion of cortisol. It has been shown that both psychological and physical stresses under arctic conditions can be expected to activate the body's response to stress, which may result in increased cortisol secretion. An increased level of cortisol was detected during an irregular trip with dog sledding in the Arctic, probably because of increased mental strain (Steine et al., 2003). Other expedition studies, however, found no increased cortisol values (Bishop et al., 2001). In our study, the only physical effort was easy walking on a treadmill six times for 6 min during the trial. Neither the cognitive tests nor physical work were major stressors, and they were performed in an identical manner during all trials.

Study Limitations

CANTAB Connect is a well-documented and reliable test method; but we did only include two cognitive parameters in our test battery for practical reasons. Short-term memory and reaction time might not be the most sensitive cognitive parameter to temperature cold stress as there might be an arousal effect of the low temperatures. Therefore, we cannot exclude the possibility that the inclusion of other cognitive parameters would have uncovered stronger negative effects in this study. Even though a practical application of our findings is that adequate clothing is of importance to protect against cooling and hence maybe protected from declines in cognitive performance, it is also a study limitation. We could have designed the protocol more like Muller et al. (2012) to provoke a more severe impact of the low ambient temperatures on skin and core temperature. The reason we selected to use protective clothing in −2°C was to simulate a realistic scenario for outdoor workers in the cold by using one of the best clothing available for the workers.

CONCLUSION

This study investigated how low ambient temperatures and night work affects some cognitive performance parameters. Lower skin- and core temperature was observed at night when exposed to low ambient temperature (−2°C), but there was no effect on short-term memory or reaction time. Increased sleepiness and lower cortisol levels were observed at night compared to daytime and was not influenced by low ambient temperature at night. The result from this study suggests that cognitive performance (short-term memory and reaction time) is not adversely affected by night work when exposed to low ambient temperatures if adequate protective clothing is worn.

DATA AVAILABILITY STATEMENT

The original contributions presented in the study are included in the article/supplementary material, further inquiries can be directed to the corresponding author.

ETHICS STATEMENT

The studies involving human participants were reviewed and approved by the Committee for Medical and Health Research Ethics, Central Norway. The patients/participants provided their written informed consent to participate in this study.

AUTHOR CONTRIBUTIONS

HF, MS, and ØW: study conception and design. ØW and JH: sample and data acquisition. HF, MS, ØW, and JH: data analysis and drafting of the manuscript. HF and MS: project supervision. All authors contributed to the article and approved the submitted version.

FUNDING

This work was funded by the Research Council of Norway (Grant No. 237779) and the Petroleum Safety Authorities of Norway.

REFERENCES

Akerstedt, T. (2007). Altered sleep/wake patterns and mental performance. *Physiol. Behav.* 90, 209–218. doi: 10.1016/j.physbeh.2006.09.007

Akerstedt, T., and Gillberg, M. (1990). Subjective and objective sleepiness in the active individual. *Int. J. Neurosci.* 52, 29–37. doi: 10.3109/00207459008994241

Akerstedt, T., Kecklund, G., and Gillberg, M. (2007). Sleep and sleepiness in relation to stress and displaced work hours. *Physiol. Behav.* 92, 250–255. doi: 10.1016/j.physbeh.2007.05.044

Bishop, S. L., Grobler, L. C., and Schjoll, O. (2001). Relationship of psychological and physiological parameters during an Arctic ski expedition. *Acta Astronaut.* 49, 261–270. doi: 10.1016/s0094-5765(01)00104-7

Castellani, J. W., and Young, A. J. (2016). Human physiological responses to cold exposure: acute responses and acclimatization to prolonged exposure. *Auton. Neurosci.* 196, 63–74. doi: 10.1016/j.autneu.2016.02.009

Coleshaw, S. R., Van Someren, R. N., Wolff, A. H., Davis, H. M., and Keatinge, W. R. (1983). Impaired memory registration and speed of reasoning caused by low body temperature. *J. Appl. Physiol.* 55, 27–31. doi: 10.1152/jappl.1983.55.1.27

Dai, L., Kloog, I., Coull, B. A., Sparrow, D., Spiro, A. III, Vokonas, P. S., et al. (2016). Cognitive function and short-term exposure to residential air temperature: a repeated measures study based on spatiotemporal estimates of temperature. *Environ. Res.* 150, 446–451. doi: 10.1016/j.envres.2016.06.036

Durnin, J. V. G. A., and Womersley, J. (1974). Body fat assessed from total body density and its estimation from skinfold thickness: measurements on 481 men and women aged from 16 to 72 Years Body fat assessed from total body density and its estimation from skinfold thickness : measurements on 481 men and women aged from 16 to 72 years. *Br. J. Nutr.* 32, 77–97. doi: 10.1079/BJN19740060

Faerevik, H., and Reinertsen, R. E. (2003). Effects of wearing aircrew protective clothing on physiological and cognitive responses under various ambient conditions. *Ergonomics* 46, 780–799. doi: 10.1080/0014013031000085644

Friborg, O., Rosenvinge, J. H., Wynn, R., and Gradisar, M. (2014). Sleep timing, chronotype, mood, and behavior at an Arctic latitude (69°N). *Sleep Med.* 15, 798–807. doi: 10.1016/j.sleep.2014.03.014

Gerra, G., Volpi, R., Delsignore, R., Maninetti, L., Caccavari, R., Vourna, S., et al. (1992). Sex-related responses of beta-endorphin, ACTH, GH and PRL to cold exposure in humans. *Acta Endocrinol.* 126, 24–28. doi: 10.1530/acta.0.1260024

Gibbs, M., Hampton, S., Morgan, L., and Arendt, J. (2002). Adaptation of the circadian rhythm of 6-sulphatoxymelatonin to a shift schedule of seven nights followed by seven days in offshore oil installation workers. *Neurosci. Lett.* 325, 91–94. doi: 10.1016/s0304-3940(02)00247-1

Gibbs, M., Hampton, S., Morgan, L., and Arendt, J. (2007). Predicting circadian response to abrupt phase shift: 6-sulphatoxymelatonin rhythms in rotating shift workers offshore. *J. Biol. Rhythms* 22, 368–370. doi: 10.1177/0748730407302843

Granberg, P. O. (1995). Human endocrine responses to the cold. *Arctic Med. Res.* 54, 91–103.

Hancock, P. A., Ross, J. M., and Szalma, J. L. (2007). A meta-analysis of performance response under thermal stressors. *Hum. Factors* 49, 851–877. doi: 10.1518/001872007x230226

Hansen, J. H., Geving, I. H., and Reinertsen, R. E. (2010). Adaptation rate of 6-sulfatoxymelatonin and cognitive performance in offshore fleet shift workers: a field study. *Int. Arch. Occup. Environ. Health* 83, 607–615. doi: 10.1007/s00420-010-0547-x

Harris, A. (2011). *Adaptation and health in extreme and isolated environments: from 78°N to 75°S*. Ph.D. thesis. Norway: University of Bergen.

Kazemi, R., Haidarimoghadam, R., Motamedzadeh, M., Golmohamadi, R., Soltanian, A., Zoghipaydar, M. R., et al. (2016). Effects of Shift Work on Cognitive Performance, Sleep Quality, and Sleepiness among Petrochemical Control Room Operators. *J. Circadian Rhythms* 14:1. doi: 10.5334/jcr.134

Kräuchi, K. (2002). How is the circadian rhythm of core body temperature regulated? *Clin. Auton. Res.* 12, 147–149. doi: 10.1007/s10286-002-0043-9

Kräuchi, K., Cajochen, C., Werth, E., and Wirz-Justice, A. (2000). Functional link between distal vasodilation and sleep-onset latency? *Am. J. Physiol. Regul. Integr. Comp. Physiol.* 278, R741–R748. doi: 10.1152/ajpregu.2000.278.3.R741

Leppäluoto, J., Pääkkönen, T., Korhonen, I., and Hassi, J. (2005). Pituitary and autonomic responses to cold exposures in man. *Acta Physiol. Scand.* 184, 255–264. doi: 10.1111/j.1365-201X.2005.01464.x

Mäkinen, T. M. (2007). Human cold exposure, adaptation, and performance in high latitude environments. *Am. J. Hum. Biol.* 19, 155–164. doi: 10.1002/ajhb.20627

Mitler, M. M., Carskadon, M. A., Czeisler, C. A., Dement, W. C., Dinges, D. F., Graeber, R. C., et al. (1988). Catastrophes, sleep, and public policy: consensus report. *Sleep* 11, 100–109. doi: 10.1093/sleep/11.1.100

Muller, M. D., Gunstad, J., Alosco, M. L., Miller, L. A., Updegraff, J., Spitznagel, M. B., et al. (2012). Acute cold exposure and cognitive function: evidence for sustained impairment. *Ergonomics* 55, 792–798. doi: 10.1080/00140139.2012.665497

Naesgaard, O. P., Storholmen, T. C. B., Wiggen, ØN., and Reitan, J. (2017). A user-centred design process of new cold-protective clothing for offshore petroleum workers operating in the Barents Sea. *Ind. Health* 55, 564–574. doi: 10.2486/indhealth.2017-0127

Nielsen, R., Gavhed, D. C. E., and Nilsson, H. (1989). Thermal function of a clothing ensemble during work: dependency on inner clothing layer fit. *Ergonomics* 32, 1581–1594. doi: 10.1080/00140138908966927

Palinkas, L. A. (2001). Mental and cognitive performance in the cold. *Int. J. Circumpolar Health* 60, 430–439.

Panda, S. (2016). Circadian physiology of metabolism. *Science* 354, 1008–1015. doi: 10.1126/science.aah4967

Pilcher, J. J., Nadler, E., and Busch, C. (2002). Effects of hot and cold temperature exposure on performance: a meta-analytic review. *Ergonomics* 45, 682–698. doi: 10.1080/00140130210158419

Ramanathan, N. L. (1964). A new weighting system for mean surface temperature of the human body. *J. Appl. Physiol.* 19, 531–533. doi: 10.1152/jappl.1964.19.3.531

Ramsey, J. D. (1995). Task performance in heat: a review. *Ergonomics* 38, 154–165. doi: 10.1080/00140139508925092

Shurtleff, D., Thomas, J. R., Schrot, J., Kowalski, K., and Harford, R. (1994). Tyrosine reverses a cold-induced working memory deficit in humans. *Pharmacol. Biochem. Behav.* 47, 935–941. doi: 10.1016/0091-3057(94)90299-2

Stang, P. R., and Wiener, E. L. (1970). Diver performance in cold water. *Hum. Factors* 12, 391–399.

Steine, K., Røseth, A. G., Sandbaek, G., Murison, R., Slagsvold, C. E., Keller, A., et al. (2003). [Increased cortisol levels, frostbite and effects on the muscles and skeleton during extreme polar conditions]. *Tidsskr. Nor. Laegeforen.* 123, 3529–3532.

Taylor, L., Watkins, S. L., Marshall, H., Dascombe, B. J., and Foster, J. (2015). The Impact of Different Environmental Conditions on Cognitive Function: a Focused Review. *Front. Physiol.* 6:372. doi: 10.3389/fphys.2015.00372

Tikuisis, P., Ducharme, M. B., Moroz, D., and Jacobs, I. (1999). Physiological responses of exercised-fatigued individuals exposed to wet-cold conditions. *J. Appl. Physiol.* 86, 1319–1328. doi: 10.1152/jappl.1999.86.4.1319

Turek, F. W., and Zee, P. C. (1999). "Lung biology in health and disease," in *Regulation of sleep and circadian rhythms*, ed C. Lenfant (New York: Marcel Dekker), 133

Wagner, J. A., Horvath, S. M., Kitagawa, K., and Bolduan, N. W. (1987). Comparisons of blood and urinary responses to cold exposures in young and older men and women. *J. Gerontol.* 42, 173–179. doi: 10.1093/geronj/42.2.173

Wiggen, ØN., Heen, S., Færevik, H., and Reinertsen, R. E. (2011). Effect of cold conditions on manual performance while wearing petroleum industry protective clothing. *Ind. Health* 49, 443–451. doi: 10.2486/indhealth.ms1236

Wittert, G. A., Or, H. K., Livesey, J. H., Richards, A. M., Donald, R. A., and Espiner, E. A. (1992). Vasopressin, corticotrophin-releasing factor, and pituitary adrenal responses to acute cold stress in normal humans. *J. Clin. Endocrinol. Metab.* 75, 750–755. doi: 10.1210/jcem.75.3.1517364

Wright, K. P., Hull, J. T., and Czeisler, C. A. (2002). Relationship between alertness, performance, and body temperature in humans. *Am. J. Physiol. Regul. Integr. Comp. Physiol.* 283, R1370–R1377. doi: 10.1152/ajpregu.00205.2002

Conflict of Interest: The authors declare that the research was conducted in the absence of any commercial or financial relationships that could be construed as a potential conflict of interest.

Advantages of publishing in Frontiers

OPEN ACCESS
Articles are free to read for greatest visibility and readership

FAST PUBLICATION
Around 90 days from submission to decision

HIGH QUALITY PEER-REVIEW
Rigorous, collaborative, and constructive peer-review

TRANSPARENT PEER-REVIEW
Editors and reviewers acknowledged by name on published articles

Frontiers
Avenue du Tribunal-Fédéral 34
1005 Lausanne | Switzerland

Visit us: www.frontiersin.org
Contact us: frontiersin.org/about/contact

REPRODUCIBILITY OF RESEARCH
Support open data and methods to enhance research reproducibility

DIGITAL PUBLISHING
Articles designed for optimal readership across devices

FOLLOW US
@frontiersin

IMPACT METRICS
Advanced article metrics track visibility across digital media

EXTENSIVE PROMOTION
Marketing and promotion of impactful research

LOOP RESEARCH NETWORK
Our network increases your article's readership